MARÍLIA FERNANDES MANCHOPE

EFEITO TERAPÊUTICO E MECANISMOS DE AÇÃO DA RESOLVINA D5 EM MODELOS DE ARTRITE

Londrina
2021

MARÍLIA FERNANDES MANCHOPE

EFEITO TERAPÊUTICO E MECANISMOS DE AÇÃO DA RESOLVINA D5 EM MODELOS DE ARTRITE

Tese apresentada ao programa de Pós-Graduação em Patologia Experimental da Universidade Estadual de Londrina, como requisito parcial para à obtenção do título de Doutora em Patologia Experimental.

Orientador: Prof. Dr. Waldiceu A. Verri Jr.

Londrina
2021

Ficha de identificação da obra elaborada pelo autor, através do Programa de Geração Automática do Sistema de Bibliotecas da UEL

M268e Manchope, Marília Fernandes.
Efeito terapêutico e mecanismos de ação da resolvina d5 em modelos de artrite / Marília Fernandes Manchope. - Londrina, 2021.
169 f. : il.

Orientador: Waldiceu Aparecido Verri Jr.
Tese (Doutorado em Patologia Experimental) - Universidade Estadual de Londrina, Centro de Ciências Biológicas, Programa de Pós-Graduação em Patologia Experimental, 2021.
Inclui bibliografia.

1. Artrite - Tese. 2. Dor crônica - Tese. 3. Mediadores lipídicos pró-resolução - Tese. 4. Inflamação - Tese. I. Aparecido Verri Jr, Waldiceu . II. Universidade Estadual de Londrina. Centro de Ciências Biológicas. Programa de Pós-Graduação em Patologia Experimental. III. Título.

CDU 616

MARÍLIA FERNANDES MANCHOPE

EFEITO TERAPÊUTICO E MECANISMOS DE AÇÃO DA RESOLVINA D5 EM MODELOS DE ARTRITE

Tese apresentada ao programa de Pós-Graduação em Patologia Experimental da Universidade Estadual de Londrina, como requisito parcial para à obtenção do título de Doutora em Patologia Experimental.

BANCA EXAMINADORA

_____
Orientador: Dr. Waldiceu A. Verri Jr
Universidade Estadual de Londrina – UEL

_____
Dra. Camila Rodrigues Ferraz
University of Maryland School of Medicine

_____
Dr. Fábio Henrique Kwasniewski
Universidade Estadual de Londrina – UEL

_____
Dr. Felipe Pinho Ribeiro
Havard Medical School

_____
Dra. Larissa Garcia Pinto
King's College London

Londrina, 22 de setembro de 2021

“O sucesso é ir de fracasso em fracasso sem perder entusiasmo.”

(Winston Churchill)

AGRADECIMENTOS

Agradeço primeiramente a todos os esforços e incentivos dos meus pais Eliana e Sidney. Reconheço e agradeço as abdicações que fizeram para proverem a melhor educação durante a minha formação, sem dúvidas isso me auxiliou durante minha jornada e me oportunizou importantes experiências pessoais e profissionais. Em especial a minha mãe que sempre acreditou em mim e me incentivou a batalhar pelos meus sonhos. Você quem plantou a sementinha do meu sonho em morar fora do país. Feliz em saber que esse sonho logo será concretizado.

Agradeço ao meu marido Danilo pela companhia em todos esses anos juntos. Sem dúvidas você fez da pós-graduação um momento mais fácil para mim, em especial nesse último ano em que o trabalho sobrecarregou, e você sempre compreensível de que essa fase passaria e chegaríamos ao tão sonhado título de Doutora. Obrigada por sonhar esse sonho comigo e acreditar mais do que eu mesma onde conseguiríamos chegar.

Agradeço aos meus sogros Celiane e Sidney por todo auxílio dado a mim e ao Danilo nessa trajetória. Pelas palavras de sabedoria e acolhimento de sempre. Obrigada por sonharem conosco esse sonho, e por não nos deixarem desistir.

Agradeço ao meu orientador prof Waldiceu, que aceitou me orientar durante a iniciação científica, mestrado e doutorado. Foram 9 anos de muito aprendizado e trabalho. Obrigada por sempre incentivar a realização de um período do doutoramento no exterior. Sem dúvidas essa oportunidade acrescenta muito a nós alunos.

Agradeço a todos do LabDor por terem me acolhido durante a iniciação científica em 2012. Gratidão por ter trabalhado com cada dos alunos de graduação, mestrado, doutorado e pós-doutorado que passaram por aqui entre 2012 a 2021, tenho certeza que de alguma maneira cada um de vocês teve papel no meu crescimento pessoal e profissional.

Agradeço aos queridos amigos que fiz aqui no labdor Cássia, Thacyana, Camila, Sandra, Ana Carla, Ana Carolina, Talita, Miram, Telma, Tiago, Anelise, Nayara, Felipe, Victor, Fernanda, Mariana. Vocês sempre fizeram os dias de experimentos mais leves e construtivos.

Agradeço aos queridos amigos que fiz em Londres e no King's College London, em especial a Lalazinha e Fabi vocês fizeram do meu ano em Londres muito especial. Obrigada por sempre se fazerem presentes apesar da distância física em que estamos atualmente. Ansiosa para nosso reencontro.

Agradeço a companhia, carinho e amor da mina filhas de quatro patas Amora e Zara

que fazem meus dias mais prazerosos e cheios de alegria.

Agradeço aos meus cunhados, primos e amigos que sempre compreenderam e aceitarem o ritmo de trabalho do labdor, e por nunca me desencorajarem, mesmo quando eu estava trabalhando durante o fim de semana do computador ou por nos ausentarmos mais cedo no fim de semana pois precisávamos passar no lab no retorno para Londrina.

Agradeço ao apoio técnico e amizade da Rosana, Pedro e Zui.

Por última, mas não menos importante, agradeço ao financiamento das agências de fomento CNPq e CAPES que financiaram as bolsas de estudo desde a iniciação científica até o doutoramento, e assim possibilitaram a dedicação exclusiva ao longo da minha jornada científica no Brasil e Londres. Desejo sorte e resistência aos cientistas brasileiros que ficarem no Brasil. A ciência, tecnologia e inovação no país sofrerá duramente a falta de investimentos. O que se constrói com décadas de trabalho e financiamento é facilmente destruído pela falta de investimentos e absorção do mercado de trabalho.

MANCHOPE, Marília Fernandes. **Efeito terapêutico e mecanismos de ação da resolvina d5 em modelos de artrite.** 2021. 169 f. Tese (Doutorado em Patologia Experimental) – Universidade Estadual de Londrina, Londrina, 2021.

RESUMO

A dor e inflamação articular acomete pacientes com artrite reumatoide (AR), ou que passaram por um procedimento que falhou de artroplastia/implante e tratamentos mais eficazes são necessários nestes casos. Utilizou-se neste trabalho dois modelos experimentais: 1) artrite induzida pelo antígeno albumina de soro bovino metilada (mBSA) em camundongos imunizados com mBSA emulsificado em CFA ou IFA; 2). artrite crônica induzida por dióxido de titânio (TiO2). Como abordagem terapêutica utilizou-se a resolvina (Rv)D5, que é um mediador lipídicos pró-resolução, e estes mediadores possuem potente ação resolutiva da inflamação e induzem analgesia prolongada. Camundongos C57BL/6 (20-25g) foram pré-tratados com RvD5 [3, 10 e 30 ng, i.p.) 30 minutos antes do desafio intra-articular (i.a.) com mBSA (100 µg). A hipersensibilidade mecânica e edema foram avaliados (1-24h) após o desafio, e infiltrado de neutrófilos (9-48h). Avaliou-se 24h após o desafio, a ativação de neurônios do gânglio da raiz dorsal (GRD) e expressão de RNAm para os canais TRPV1 e Nav1.8. Determinou-se no GRD 9h após o desafio: i) níveis do peptídeo relacionado ao gene da calcitonina (CGRP), ii) p-NF□B, iii) porcentagem de p-NF□B na população de neurônicos CGPR+. Na medula espinal, 9h após desafio avaliou-se a expressão de RNAm para GFAP, Olig-2, Iba-1, CX3CR1, ST2, IL-33, TNFα, pro-IL-1β e IL-10. Utilizou-se um protocolo prolongado consistindo de 2 desafios i.a. com mBSA primeiro no tempo zero e após 120h. Os animais foram pré-tratados 30 minutos antes do primeiro desafio e o tratamento com RvD5 repetido a cada 48h. A hipersensibilidade mecânica e edema foram avaliados diariamente até 240h após o primeiro desafio com mBSA nos camundongos. No contexto da artrite crônica induzida por TiO2, camundongos Swiss ou LysM-eGFP / CCR2-RFP (20-25g) foram tratados com RvD5 (1, 3 e 10 ng, i.p.) e 24h após o estímulo i.a. com TiO2 (3mg), e o tratamento repetido a cada 72h. Fenótipo da artrite (comportamento nociceptivo e edema articular) foi avaliado ao longo de 30 dias. Após 30 dias avaliou-se, o dano histopatológico, recrutamento de leucócitos, estresse oxidativo, e RNAm para gp91phox, iNOS TNFα, pró-IL-1β. In vitro utilizou-se macrófagos derivados da medula óssea, as células foram pré-tratados por 12h com RvD5 (0,1-100 ng/ml), primados com LPS e exposto ao TiO2. O sobrenadante foi utilizado para dosagem de TNFα, IL-1β por ELISA, lactato desidrogenase, e os macrófagos para a translocação nuclear de p-NF□B por imunofluorescência. A RvD5 induziu analgesia e efeito anti-inflamatório em ambos os modelos avaliados, reduzindo a hipersensibilidade mecânica, térmica, edema e alteração na distribuição do peso corpóreo das patas traseiras do camundongo. Na AR, a RvD5 reduziu a ativação neuronal, a ativação de neurônicos CGRP+ no GRD, inibiu a neuroinflamação na medula espinal reduzindo a ativação de células da glia e expressão de citocinas e o receptor ST2. Já na artrite crônica induzida por TiO2 RvD5 inibiu o infiltrado de leucócitos Lysm+ e CCR2+, estresse oxidativo articular, expressão de RNAm para TNFα e pro-IL-1β in vivo e produção de TNFα e ativação do NF□B induzidos por TiO2 in vitro. Portanto a RvD5 é uma abordagem terapêutica promissora no contexto da dor articular, minimizando a dor e inflamação,

e modulando mecanismos inflamatórios periféricos e mecanismo sensoriais de camundongos acometido com dor articular.

Palavras-chave: artrite; inflamação; dor crônica; mediadores lipídicos pró-resolução; nocicepção

Manchope, Marília Fernandes. **Therapeutical effect and mechanism of action of resolvin D5 in models of arthritis.** 2021. 169 p. Thesis (Doctorade in Experimental Pathology) – Universidade Estadual de Londrina, Londrina, 2021.

ABSTRACT

Patients with rheumatoid arthritis (RA) or that went through an arthroplasty/implant procedure that failed suffer from arthritic pain and inflammation, and new treatment are needed. In this work, we used two experimental models: 1) arthritis induced by methylated bovine serum albumin (mBSA) challenge in immunized mice; 2) chronic arthritis induced by titanium dioxide (TiO2) in mice. Resolvin (Rv) D5 was used as a therapeutic approach because it is a specialized pro-resolving mediator. These kinds of mediators have potent proprieties of inflammation resolution and prolonged analgesia. C57BL/6 mice (20-25g) were pre-treated with RvD5 [3, 10 e 30 ng, (intraperitoneally) i.p.] 30 minutes before mBSA intra-articular (i.a.) challenge (100 µg). Mechanical hypersensitivity and edema were evaluated (1-24h), neutrophilic infiltration (9-48h) after mBSA challenge. At 24h after mBSA challenge, neuronal activation was evaluated in neurons from dorsal root ganglion (DRG) and mRNA expression for TRPV1 and Nav1.8 ion channels. At the DRGs 9h after challenge it was evaluated: i) calcitonin gene-related peptide (CGRP) levels, ii) p-NF□B, iii) percentage of p-NF□B in CGRP+ neurons by immunofluorescence. At the spinal cord 9h after challenge, mRNA expression was evaluated for GFAP, Olig-2, Iba-1, CX3CR1, ST2, IL-33, TNFα, pro-IL-1β, and IL-10. A prolonged protocol with two i.a. mBSA challenges 120 h apart from each other was used for mechanical hypersensitivity and edema assessment in arthritic mice up to 240h after the first challenge. In chronic arthritis induced by TiO2, swiss and LysM-eGFP / CCR2-RFP mice (20-25g) were treated with RvD5 (1, 3 e 10 ng, i.p.) 24h after TiO2 stimulus (3mg, i.a.), the treatment was repeated every other 72h. Arthritis phenotype (nociceptive behaviour and edema) was assessed throughout 30 days. After 30 days was assessed in the joint histopathological damage, leukocytes recruitment, oxidative stress, and mRNA expression for gp91phox e iNOS TNFα, pro-IL-1β. Bone-marrow derived macrophages were pre-treated for 12h with RvD5 (0,1-100 ng/ml), primed with LPS, and exposed to TiO2. The supernatant was used for TNFα, IL-1β, and lactate dehydrogenase assessment, and in the macrophages for p-NF□B nuclear translocation by immunofluorescence. RvD5 induced analgesia and anti-inflammatory activities in both models used here by decreasing mechanical and thermal hypersensitivity, edema, and static weight distribution in the rear paws of mice. In RA, RvD5 inhibited neuronal activation assessed by calcium imaging, CGRP levels, and neuronal activation of CGRP+ neurons in the DRG. RvD5 inhibited neuroinflammation at the spinal cord by reducing glial cells markers, cytokines, and ST2 receptor mRNA expression. In chronic arthritis induced by TiO2, RvD5 inhibited histopathological damage, leukocyte infiltration of Lysm+ e CCR2+ cells, oxidative stress, mRNA expression of TNFα e pro-IL-1β in vivo, and the release of TNFα in the supernatant and p-NF□B nuclear translocation induced by TiO2 in vitro. Thus, RvD5 is a conceivable approach to inhibit arthritic pain by modulating peripheral inflammation and sensorial mechanism in mice affected.

Key words: arthritis; inflammation; chronic pain; specialized pro-resolving mediators; nociception.

LISTA DE FIGURAS

LISTA DE ABREVIATURAS E SIGLAS

a.C	Antes de cristo
ACKR	Receptor atípico de quimiocina
AIA	Artrite induzida por antígeno
AR	Artrite reumatoide
ATP	Trifosfato de adenosina
BAI1	Inibidor de angiogênese específico do cérebro 1
CFA	Adjuvante completo de Freund
CGRP	Peptídeo relacionado ao gene da calcitonina
d.C.	Depois de cristo
DAMPS	Padrões moleculares associados ao dano
DHA	Ácido docosahexaenóico
DMDAR	Agentes modificadores de doenças reumáticas
EGF	Fator de crescimento epidérmico
EPA	Ácido eicosapentaenóico
ERNs	Espécies reativas de nitrogênio
EROs	Espécies reativas de oxigÊnio
ET-1	Endotelina-1
fMLP	N-formilmetionil-leucil-fenilalanina
G2A	Receptor acoplado à proteína G 132
GFAP	Proteína ácida fibrilar glial
GPCR	Receptores acoplados a proteína G
GRD	Gânglio da raiz dorsal
HPETE	Ácido hidroxieicosatetraenóico
i.p.	Intraperitoneal
Iba-1	Molécula adaptadora ionizada de ligação ao cálcio 1
IL	Interleucina
IL-1R1	Receptor de interleucina 1, tipo I
iNOS	Óxido nítrico-sintase induzida
I□B	Molécula inibidora do fator de transcrição □B
KO	Nocaute
LDH	Lactato desidrogenase
LPS	Lipopolissacarídeo

LTB4	Leucotrieno B4
Lx	Lipoxinas
MaR	Maresina
mBSA	Albumina de soro bovina metilada
MMP-12	Metaloproteinase-12 específica de macrófago
NADPH	Fosfato de dinucleotídeo de adenina e nicotinamida
Nav	Canal de sódio voltagem dependente
NF□B	Fator de transcrição □B
NLR	Receptores do tipo NOD
NO	Óxido nítrico
Olig-2	Fator de transcrição de oligodendrócitos
P2Y2	Receptor purinérgico P2Y2
PAMPS	Padrões moleculares associados a patógenos
PGE2	Prostaglandina E2
PKA	Proteína quinase A
PRRs	Receptores de reconhecimento de padrões
RANK	Receptor ativador do fator nuclear □B
RANKL	Ligante do receptor ativador do fator nuclear □B
Rv	Resolvina
S1P1-5	Receptor 1-5 de esfingosina-1-fosfato
SOD	Superóxido dismutase
SPMs	Mediadores lipídicos pró-resolução
TGFβ	Fator de transformação do crescimento b
TIM4	Imunoglobulina das células T contendo o domínio 4 da mucina
TiO2	Dióxido de titânio
TNF□	Fator de necrose tumoral α
TNFR1	Receptor do fator de necrose tumoral 1
TRL	Receptores do tipo Toll
TRP	Canal de potencial transitório
TRPA1	Canal de potencial transitório anquirina 1
TRPV1	Canal de potencial transitório da subfamília vaniloide 1
UTP	Uridina trifosfato
VGEF	Fator de crescimento endotelial vascular

SUMÁRIO

1 INTRODUÇÃO

1.1 INFLAMAÇÃO

O processo inflamatório e os sinais cardinais: vermelhidão, calor, edema e dor são descritos desde a antiguidade em hieróglifos da civilização suméria datados de 2700 a.C. e posteriormente por Celsius no primeiro século d.C. (ROCHA E SILVA, 1994). A inflamação é uma resposta adaptativa do organismo que tem início por um estímulo ou condição nociva, como infecção e/ou injuria tecidual (MEDZHITOV, 2008). O processo inflamatório é essencial para a sobrevivência do indivíduo e orquestra a defasa do organismo frente a uma condição nociva. A inflamação pode ser dividida na iniciação do processo seguido da resolução que é imprescindível para o reestabelecimento da homeostase tecidual (MADERNA; GODSON, 2009). Falhas no processo de resolução, exacerbação e/ou persistência do processo infamatório acarreta na destruição tecidual, fibrose e culmina no 5º sinal da inflamação que é a perda de função do tecido e/ou órgão acometido (GUERRERO; VERRI; CUNHA; SILVA *et al.*, 2008; MADERNA; GODSON, 2009).

A inflamação tem sua iniciação, por exemplo, pelo reconhecimento de padrões moleculares associados a patógenos (PAMPs) e padrões moleculares associados ao dano (DAMPs) por receptores do reconhecimento do padrão (PRRs) como por exemplo receptor do tipo toll (TLR), receptor do tipo NOD (NLR) que estão presente em células residentes do tecido como macrófagos e mastócitos (MEDZHITOV, 2008; TAKEUCHI; AKIRA, 2010). Ativação de PRRs promove a ativação de vias de sinalização que culminam na ativação de fatores de transcrição e produção de mediadores como citocinas e lipídeos pró-inflamatórios. Por exemplo, a ativação do fator de transcrição κB (NFκB) leva a produção de citocinas inflamatórias como fator de necrose tumoral α (TNFα), interleucina (IL)-1β e IL-6 (MEDZHITOV, 2008; TAKEUCHI; AKIRA, 2010). A ativção do NFκB e produção de mediadores inflamatóriosestá exemplificado abaixo na figura 1. Em consequência outros mediadores inflamatórios são produzidos como aminas vasoativas, quimiocinas, leucotrieno B_4 (LTB_4), prostaglandina E_2 (PGE_2) que propiciam a ampliação da reação inflamatória (CUNHA; CACINI; FERREIRA, 1986; PARADA; TAMBELI; CUNHA; FERREIRA, 2001; RIBEIRO; SOUZA-FILHO; SOUZA; OLIVEIRA *et al.*, 1997; SPECTOR; WILLOUGHBY, 1964; VERRI; CUNHA; PARADA; POOLE *et al.*, 2006).

Figura 1 – Figura esquemática demonstrando a ativação do NFκB e produção de citocinas e lipídeos pró-inflamatórios em macrófago.

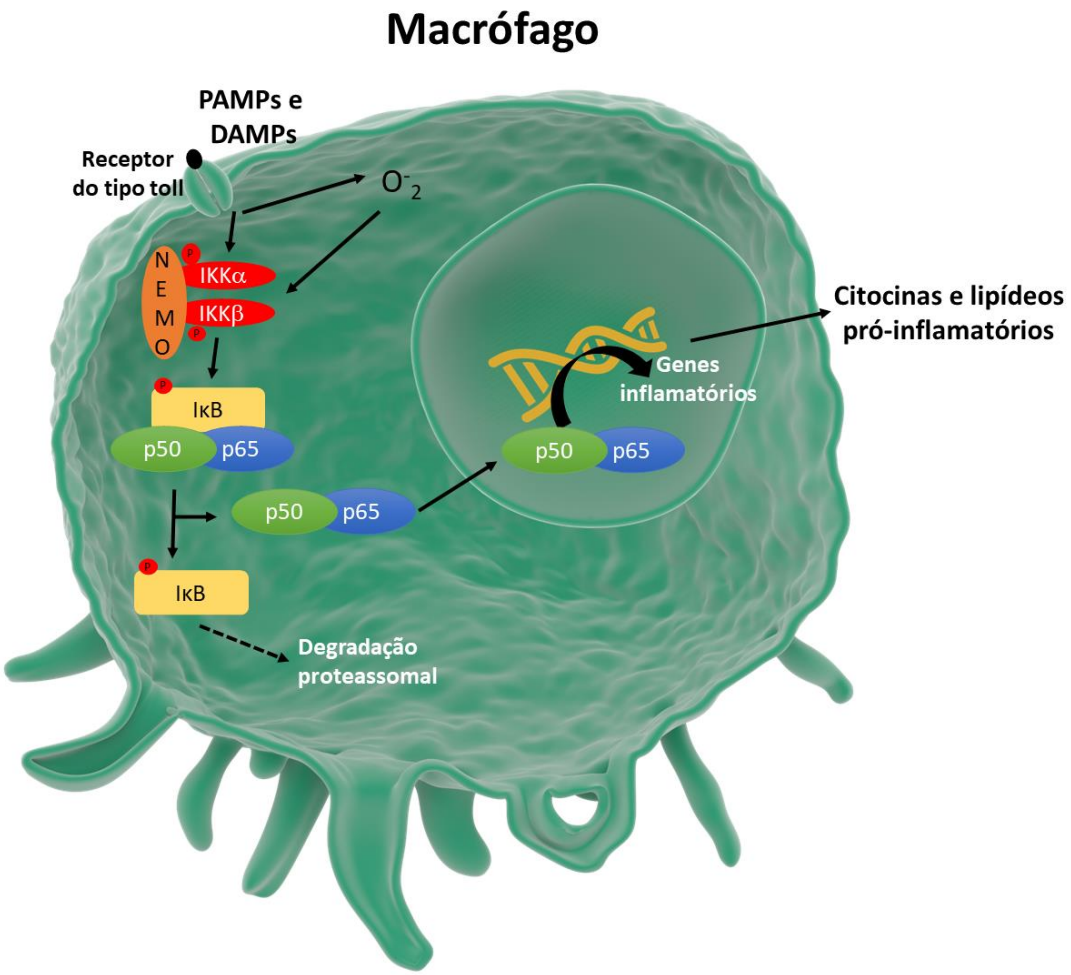

Fonte: Adaptado de Manchope, Casagrande e Verri, 2017.

Alterações na vasculatura e leito capilar ocorrem na região proximal ao foco inflamatório com aumento no calibre do leito vascular e aumento no fluxo sanguíneo local, associado a aumento na permeabilidade vascular e extravasamento de líquido rico em proteínas que contribui para formação do edema. Essas modificações no leito vascular alteram o fluxo hemodinâmico favorecendo a marginalização de leucócitos, principalmente neutrófilos (ABBAS; KUMAR; FAUSTO, 2016; BOTTARO; SHEPRO; PETERSON; HECHTMAN, 1986; SPECTOR; WILLOUGHBY, 1964; THEOHARIDES; KEMPURAJ; TAGEN; CONTI *et al.*, 2007). Além disso a células epiteliais são ativadas por citocinas pró-inflamatórias como TNFα, e contribuem para a quimiotaxia de neutrófilos até o foco inflamatório (WOODFIN; VOISIN; IMHOF; DEJANA *et al.*, 2009). Os agentes quimiotáticos

possuem participação hierárquica para precisamente guiar os neutrófilos (FOXMAN; CAMPBELL; BUTCHER, 1997). O estímulo com TNFα no músculo cremaster induz a produção de quimiocinas CXCL1 e CXCL2, e interessantemente estas quimiocinas são produzidas sequencialmente, e por diferentes fontes celulares. Estas quimiocinas medeiam a adesão firme, arrastamento e transmigração do neutrófilo pelo lúmen endotelial, junções endoteliais e espaço subluminal até transmigrarem para o tecido (GIRBL; LENN; PEREZ; ROLAS *et al.*, 2018). O CXCL1 é produzido pela célula endotelial e pericitos e promove a adesão e arrastamento do neutrófilo pelo lúmen e espaço subluminal do vaso. Para os neutrófilos transmigrarem pela junção endotelial e atingirem o espaço subluminal, o TNFα induz a liberação CXCL2 pelo neutrófilo, e esta quimiocina se liga a célula endotelial no receptor atípico de quimiocina (ACKR)1, o qual mantém o CXCL2 exposto na célula endotelial, permitindo a interação CXCL2/CXCR2 entre célula endotelial e neutrófilo. Assim, o neutrófilo transmigra entre as junções das células endoteliais atingindo o espaço subluminal por onde transmigra até o tecido (GIRBL; LENN; PEREZ; ROLAS *et al.*, 2018). Este gradiente hierárquico ainda pode ser dividido conforme a distância do foco inflamatório. Na injúria focal térmica hepática como modelo de inflamação estéril, os neutrófilos são qumioatraidos até a vasculatura pelo CXCL2. Já no espaço intersticial os neutrófilos são guiados até o foco necrótico pela sinalização de formilmetionina-leucil-fenilalanina (fMLP) no receptor FPR1 dos neutrófilos (MCDONALD; PITTMAN; MENEZES; HIROTA *et al.*, 2010).

Radicais livres como as espécies reativas de oxigênio (EROs) e nitrogênio (ERNs) desempenham importante papel na inflamação. Ânion superóxido pode ser produzido pelo fosfato de dinucleotídeo de nicotinamida e adenina (NADPH) oxidase (BABIOR, 2004). Mediadores inflamatórios como TNFα e endotelina-1 (ET-1) induzem a NADPH oxidase produzir ânion superóxido (KILPATRICK; SUN; LI; VARY *et al.*, 2010; LÓPEZ-SEPÚLVEDA; GÓMEZ-GUZMÁN; ZARZUELO; ROMERO *et al.*, 2011). O ânion superóxido pode se transmutar em outros mediadores como peróxido de hidrogênio, radical hidroxila, ou peroxinitrito ao se combinar com o óxido nítrico (NO) produzido pela óxido nítrico sintase induzível (iNOS) (CUMPSTEY; FEELISCH, 2017). Em condições patológicas e inflamatórias, o desbalanço pelo aumento da produção de espécies reativas e diminuição de defesas antioxidantes induz o estresse oxidativo. O acúmulo de espécies reativas levará a ativação de vias de sinalização, fatores de transcrição e

promoverá o dano a biomoléculas como membrana lipídica, proteínas, e material genético (CUMPSTEY; FEELISCH, 2017; GLOIRE; PIETTE, 2009; TORRES; FORMAN, 2003; ZHANG; WANG; VIKASH; YE *et al.*, 2016). Radicais livres podem levar a ativação de quinases como proteína quinase ativada por mitógenos (MAPK) e NFκB (GLOIRE; PIETTE, 2009; TORRES; FORMAN, 2003). A via de sinalização do NFκB é redox sensível, a molécula inibidora do fator de transcrição κB (IκB) é ubiquitinada e degradada liberando as subunidades p65 e p50 do NFκB. A subunidade p65 é fosforilada em resíduos específicos, como a Serina 276 pela proteína quinase A (PKA). A ativação do NFκB pela PKA tem ação aumentada por radicais livres, e o uso de antioxidantes como N-acetilcisteína inibe a ligação do NFκB na região promotora do gene IL-8 (JAMALUDDIN; WANG; BOLDOGH; TIAN *et al.*, 2007), ou M40403 [mimético da superóxido dismutase (SOD)], inibe a ativação do NFκB e liberação de TNFα e IL-6 (NDENGELE; MUSCOLI; WANG; DOYLE *et al.*, 2005). Corroborando que a produção de radicais livres potencializa o processo inflamatório. Por outro lado, é importante ressaltar que a produção de radicais livres também tem importância no contexto fisiológico. Por exemplo, a ativação de via de sinalização do fator de crescimento epidermal (EGF) induz a ativação da enzima tirosina fosfatase, sendo que esta enzima depende da ação de EROs para a ativação. Além disso, a tirosina fosfatase é inativada por produtos de oxidação como a glutationa oxidada (TRUONG; CARROLL, 2012). Comprovando que existe um fino balanço na regulação das vias de sinalização redox sensíveis pelas EROs e os produtos de oxidação (HOLMSTRÖM; FINKEL, 2014).

1.2 RESOLUÇÃO

A progressão temporal da inflamação é importante e progride para a resolução do processo inflamatório por meio de um processo coordenado e ativo que visa restaurar a função e homeostase tecidual. A resolução é induzida pelos mediadores lipídicos pró-resolução (SPMs) (SERHAN, 2014). Esses mediadores lipídicos são derivados da transformação dos ácidos graxos essenciais do ômega-6 e ômega-3, como ácido araquidônico, ácido eicosapentaenóico (EPA) e ácido docosaexaenóico (DHA). Os SPMs são subdivididos nas famílias das lipoxinas (única ômega-6), resolvinas (Rv), protectinas e maresinas (MaR) (Figura 2) (SERHAN, 2014). Embora tenham sido primeiramente identificados na resolução do processo inflamatório, os mediadores lipídicos pró-resolução desempenham papel

na defesa do hospedeiro contra micro-organismos, injúrias teciduais, e remodelamento tecidual (SERHAN, 2014). A sinalização da PGE_2 nos neutrófilos induz a expressão da enzima 15-lipoxigenase e ocorre a mudança na classe de mediadores lipídicos inflamatórios para os SPMs, como a lipoxina $(Lx)A_4$ (LEVY; CLISH; SCHMIDT; GRONERT *et al.*, 2001). A sinalização dos SPMs reduz o recrutamento de neutrófilos para o foco inflamatório, bem como promove a retirada dos neutrófilos da superfície endotelial. Além disso, induz a apoptose dos neutrófilos para posterior eferocitose dos corpos apoptóticos por macrófagos não-flogísticos bem como a remoção de *debris* inflamatórios e infecciosos (SERHAN, 2014). Assim, esse processo reduz a quantidade de citocinas pró-inflamatórias, aumenta as citocinas anti-inflamatórias e o promove o retorno da homeostase tecidual (SERHAN, 2014).

Figura 2 – Figura esquemática da conversão do DHA e EPA em SPMs.

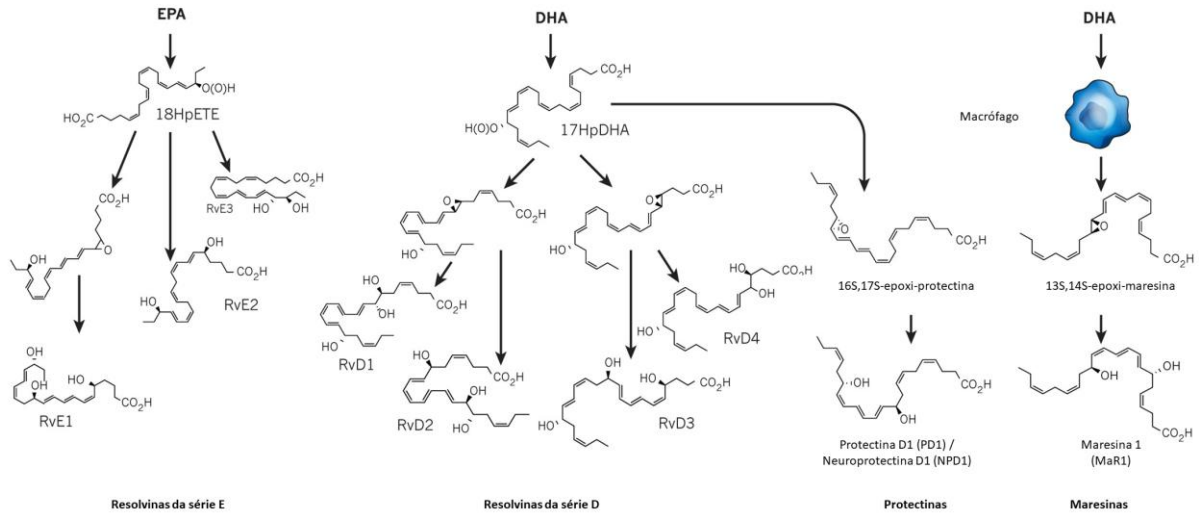

Fonte: Adaptado de Serhan 2014

A redução do recrutamento de neutrófilos é imprescindível para a fase resolutiva. Mecanisticamente, ocorre a clivagem proteolítica de quimiocinas ou até mesmo o sequestramento destes mediadores favorecendo a redução do infiltrado leucocitário e, assim, a resolução da inflamação (ORTEGA-GOMEZ; PERRETTI; SOEHNLEIN, 2013). A metaloproteinase-12 específica de macrófago (MMP-12) cliva a região ELR de quimiocinas da família CXC como CXCL1, -2, -3, -5 e -8. Sendo esta região importante para a ligação da quimiocina da família CXC ao receptor e promoção da quimioatração de neutrófilos. Portando a clivagem dessa região favorece a inibição do recrutamento de neutrófilos e adesão dos mesmo a

vasculatura (DEAN; COX; BELLAC; DOUCET *et al.*, 2008). Além disso, a MMP-12 também é responsável pela clivagem de quimiocinas da família CC relacionas ao recrutamento de monócitos inflamatórios como CCL2, -7, -8, e -13. Interessantemente, animais nocaute (KO) para MMP-12 quando estimulados intranasalmente com lipopolissacarídeo (LPS) apresentam maiores níveis de neutrófilos e macrófagos no lavado broncoalveolar 72h após o estímulo quando comparado com os animais selvagens (DEAN; COX; BELLAC; DOUCET *et al.*, 2008). Portanto a clivagem das quimiocinas tem importância para reduzir o infiltrado leucocitário. Os receptores atípicos de quimiocinas também desempenham papel no processo resolutivo. Estes receptores não possuem a região intracelular requerida para ativação de vias de sinalização intracelular. Em oposição ao efeito do ACKR1 que é importante para o recrutamento de neutrófilos no contexto de inflamação aguda induzida por TNFα (GIRBL; LENN; PEREZ; ROLAS *et al.*, 2018), o ACKR2 sequestra quimiocinas e promove a internalização e direcionamento para compartimentos intracelulares com ação proteolíticas, reduzindo a biodisponibilidade destas quimiocinas, e por conseguinte diminui o recrutamento de leucócitos. Por exemplo, no estímulo subcutâneo com adjuvante completo de Freund (CFA) após 7 dias houve um aumento na formação de granulomas na pele de animais KO para a ACKR2 comparado com os animais selvagens (MARTINEZ DE LA TORRE; LOCATI; BURACCHI; DUPOR *et al.*, 2005). Portanto, a redução da biodisponibilidade das quimiocinas é importante no contexto resolutivo para redução do recrutamento de neutrófilos e macrófagos inflamatórios e assim progressão para a resolução da inflamação.

Neutrófilos em apoptose são outro marco durante a resolução. Os corpos apoptóticos tem importante ação resolutiva por liberarem Anexina A1, um mediador que induz ações resolutivas como indução de apoptose de neutrófilos e eferocitose dos corpos apoptóticos por macrófagos (PERRETTI; SOLITO, 2004; SCANNELL; FLANAGAN; DESTEFANI; WYNNE *et al.*, 2007). Células em apoptose liberam sinais quimiotáticos (*find me signal*) para atrair macrófagos não-flogístico, como lisofosfatidilcolinas, esfingosina-1-fosfato, CX_3CL_1, nucleotídeos como trifosfato de adenosina (ATP) e uridina trifosfato (UTP) os quais sinalizam nos receptores: receptor acoplado à proteína G 132 (G2A), receptor 1-5 de esfingosina-1-fosfato (S1P1-5), CX_3CR_1, e receptor purinérgico P2Y2 (P2Y2), respectivamente (ELLIOTT; CHEKENI; TRAMPONT; LAZAROWSKI *et al.*, 2009; GUDE; ALVAREZ;

PAUGH; MITRA *et al.*, 2008; LAUBER; BOHN; KROBER; XIAO *et al.*, 2003; TRUMAN; FORD; PASIKOWSKA; POUND *et al.*, 2008). Além disso, as células em apoptose apresentam sinais de morte na membrana celular que medeiam a eferocitose, conhecidos como *eat me signal*. Por exemplo, fosfatidilserina é um componente interno da membrana lipídica e durante a apoptose é exteriorizado na bicamada lipídica possibilitando o reconhecimento pelos receptores imunoglobulina das células T contendo o domínio 4 da mucina (TIM4), inibidor de angiogênese específico do cérebro 1 (BAI1), estabilina 2 e receptor de produtos avançados finais de glicação (HE; KUBO; MORIMOTO; FUJINO *et al.*, 2011; RAVICHANDRAN, 2011) levando assim a eferocitose dos corpos apoptóticos e favorecendo a retirada dos *debris* inflamatórios. Após a eferocitose os macrófagos mudam seu padrão de inflamatório com produção de TNFα e LTB_4, para um perfil resolutivo com a produção fator de transformação do crescimento β (TGFβ), IL-10, LXA_4, fator de crescimento endotelial vascular (VGEF) (ORTEGA-GOMEZ; PERRETTI; SOEHNLEIN, 2013) contribuindo assim para o retorno da homeostase tecidual e reparo.

A falha na resolução do processo inflamatório aumenta a quantidade de neutrófilos no local injuriado, com elevação de mediadores pró-inflamatórios como prostaglandinas, leucotrienos, citocinas inflamatórias como TNFα os quais contribuem para cronificação do processo inflamatório (ARNARDOTTIR; DALLI; NORLING; COLAS *et al.*, 2016; HSIAO; THATCHER; COLAS; SERHAN *et al.*, 2015; LEVY; CLISH; SCHMIDT; GRONERT *et al.*, 2001). Doenças inflamatórias crônicas podem ser relacionadas a falhas na resolução da inflamação, por exemplo, pacientes com enfisema pulmonar possuem níveis elevados da enzima 15-prostaglandina desidrogenase que promove a degradação de mediadores lipídicos (HSIAO; THATCHER; COLAS; SERHAN *et al.*, 2015). Esse aumento da 15-prostaglandina desidrogenase reduz os mediadores lipídicos pró-resolução (CROASDELL; THATCHER; KOTTMANN; COLAS *et al.*, 2015). A artrite induzida pelo soro artritogênico K/BxN pode apresentar uma auto-resolução quando o animal é estimulado duas vezes com o soro artritogênico, ou ter a resolução atrasada quando o animal é estimulado três vezes com o soro. Durante a resolução os níveis de Rv da série D aumentaram como RvD1, RvD2, RvD3 e RvD4. Por outro lado, no contexto da resolução atrasada os níveis da RvD3 estão reduzidos. De fato, o tratamento com RvD3 inibe a migração de leucócitos, produção de mediadores

lipídicos pró-inflamatórios (PGE_2, LTB_4), edema e score clínico. Em concordância pacientes com artrite reumatoide (AR) apresentam níveis baixos de RvD3 no soro quando comparado a indivíduos saudáveis (ARNARDOTTIR; DALLI; NORLING; COLAS *et al.*, 2016). Desta maneira um fino balanço entre os mecanismos inflamatórios e resolutivos deve existir, com a finalidade do indivíduo se beneficiar dos eventos protetivos da inflamação aguda (combate de agente infeccioso, e/ou cessar uma injúria tecidual), bem como induzir a sinalização apropriada para que ocorra a resolução inflamatória e retorno a homeostase tecidual.

1.3 DOR

A dor é uma experiência sensorial e emocional desagradável que alerta o indivíduo sobre um dano real ou potencial e desencadeia uma resposta protetiva adequada (RAJA; CARR; COHEN; FINNERUP *et al.*, 2020). Fatores como humor, atenção e expectativa da intensidade dolorosa são exemplos de como o componente emocional pode interferir na percepção da sensação dolorosa (BUSHNELL; ČEKO; LOW, 2013). Indivíduos acometidos com alterações genéticas que causem a redução na expressão do canal de sódio voltagem dependente (Na_V)1.7 vivenciam a inabilidade de sentir dor e acabam acometidos em episódios de automutilação, fraturas ósseas, múltiplas cicatrizes, amputação de membros, até mesmo a morte precoce do indivíduo acometido por essa alteração genética (COX; REIMANN; NICHOLAS; THORNTON *et al.*, 2006), o que demonstra o papel protetor do processo doloroso .

A dor pode ser classificada de acordo com seus mecanismos patofisiológicos e alteração no limiar de ativação neuronal. A dor nociceptiva tem papel adaptativo protetor. A dor nociceptiva visa cessar o agente nocivo. Por exemplo, uma fonte de temperaturas nocivas induz um reflexo motor de retirada do membro acometido protegendo assim o indivíduo de injúria tecidual pela temperatura extrema e não existe alteração no limiar de ativação neuronal. Por outro lado a dor inflamatória e neuropática são classificadas como patológicas e possuem uma redução no limiar de ativação neuronal. A dor inflamatória ocorre pela interação entre o tecido injuriado, que produz mediadores inflamatórios, com neurônios sensoriais periféricos que inervam a região. A dor inflamatória objetiva auxiliar na cura do indivíduo desencorajando o contato físico com a região ou até o movimento do membro acometido pela lesão. A dor neuropática é causada por uma injúria ao

tecido nervoso periférico ou central e tem características mal-adptativa causando um funcionamento anormal do sistema sensorial. Além disso, outro tipo de dor mal-adaptativa são quando existe relato de dor pelo paciente, porém não existe mais dano ou processo inflamatório ativo, como ocorre na AR (LEE; CUI; LU; FRITS *et al.*, 2011; WOOLF, 2010), sugerindo que possa existir alterações no sistema somatossensorial.

O estímulo doloroso é transmitido pelo sistema sensorial da periferia até o sistema nervoso central (ZAKY; ZAKY; ABD-ELSAYED, 2019). O neurônio primário tem seu corpo neuronal no gânglio da raiz dorsal e possui seus axônios inervando o tecido periférico e na outra direção invervado o corno dorsal da medula espinal (ZAKY; ZAKY; ABD-ELSAYED, 2019). A percepção do estímulo doloroso e nocivo ocorre por meio da ativação de diferentes tipos de receptores e canais iônicos presentes no terminação nervosa periférica do neurônio primário, como canais de potencial transitório (TRP), canais iônicos voltagem dependente, receptores de mediadores inflamatórios como de lipídeos e citocinas. Canais do tipo TRP são ativados por diferentes tipos de estímulos como temperatura, agentes irritantes e ligantes endógenos. Por exemplo, canal de potencial transitório da subfamília Vaniloide 1 (TRPV1) é um canal de cálcio não-seletivo ativado pela capsaicina, um componente da pimenta, temperatura nocivas (> 42ºC), baixo pH, e ligantes endógenos como moléculas derivadas da ação da lipoxigenase no ácido araquidônico gerando ácido12-hidroperoxiéicosatetraenoico (HPETE) and 15-HPETE (JULIUS, 2013; PINHO-RIBEIRO; VERRI; CHIU, 2017; SZALLASI; CORTRIGHT; BLUM; EID, 2007).

A condução do estímulo sensorial ocorre por meio de fibras nervosas classificadas em A (Aα, Aβ e Aδ) e C (BRAZ; SOLORZANO; WANG; BASBAUM, 2014). As fibras Aα e Aβ possuem largo diâmetro, e maior quantidade de mielina, conduzem principalmente estímulos inócuos como toque leve e propriocepção (FERREIRA; FERRARI; CUNHA; NASCIMENTO *et al.*, 2009; JULIUS; BASBAUM, 2001). As fibras Aα e Aβ recrutam interneurônios inibitórios no corno dorsal da medula espinal que inibem a entrada ou quantidade de resposta nociceptiva na medula espinal o que explica porque um estímulo inócuo reduz a informação nociceptiva quando ambos ocorrerem no mesmo local (JULIUS; BASBAUM, 2001). As fibras de diâmetro médio Aδ são levemente mielinizadas, podem ser divididas em: i) mecanoceptoras – respondem preferencialmente a

estímulos mecânicos intensos e potencialmente danosos; ii) polimodais – respondem a estímulos mecânicos, térmicos e químicos. A ativação de fibras Aδ gera sensação dolorosa intensa em alfinetada ou pontada de forma transiente. Além disso, os mecanoceptoras podem aumentar sua despolarização frente a estímulos térmicos intensos (FEIN, 2012; JULIUS; BASBAUM, 2001). As fibras do tipo C são de diâmetro pequeno, amielinizadas e polimodais responsáveis por dor em queimação (FEIN, 2012; JULIUS; BASBAUM, 2001).

Após a ativação do nociceptor primário, este transmite a informação dolorosa periférica até o corno dorsal da medula espinal onde faz sinapse com neurônios de segunda ordem. A medula espinal é dividida em 10 lâminas, e as fibras do tipo C inervam as lâminas do tipo I e II e menos extensivamente a lâmina V. Já as fibras do tipo Aδ inervam principalmente as lâminas I, V e menos extensivamente a X da medula espinal (BRAZ; SOLORZANO; WANG; BASBAUM, 2014; ZAKY; ZAKY; ABD-ELSAYED, 2019). A percepção do estímulo ocorre pela transmissão do sinal para o córtex somatossensorial no cérebro, local onde o estímulo nociceptivo é interpretado. Ademais, as projeções que envolvem sinapses na região da amídala são responsáveis pelo componente emocional da sensação dolorosa (FEIN, 2012; JULIUS; BASBAUM, 2001; MILLAN, 1999; REICHLING; LEVINE, 2009; SCHOLZ; WOOLF, 2002)

O aumento da excitabilidade do neurônio sensorial primário é conhecido como sensibilização neuronal. No contexto da dor inflamatória o aumento da excitabilidade neuronal ocorre pela ação de citocinas como TNFα e IL-1β em seus respectivos receptores – receptor do fator de necrose tumoral 1 (TNFR1) e receptor de interleucina 1, tipo I (IL-1R1), os quais estão presentes no terminal periférico do neurônio sensorial primário (CUNHA; POOLE; LORENZETTI; FERREIRA, 1992; CUNHA; VERRI; SILVA; POOLE *et al.*, 2005; EBBINGHAUS; UHLIG; RICHTER; VON BANCHET *et al.*, 2012; GUDES; BARKAI; CASPI; KATZ *et al.*, 2015; JIN; GEREAU, 2006; SORKIN; DOOM, 2000). O aumento na excitabilidade dos neurônios aferentes primário contribui para o aumento na sensibilidade dolorosa, que pode ser dividida em duas categorias: 1) hipersensibilidade – resposta exacerbada a um estímulo doloroso; 2) alodinia – resposta nociceptiva a estímulos previamente não dolorosos (FERREIRA; FERRARI; CUNHA; NASCIMENTO *et al.*, 2009). A sinalização TNFα/TNFR1 e IL-1β/IL-1R1 ativa map quinases como a p38, que fosforila de canais como $Na_V1.8$ o que promove

um aumento na quantidade de potenciais de ação e exicitabilidede neuronal, tal fato se relaciona com o aumento na hipersensibilidade a um estímulo mecânico e/ou térmico (CUNHA; POOLE; LORENZETTI; FERREIRA, 1992; CUNHA; VERRI; SILVA; POOLE *et al.*, 2005; EBBINGHAUS; UHLIG; RICHTER; VON BANCHET *et al.*, 2012; GUDES; BARKAI; CASPI; KATZ *et al.*, 2015; JIN; GEREAU, 2006; SORKIN; DOOM, 2000). Leucócitos residentes como mastócitos, macrófagos e neutrófilos recrutados ao foco inflamatório tem relação direta com a dor inflamatória, sendo estas células importantes para a manutenção da dor inflamatória, pois são fonte importante dos mediadores inflamatórios (AICH; AFRIN; GUPTA, 2015; CUNHA; VERRI; SCHIVO; NAPIMOGA *et al.*, 2008; OLD; NADKARNI; GRIST; GENTRY *et al.*, 2014; SCHUH; PIERRE; WEIGERT; WEICHAND *et al.*, 2014).

1.3.1 Interação nociceptor e sistema imune

O sistema nervoso somatossensorial periférico se comunica com o sistema imune pois as células imunes expressam receptores para neuropeptídeos e neurotransmissores (GODINHO-SILVA; CARDOSO; VEIGA-FERNANDES, 2019). Este sistema é responsável pela percepção de estímulos do ambiente e internos do próprio indivíduo. Os corpos dos neurônios estão localizados nos gânglios da raiz dorsal (GRDs) e gânglio trigêmeo e são responsáveis pelas percepções de toque, térmicos, propriocepção, coceira e dor, sendo o nociceptor o neurônio primário responsável pela percepção dos estímulos nocivos, como térmicos, mecânicos, e inflamatórios (BASBAUM; BAUTISTA; SCHERRER; JULIUS, 2009). O nociceptor possui vesículas densas contendo neuropeptídeos que se localizam não somente na terminação nervosa central, mas também na terminação nervosa periférica. Portanto frente a uma injúria periférica o nociceptor responde liberando neuropeptídeos no sentido ortodrômico, ou seja, liberação de neuropeptídeos no terminal nervoso central, para propagação do estímulo doloroso para o sistema nervoso central, ou no sentido antidrômico por meio do reflexo axonal liberando neuropeptídeos no terminal nervoso periférico modulando a resposta inflamatória contra o agente injuriante (PINHO-RIBEIRO; VERRI; CHIU, 2017). Estes neuropeptídeos modulam a resposta inflamatória, células imunes e causam inflamação neurogênica na periferia e também ativam células da glia residentes da medula espinal causando neuroinflamação (CHIU; VON HEHN; WOOLF, 2012; CHU; ARTIS; CHIU, 2020; PINHO-RIBEIRO; VERRI; CHIU, 2017; XANTHOS; SANDKUHLER, 2014).

A liberação de neuropeptídeos como peptídeo relacionado ao gene da calcitonina (CGRP) e substância P modularam a resposta imune e inflamatória local. A inflamação neurogênica mediada pelos neuropeptídeos tem ação no leito vascular, sobre as células endoteliais e musculatura vascular lisa (BRAIN; WILLIAMS, 1989; CHIU; VON HEHN; WOOLF, 2012; MCCORMACK; MAK; COUPE; BARNES, 1989; SARIA, 1984). CGRP induz vasodilatação e substância P aumenta a permeabilidade vascular o que contribuem para o extravasamento plasmática e edema tecidual (BRAIN; WILLIAMS, 1989; MCCORMACK; MAK; COUPE; BARNES, 1989; SARIA, 1984).

Com relação a modulação da resposta imune pelo sistema sensorial. A imunidade na pele contra *Candida albicans* é modulada pelo nociceptor, e a deleção do nociceptor reduz a produção de IL-23 pelas células dendríticas e IL-17 pelas células Tγδ. Desta maneira, a deleção do nociceptor reduz a proteção do hospedeiro contra a *C. albicans* por reduzir o eixo IL-23/IL-17. O tratamento local com CGRP restaura a defesa do hospedeiro contra *C. albicans* em camundongos que não possuem o nociceptor. De fato, o zymosan presente na parede celular fúngica ativa diretamente os neurônios sensorias. Portanto, o reconhecimento de PAMPs como o zymosan pelo sistema sensorial induz a liberação de CGRP pelo nociceptor e proteção contra micro-organismos comensais como a *C. albicans* pela indução do eixo IL-23/IL-17. (KASHEM; RIEDL; YAO; HONDA *et al.*, 2015). Por outro lado, na doença fascite necrosante, o *Streptococcus pyogenes* faz uso do circuito neuro-imune para induzir a sobrevivência bacteriana e manutenção do processo infeccioso. A estreptolisina liberada pelo *S. pyogenes* é reconhecida por neurônios $TRPV1^+$ e induz dor em camundongos. Em resposta a toxina bacteriana, o nociceptor libera CGRP na periferia que suprime o recrutamento de neutrófilos, o que inibe a morte e controle dos níveis do *S. pyogenes* por neutrófilos de humano e camundongo. O bloqueio da comunicação neuro-imune com toxina botulínica, ou o uso de um antagonista do receptor de CGRP melhora o desfecho da infecção reduzindo a dermonecrose no flanco do camundongo (PINHO-RIBEIRO; BADDAL; HAARSMA; O'SEAGHDHA *et al.*, 2018). Demonstrando assim que a resposta imune é modulada diretamente pelo nociceptor, o qual pode contribuir para o controle dos níveis de micro-organismos comensais ou até mesmo reduzir a resposta imune frente a uma infecção, e isso contribuir para o descontrole infeccioso. Desta maneira, essa interação é contexto específico, podendo variar conforme o micro-organismo e

fatores de virulência.

A neuroinflamação é acompanhada por exemplo de estados de dor crônica em que existe um aumento na excitabilidade do nociceptor e aumenta da entrada de informação dolorosa no corno dorsal da medula espinal (JI; XU; GAO, 2014; XANTHOS; SANDKUHLER, 2014). Nociceptor libera neurotransmissores e neuropeptídeos. Sendo os neuropeptídeos reconhecidos por modular a ativação de células da glia as quais tem importante papel na manutenção da sensibilização central na dor crônica e desempenham o papel imune na medula espinal (JI; NACKLEY; HUH; TERRANDO *et al.*, 2018; PINHO-RIBEIRO; VERRI; CHIU, 2017; XANTHOS; SANDKUHLER, 2014). Por exemplo, no modelo de AR induzida em ratos imunizados com colágeno, a liberação pelo nociceptor de CGRP no corno dorsal da medula espinal ativa a micróglia que auxilia na manutenção do processo doloroso crônico. O tratamento dos ratos com artrite com um antagonista de receptor de CGRP reduziu a ativação da micróglia e a hipersensibilidade mecânica (NIETO; CLARK; GRIST; CHAPMAN *et al.*, 2015). O CGRP também potencia o efeito do ATP em astrócitos de rato e diretamente ativa esta célula da glia. CGRP leva ativação da via de sinalizada da ERK em astrócitos e aumenta a expressão na medula espinal de citocinas como TNFα e IL-1β os quais participam na sensibilização central na medula espinal (LAZAR; REDDINGTON; STREIT; RAIVICH *et al.*, 1991; PRILLER; REDDINGTON; HAAS; KREUTZBERG, 1998; SVENSSON; BRODIN, 2010; WANG; MA; CHABOT; QUIRION, 2009). De fato, o bloqueio da ativação de células da glia, ou de citocinas TNFα e IL-1β na medula espinal reduz o comportamento nociceptivo de camundongo com artrite induzida pelo desafio com o antígeno em camundongos imunizados (QUADROS; PINTO; FONSECA; KUSUDA *et al.*, 2015). Portanto o nociceptor tem importante papel na modulação da reposta imune tanto na periferia como no sistema nervoso central e isso tem direta relação com a modulação da percepção dolorosa.

1.4 ARTRITE

1.4.1 AR

AR é uma doença autoimune, com produção de autoanticorpos e associada com sintomas severos e sistêmicos (SMOLEN; ALETAHA; MCINNES, 2016). A deposição de complexos imunes na articulação induz inflamação que leva a um aumento no recrutamento de leucócitos, incluindo células imunes inatas como

macrófagos e neutrófilos, os quais contribuem para um microambiente inflamatório. As células da imunidade adaptativa do tipo Th1 bem como Th17 são essenciais no desenvolvimento e manutenção da AR (LEIPE; GRUNKE; DECHANT; REINDL *et al.*, 2010). Além da resposta imune adaptativa na AR, a contribuição de células relacionadas à resposta imune inata como macrófagos, mastócitos e neutrófilos, bem como o papel de receptores da imunidade inata como TLR, tem sido demonstrado em diversos estudos (BRENTANO; SCHORR; GAY; GAY *et al.*, 2005; GIERUT; PERLMAN; POPE, 2010). Portanto, a AR apresenta uma resposta imune complexa envolvendo tanto um componente da imunidade adaptativa, como participação do sistema imune inato.

Um dos modelos animais utilizados para estudar a AR, é o modelo de artrite induzida por antígeno (AIA). Este modelo consiste em imunizar o animal com três administração por via subcutânea no animal (7 dias entre cada inoculação) com uma emulsão contendo o antígeno mBSA (albumina de soro bovino metilada). No 21º dias após a primeira imunização o animal é desafiada com uma administração intra-articular do antígeno. Portanto este modelo induz uma resposta que se assemelha a da AR, entretando apenas na articulação desafiada. A indução da AIA induz uma reposta transiente que pode durar por semanas ou meses dependendo da retenção do antígeno. Neste modelo existe a ativação de sinoviócitos tipo- macrófagos, participação de células T e da imunidade adaptativa, produção de citocinas inflamatórias tais como TNFα, IL-1β, IL-33, IL-17, CXCL1 e CXCL2, quimioatração de neutrófilos, degradação de proteoglicanos da cartilagem e dor (BAS; SU; WIGERBLAD; SVENSSON, 2016; COELHO; PINHO; AMARAL; SACHS *et al.*, 2008; MCDOUGALL, 2006; VERRI; GUERRERO; FUKADA; VALERIO *et al.*, 2008; VERRI; SOUTO; VIEIRA; ALMEIDA *et al.*, 2010).

O processo doloroso de pacientes acometidos com a AR é complexo e de difícil controle. Pacientes relatam dor mesmo quando o processo inflamatório periférico está sob controle, sugerindo a participação da sensibilização central e alteração no processamento doloroso (LEE; CUI; LU; FRITS *et al.*, 2011; MCWILLIAMS; WALSH, 2017). O aumento da entrada da informação dolorosa da periferia no contexto da AR aumenta a liberação de CRGP na terminação nervosa central e contribui para a ativação das células da glia na artrite induzida pela imunização com colágeno em ratos. A administração intratecal de um antagonista de receptor de CGRP inibe a hipersensibilidade mecânica dos animais demonstrando

que a redução da entrada da informação dolorosa na medula espinal contribui para a redução do comportamento nociceptivo (NIETO; CLARK; GRIST; CHAPMAN *et al.*, 2015). Além disso, o desafio com mBSA leva a ativação de células da glia e neuroinflamação na medula espinal de camundongos imunizados. A inibição de astrócitos e micróglia, bem como as citocinas TNFα e IL-1β na medula espinal inibe o comportamento nociceptivo em camundongos, o que demonstra a contribuição da neuroinflamação e ativação de células da glia no contexto da AR e dor articular (QUADROS; PINTO; FONSECA; KUSUDA *et al.*, 2015).

A terapêutica no Brasil para o tratamento de pacientes com AR segundo a sociedade brasileira reumatologia em 2017 envolve três níveis de protocolos terapêuticos. O primeiro nível se inicia pelo uso de agentes modificadores de doenças reumáticas (DMARD) convencionais como metotrexato, sulfalazina, leflumide, ou drogas antimaláricas (hidroxicloroquina e cloroquina). Normalmente, deve ser feito o uso de DMARD convencionais se inicia com o metotrexato, e após 3-6 meses é feito a avaliação do paciente. Ocorrendo efeitos adversos ao medicamento nos 3 primeiros meses ocorrerá a substituição dentro dos fármacos DMARD convencionais. Caso a efetividade do tratamento ou objetivos terapêuticos não sejam atingidos em 6 meses será realizado a adição de mais um DMARD convencional ou a substituição por outro desta mesma classe. A segunda linha de escolha da terapêutica inclui o uso de um DMARD biológico como anti-TNF (adalimumab, certolizumab, golimumab, infliximab) ou moduladores da estimulação de linfócitos T (abatacept) ou bloqueador do receptor de IL-6 (tocilizumab). Preferencialmente, deve ser feito a associação do metotrexato ou outro DMARD convencional com o imunobiológico. Alternativamente, pode ser utilizado o DMARD alvo-específico tofacitinib associado ao metotrexato. Como terceiro nível terapêutico, ocorrerá a troca de classe dentro os DMARD biológico citados anteriormente ou ainda o anti-CD20 (rituximab), combinado com DMARD convencionais (preferencialmente metotrexato, não havendo efeitos adversos), ou o DMARD alvo-específico tofacitinib (inibidor da quinase Janus) associado o metotrexato. Não sendo atingido os objetivos terapêuticos, é realizada a trocado dentro das classes ainda não utilizadas dentro do terceiro nível terapêutico. Em qualquer fase do processo terapêutico poderá ser utilizado corticosteroides em doses baixas de forma sistêmica por curto período de tempo, ou aplicação local na articulação de corticoides ou anti-inflamatórios não esteroidais para auxiliar no controle de recidivas

inflamatórias. A complexidade do esquema terapêutico evidencia a complexidade da fisiopatologia da AR bem como a dificuldade no controle sintomatológico (MOTA; KAKEHASI; GOMIDES; DUARTE *et al.*, 2018). A terapêutica atual consegue controles razoáveis do processo inflamatório local comparado a décadas anteriores, pois atualmente o início do tratamento ocorre em fases iniciais da doença, e não se encontra com frequência pacientes acometidos com alterações anatômicas em decorrência do processo inflamatório crônico articular. Destaca-se como exemplo a deformidade de falanges conhecido como pescoço de cisne. Entretanto a dor ainda é destacado pelos pacientes mesmo sem inflamação articular ativa (LEE; CUI; LU; FRITS *et al.*, 2011; MINNOCK; FITZGERALD; BRESNIHAN, 2003; SHARIF; SHARIF; JUMAH; OSKOUIAN *et al.*, 2018). Portanto, o estudo de novas abordagens terapêuticas se faz necessário, em especial de moléculas que tenham a capacidade de modular o sistema imune a fim de promover a resolução da inflamação periférica, bem como modular o sistema somatossensorial reduzindo a ativação e atividade de nociceptores e a neuroinflamação a fim de reduzir o processo doloroso apresentado pelos pacientes com AR.

1.4.2 Artrite Relacionada A Implantes

Alterações morfológicas como a destruição superfícies de suporte de peso articular ocorrem devido ao processo inflamatório crônico. O procedimento cirúrgico de artroplastia faz a substituição articular por próteses, compreendendo desde de a troca total articular, ou seja substituição de ambas as cabeças articulares que que compõe a articulação; ou a troca parcial de apenas uma das cabeças ósseas por uma prótese (COBELLI; SCHARF; CRISI; HARDIN *et al.*, 2011). Pacientes em estágios avançados de AR, osteoartrite, fraturas e necrose avascular podem ser indicados a procedimentos de artroplastia de joelho e quadril, por exemplo (SIDDIQUI; YEO; SIVAIAH; CHIA *et al.*, 2012; SOEVER; MACKAY; SARYEDDINE; DAVIS *et al.*, 2010). Em 2010 aproximadamente 7 milhões de cidadãos dos EUA realizaram a substituição total do joelho ou quadril, e até 2030, aproximadamente 11 milhões de estadunidenses irão realizar a substituição do joelho ou quadril por uma prótese (MARADIT KREMERS; LARSON; CROWSON; KREMERS *et al.*, 2015).

Os materiais de implantes e próteses podem ser de aço inoxidável, liga metálica de cobalto, crômio e molibdênio, titânio e ligas metálicas de titânio (como titânio, alumínio e vanádio), polietileno e polimetilmetacrilato. Falhas

protéticas podem ocorrer, e em torno de 10-15% dos procedimentos de artroplastia falham, e a osteólise é um dos principais fatores que promovem isto (GOODMAN, 2007; HARRIS, 2001; LOONEY; SCHWARZ; BOYD; O'KEEFE, 2006; SARGEANT; GOSWAMI, 2006; SUNDFELDT; CARLSSON; JOHANSSON; THOMSEN *et al.*, 2006). Nanopartículas são liberadas pela prótese e induzem uma resposta inflamatória estéril (COBELLI; SCHARF; CRISI; HARDIN *et al.*, 2011). Os primeiros casos de ostéolise foram reportados na década de 70 em que partículas protéticas induziram a erosão óssea (HARRIS; SCHILLER; SCHOLLER; FREIBERG *et al.*, 1976). Óxidos metálicos, hidróxidos metálicos e fosfatos metálicos são as principais partículas provenientes do desgaste da prótese. As partículas metálicas (<50 nm) são marcadamente menores e numerosas comparando com as partículas de polietileno (>0,1 μm) (COBB; SCHMALZREID, 2006).

Macrófagos residentes são ativados e fagocitam as nanopartículas metálicas (ST PIERRE; CHAN; IWAKURA; AYERS *et al.*, 2010) e produzem mediadores inflamatórios como ligante do receptor ativador do NFκB (RANKL), TNFα, IL-1β e IL-6 bem como produção de espécies reativas de oxigênio. E levam a ativação de NFκB que atuará na manutenção do processo inflamatório asséptico no tecido periprotético (COBELLI; SCHARF; CRISI; HARDIN *et al.*, 2011). O aumento dos mediadores inflamatórios em especial RANKL, TNFα e IL-6 promovem a ativação de osteoclastos de maneira dependente ou independente do receptor ativador do NFκB (RANK), respectivamente. Ativação dos osteoclastos promoverá a reabsorção óssea e consequente progressão do processo de osteólise.(COBELLI; SCHARF; CRISI; HARDIN *et al.*, 2011; DANKS; KOMATSU; GUERRINI; SAWA *et al.*, 2016; O'BRIEN; FISSEL; MAEDA; YAN *et al.*, 2016). Portanto, o processo inflamatório crônico induzido pelas nanopartículas resultará na rejeição da prótese e um novo procedimento será necessário, o que pode não ser possível dependendo da condição de saúde e idade do paciente.

O dióxido de titânio (TiO_2) é usado na fabricação de próteses ortopédicas, pigmento de tintas, corante alimentar, protetor solar e cremes cosméticos (GURR; WANG; CHEN; JAN, 2005) As nanopartículas de TiO_2 acumulam-se em tecidos como pele, pulmão e tecido sinovial, apresentando-se como um pigmento preto depositado no tecido acompanhado de alterações teciduais como fibrose, necrose ou reação granulomatosa (MORAN; MULLICK; ISHAK;

JOHNSON *et al.*, 1991). Além disso, o TiO_2 pode causar danos ao material genético ao penetrar na pele e induzir dano oxidativo ao DNA, e ainda causar outros danos oxidativos aos tecidos e órgãos (CHEN; DONG; ZHAO; TANG, 2009; DUNFORD; SALINARO; CAI; SERPONE *et al.*, 1997; WANG; FAN; GAO; HU *et al.*, 2009). A quantidade e formato das partículas de TiO_2 são importantes para a magnitude da resposta inflamatória induzida pelo TiO_2 (BAISCH; CORSON; WADE-MERCER; GELEIN *et al.*, 2014; SILVA; TEESY; FRANZI; WEIR *et al.*, 2013).

Em um relato de um caso clínico, o paciente com um implante cervical de titânio e vanádio, e sem casos prévios de doenças reumáticas na família, desenvolveu artrite. E o desenvolvimento da artrite foi correlacionada com liberação de partículas metálicas provenientes do implante após meses de descontrole da doença. Macrófagos provenientes do sangue periférico do paciente reagiram com TiO_2 produzindo TNFα diferente de amostras controles de pacientes controle. Terapeuticamente, o paciente recebeu por 5 dias corticosteroide que promoveu a melhora parcial dos sintomas. Adicionalmente, usou-se paracetamol, anti-inflamatórios não-esteroidais como ibuprofeno, diclofenaco e celecoxib, e o DMARD metotrexato, que não foram capazes de controlar os sintomas. Por fim, usou-se a combinação de corticosteroide e leflumide e preveniu-se os sintomas, mas não a atividade da doença. Somente a retirada do implante metálico fez cessar o caso de artrite após 14 dias (DÖRNER; HAAS; LODDENKEMPER; VON BAEHR *et al.*, 2006). Este caso demonstra a capacidade das nanoparticulas metálicas migrarem pelo corpo e se acumulam em outros tecidos articulares promovendo artrite. Desta forma, nosso grupo de pesquisa padronizou a indução de artrite crônica com estímulo intra-articular com TiO_2. O TiO_2 induz hipersensibilidade mecânica, edema, estresse oxidativo, produção de IL-33, TNFα, IL-1β, e IL-6, ativação da via de sinalização RANKL/ receptor Ativador do Fator Nuclear κB (RANK). Neste contexto o TiO_2 induz a destruição da cartilagem, e aumento na reabsorção óssea e consequentemente destruição articular de camundongos expostos ao TiO_2 por 30 dias (BORGHI; MIZOKAMI; PINHO-RIBEIRO; FATTORI *et al.*, 2017; MANCHOPE; ARTERO; FATTORI; MIZOKAMI *et al.*, 2018). Portanto a artrite crônica induzido por TiO_2 é um modelo translacional que possibilita a compreensão dos mecanismos celulares e moleculares relacionado ao processo inflamatório asséptico mediado por partículas de TiO_2 liberadas no espaço periprotético, ou que se translocam pelo organismo, bem como avaliar abordagens terapêuticas que possam induzir a

resolução da inflamação e dor crônica induzida pelo TiO_2 no tecido articular.

1.5 RvD5

A RvD5 é membro da família das Rv da série D derivado do DHA e foi descrita por sinalizar no receptor acoplado a proteína G (GPCR) GPR32 (CHIANG; FREDMAN; BACKHED; OH *et al.*, 2012; SERHAN, 2014), e possui o epímero $RvD5_{n\text{-}3DPA}$ derivado do ácido 3-docosapentanóico (3-DPA) que sinaliza nos GPCR GPR101 e GPR32 (FLAK; KOENIS; SOBRINO; SMITH *et al.*, 2020). Portanto, é razoável que a RvD5 também sinalize no GPR101 uma vez que é um epímero da $RvD5_{n\text{-}3DPA.}$ Similarmente como ocorre com a LXA_4 e seu epímero 15-epi-LXA_4 que agem no recepto FPR2 (TYLEK; TROJAN; REGULSKA; LACIVITA *et al.*, 2021).

Durante o processo resolutivo, existe a produção de RvD5 em níveis superiores a outros SPMs. Na peritonite induzida por tioglicolato em camundongos a RvD5 foi detectada no exsudato peritoneal após 4h, com pico de produção em 24h, e manteve-se nesse nível por até 120h após o estímulo. Outras moléculas derivadas do DHA como RvD2, RvD5, e MaR1 foram produzidas de forma transiente após estímulo com tioglicolato, sendo a RvD5 a única a ser produzida continuamente. Além disso a produção de SPMs é dependente do tipo de estímulo, uma vez comparando animais estimulados com tioglicolato ou zymosan, observou-se que os níveis de RvD5 no exsudato peritoneal são superiores no grupo tioglicolato comparado ao grupo estimulado com zymosan após 72h (LASTRUCCI; BAILLIF; BEHAR; AL SAATI *et al.*, 2015). Jordan e colaboradores evidenciaram o efeito do *Staphylococcus aureus* em macrófagos humanos polarizados em M1 ou M2, e observou que o agente infeccioso induziu rápida resposta com produção dos mediadores lipídicos pró-inflamatórios LTB_4 e PGE_2 nos macrófagos polarizados em M1, mas sem a produção de SPMs. O macrófago polarizado em M2 produziu, de forma lenta, porém, potente os SPMs. Em especial, a RvD5 foi produzida em níveis elevados quando comparados a RvD1 e RvD2 neste contexto de infecção por *S. aureus* de macrófagos humanos polarizados em M2. O que demonstra que a RvD5 é produzida por macrófagos do tipo M2 frente a um estímulo infeccioso (JORDAN; GERSTMEIER; PACE; BILANCIA *et al.*, 2020). Demonstrando que existe diferenças na resposta resolutiva comparando um processo não infeccioso e infeccioso, mas os níveis de RvD5 ainda são superiores independente do contexto infeccioso ou não.

A respeito das ações resolutivas da RvD5, a $RvD5_{n-3\ DPA}$ inibe a quimoatração de neutrófilos ao gradiente de LTB_4, e a diapedese frente a uma monocamada endotelial, e induz a eferocitose de corpos apoptóticos por macrófagos *in vitro* via sinalização no receptor GRP101 (FLAK; KOENIS; SOBRINO; SMITH *et al.*, 2020). Já *in vivo* a $RvD5_{n-3\ DPA}$ inibe o edema articular, score clínico produção de LTB_4 e PGE_2 na artrite causada pelo estímulo com soro artritogênico K/BxN em camundongo (FLAK; KOENIS; SOBRINO; SMITH *et al.*, 2020). Estas ações *in vivo* também foram pela a ação no GRP101, uma vez que o *knockdown* deste receptor inibiu as ações da $RvD5_{n-3\ DPA}$ na artrite induzida pelo soro artritogênico (FLAK; KOENIS; SOBRINO; SMITH *et al.*, 2020). Além disso, a RvD5 modula a diferenciação de células T efetoras. Por exemplo, RvD5 inibiu a diferenciação de células $Ror\gamma t^+$ Th17, quando cultivadas em meio propício para se diferenciarem em Th17, e ainda aumentou a população de células $Foxp3^+$ Tregs, sendo que na concentração de 500 nM a inibição da população $Ror\gamma t^+$ Th17 foi de 66% (YAMADA; SAEGUSA; SENDO; UEDA *et al.*, 2021). Sugerindo assim que a RvD5 é uma abordagem interessante no contexto da AR.

A RvD5 tem efeito analgésico na dor neuropática induzida pelo paclitaxel e inibe a segunda fase da formalina, mas não a primeira fase, sugerindo que suas ações modulam o sistema somatossensorial por inibir a dor neuropática induzida pelo paclitaxel (LUO; GU; TAO; SERHAN *et al.*, 2019), mas não tem sua ação via a inibição de canal de potencial transitório anquirina 1 (TRPA1) uma vez que não inibiu a primeira fase da formalina que induz comportamentos nociceptivos via ativação do TRPA1 (MCNAMARA; MANDEL-BREHM; BAUTISTA; SIEMENS *et al.*, 2007). Ainda sugere que a RvD5 tem ações relacionadas a inibir a dor de origem inflamatória, uma vez que inibiu a segunda fase da formalina que é de origem inflamatória (LUO; GU; TAO; SERHAN *et al.*, 2019). Portanto, a RvD5 tem papel importante na resolução do processo inflamatório e doloroso e estes achados demonstram que a RvD5 é uma abordagem interessante no contexto da dor articular por inibir a produção de mediadores lipídicos inflamatórios, o quimioatração de neutrófilos, e ainda no contexto de doenças autoimunes modula a diferenciação de células T auxiliares e induz efeitos analgésico. Assim este trabalho avança na avaliação dos efeitos e mecanismos da RvD5 na dor articular envolvendo um modelo de AR induzido pelo desafio com antígeno em animais imunizados, e outro de artrite crônica induzido por TiO_2.

2 OBJETIVOS

2.1 OBJETIVO GERAL

Avaliar o efeito analgésico, resolutivo e os mecanismos de ação da RvD5 na dor articular por meio de dois modelos murinos de artrite: AR induzida por desafio com antígeno em animais imunizados, e artrite crônica induzida por estímulo i.a. com TiO_2.

2.1.1 Objetivos Específicos Do Modelo De AR

- Avaliar o efeito analgésico e anti-edematogênico da RvD5 na AIA no protocolo agudo e protocolo prolongado;
- Avaliar o efeito da RvD5 no infiltrado neutrofílico na AIA;
- Avaliar o efeito da RvD5 na ativação neuronal por imageamento de cálcio com neurônios do GRD e expressão de canais iônicos no GRD de animais com AIA após 24h do desafio com mBSA;
- Avaliar o efeito da RvD5 nos níveis de CGRP, p-NFκB, e a porcentagem de p-NFκB em neurônios $CGRP^+$ no GRD de animais com AIA 9h após o desafio com mBSA;
- Avaliar o efeito da RvD5 na expressão de RNAm de marcadores de células da glia [proteína ácida fibrilar glial (GFAP), fator de transcrição de oligodendrócitos (olig-2), molécula adaptadora ionizada de ligação ao cálcio 1 (Iba-1), CX_3CR_1] na medula espinal de animais com AIA 9h após o estimulo com mBSA;
- Avaliar o efeito da RvD5 na expressão de RNAm do receptor ST2, IL-33, TNFα, pro-IL-1β, IL-10 na medula espinal de animais com AIA 9h após o estimulo com mBSA.

2.1.2 Objetivos Específicos Do Modelo De Artrite Crônica

- Avaliar o efeito analgésico na hipersensibilidade mecânica, hipersensibilidade térmica, distribuição estática do peso corpóreo nas patas traseiras, e efeito anti-edematogênico na artrite crônica induzida por TiO_2;
- Avaliar o efeito da RvD5 no dano histopatológico e infiltrado leucocitário na artrite crônica induzida por TiO_2;

- Avaliar o efeito da RvD5 na expressão de RNAm para TNFα e pró-IL-1β na artrite crônica induzida pelo TiO_2;
- Avaliar o efeito da RvD5 na produção das citocinas TNFα e IL-1β *in vitro* em macrófagos derivados da medula óssea primados com LPS e estimulados com TiO_2;
- Avaliar o efeito da RvD5 na ativação do NFκB *in vitro* em macrófagos derivados da medula óssea primados e estimulados com TiO_2;
- Avaliar o efeito citotóxico da RvD5 *in vitro* pela liberação da enzima lactato desidrogenase (LDH) em macrófagos derivados da medula óssea primados e estimulados com TiO_2;
- Avaliar o efeito da RvD5 no estresse oxidativo na artrite crônica induzida pelo TiO_2.

3.ARTIGO A SER SUBMETIDO NO NEUROPHARMACOLOGY

O presente trabalho foi realizado no Laboratório de Dor, Inflamação Neuropatia e Câncer, da Universidade Estadual de Londrina e no McNaughton Lab no King's College London e segue as normas da revista Neuropharmacology. Os resultados parciais estão descritos no artigo intitulado: "Resolvin D5 ameliorates arthritic pain related to rheumatoid arthritis resolving inflammation, targeting the sensorial system: primary neurons and glial cells".

Resolvin D5 ameliorates arthritic pain related to rheumatoid arthritis resolving inflammation, targeting the sensorial system: primary neurons and glial cells

Marília F. Manchope[1], Santos-Saraiva T.[1], Ferraz C.R.[1], Pinto, L.G.[2], Zaninelli T.H.[1], McNaughton P.[2], Casagrande, R[3], Verri W.A.[1]

[1] Laboratory of Pain, Inflammation, Neuropathy, and Cancer, Department of Pathology, Londrina State University, Londrina, Paraná, Brazil

[2] Wolfson Centre for Age-Related Diseases, King's College London, Guy's Campus, London Bridge, London, SE1 1UL, UK.

[3] Laboratory of Oxidative Stress and Inflammation, Department of Pharmaceutical Sciences, Londrina State University, Londrina, PR, Brazil

Highlights

- RvD5 accelerated neutrophilic flare resolution in mBSA-induced arthritis in immunized animals
- RvD5 reduced primary neurons activation in arthritic animals
- RvD5 reduced CGRP levels in DRGs neurons induced by mBSA challenge in immunized animals
- RvD5 inhibited neuroinflammation in the spinal after mBSA-induced arthritis in immunized animals

Abstract

In rheumatoid arthritis, pain is the main symptom reported by patients, even with synovitis under control and no sign of inflammation in the joints the pain remains. This demonstrates the complexity of rheumatoid arthritis chronic pain which involves a peripheral inflammatory pain input, changes into the sensorial system at the dorsal root ganglion (DRG) and spinal cord levels. Resolutive mediators have been described as having potent analgesic properties, especially in conditions related to neurogenic inflammation and neuroinflammation. Herein, we assessed the analgesic and resolutive activities of Resolvin (Rv) D5 in a monoarthritis model of rheumatoid arthritis induced by methylated bovine serum albumin (mBSA) challenge in immunized animals. RvD5 induced analgesia, and reduced oedema, and resolved the neutrophilic accumulation in the synovial cavity. In addition, RvD5 targeted the DRG by reducing primary neuronal activation in arthritic mice, calcitonin gene-related peptide (CGRP) levels, and phosphorylated nuclear factor κB (p-NFκB) increase in $CGRP^+$ neurons. In the spinal cord, RvD5 inhibited neuroinflammation by reducing glial cells activation and mRNA expression of *ST2*, *IL-33*, *TNFα*, and *pro-IL-1β*. Thus, RvD5 ameliorates arthritic pain in rheumatoid arthritis resolving the neutrophilic flare-up, and more importantly targeting sensorial systems: primary neuron and glial cells in the spinal cord.

Keywords: resolution, specialized pro-resolution mediator, CGRP, neuroinflammation, glial cells.

1. Introduction

Arthritic pain is the main symptom reported by patients with rheumatoid arthritis. It is noteworthy that arthritic chronic pain persists even when the inflammatory flare-up is under control, and there is no sign of inflammation, demonstrating the complexity regarding pain in rheumatoid arthritis (Lee et al., 2011; Minnock et al., 2003).

Inflammatory pain occurs during the flaring up of rheumatoid arthritis with an increase in neutrophils influx into the joint in an IL-33- and IL-17-dependent manner in the monoarthritis model induced by mBSA challenge in immunized animals (Pinto et al., 2010; Verri et al., 2008; Verri et al., 2010). Sinoviocytes and recruited cells contribute to the inflammatory pain by releasing inflammatory cytokines and lipids such as TNFα, IL-1β, PGE_2 (Pinto et al., 2010; Verri et al., 2008; Verri et al., 2010). The neutrophilic flare in mBSA antigen challenge is autoresolutive (Barroso et al., 2017) but with a long-lasting nociceptive behaviour-related, which resembles patients with no sign of synovitis but with pain still being reported as a symptom (Lee et al., 2011; Minnock et al., 2003).

Joints are innervated by sensory fibber and have a plethora of receptors and ion channels responsible for sensing the microenvironment around the peripheral ending (Donaldson, 2009; Pinho-Ribeiro et al., 2017). The inflammatory milieu produced during the synovitis flare-up in rheumatoid arthritis sensitizes the sensorial neuron reducing the activation threshold, increasing pain sensation (Donaldson, 2009; Pinho-Ribeiro et al., 2017). Primary sensory neuron conducts the painful input to the dorsal horn of the spinal cord in an orthodromic manner releasing *e.g.,* CGRP which contributes to neuroinflammation in the spinal cord in arthritic conditions (Nieto et al., 2015). On the other hand, the sensorial neuron can respond in an antidromic manner releasing neuropeptides into the periphery causing neurogenic inflammation. CGRP released at peripheral tissue increases vasodilatation and blood flow (Brain et al., 1985) and acts synergically with IL-1β potentiating oedema and neutrophil recruitment (Buckley et al., 1991). Of note, CGRP is upregulated in synovial fluid (Appelgren et al., 1995; Larsson et al., 1991), suggesting that the neuropeptide is being released into the joint.

Neuroinflammation is present in chronic pain due to increased nociceptive input into the sensorial system leading to glial cells activation (Xanthos and Sandkuhler, 2014). mBSA-induced rheumatoid arthritis leads to glial cells activation

with increased TNFα and IL-1β production in the spinal cord (Quadros et al., 2015). Specialized pro-resolving mediators are already known to induce pain resolution with long-lasting action. For instance, MaR1 analgesic activity lasted up to 5 days, reducing neuronal activation and neuroinflammation in CFA-induced inflammatory pain (Fattori et al., 2019). RvD5 inhibits chemotherapy-induced-neuropathic pain (Luo et al., 2019). $RvD5_{n\text{-}3\ DPA}$ improves arthritogenic serum-induced arthritis reducing oedema, and PGE_2 and LTB_4 inflammatory lipids release (Flak et al., 2020) which leads to neuronal sensitization and neutrophil recruitment, respectively (Verri et al., 2006). Herein, we evaluated the analgesic and resolutive activities of RvD5 in the monoarthritis model induced by mBSA challenge of immunized animals by demonstrating a decrease in the neutrophilic flare-up and activation of the sensorial system focusing on the primary neurons in the DRGs and glial cells in the spinal cord.

2. Materials and Methods

2.1. Animals

Animal care and handling procedures followed the International Association for Study of Pain (IASP) guidelines and the Animals (Scientific Procedures) Act 1986. This study was approved by the Londrina State University Ethics Committee on Animal Research and Welfare (process number 16567.2019.51) and experiments conducted in the UK were approved under the project license PB1C5C31C by King's College London Animal Welfare and Ethical Review Body and Home office. Male C57BL/6 (20-30g, 7-9 weeks old) were provided from Charles River (UK) or Londrina State University. Mice were housed in standard clear plastic cages with water and food *ad libitum*, light/dark cycle of 12/12 h, and controlled temperature (21 °C) at the biological services unit in New Hunt's House, King's College London or vivarium from the Department of Pathology in Londrina State University for at least 7 days before experiments. Behavioural assessments were conducted between 9 am to 5 pm.

2.2. Immunization and antigen challenging protocols

Mice were immunized on day zero and boosted on days 7^{th} and 14^{th} with 500 µg of methylated serum albumin bovine (mBSA – Sigma-Aldrich, St. Louis, MO) diluted in 100 µL of CFA (1^{st} immunization – Santa Cruz Biotechnology, Inc.) or IFA (1^{st} and 2^{nd} boost – Santa Cruz Biotechnology, Inc.) emulsified with 100 µL of sterile saline in

glass syringes connected with a three-way stopcock. Mice received 200 µL of emulsion for each immunization or boost procedure. To induce the acute protocol, mice were challenged with 100 µg of mBSA diluted in 10 µL in the knee on the 21st day. For the chronic protocol, a re-challenge was made 120 h after the 1st challenge.

2.3. Experimental Design

Herein 2 arthritic protocols were used to assess the ability of RvD5 to ameliorate rheumatoid arthritis. First, the acute protocol was used to assess Rvd5 analgesic and resolutive activity in a rheumatoid arthritis model and to investigate the underlying mechanism. Mice were treated with RvD5 [3, 10, and 30 ng, intraperitoneal (i.p.), 30 min before antigen challenge] (#10007280; Cayman Chemical, Michigan, USA). Mechanical hypersensitivity was evaluated 1, 3, 5, 7, and 24h, and oedema 7 and 24h after antigen challenge. Neutrophils were counted and their levels in the synovial cavity were used to quantify the resolution indices 9, 12, 24, and 48h after antigen challenge. DRGs neurons from the L4, L5, and L6 segments were used to evaluate neuronal activation through calcium flux and *TRPV1* mRNA expression in arthritic mice 24h after antigen challenge. CGRP levels and p-NFκB activation in $CGRP^+$ neurons were assessed 9h after antigen challenge in DRGs primary neurons. Glial cells activation at L4, L5, and L6 spinal cord segments were evaluated by mRNA expression (*GFAP*, *Olig-2*, CX_3CR_1, and *Iba-1* 9h after antigen challenge). Also, *ST2*, *IL-33*, *TNFα*, and *pro-IL-1β* mRNA expression were assessed 9h after antigen challenge in the spinal cord. For the chronic protocol, 2 challenges were made 120 h apart from each other in the mice. Animals were assessed for mechanical hypersensitivity and oedema between 0-240 h after 1st antigen challenge, and mice were pre-treated 30 minutes before the 1st challenge and after every 48h.

2.4. Mechanical hypersensitivity

Mice were acclimatized to the room and apparatus (plexiglass chamber and wire grid) at least 3 times for 1h and before measurement for a 30 min minimum. A blind experimenter for the treatments stimulated the hind paw with a logarithmic series of von Frey monofilaments using the up-and-down method (1.4g – 0.008g). Briefly, mechanical hypersensitivity was assessed by measuring the mechanical threshold which was considered as the lowest force needed to observe a hind paw flinch. The nociceptive assessment started with the intermediate filament of 0.4 g and going up

for the 0.6g if the mice did have not a nociceptive behaviour (Chaplan et al., 1994) or going down to 0.16 g whether mice had a nociceptive behaviour. The lowest filament was able to elicit a nociceptive behaviour was considered as the mechanical threshold. Results were expressed as the log of the mechanical threshold in mg (Sant'Anna et al., 2016)

2.5. Oedema

Mice transversal and lateral knee thickness were measured using a digital caliper (Duratool – UK) before, 7h, and 24h after antigen challenge. The knee circumference was determined as the average between transversal and lateral knee thickness multiplied by 3.14. Oedema was expressed as the variance between the knee circumference between the time point by the baseline measurement.

2.6. Leukocytes recruitment

Mice synovial cavity was washed 3 times with 3.33 µL of 2mM EDTA containing 0.5% of BSA. The recovered leukocyte suspension was diluted 1:1 with Turkey's solution and counted using a hemocytometer. The remaining leukocyte suspension was cytocentrifuged in a cytospin at 500 rpm for 5 minutes and proceed for differential counting of neutrophils and mononuclear cells after Diff-Quick staining (Fast Panotico, Labonclin – Brazil). The resolution index was determined as previously described (Serhan et al., 2008): a) Magnitude as the time after antigen challenge (T_{max}) when neutrophils reach the maximum number (Ψ_{max}); b) Duration (T_{50}) as the time after antigen challenge when the neutrophil numbers reduce to 50% of Ψ_{max}; c) Resolution Interval (Ri) as the time interval between T_{max} and T_{50}.

2.7. Calcium imaging

Calcium imaging was performed as described previously (Fattori et al., 2019). DRG neurons from the segments L4, L5, and L6 were dissected into Neurobasal-A medium (NBM – Life Technologies, Thermo Fisher Scientific), dissociated in HEPES-buffered saline (MilliporeSigma) containing collagenase A (1 mg/mL) and dispase II (2.4 U/mL RocheApplied Sciences, Indianapolis, IN, USA) for 15 minutes at 37ºC. Mechanical dissociation was also made using glass Pasteur pipettes of decreasing size. Dissociated neurons were centrifuged against a 10% BSA gradient and plated on laminin-coated cell culture dishes. DRG neurons were loaded with 1.2 µM of Fluo-

4AM in NBM for 40 minutes for 37º C, washed with HBSS, and imaged in a confocal microscope (TCS SP8, Leica Microsystems). To evaluate TRPV1 activation, neurons were recorded for 6 minutes, which was divided into 2 minutes of baseline reading (0-s mark), followed by 1 µM Capsaicin stimulation for 2 minutes (120-s mark), and for the last 40 mM of KCl stimulation for 2 minutes (240-s mark) to activate all neurons. Calcium flux was assessed from the mean fluorescence measured with the LAS X software (Leica Microsystems).

2.8. RT-qPCR

DRG or spinal cord from the segments L4, L5, and L6 were dissected into TRIzol™ reagent, and total RNA was isolated following the manufacturer's instructions. The purity of total RNA was measured with a spectrophotometer, and the wavelength absorption ratio (260/280 nm) was between 1.8 and 2.0 for all preparations. Reverse transcription of total RNA to cDNA and qPCR were performed using GoTaq® 2-Step RT-qPCR System (Promega, Madison, WI, USA) on a StepOnePlus™ Real-Time PCR System (Applied Biosystems®, Thermo Fisher Scientific, Waltham, MA, USA). The relative gene expression was determined using the comparative $2^{-(\Delta\Delta Ct)}$ method. The primers sequence used in this study were *Trpv1* sense: 5′-TTC CTG CAG AAG AGC AAG AAGC-3′, antisense: 5′- GTG TGC ATG ACC CGA ACT GAT-3′; *Na_V1.8* sense: 5′-GTG TGC ATG ACC CGA ACT GAT-3′, antisense: 5′-CAA AAC CCT CTT GCC AGT ATCT-3′; *Gfap* sense: 5′-GGC GCT CAA TGC TGG CTT CA-3′, antisense: 5′-TCT GCC TCC AGC CTC AGG TT-3′; *Iba-1* sense: 5′-ATG GAG TTT GAT CTG AAT GGA AAT-3′, antisense: 5′-TCA GGG CAG CTC GGA GAT AGC TTT-3′; *ST2* sense:5'-GCA ATT CTG ACA CTT CCC ATG-3', antisense: 5'-ACG ATT TAC TGC CCT CCG TA-3'; *IL-33* sense: 5'-TCC TTG CTT GGC AGT ATC CA-3', antisense: 5'-TGC TCA ATG TGT CAA CAG ACG-3'; *TNFα*, sense: 5′-TCT CAT CAG TTC TAT GGC CC-3′, antisense: 5′-GGG AGT AGA CAA GGT ACAAC-3′; *pro-IL-1β*, sense: 5-′GAA ATG CCA CCT TTT GAC AGTG-3′, antisense: 5′-TGG ATG CTC TCA TCA GGA CAG-3′; *GAPDH* sense: 5′-CAT ACC AGG AAA TGA GCT TG-3′, antisense: 5′-ATG ACA TCA AGA AGG TGG TG-3′; The expression of *GAPDH* mRNA was used as a reference gene to normalise data.

2.9. Immunofluorescence

Animals were terminally anesthetized (isoflurane 5%) and perfused with saline followed by 4% paraformaldehyde through the ascending aorta. DRGs were dissected, post-fixed for 24h, and dehydrated overnight with 30% sucrose. Tissues were embedded in optimum cutting temperature, and 15 µm sections were cut in a cryostat and proceeded for immunofluorescence assay. Sections were blocked with 3% BSA and then incubated with primary antibodies overnight followed by secondary antibody for 1h. DRGs were stained for CGRP (C8198, Sigma-Aldrich) followed by Alexa Fluor 488 (#A-11008, Invitrogen), p-NFκB p65 [p-NFκB p65 (27.Ser 536): sc-136548, Santa Cruz Biotechnology, INC], followed by Alexa fluor 647 (# A-21240, Invitrogen). The image acquisition and analysis were performed using a Confocal Microscope (TCS SP8, Leica Microsystems, Mannheim, Germany).

2.10. Statistical analysis

The results are presented as means ± SEM of measurements made on six mice in each group per experiment and are representative of two separate experiments. Two-way repeated-measures analysis of variance (ANOVA) followed by Tukey's post hoc was used to compare all groups and doses at all times when responses were measured at different times after the antigen challenge in mechanical hypersensitivity and oedema. Two-way ANOVA followed by Tukey's post hoc was used to compare all groups in the leukocyte recruitment evaluated at different times. Differences between responses were evaluated by one-way ANOVA followed by Tukey's post hoc for data of a single time point. Statistical differences were considered significant when $p < 0.05$.

3. Results

3.1. RvD5 inhibits mechanical hypersensitivity and oedema and accelerates neutrophilic resolution in antigen-induced arthritis (acute protocol)

In the first set of experiments, the analgesic and anti-edematogenic activity of dose-response curve of RvD5 (3, 10, and 30 ng/animal, i.p.) were assessed over 24h after the antigen challenge. Mechanical hypersensitivity was inhibited with all doses tested at 1, 3, 5, 7, and 24 h after the challenge. The dose of 10 ng had a

superior analgesic effect at the end of the 24 h when compared to 3 and 30 ng doses (Fig. 1a). Oedema was assessed 7 and 24 h and all doses inhibited knee oedema without any difference in anti-oedematogenic activity among the doses (Fig 1b). The dose of 10 ng was chosen for the following experiments once it had a superior analgesic effect compared to the other doses tested here. RvD5 ability to induce neutrophilic resolution was assessed through the resolutive indices ψ_{max}, T_{max}, T_{50}, and R_i 9 – 48 h after antigen challenge. RvD5 decreased the ψ_{max} of neutrophils accumulation in the synovial cavity without changing the T_{max} to neutrophils accumulated at the synovial cavity. In addition, RvD5 decreased the T_{50} from 23h to 15h, thus shortening the R_i from 11h to 3h (Fig 1c). Demonstrating though that RvD5 induces analgesia, decreases edema, and accelerates the neutrophilic resolution in antigen-induced arthritis.

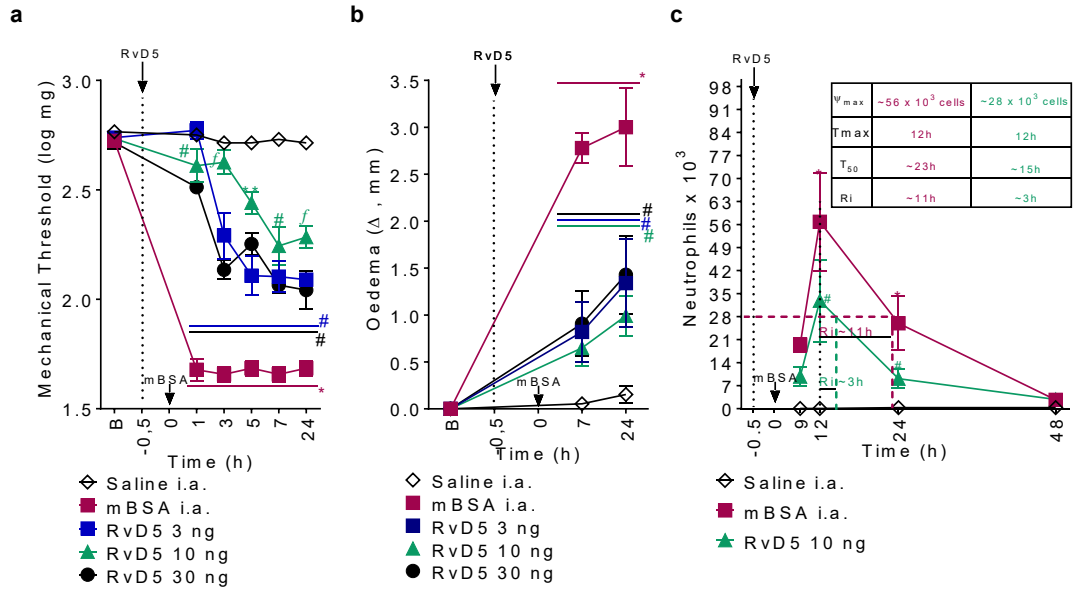

Fig. 1. RvD5 inhibits mechanical hypersensitivity and oedema and accelerates neutrophilic flare-up resolution induced by mBSA challenge in immunized animals. Immunized mice were treated with RvD5 (3, 10, 30 ng/animal, i.p.) and 30 minutes after challenge with 100 µg mBSA. Mechanical hypersensitivity was evaluated 1-24 (a), oedema 7 and 24h, and (c) resolution indices 9, 12, 24, and 48h after mBSA challenge. Results are presented as mean ± SEM of six mice per group per experiment and are representative of two separate experiments. [$^{*}p < 0.05$ compared to the saline group; #$p < 0.05$ compared to the mBSA group; $^{**}p < 0.05$ compared mBSA and 3ng dose;

[$^{f}p < 0.05$ compared mBSA and 3 and 30 ng doses.]

3.2. RvD5 inhibits mechanical hypersensitivity and oedema in antigen-induced arthritis chronic protocol

Aiming to evaluate whether the RvD5 has analgesic and anti-oedematogenic effects in a prolonged protocol of antigen-induced arthritis mechanical hypersensitivity and oedema, these parameters were assessed up to 240h after the 1st challenge. The animals were submitted to a 2nd challenge 120h after the 1st challenge. RvD5 presented an analgesic effect that had a 48h duration (data not shown), thus the treatment was performed every 48h. RvD5 inhibited mechanical hypersensitivity (Fig. 2a) and oedema (Fig. 2b) in all-time points evaluated. Demonstrating that RvD5 induces analgesia and anti-oedematogenic effects under a prolonged protocol involving two antigens challenges.

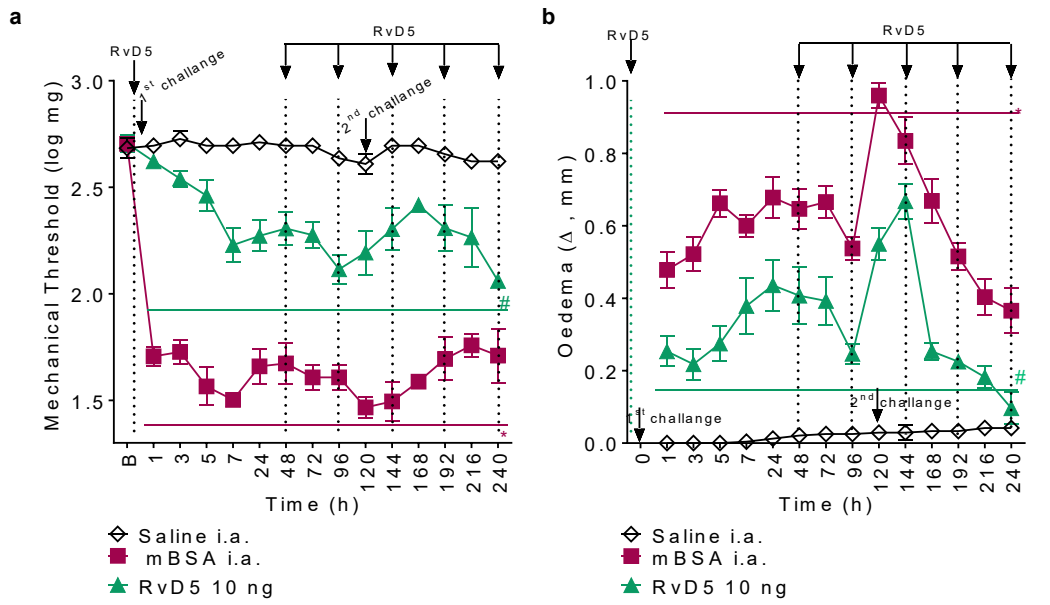

Fig. 2. RvD5 inhibits mechanical hypersensitivity and oedema in a chronic protocol induced by two challenges with mBSA 120h apart of each other in immunized mice. Immunized mice were treated with RvD5 (10 ng/animal, i.p.) 30 minutes after being challenged with 100 µg mBSA. RvD5 treatment was repeated every other 48h. 2nd challenge was performed 120 h after the first one. Mechanical hypersensitivity (a) and oedema (b) were evaluated up to 240h after mBSA 1st challenge. Results are presented as mean ± SEM of six mice per group per experiment and are representative of two separate experiments.

[$^{*}p < 0.05$ compared to the saline group; $^{\#}p < 0.05$ compared to the mBSA group.]

3.3. RvD5 reduces calcium influx and *TRVP1* and *Na_V 1.8* mRNA expression in DRG neurons 24 h after antigen-induced arthritis

Neuronal activity is increased in painful conditions such as rheumatoid arthritis (Pinho-Ribeiro et al., 2017), thus we wondered whether RvD5 would reduce neuronal activity. Calcium influx was used to assess changes in neuronal response to capsaicin in DRG neurons from arthritic mice 24h after antigen-induced arthritis. The neuronal basal activity was increased in animals challenged with mBSA (Fig 3 a-c). RvD5 reduced both baseline neuronal activity and the response to capsaicin in DRG neurons from arthritic mice (Fig 3 a-c). In agreement, RvD5 inhibits the mRNA expression of *TRPV1* (Fig 3d) and *Na_V 1.8* (Fig 3 e) induced by antigen-induced arthritis. Suggesting that RvD5 reduces neuronal activity by decreasing channels related to pain activation and sensitization (Pinho-Ribeiro et al., 2017).

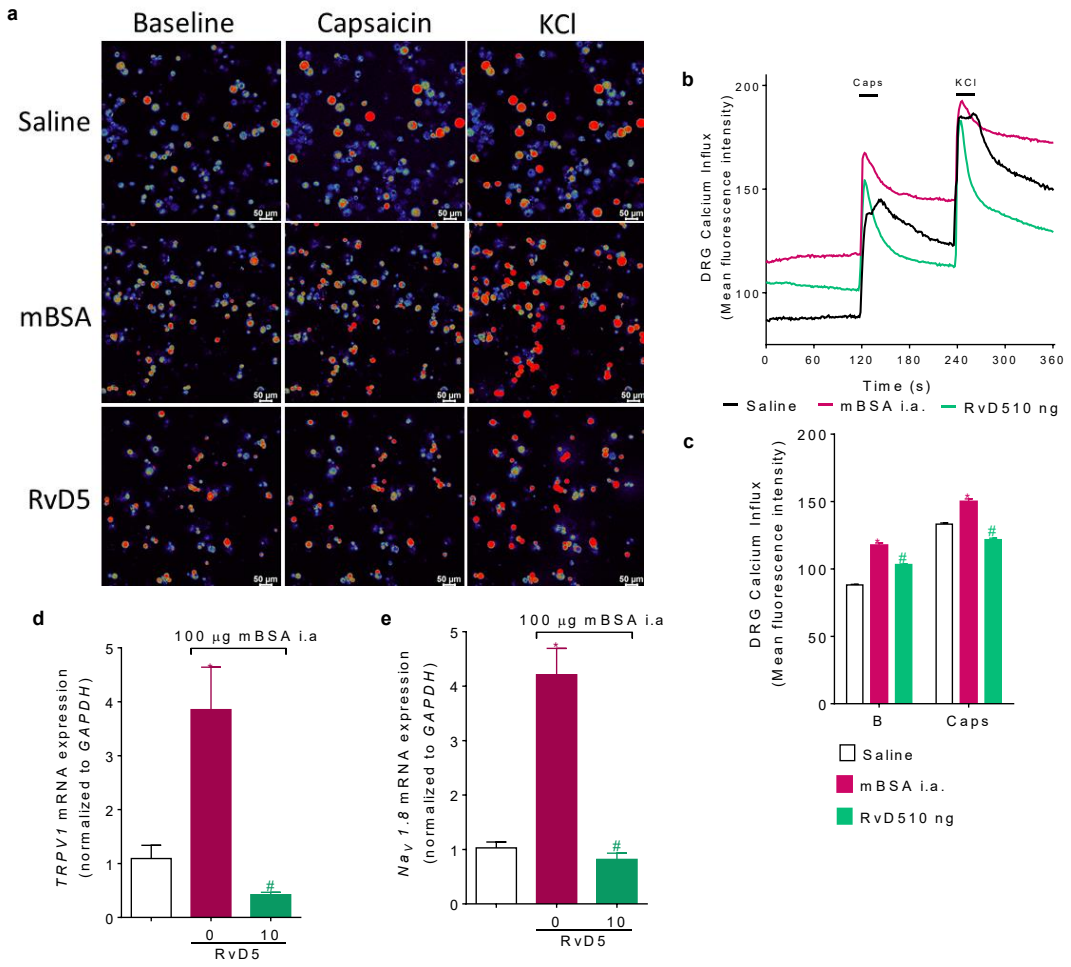

Fig. 3. RvD5 reduces antigen-induced DRG primary neuron activation. Mice were treated with RvD5 (10ng, i.p.) and after 30 minutes arthritis was induced by mBSA challenge in immunized animals. After 24h, DRGs were collected for calcium imaging (a-c) or RT-qPCR (d-e). (a) Representative fields of DRG neurons were dissected from mice challenged with saline, mice challenged with mBSA, or treated with RvD5 and challenged with mBSA. Baseline mean fluorescence intensity (0-120s – first column), mean fluorescence intensity after capsaicin (120-240s – second column), and after KCl control (240-360s – third column). (b) mean fluorescence intensity traces of calcium influx throughout the 360s of recording. (c) Mean fluorescence intensity of calcium influx of the baseline, and that following the stimulus with capsaicin. mRNA expression was evaluated with RT-qPCR for *Trpv1* (d) Nav1.8 (e) in the DRG neurons. Results are expressed as mean ± SEM, n = 2 DRG plates (each plate is a neuronal culture pooled from six mice) per group. RT-qPCR used n =

6 DRG per group per experiment. Data is the representative of two independent experiments [*P < 0.05 compare to saline, #P < 0.05 compared to mBSA group. Scale bar: 50 μm.].

3.4. RvD5 reduces CGRP levels and NFκB activation in primary neurons after antigen-induced arthritis

CGRP is a neuropeptide released after sensory neuron activation at the innervating periphery leading to neurogenic inflammation or at the central terminal in the spinal cord inducing neuroinflammation (Xanthos and Sandkuhler, 2014). Neuronal release of neuropeptides has an important role in inducing neurogenic inflammation (Xanthos and Sandkuhler, 2014). CGRP neuronal levels were increased in DRG neurons 9h after antigen-induced arthritis (Fig 4 a-b) and more importantly p-NFκB activity is increased in those $CGRP^+$ neurons (Fig 4 a-d). Suggesting an increase of neuronal activity of this peptidergic population. Herein CGRP increased levels in DRG and p-NFκB in $CGRP^+$ neurons were inhibited by RvD5 in antigen-induced arthritis, suggesting that a reduction of the availability of CGRP by RvD5 might be decreasing neurogenic inflammation in the periphery and neuroinflammation in the spinal cord.

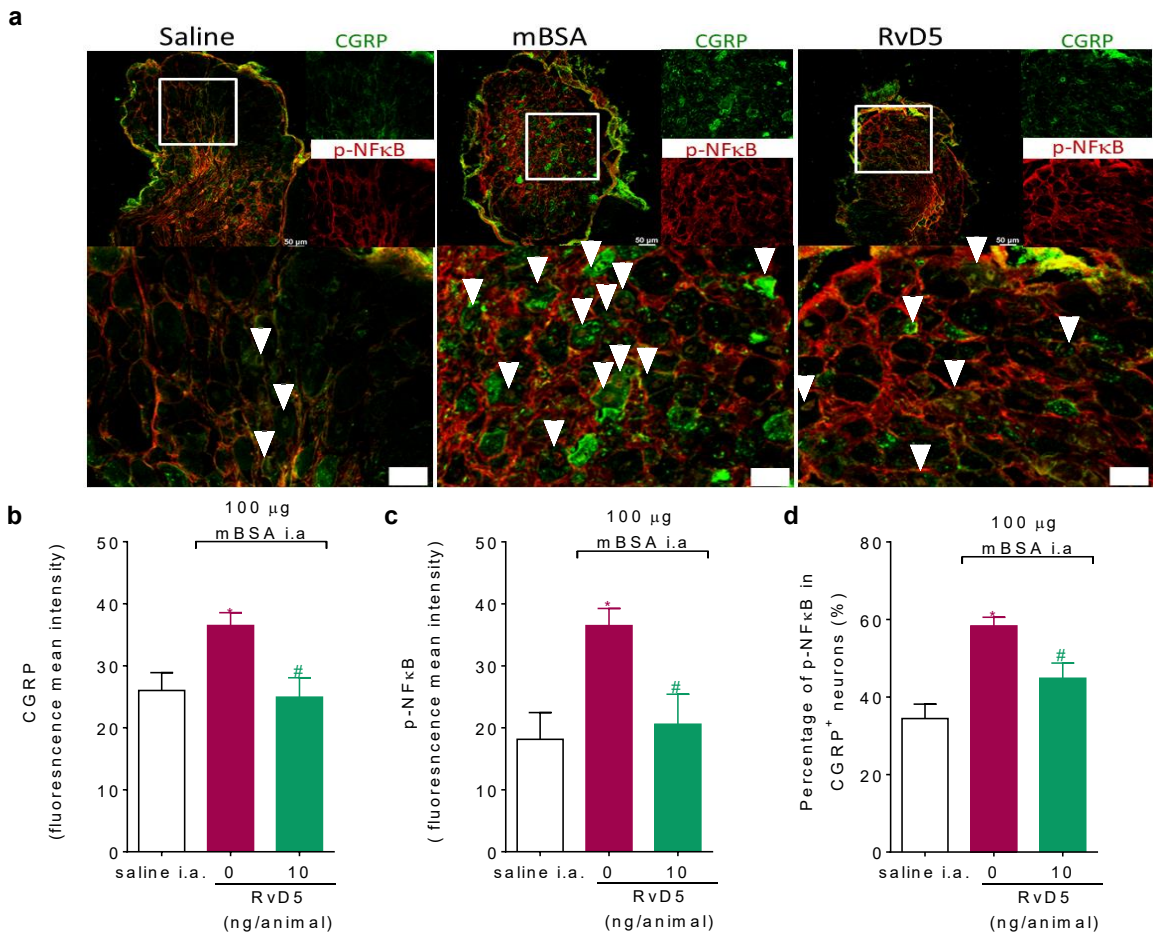

Fig 4. RvD5 reduces CGRP levels, p-NFκB, and p-NFκB in CGRP⁺ neurons 9h after antigen-induced arthritis. Mice were treated with RvD5 (10ng, i.p.) and after 30 minutes arthritis was induced by mBSA challenge. After 9h, DRGs were collected for immunofluorescence assay. (a) Representative DRGs stained for CGRP and p-NFκB are displayed at the left side upper row. The blank square demonstrates the zoom-in area. At the right-side upper row zoom-in of which channel is displayed, and the bellow row displays the zoom-in merge of CRGP with p-NFκB. The first column is shown the saline stimulated group, the second column mBSA stimulated group, and the third column RvD5 treated group and stimulated with mBSA. (b) CGRP mean fluorescence intensity; (c) p-NFκB mean fluorescence intensity; d) the percentage of p-NFκB in CGRP⁺ neurons. Results are presented as mean ± SEM of six mice per group per experiment and are representative of two separate experiments. [$^{*}p < 0.05$ compared to the saline group; $^{\#}p < 0.05$ compared to the mBSA group. Scale bar in whole DRG photomicrograph is 50 µm and in the zoom-in 25 µm. Arrowheads p-

NFκB in CGRP^{+} neurons]

3.5. RvD5 inhibits glial cells activation in the spinal cord of arthritic animals

Neuroinflammation is highlighted by glial cells activation which contributes to antigen-induced arthritis as described by Quadros *et al.* (Quadros et al., 2015). In antigen-induced arthritis, astrogliosis occurred with an increase in *GFAP* mRNA expression, and protein expression at 9h after mBSA challenge. Unlike microgliosis in which the Iba-1 mRNA expression peaked at 9h and the protein expression only 24h after the antigen challenge (Quadros et al., 2015). Herein, we evaluated the activation of astrocytes (*GFAP*), oligodendrocytes (*Olig-2*), and microglia (CX_3CR_1 and *Iba-1*) assessing the mRNA expression with RT-qPCR 9h after the antigen challenge. RvD5 treatment reduced the expression of *GFAP*, *Olig-2*, CX_3CR_1, and *Iba-1*. Hence, demonstrating that RvD5 targets glial cells which have a role in inducing neuroinflammation and in the maintenance of arthritic pain (Christianson et al., 2010; Nieto et al., 2015; Quadros et al., 2015).

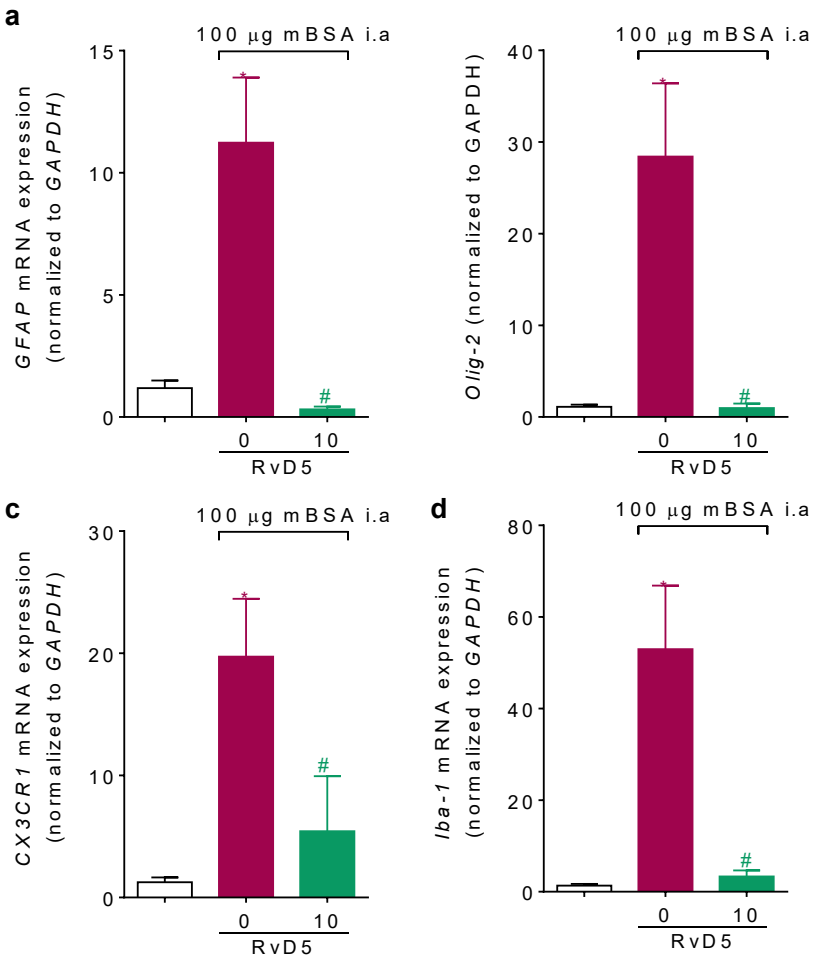

Fig 5. RvD5 reduces glial cells activation in the spinal cord 9h after mBSA-induced arthritis in immunized animals. Mice were treated with RvD5 (10ng, i.p.) and after 30 minutes arthritis was induced by mBSA challenge. After 9h, spinal cord was collected for RT-qPCR. (a) *GFAP;* (b) *Olig*-2, (c), *CX$_3$CR$_1$*, and (d) *Iba-1* mRNA expression was evaluated. *GAPDH* mRNA expression was used to assess the relative gene expression. Results are presented as mean ± SEM of six mice per group per experiment and are representative of two separate experiments. [$^{*}p < 0.05$ compared to the saline group; $^{\#}p < 0.05$ compared to the mBSA group.]

3.6. RvD5 inhibits the expression of ST2 and cytokines in the spinal cord of arthritic animals

Inflammatory receptors such as ST2 and cytokines promote in the spinal cord the maintenance of chronic pain. Herein, we evaluated the effect of the RvD5 in the

mRNA expression of *ST2*, *IL-33*, *TNFα*, and *pro-IL-1β*, 9h after the antigen challenge. RvD5 inhibited the increase of mRNA expression of *ST2*, *IL-33*, *TNFα*, and *pro-IL-1β* in the spinal cord induced by antigen challenge. Suggesting that the inhibition of glial cells activation by RvD5 is also accompanied by the inhibition of the expression of ST2 and cytokines. Thus, both contributing to RvD5 inhibition of neuroinflammation in the spinal cord induced by antigen challenge.

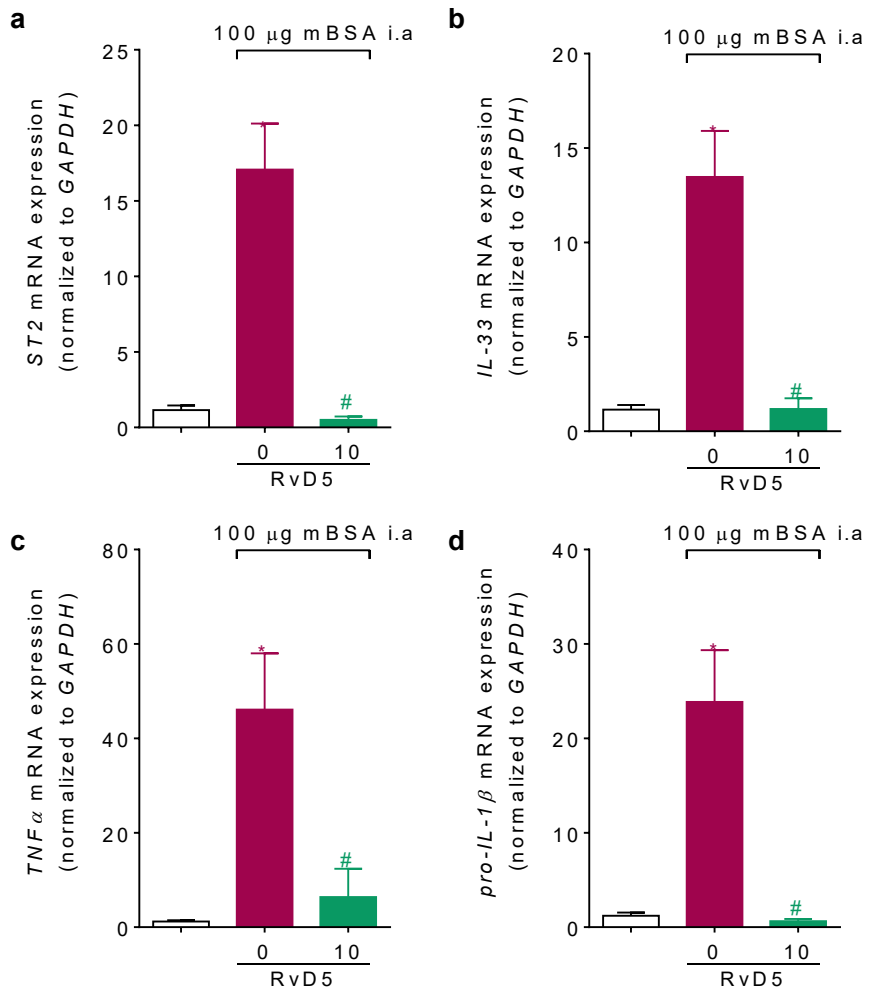

Fig 6. RvD5 reduces mRNA expression of the *ST2* receptor and *IL-33*, *TNFα*, and *pro-IL-1β*. Mice were treated with RvD5 (10ng, i.p.) and after 30 minutes arthritis was induced by mBSA challenge. After 9h, the spinal cord was collected for RT-qPCR. (a) *ST2;* (b) *IL-33*, (c), *TNFα*, and (d) *pro-IL-1β* mRNA expression was evaluated. *GAPDH* mRNA expression was used to assess the relative gene expression. Results are presented as mean ± SEM of six mice per group per experiment and are representative of two separate

experiments. [$^{*}p < 0.05$ compared to the saline group; $^{\#}p < 0.05$ compared to the mBSA group.]

4. Discussion

Rheumatoid arthritis is an autoimmune disease affecting several systems such as joints at the musculoskeletal system and the sensorial system. Acute flares in the joint might relate to synoviocytes responding to immune-complex deposition leading to the inflammatory response and neutrophil recruitment (Lee et al., 2011). These events align with an increase in painful input into the sensorial system by the release of inflammatory mediators from recruited and local synoviocytes-like macrophages. Interestingly, pain is reported even with the inflammation well controlled in the joints. Thus, pain is highlighted as the main symptom by patients with rheumatoid arthritis (Lee et al., 2011; Minnock et al., 2003) suggesting though that the nociceptive circuit is sensitized and a neuroinflammation process may contribute to pain maintenance (Ji et al., 2014a; Minnock et al., 2003). Herein, we reported that RvD5 induces analgesia, reduces oedema, and accelerates the resolution of neutrophilic inflammation in an acute flare by decreasing 72% the R_i (11h for mBSA group to 3h for the RvD5 group) and also had analgesic and anti-oedematogenic activities in the chronic protocol. Together, these data suggest that RvD5 mechanisms also involve the sensorial system, since the neutrophilic infiltrate is resolved in 48h, RvD5 still presents its analgesic and anti-oedematogenic effects in the maintenance phase of arthritic pain. RvD5 decreases DRG primary neuron activity after antigen-induced arthritis by downregulating *TRPV1* and Na_V 1.8 mRNA. Further, RvD5 is acting in the CGRP peptidergic population, reducing CGRP levels and the p-NFκB in $CGRP^+$ neurons, then demonstrating a reduction in $CGRP^+$ neurons activity. Ascending into the sensorial system, at the spinal cord level, RvD5 targets neuroinflammation by inhibiting the mRNA expression markers of astrocytes, oligodendrocytes, and microglia and the mRNA expression of *ST2* and cytokines such as *IL-33*, *TNFα*, and *pro-IL1β*.

Joint inflammation has an important role in the painful pathogenesis of rheumatoid arthritis. Neutrophils constitute over 90% of the cells found in the synovial fluid of patients with rheumatoid arthritis (Chen et al., 2018), and have an important role in the rheumatoid arthritis initiation. Depletion of neutrophils before arthritogenic serum-

induced arthritis mitigates inflammatory signs in the joint (Wipke and Allen, 2001). Synoviocytes and neutrophils are important sources of inflammatory mediators which are responsible for neuronal activation and sensitization. For instance, neutrophils are an important source of PGE_2 which causes pain and primary neuron sensitization (Cunha et al., 2008). Thus, accelerating the resolution of neutrophil inflammation is a conceivable approach for pain resolution in rheumatoid arthritis. Herein, mBSA challenge induced neutrophil accumulation in the synovial lavage peaking 12h after the challenge and took 11h to reduce neutrophil levels by half. RvD5 reduced the magnitude of neutrophil accumulation in the synovial lavage and accelerated up to 3h the time needed to reduce by half the neutrophil levels. These results demonstrate that RvD5 accelerated the neutrophilic resolution. It remains to be assessed the mechanisms underlying RvD5 reducing neutrophil accumulation and accelerating the neutrophilic reduction in antigen-induced arthritis.

Inflammation is an important feature of rheumatoid arthritis pain, and it is already known that pain goes beyond inflammation in this disease. Patients report pain as a symptom without any inflammatory sign at the joint (Lee et al., 2011). Suggesting that rheumatoid arthritis pain is more complex than driven by inflammation (Krock et al., 2018). Treatment targeting lower neuronal activation is a conceivable approach to pain management in conditions that inflammation is already under control. Herein RvD5 lowered neuronal activation (baseline) and the TRPV1 responsiveness to capsaicin in DRGs neurons from arthritic mice after 24h of antigen challenge. In line with the decrease in neuronal activation, RvD5 reduced *TRPV1* and *Na_V 1.8* mRNA expression in DRG neurons, which are important channels involved in pain conduction (Pinho-Ribeiro et al., 2017).

Neuropeptides are important for neuronal communication. Neurogenic inflammation occurs through the release of neuropeptides *e.g.,* CGRP after a stimulus input into the sensorial system through an antidromically axonal response releasing those molecules at the peripheral end terminal (Chiu et al., 2012). For instance, peptidergic nerve fibers are altered in arthritic synovium of patients displaying reduced immunostaining for CGRP (Mapp et al., 1990; Pereira da Silva and Carmo-Fonseca, 1990), which opposes to increases of CGRP in synovial fluid (Appelgren et al., 1995; Larsson et al., 1991). Suggesting though that the neuropeptide is being released into the joint. CGRP increases vasodilatation and blood flow in rabbit skin (Brain et al., 1985) and acts synergically with IL-1β

potentiating oedema and neutrophil recruitment (Buckley et al., 1991). Increased levels of CGRP in synovial fluid are correlated positively with pain and impaired mobility in the temporomandibular joint from rheumatoid arthritis patients (Appelgren et al., 1995). In addition, fibroblast from rheumatoid arthritis patients stimulated with CGRP release IL-6 and IL-8, which would contribute to inflammatory pain flare-up and neutrophil recruitment (Raap et al., 2000; Verri et al., 2006). Besides, the role of CGRP in rheumatoid arthritis remains to be determined, those data suggest that CGRP may have an important contribution to rheumatoid arthritis. At the level of the neuronal cell body in the DRG, the percentage of $CGRP^+$ neurons innervating the joint is increased in collagen-induced rheumatoid arthritis in rats (Nieto et al., 2015). Increased levels of CGRP would be available to be released into the peripheral and central terminal ending. CGRP released at the central terminal end contributes to neuroinflammation in collagen-induced rheumatoid arthritis in rats (Nieto et al., 2015). Herein, we reported an increase in neuronal CGRP levels and p-NFκB in $CGRP^+$ neurons from DRGs of arthritic mice. RvD5 decreased both CGRP levels and p-NFκB in $CGRP^+$ neurons reducing the availability of neuropeptide to be released into the periphery inducing neurogenic inflammation or into the central terminal contributing to neuroinflammation in the spinal cord.

Neuroinflammation accompanies chronic painful states through increased neuronal excitability input into the dorsal horn of the spinal cord. Primary neurons release CGRP which contributes to glial cell activation (Nieto et al., 2015; Priller et al., 1998). Neuroinflammation and glial cell activation are important mechanisms in chronic pain such as in rheumatoid arthritis models (Christianson et al., 2010; Ji et al., 2014b; Nieto et al., 2015; Quadros et al., 2015). Blocking CGRP or fractalkine activating glial cells or glial cells releasing TNFα and IL-1β inhibit nociceptive beheviour in a rheumatoid arthritis model (Clark et al., 2012; Nieto et al., 2015; Quadros et al., 2015). Herein, we reported that RvD5 inhibited the expression of glial cells markers related to their activation. Thus, RvD5 decreased astrocyte activation showed by inhibition of *GFAP* mRNA expression, microglia activation by the inhibition of *Iba-1* and CX_3CR_1 mRNA expression, and oligodendrocyte activation by the inhibition of *Olig-2* mRNA expression.

IL-33 through its ST2 receptor acts as an alarmin in CNS and is released mainly by oligodendrocytes (Zarpelon et al., 2016). Intrathecal IL-33 dosing in mice induces nociceptive behaviour through astrocyte and microglia activation and the

release of TNFα and IL1-β in a PI3K-, mTOR-, MAPK-, and NF-κB-dependent manner (Zarpelon et al., 2013). In the rheumatoid arthritis context, TNFα and IL1-β inhibition in the spinal cord at 6h or 24h after mBSA challenge demonstrate the contribution of those mediators to initiation or maintenance phases of arthritic pain. Suggesting that even without an increase in glial cell activation markers in the early time, glial cells are already activated and are releasing inflammatory cytokines. Herein, RvD5 inhibited antigen-induced expression of *ST2*, *IL-33*, *TNFα*, and *pro-IL-β* in the spinal cord 9h after mBSA challenge. We hypothesized that RvD5 analgesic and anti-oedematogenic activities observed here are related to the reduction of neurogenic inflammation and neuroinflammation since 48h after the challenge neutrophilic flare is under control and pain and oedema last longer. Continued treatment with RvD5 remained to induce analgesia and anti-oedematogenic activities. After the second challenge, a new neutrophilic wave is expected to last 48h (120 – 148h after the first mBSA challenge), and once again RvD5 maintained its actions until the end of the evaluation. Thus, RvD5 would be reducing primary neuron activation, neurogenic inflammation with CGRP release in the periphery, and neuroinflammation with CGRP release in the central neural ending. Also, reduction of CGRP release in the CNS contributes to the reduction of glial cell activation but also RvD5 may be acting directly at the glial cells in the spinal cord and reducing neuroinflammation.

Conclusion

Our data show that RvD5 resolves pain, oedema, and neutrophilic flare in a rheumatoid arthritis mouse model targeting the sensorial system encompassing primary neuronal in the DRG resulting in decreased levels of CGRP and p-NFκB in $CGRP^{+}$ neurons and inhibiting neuroinflammation by reducing glial cell activation and expression of cytokines.

Acknowledgements

Coordenação de Aperfeiçoamento de Pessoal de Nível Superior (CAPES; Finance Code 001), and Programa de Pesquisa para o SUS (PPSUS) grant supported by Ministério da Ciência, Tecnologia e Inovação (MCTI), Secretaria da Ciência, Tecnologia e Ensino Superior (SETI), Decit/SCTIE/MS through CNPq with the

support of Fundação Araucária and Secretaria da Saúde do Estado do Paraná (SESA-PR), and Parana State Government (Brazil).

References

Appelgren, A., Appelgren, B., Kopp, S., Lundeberg, T., Theodorsson, E., 1995. Neuropeptides in the arthritic TMJ and symptoms and signs from the stomatognathic system with special consideration to rheumatoid arthritis. J Orofac Pain 9, 215-225.

Barroso, L. C., Magalhaes, G. S., Galvao, I., Reis, A. C., Souza, D. G., Sousa, L. P., Santos, R. A. S., Campagnole-Santos, M. J., Pinho, V., Teixeira, M. M., 2017. Angiotensin-(1-7) Promotes Resolution of Neutrophilic Inflammation in a Model of Antigen-Induced Arthritis in Mice. Front Immunol 8, 1596.

Brain, S. D., Williams, T. J., Tippins, J. R., Morris, H. R., MacIntyre, I., 1985. Calcitonin gene-related peptide is a potent vasodilator. Nature 313, 54-56.

Buckley, T. L., Brain, S. D., Collins, P. D., Williams, T. J., 1991. Inflammatory edema induced by interactions between IL-1 and the neuropeptide calcitonin gene-related peptide. J Immunol 146, 3424-3430.

Chaplan, S. R., Bach, F. W., Pogrel, J. W., Chung, J. M., Yaksh, T. L., 1994. Quantitative assessment of tactile allodynia in the rat paw. J Neurosci Methods 53, 55-63.

Chen, W., Wang, Q., Ke, Y., Lin, J., 2018. Neutrophil Function in an Inflammatory Milieu of Rheumatoid Arthritis. J Immunol Res 2018, 8549329.

Chiu, I. M., von Hehn, C. A., Woolf, C. J., 2012. Neurogenic inflammation and the peripheral nervous system in host defense and immunopathology. Nat Neurosci 15, 1063-1067.

Christianson, C. A., Corr, M., Firestein, G. S., Mobargha, A., Yaksh, T. L., Svensson, C. I., 2010. Characterization of the acute and persistent pain state present in K/BxN serum transfer arthritis. Pain 151, 394-403.

Clark, A. K., Grist, J., Al-Kashi, A., Perretti, M., Malcangio, M., 2012. Spinal cathepsin S and fractalkine contribute to chronic pain in the collagen-induced arthritis model. Arthritis Rheum 64, 2038-2047.

Cunha, T. M., Verri, W. A., Schivo, I. R., Napimoga, M. H., Parada, C. A., Poole, S., Teixeira, M. M., Ferreira, S. H., Cunha, F. Q., 2008. Crucial role of neutrophils in the development of mechanical inflammatory hypernociception. Journal of Leukocyte Biology 83, 824-832.

Donaldson, L. F., 2009. Neurogenic mechanisms in arthritis. NeuroImmune biology 8, 211-241.

Fattori, V., Pinho-Ribeiro, F. A., Staurengo-Ferrari, L., Borghi, S. M., Rossaneis, A. C., Casagrande, R., Verri, W. A., Jr., 2019. The specialised pro-resolving lipid mediator maresin 1 reduces inflammatory pain with a long-lasting analgesic effect. Br J Pharmacol 176, 1728-1744.

Flak, M. B., Koenis, D. S., Sobrino, A., Smith, J., Pistorius, K., Palmas, F., Dalli, J., 2020. GPR101 mediates the pro-resolving actions of RvD5n-3 DPA in arthritis and infections. J Clin Invest 130, 359-373.

Ji, R.-R., Xu, Z.-Z., Gao, Y.-J., 2014a. Emerging targets in neuroinflammation-driven chronic pain. Nature Reviews Drug Discovery 13, 533-548.

Ji, R. R., Xu, Z. Z., Gao, Y. J., 2014b. Emerging targets in neuroinflammation-driven chronic pain. Nat Rev Drug Discov 13, 533-548.

Krock, E., Jurczak, A., Svensson, C. I., 2018. Pain pathogenesis in rheumatoid arthritis-what have we learned from animal models? Pain 159 Suppl 1, S98-S109.

Larsson, J., Ekblom, A., Henriksson, K., Lundeberg, T., Theodorsson, E., 1991. Concentration of substance P, neurokinin A, calcitonin gene-related peptide, neuropeptide Y and vasoactive intestinal polypeptide in synovial fluid from knee joints in patients suffering from rheumatoid arthritis. Scand J Rheumatol 20, 326-335.

Lee, Y. C., Cui, J., Lu, B., Frits, M. L., Iannaccone, C. K., Shadick, N. A., Weinblatt, M. E., Solomon, D. H., 2011. Pain persists in DAS28 rheumatoid arthritis remission

but not in ACR/EULAR remission: a longitudinal observational study. Arthritis Res Ther 13, R83.

Luo, X., Gu, Y., Tao, X., Serhan, C. N., Ji, R. R., 2019. Resolvin D5 Inhibits Neuropathic and Inflammatory Pain in Male But Not Female Mice: Distinct Actions of D-Series Resolvins in Chemotherapy-Induced Peripheral Neuropathy. Front Pharmacol 10, 745.

Mapp, P. I., Kidd, B. L., Gibson, S. J., Terry, J. M., Revell, P. A., Ibrahim, N. B., Blake, D. R., Polak, J. M., 1990. Substance P-, calcitonin gene-related peptide- and C-flanking peptide of neuropeptide Y-immunoreactive fibres are present in normal synovium but depleted in patients with rheumatoid arthritis. Neuroscience 37, 143-153.

Minnock, P., FitzGerald, O., Bresnihan, B., 2003. Women with established rheumatoid arthritis perceive pain as the predominant impairment of health status. Rheumatology (Oxford) 42, 995-1000.

Nieto, F. R., Clark, A. K., Grist, J., Chapman, V., Malcangio, M., 2015. Calcitonin gene-related peptide-expressing sensory neurons and spinal microglial reactivity contribute to pain states in collagen-induced arthritis. Arthritis Rheumatol 67, 1668-1677.

Pereira da Silva, J. A., Carmo-Fonseca, M., 1990. Peptide containing nerves in human synovium: immunohistochemical evidence for decreased innervation in rheumatoid arthritis. J Rheumatol 17, 1592-1599.

Pinho-Ribeiro, F. A., Verri, W. A., Chiu, I. M., 2017. Nociceptor Sensory Neuron–Immune Interactions in Pain and Inflammation. Trends in Immunology 38, 5-19.

Pinto, L. G., Cunha, T. M., Vieira, S. M., Lemos, H. P., Verri, W. A., Jr., Cunha, F. Q., Ferreira, S. H., 2010. IL-17 mediates articular hypernociception in antigen-induced arthritis in mice. Pain 148, 247-256.

Priller, J., Reddington, M., Haas, C. A., Kreutzberg, G. W., 1998. Stimulation of P2Y-purinoceptors on astrocytes results in immediate early gene expression and potentiation of neuropeptide action. Neuroscience 85, 521-525.

Quadros, A. U., Pinto, L. G., Fonseca, M. M., Kusuda, R., Cunha, F. Q., Cunha, T. M., 2015. Dynamic weight bearing is an efficient and predictable method for evaluation of arthritic nociception and its pathophysiological mechanisms in mice. Sci Rep 5, 14648.

Raap, T., Justen, H. P., Miller, L. E., Cutolo, M., Scholmerich, J., Straub, R. H., 2000. Neurotransmitter modulation of interleukin 6 (IL-6) and IL-8 secretion of synovial fibroblasts in patients with rheumatoid arthritis compared to osteoarthritis. J Rheumatol 27, 2558-2565.

Sant'Anna, M. B., Kusuda, R., Bozzo, T. A., Bassi, G. S., Alves-Filho, J. C., Cunha, F. Q., Ferreira, S. H., Souza, G. R., Cunha, T. M., 2016. Medial plantar nerve ligation as a novel model of neuropathic pain in mice: pharmacological and molecular characterization. Sci Rep 6, 26955.

Serhan, C. N., Chiang, N., Van Dyke, T. E., 2008. Resolution Lipid Mediators. Nat Rev Immunol 8, 349-361.

Verri, W. A., Cunha, T. M., Parada, C. A., Poole, S., Cunha, F. Q., Ferreira, S. H., 2006. Hypernociceptive role of cytokines and chemokines: Targets for analgesic drug development? Pharmacology & Therapeutics 112, 116-138.

Verri, W. A., Guerrero, A. T. G., Fukada, S. Y., Valerio, D. A., Cunha, T. M., Xu, D., Ferreira, S. H., Liew, F. Y., Cunha, F. Q., 2008. IL-33 mediates antigen-induced cutaneous and articular hypernociception in mice. Proceedings of the National Academy of Sciences of the United States of America 105, 2723-2728.

Verri, W. A., Jr., Souto, F. O., Vieira, S. M., Almeida, S. C., Fukada, S. Y., Xu, D., Alves-Filho, J. C., Cunha, T. M., Guerrero, A. T., Mattos-Guimaraes, R. B., Oliveira, F. R., Teixeira, M. M., Silva, J. S., McInnes, I. B., Ferreira, S. H., Louzada-Junior, P., Liew, F. Y., Cunha, F. Q., 2010. IL-33 induces neutrophil migration in rheumatoid arthritis and is a target of anti-TNF therapy. Ann Rheum Dis 69, 1697-1703.

Wipke, B. T., Allen, P. M., 2001. Essential role of neutrophils in the initiation and progression of a murine model of rheumatoid arthritis. J Immunol 167, 1601-1608.

Xanthos, D. N., Sandkuhler, J., 2014. Neurogenic neuroinflammation: inflammatory CNS reactions in response to neuronal activity. Nat Rev Neurosci 15, 43-53.

Zarpelon, A. C., Cunha, T. M., Alves-Filho, J. C., Pinto, L. G., Ferreira, S. H., McInnes, I. B., Xu, D., Liew, F. Y., Cunha, F. Q., Verri, W. A., 2013. IL-33/ST2 signalling contributes to carrageenin-induced innate inflammation and inflammatory pain: role of cytokines, endothelin-1 and prostaglandin E2. British journal of pharmacology 169, 90-101.

Zarpelon, A. C., Rodrigues, F. C., Lopes, A. H., Souza, G. R., Carvalho, T. T., Pinto, L. G., Xu, D., Ferreira, S. H., Alves-Filho, J. C., McInnes, I. B., Ryffel, B., Quesniaux, V. F. J., Reverchon, F., Mortaud, S., Menuet, A., Liew, F. Y., Cunha, F. Q., Cunha, T. M., Verri, W. A., 2016. Spinal cord oligodendrocyte-derived alarmin IL-33 mediates neuropathic pain. The FASEB Journal 30, 54-65.

4. ARTIGO A SER SUBMETIDO NO THE JOURNAL OF NUTRITIONAL BIOCHEMISTRY

O presente trabalho foi realizado no Laboratório de Dor, Inflamação Neuropatia E Câncer, da Universidade Estadual de Londrina e segue as normas da revista The Journal Of Nutritional Biochemistry. Os resultados parciais estão descritos no artigo intitulado: “Resolvin D5, a docosahexaenoic acid-derived pro-resolution lipid, resolves titanium dioxide (TiO_2)-induced chronic arthritis”.

Resolvin D5, a docosahexaenoic acid-derived pro-resolution lipid, resolves titanium dioxide (TiO_2)-induced chronic arthritis

Marília F. Manchope[a]; Telma Saraiva-Santos[a], Camila R. Ferraz[a]; Anelise Franciosi[a], Tiago H. Zaninelli[a], Nayara A. Artero[a], Rubia Casagrande[b], Waldiceu A. Verri Jr[a*]

[a] Laboratory of Pain, Inflammation, Neuropathy, and Cancer, Department of Pathology, Londrina State University, Londrina, Paraná, Brazil

[b] Laboratory of Oxidative Stress and Inflammation, Department of Pharmaceutical Sciences, Londrina State University, Londrina, PR, Brazil

[*]**Corresponding author: Prof. Waldiceu A. Verri Jr, Ph.D.** Present address: Departamento de Ciências Patológicas, Universidade Estadual de Londrina, Rod. Celso Garcia Cid Km480 PR445, CEP 86057-970, Cx Postal 10.011, Londrina, Paraná, Brasil. Tel: +55 43 3371 4979. Fax: +55 43 3371 4387. E-mails: waverri@uel.br or waldiceujr@yahoo.com.br

Running title: Resolvin D5 resolves TiO_2-induced chronic arthritis

Abstract

Nanoparticles inducing chronic arthritis occur in cases of a prosthesis or implants loosening nanoparticle material such as titanium dioxide (TiO_2). TiO_2 induces pain, inflammatory response, and oxidative stress in patients. New therapeutic approaches are needed to control pain, inflammatory response, and oxidative stress induced by TiO_2 and further improve patients' quality of life. Specialized pro-resolving mediators are derived from omega-6 and omega-3 and induce inflammation resolution and tissue homeostasis. Herein, we assessed the resolutive effect of resolving d5 (RvD5), a docosahexaenoic acid-derived pro-resolution lipid, in chronic arthritis induced by TiO_2 in mice. RvD5 inhibited nociceptive behavior, edema, histopathological damage, leukocyte infiltration (polymorphonuclear and mononuclear $LysM^+$ and $CCR2^+$) in the synovial tissue, and synovial cavity, mRNA expression of TNFα and pro-IL-1β, and oxidative stress in the knee joint stimulated with TiO_2. Additionally, RvD5 inhibited the release of TNFα, but not IL-1β and the activation of NFκB in macrophages stimulated with TiO_2. Thus, RvD5 resolves chronic arthritis induced by TiO_2 by decreasing NFκB activation, the release of TNFα, and oxidative stress.

Keywords: Nanoparticles, specialized pro-resolving mediators, DHA, chronic pain, inflammation.

1. Introduction

Chronic arthritis related to prosthesis and implants occurs through the loosening of nanoparticles from implant material inducing pain, inflammation, and oxidative stress in the periprosthetic tissue [1-4]. The nanoparticles even translocate throughout the body and accumulated in other tissues causing damage such as in the joints causing arthritis [5]. Inflammation and the oxidative stress caused by the nanoparticles induce osteolysis [6] with osteoclasts activation by the release of cytokines such as RANKL, TNFα, and IL-6 which activate osteoclast in a RANKL dependent manner [7] or a RANKL independent manner [8]. This whole scenario causes the failure of the procedure and requires revision surgery, which may not be possible depending on the patients' health condition.

Specialized pro-resolving mediators (SPMs) are derived from omega-6 (lipoxins) or omega-3 docosahexaenoic acid (DHA) and eicosapentaenoic acid (EPA). DHA originates the maresins and resolvins D series, and EPA the resolvins E series [9]. SPMs induce the resolution of inflammation and restore tissue homeostasis. Chronic inflammatory diseases such as chronic obstructive pulmonary disease (COPD) emphysema have been related to failures in the resolution process [10] due to an increase in the enzyme 15-prostaglandin dehydrogenase/eicosanoid oxidoreductase which degradants lipid mediator [10] reducing the levels of resolving (Rv) D1 in the patients with (COPD) emphysema [11]. Patients with rheumatoid arthritis have lower levels of RvD3 and increase levels of thromboxane A_2 in the serum compared to healthy individuals [12]. RvD3 inhibited clinical score, edema, and leukocyte recruitment in arthritis induced by K/BxN serum in mice [12]. In addition, SPMs induce analgesia with potent and long-lasting activity, Maresin-1 (MaR1) decreases neuronal activation leading to analgesia in mice stimulated with Freund’s complete adjuvant (CFA). It is noteworthy to highlight that one intrathecal (i.t.) administration of MaR1 inhibits CFA-induced inflammatory pain for 5 days. Thus, assessing the ability of SPMs to restore tissue homeostasis, decrease inflammation, oxidative stress, and resolves pain in chronic arthritis induced by nanoparticles loosening is an innovative approach. Herein, we assessed the effect of the DHA-derived RvD5 resolving pain, inflammation, and oxidative stress in chronic arthritis induced by TiO_2.

2. Materials and Methods

2.1 Animals

Male Swiss and C57BL/6 mice (20-25 g) from the Londrina State University, Londrina, Paraná, Brazil, were used in this study. LysM-eGFP / CCR2-RFP C57BL/6 background mice (19-22g) from Ribeirão Preto Medical School, São Paulo, Brazil were used in this study. Mice were housed in standard clear plastic cages with a light / dark cycle of 12 / 12h, controlled temperature (21°C), and water and food *ad libitum*. Mice were maintained in the vivarium of the Department of Pathology of Londrina State University for at least two days before experiments. Mice were used only once and were acclimatized to the testing room at least 1 hour before the experiments, which were conducted during the light cycle. Animal care and handling procedures were under the International Association for Study of Pain (IASP) guidelines and approved by the Londrina State University Ethics Committee on Animal Research and Welfare (process number 1147.2016.40). All efforts were made to minimize the number of animals used and their suffering.

2.2 Experimental section

Mice were stimulated in the right knee joint with 3 mg of TiO_2 intra-articular [i.a.] and 24h later treated with RvD5 [1, 3, 10 ng, intraperitoneal (i.p.)] and then every other 72h up to 30 days after TiO_2. Behavior nociception evaluation and edema were measured before (baseline) and 24h after TiO_2 stimulus to assure arthritis induction. Mechanical hyperalgesia measurements continued after RvD5 treatment (1, 3, 5, 7 h after treatment on the 1st day) and continued on the 2nd and every other day up to the 30th day. Thermal hyperalgesia and the static weight ratio were assessed on the 1st day and 4th, and every other 4 days until the 28th day. Joint edema was assessed on the 1st day and 2nd, and every other day up to the 30th day. Behavior nociception was assessed 1h after the treatment on the days when treatment and behavior assessment matched. Histopathology, leukocyte recruitment and synovial infiltration, oxidative stress, and TNFα and pro-IL1β mRNA expression in the joint were evaluated on the 30th day. Bone marrow-derived macrophages (BMDM) were used to assess the effect of RvD5 modulating TNFα and IL-1β production and p-NFκB activation in primed BMDM stimulated with TiO_2. Briefly, BMDM were pre-treated with RvD5 (0.1-100 ng/mL) 12 h after LPS priming (500ng/mL). After 3h of primming, BMDM were stimulated with TiO_2 (500 µg/mL) for 5h. The supernatant was used for

cytokines and cytotoxicity evaluation and the BMDM for the immunofluorescence assay.

2.3 Mechanical hyperalgesia

Mechanical hyperalgesia was evaluated as previously described [13]. Mice were placed individually in acrylic cages (12 x 10 x 17 cm) with a wire grid floor. Mice were acclimatized for 4 days before the experiment and 15-30 minutes before the measurements. An electronic pressure-meter test consisting of a hand-held force transducer fitted with a polypropylene tip (electronic von Frey Anesthesiometer; Insight, Ribeirão Preto, SP, Brazil) was used to evaluate mechanical threshold. An increasing perpendicular force was applied to the central area of the plantar surface of the hind paw to induce a flexion movement of the tibiofemoral joint followed by paw withdrawal. A large tip (4.15 mm2) was adapted to the probe. The electronic pressure-meter apparatus automatically recorded the mechanical threshold applied when the paw was withdrawn. The flexion-elicited mechanical threshold was expressed in grams (g) [13].

2.4 Thermal hyperalgesia

Thermal latency to a heat stimulus was used to assess thermal hyperalgesia. Mice were placed on a glass plate of a Hargreaves apparatus (Ugo Basille, Italy). An infrared heat source (infrared intensity 30%) was used to stimulate the plantar surface and latency (in seconds) to evoke a paw withdrawal response was recorded. The mean of two measurements was determined for each animal at each time point. An exposure limit of 20 s was used to avoid tissue damage.

2.5 Edema assessment

Tibiofemoral articular edema was evaluated by the average between transverse and anterolateral joint diameter using a caliper (Digmatic Caliper, Mitutoyo Corporation, Kanagawa, Japan). Edema was expressed as delta, the difference between the diameters measured after TiO_2 and baseline before the stimulus.

2.6 Static weight bearing (SWB) ratio distribution

Changes in rear paw weight distribution due to joint inflammation were evaluated using the SWB apparatus (model BIO-SWB-TOUCH-M, Bioseb, France).

In a quiet room, mice were placed into an acrylic chamber with the hind paws resting on two separate sensor plates. The animal stands and makes a natural adjustment to the degree of pain by adapting weight distribution on the noninjured contralateral joint. Mice were habituated for at least four consecutive days before the behavioral test. The weight applied on each paw by the mice is displayed on the LCD screen of the SWB apparatus. Mice were tested before (baseline values) and after stimulus and treatments. The mean of two weight measurements was calculated. Results are expressed by variation of the left/right paw weight ratio between time-point after stimulus and baseline assessments.

2.7 Histopathology

Joints were fixed in 4% formaldehyde for 1 day before decalcification in NaOH/EDTA solution (pH 7.3-7.4) and processed for paraffin embedding. Tissue longitudinal sections (7 µm) were prepared and hematoxylin and eosin (HE) stained. Sections were examined blinded and scored under light microscopy. Synovial hyperplasia; inflammatory infiltrate and vascular proliferation were scored as described previously [14]. The following parameters were degreed: a) synovial hyperplasia (from 0 = no pannus formation, to 3 = most severe pannus formation); b) inflammatory infiltrate (from 0 = no inflammation, to 3 = most severe inflammation; and c) vascularity (from 0 = no vascular proliferation, to 3 = most severe proliferation). The score was determined by summing all parameters (a-c). Two to three sections were evaluated from each animal.

2.8 Immunofluorescence assay

Mice LysM-eGFP / CCR2-RFP C57BL/6 background were terminally anesthetized (isoflurane 5%). Macrophages and neutrophils have LysM-eGFP mice express enhanced green fluorescent protein (eGFP) expression controlled by lysozyme M promoter (LysM) [15] and inflammatory macrophages express a red fluorescent protein (RFP) expression controlled by the C-C Motif Chemokine Receptor 2 (CCR2-RFP) [16]. The ascending aorta was used to perfuse the mice with saline followed by 4% paraformaldehyde (PFA). The knee joint was dissected and fixed for 24 h in 4% PFA, and decalcified (2.35mM tetrasodium EDTA, 27.8mM sodium potassium tartrate, 707,3µM sodium tartrate containing 11.8% hydrochloric acid). The tissue was cryopreserved in 30% sucrose for 72 h and embedded in

optimum cutting temperature, and 15 µm sections were cut in a cryostat and proceeded for fluorescence assay. Sections were blocked with 3% BSA and then incubated with DAPI (diamidino-2-phenylindole – Thermo Fischer scientific). Coverslips containing BMDM cells were fixed for 10 minutes. Fixative was washed 3 times with PBS 1x, blocked with 3% BSA, and incubated overnight with primary antibody for p-NFκB [p-NFκB p65 (27.Ser 536): sc-136548, Santa Cruz Biotechnology, INC]. Secondary antibody (Alexa Fluor 647, # A-21240, Invitrogen) was incubated with DAPI for 1h and coverslips were mounted within Fluormount (SouthernBiotech) into a microscope slide. Images acquisition and analysis were performed using a Confocal Microscope (TCS SP8, Leica Microsystems, Mannheim, Germany).

2.9 BMDM cell culture

Femora and tibiae of C57BL/6 mice were flushed with RPMI 1640 media with a syringe into a 15 ml sterile tube. Cells were homogenized with a Pasteur glass pipette and then seeded and cultured in treated Optilux Petri dishes containing RPMI 1640 media supplemented with 10% FBS, 2 mM L-glutamine, 100 U/ml penicillin, 100 µg/ml streptomycin, and 15% of L929 cell-conditioned medium and incubated at 37°C in a 5% CO_2 atmosphere for 7 days [17]. BMDM supernatants were discarded and 10 mL of cold PBS was used to detached the cells. The BMDM cells were counted and seeded in a 96-well tissue culture plate with a 0,8 x10^6/mL density for ELISA and cytotoxicity (LDH release). For the immunofluorescence assay, cells were seeded in a glass coverslip into a 24-well plate at a density of 2x 10^6/mL. BMDM were pretreated with RvD5 0.1, 1, 10, and 100 ng/mL 12h before LPS priming (500 ng/mL – Escherichia coli, Santa Cruz Biotechnology, California, USA). Three h after primming, BMDM was stimulated with TiO2 (500µg/mL), the supernatant or coverslips were collected 5h TiO_2 and proceed for ELISA and viability or immunofluorescence assay.

2.10 qPCR

The joint was homogenized in TRIzol reagent® and total RNA extracted using the SV Total RNA Isolation System (Promega). RNA purity was measured using a spectrophotometer (Multiskan GO Microplate Spectrophotometer, Thermo Scientific, Vantaa, Finland) and the wavelength absorption ratio (260/280) was between 1.8 and

2.0 for all preparations. Reverse transcription of total RNA to cDNA and qPCR was carried out using GoTaq® 2-Step RT-qPCR System (Promega). qPCR was performed in a StepOnePlusTM Real-Time PCR System (Applied Biosystems®). The relative gene expression was measured using the comparative $2^{-(\Delta\Delta Cq)}$ method. The primers used were: TNFα sense: 5´-TCT CAT CAG TTC TAT GGC CC-3´, antisense: 5´-GGG AGT AGA CAA GGT ACAAC-3´; pro-IL-1β sense: 5-´GAA ATG CCA CCT TTT GAC AGTG-3´, antisense: 5´-TGG ATG CTC TCA TCA GGA CAG-3´; gp91phox sense: 5´-AGC TAT GAG GTG GTG ATG TTA GTGG-3´, antisense: 5´-CAC AAT ATT TGT ACC AGA CAG ACT TGAG-3´; iNOS sense: 5'- CGA AAC GCT TCA CTT CCAA-3', antisense: 5'- TGA GCC TAT ATT GCT GTG GCT3'-; β-actin: sense: 5´-AGC TGC GTT TTA CAC CCT TT-3', antisense: 5´-AAG CCA TGC CAA TGT TGT CT-3´. The expression of β-actin mRNA was used as a reference gene, and the results were expressed as mRNA expression (normalized to β-actin).

2.11 Cytokine release

TNFα and IL-β release in the BMDM supernatant was assessed using a commercial enzyme-linked immunosorbent assay (ELISA) assay (ELISA MAX™ Deluxe Set, BioLegend®, San Diego, CA). Cytokines concentration was assessed with a commercial kit following the manufacture's protocol and read in 450 nm using a spectrophotometer (Multiskan GO Microplate Spectrophotometer, Thermo Scientific, Vantaa, Finland). Results were expressed in pg/mL.

2.12 Antioxidant capacity assessment

Total antioxidant capacity was evaluated by the ferric reducing antioxidant power (FRAP) assay and the ability to scavenger the radical ABTS (2,2'-azino-bis(3-ethylbenzothiazoline-6-sulfonic acid) [18]. The joint was homogenized into ice-cold buffer containing 1.15% KCl, centrifuged (1,000 g in 4 °C for 10 min) and the antioxidant capacity assessed as described elsewhere [18, 19]. Reading was performed at 734 nm and 595 nm, respectively, using a spectrophotometer (Multiskan GO Microplate Spectrophotometer, Thermo Scientific, Vantaa, Finland). All results were compared to a standard curve of trolox (concentration ranging between 0.01–20 nmol). Protein concentration was used to normalize data. Results are presented as nmol trolox equivalent per mg of protein.

2.13 Superoxide anion production

The redox reduction of Nitroblue tetrazolium (NBT) was used to measure superoxide anion production [14]. The joint was homogenized with 300 µL of saline using an ultra-turrax (Tissue-Tearor 985370, BioSpec Products, Bartlesville, OK, USA) and 50 µL of the homogenate was incubated with 100 µL of nitro blue tetrazolium solution (1 mg/mL) (NBT, Sigma) on a 96-well plate and maintained at 37°C in a warm bath for 5 minutes. The supernatant was removed, and the formazan precipitated was then solubilized by adding 120 µL of 2 M KOH and 120 µL of dimethyl sulfoxide (DMSO). The optical density was measured using a microplate spectrophotometer reader (Multiskan GO Microplate Spectrophotometer, Thermo Scientific, Vantaa, Finland) at 600 nm. The NBT reduction levels were normalized with protein concentration and the results were presented as NBT reduction (OD/mg of protein).

2.15. Statistical analysis

The results are presented as means ± SEM of measurements made on six mice in each group per experiment and are representative of two separate experiments. Two-way repeated-measures analysis of variance (ANOVA) followed by Tukey's post hoc was used to compare all groups and doses at all times when responses were measured at different times after TiO_2 stimulus in the behavior assessment. Differences between responses were evaluated by one-way ANOVA followed by Tukey's post hoc for data of a single time point. For histopathology score results are presented as a median and interquartile range of measurements made on six mice in each group (2-3 knee sections per animal) per experiment and are representative of two separate experiments. The difference in histopathological score was determined with the Kruskal-Wallis test followed by Dunn's post hoc. Statistical differences were considered significant when $p < 0.05$.

3. Results

3.1. RvD5 inhibits nociceptive and inflammatory disease phenotype induced by TiO_2

Disease phenotype in chronic arthritis induced by TiO_2 was evaluated by nociceptive behavior (mechanical hyperalgesia, thermal hyperalgesia, and static weight ratio – Fig. 1a, b, and d) and edema (Fig 1c, inflammatory phenotype). We started assessing a titrated curve dose-response of RvD5 in mechanical hyperalgesia. TiO_2 decreased the mechanical threshold (Fig 1a). The minor dose of 1 ng of RvD5 induced transient analgesia throughout the 30 days of the behavior nociception assessment. The 3 and 10 ng doses induced analgesia during the 30 days. The best analgesic activity was presented by the 10 ng dose and was chosen for further experiments. Thermal latency was decreased by TiO_2 and RvD5 improved the latency by 70 %. TiO_2 increased the joint edema (Fig 1c) and destabilized the weight ratio in the rear paw increasing the weight on the rear left paw (Fig 1d). RvD5 decreased by 68 % the edema induced by TiO_2 (Fig 1c) and balanced the weight ratio by 83% destabilized by TiO_2 (Fig 1d). Thus, TiO_2 induced chronic nociceptive behavior and inflammatory disease phenotype which is mitigated by RvD5.

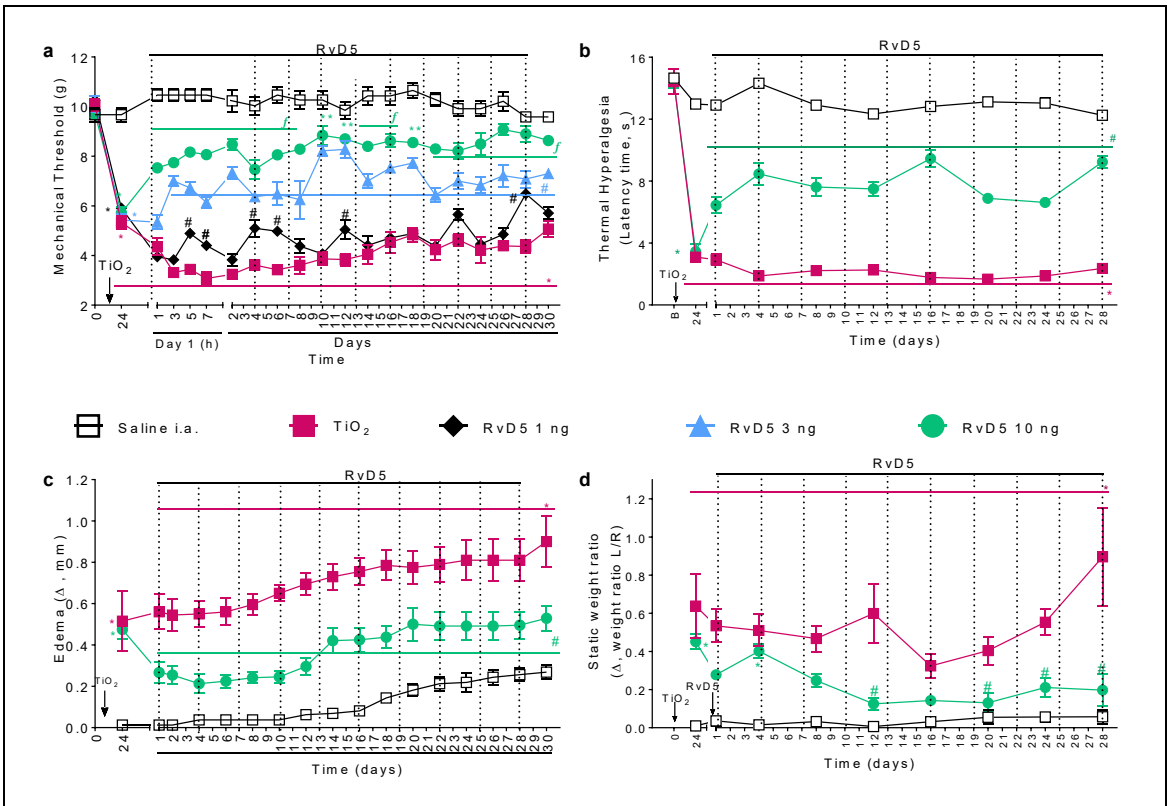

Fig 1. RvD5 inhibited nociceptive behavior and edema in chronic arthritis

induced by TiO_2. Mice were treated with RvD5 (1, 3, and 30 ng/ animal, i.p.) every other 72 h starting 24h after TiO_2 stimulus. Mechanical hyperalgesia (a), thermal hyperalgesia (b), edema (c), and (d) static weight ratio were assessed throughout 30 days of chronic arthritis. Results are presented as mean ± SEM of six mice per group per experiment and are representative of two separate experiments. *p < 0.05 compared to the saline group; #p < 0.05 compared to the TiO2 group; **p < 0.05 compared to the TiO_2 and RvD5 (1 ng/ animal) groups; ^{f}p < 0.05 compared to the TiO_2 and RvD5 (1 and 30 ng/ animal) groups, repeated measures two-way ANOVA followed by Tukey's post hoc.

3.2. RvD5 inhibits histopathological damage and leukocyte recruitment and synovial infiltrate

TiO_2 nanoparticles induced a local response with increased synovial hyperplasia lining, leukocyte infiltrate, and neovascularization which was inhibited by RvD5 in a histopathological analysis with HE staining after 30 days of chronic arthritis (Fig 2 a,b). In the synovial cavity leukocytes recruitment were evaluated and TiO_2 increased total leukocytes (Fig 2c), polymorphonuclear (Fig 2d), and mononuclear cells (Fig 2e) in synovial lavage and RvD5 inhibited leukocytes recruitment (Fig 2c-e). Aiming to assess leukocyte infiltration type we used reporter mice with $LysM^{-}eGFP$ and $CCR2^{-}RFP$ cells. TiO_2 increased the infiltration of $LysM^{+}$ (Fig 3a,b) and $CCR2^{+}$ leukocytes (Fig 3a,c). RvD5 inhibited LyM^{+} (Fig 3a,b) and $CCR2^{+}$ leukocyte infiltration (Fig 3a,c) after 30 days of chronic arthritis.

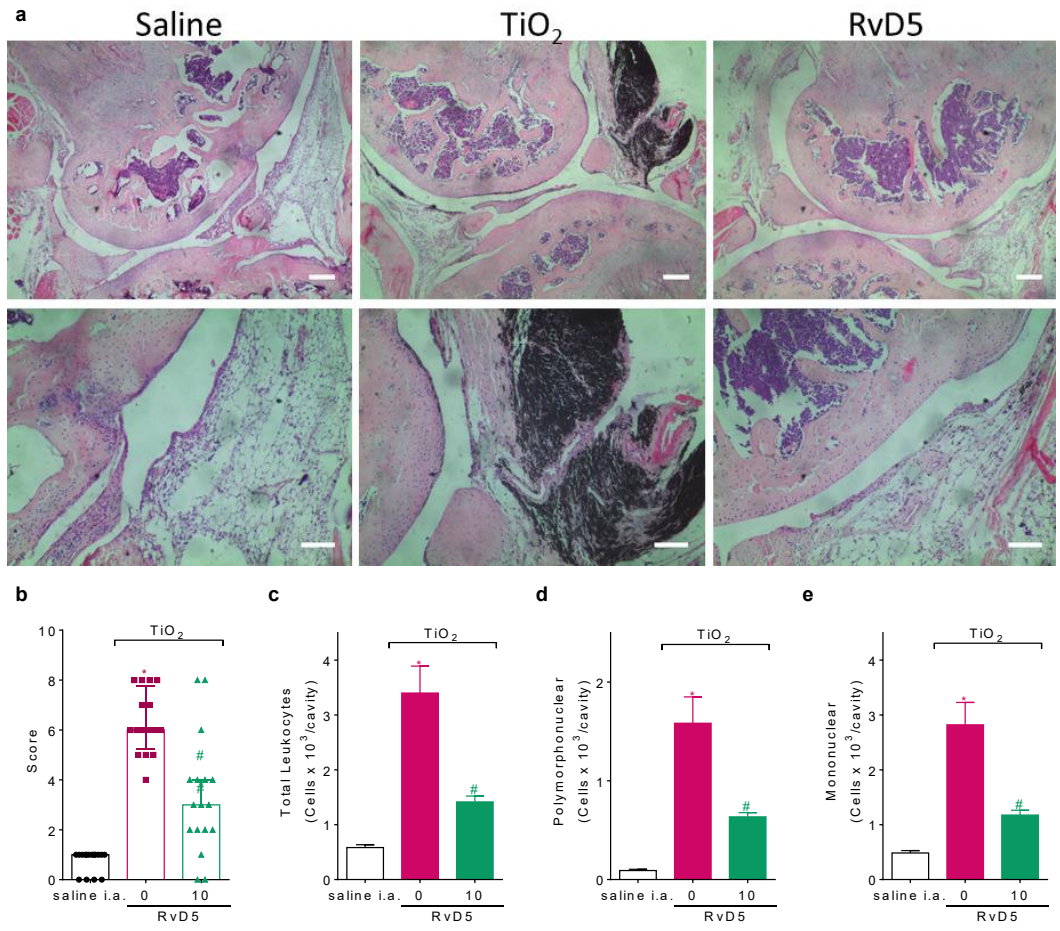

Fig 2. RvD5 inhibited TiO_2 chronic arthritis-induced histopathological damage and leukocyte recruitment. Mice were treated with 10 ng RvD5 every other 72h for 30 days starting 24h after TiO_2 stimulus. Representative photomicrography of saline, TiO_2, and RvD5 groups, histopathological score (b), total leukocytes (c), polymorphonuclear (d), and mononuclear cells (e) were evaluated after 30 days of TiO_2-induced chronic arthritis. Results are presented as median ± IQR (a) or mean ± SEM (c-e) of six mice per group per experiment and are representative of two separate experiments. *p < 0.05 compared to the saline group; #p < 0.05 compared to the TiO2 group, Kruskal-Wallis test followed by Dunn's post hoc (a) or One-way ANOVA followed by Tukey's post hoc (c-e). Scale bar 200 μm (upper line), 100 μm (lower line)

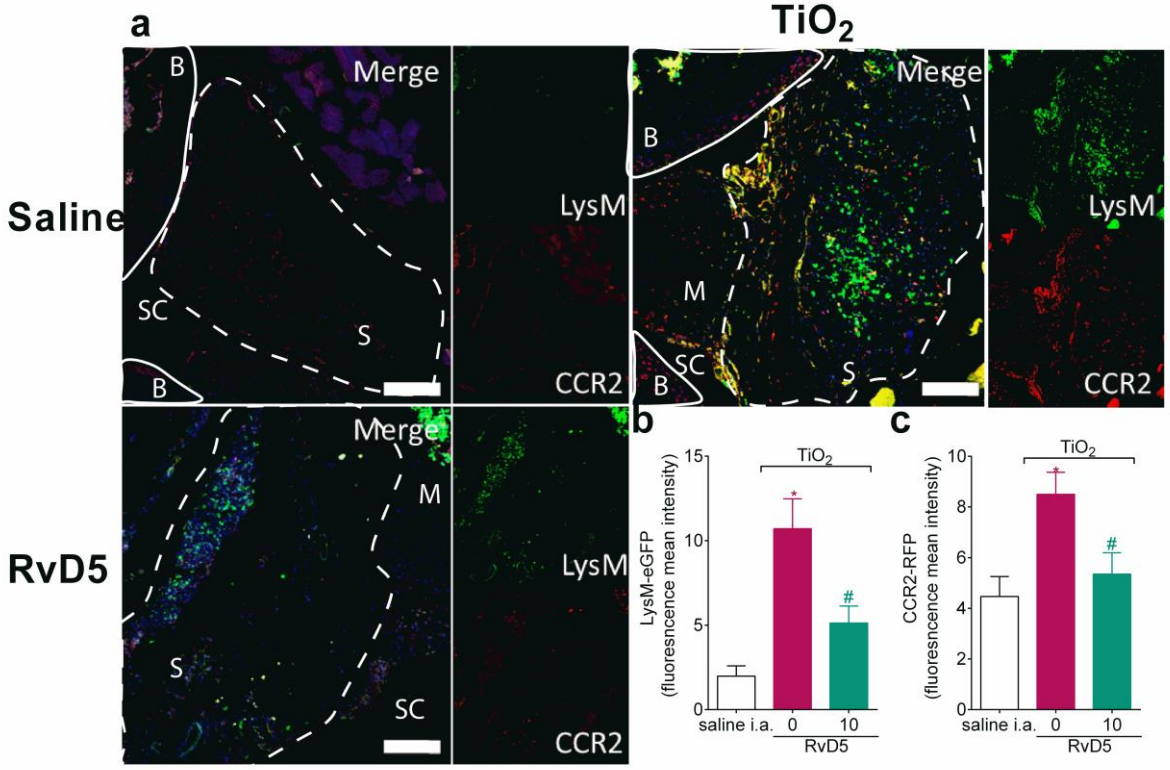

Fig 3 RvD5 inhibits TiO2-induced infiltrate of LysM+ and CCR2+ leukocytes. Mice were treated with 10 ng of RvD5 every other 72h up to 30 days starting 24h after TiO_2. Representative images of the groups Saline, TiO_2, and RvD5(a), $LysM^{+}$eGFP fluorescence mean intensity (b) and $CCR2^{+}$RFP fluorescence mean intensity (c). Results are presented as mean ± SEM of six mice per group per experiment and are representative of two separate experiments. *p < 0.05 compared to the saline group; #p < 0.05 compared to the TiO2 group, One-way ANOVA followed by Tukey's post hoc. Scale bar 100 μm. B= Bone; M= Meniscus S.C.= synovial cavity; S= synovial tissue.

3.3. RvD5 modules cytokine production

Inflammatory cytokines are produced by synoviocytes-like fibroblast and synoviocytes-like macrophages upon nanoparticles stimulus such as TiO_2 [4]. We addressed the effect of RvD5 in the mRNA expression *in vivo* after 30 days of chronic arthritis induced by TiO_2, and the cytokine release and NFκB activation in an *in vitro* approach in primed BMDM stimulated with TiO_2. RvD5 inhibited the TNFα (Fig 4a) and pro-IL-1β mRNA expression (Fig 4b) in chronic arthritis induced by TiO_2. Primed BMDM stimulated for 5h with TiO_2 released TNFα (Fig 4c) and IL-1β (Fig 4d) and a titrated curve dose-response of RvD5 inhibited TNFα (Fig 4c) release but not IL-1β (Fig 4d). Suggesting then RvD5 is modulating NFκB activation but not

inflammasome-induced IL-1β maturation. RvD5 or TiO_2 had no cytotoxicity effect in the BMDM, which was measured by the release of LDH in the supernatant, and triton treatment was used as a positive control of cytotoxicity (Fig 4g). The dose of 10 ng/mL was chosen for the next experiment since its abolished TNFα release. RvD5 inhibited the translocation of p-NFκB (Fig 4e,f) to the nucleus induced by TiO_2 stimulus in BMDM. Thus, RvD5 modulated cytokine expression in the knee joint and TNFα release in macrophages through inhibition of NFκB activation upon TiO_2.

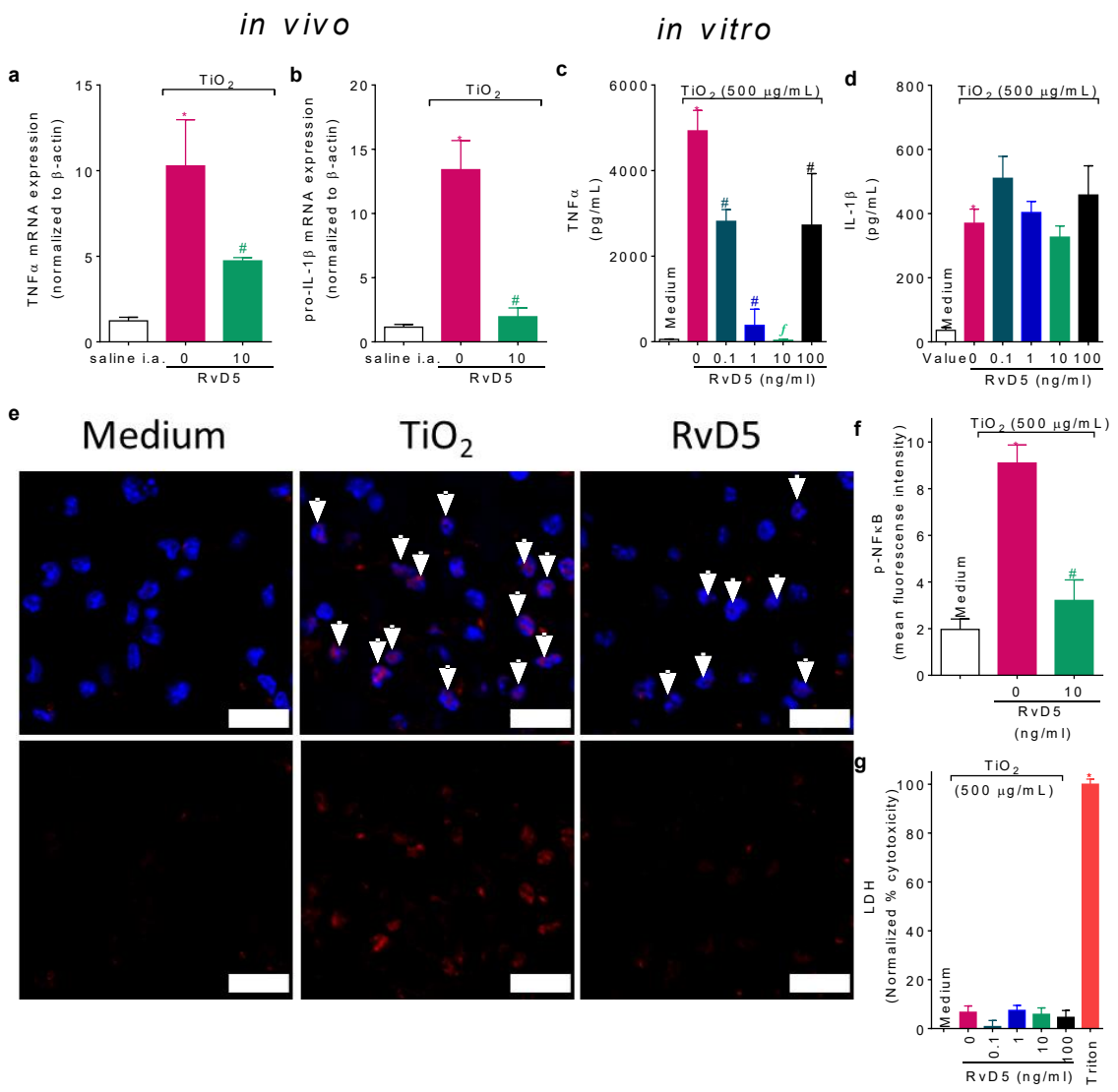

Fig 4. RvD5 modulates cytokine production. Mice were treated with 10 ng RvD5 every other 72h up to 30 days starting 24h after TiO_2 stimulus(a-b). TNFα (a) and pro-IL-1β (b) mRNA expression in chronic arthritis induced by TiO_2. TNFα (c) and IL-1β production (d) were evaluated in the supernatant of primed BMDM stimulated 5h withTiO_2. Representative images of merged images and the groups medium, TiO_2 and RvD5 (e) of p-NFκB mean

fluorescence intensity (f). Cytotoxicity induced by RvD5 was evaluated by the release of LDH in the supernatant (f). Results are presented as mean ± SEM of six measurements per group per experiment and are representative of two separate experiments. *p < 0.05 compared to the saline group; #p < 0.05 compared to the TiO2 group, One-way ANOVA followed by Tukey's post hoc. Scale bar 20μm. Arrowheads positive nuclear p-NFκB.

3.4. RvD5 inhibits oxidative stress induced by TiO_2

TiO_2 uptake by resident cells in the joint induces oxidative stress with a decrease in antioxidant response and increase in the oxidants release [4]. Here we sought that RvD5 would decrease the oxidative stress in chronic arthritis induced by TiO_2. RvD5 reestablished the total antioxidant response in the joint tissue decreased by TiO_2 stimulus after 30 days of chronic arthritis (Fig 5a,b). In addition, TiO_2 increased the mRNA expression of $gp91^{phox}$ (Fig 5c) and iNOS (Fig 5d), enzymes responsible for the superoxide anion production by reduced nicotinamide adenine dinucleotide phosphate (NADPH) oxidase2 and nitric oxide by iNOS [20, 21]. TiO_2 increased the production of superoxide anion in the joint after 30 days of chronic arthritis (Fig 5e) and RvD5 treatment inhibited the mRNA expression of $gp91^{phox}$ (Fig 5c) and iNOS (Fig 5d) and the production of superoxide anion (Fig 5e). Thus, RvD5 inhibits oxidative stress induced by TiO_2 reestablishing the antioxidant capacity and decreasing the expression of enzymes related to nitric oxide production and superoxide anion release in the knee joint.

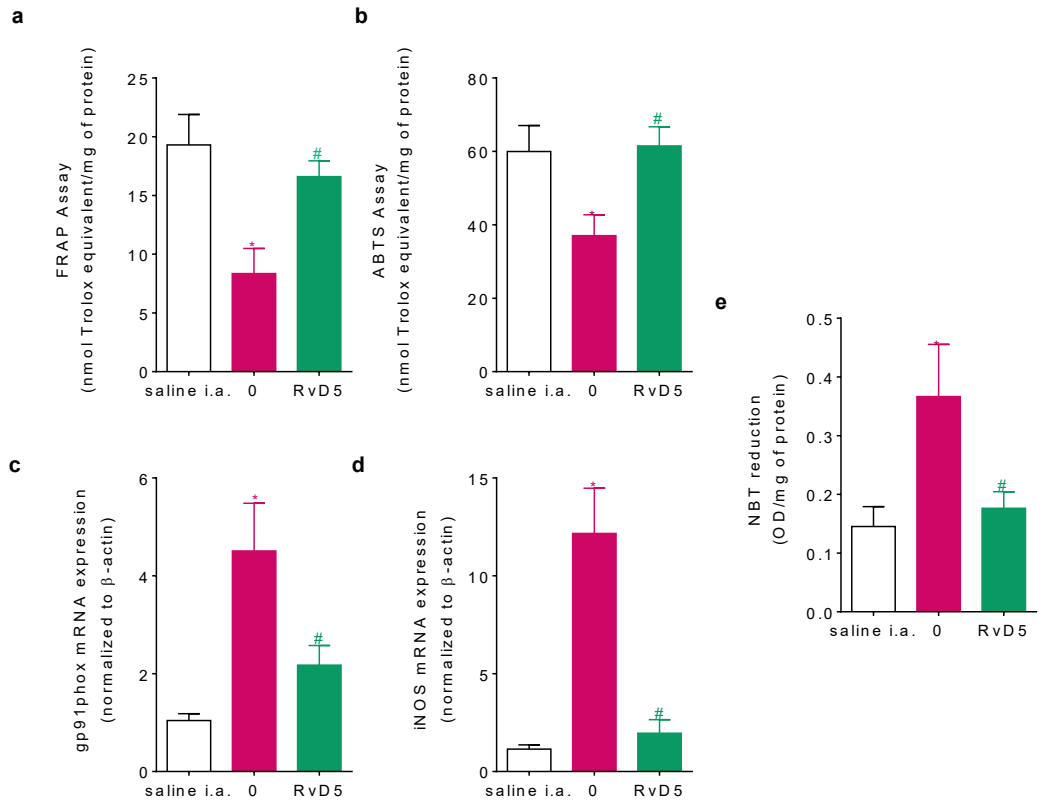

Fig 5 RvD5 inhibits oxidative stress induced by TiO_2 in chronic arthritis. Mice were treated with RvD5 every other 72h up 30 days starting 24h after TiO_2 stimulus. The total antioxidant capacity of the joint tissue was assessed by FRAP (a) and ABTS (b) assays. $Gp91^{phox}$ (c) iNOS mRNA expression (d) and superoxide anion production (e) were determined in chronic arthritis 30 days after TiO_2 stimulus. Results are presented as mean ± SEM of six mice per group per experiment and are representative of two separate experiments. *p < 0.05 compared to the saline group; #p < 0.05 compared to the TiO2 group, One-way ANOVA followed by Tukey's post hoc.

4. Discussion

Chronic arthritis induced by TiO_2 is a problem for some patients that went through arthroplasty or implanting that is made of titanium alloys [4, 5]. Besides this procedure has a beneficial outcome for the majority of the patients by improving quality of life and mobility. Some patients suffer from the nanoparticles loosening which induces inflammation and oxidative stress in the periprosthetic tissue or even migrate through the body inducing arthritis in another unrelated joint [3, 5, 22] Herein, we addressed the resolutive activity of RvD5, a DHA-derived pro-resolution lipid in chronic arthritis induced by a knee joint injection of TiO_2 which resembles prothesis-

like arthritis with nociceptive behavior, inflammation, oxidative stress and histopathological alteration such as synovitis, cartilage damage and bone resorption [14]. RvD5 inhibited the disease phenotype induced by TiO_2 involving pain, inflammation, destabilization in the weight ratio, edema, and histopathological damage induced by TiO_2-induced chronic arthritis. RvD5 inhibited the infiltrate of total leukocytes involving polymorphonuclear and mononuclear cells $LysM^+$ and $CCR2^+$, which are markers related to inflammatory polymorphonuclear and mononuclear cells [15, 16]. Mechanistically, RvD5 modulated TNFα and pro-IL-1β mRNA expression *in vivo* by inhibiting p-NFκB activation in macrophages, and also inhibited oxidative stress *in vivo*.

SPMs actively induce acute inflammation resolution by ceasing cellular events as neutrophil influx and activation, shaping macrophages responses inducing efferocytosis and phagocytoses for cleansing of inflammatory debris, inducing return of tissue homeostasis, and also causing pain relief by neuronal modulation [23]. Herein, RvD5 modulated ongoing pain with a dose in a nanograms range, and the treatment was repeated every other 72h up to 30 days after TiO_2 stimulus. Another DHA-derived induces analgesia with potent and long-lasting analgesia, MaR1 inhibits CFA-induced pain with one i.t. treatment for 5 days by decreasing neuronal activation with inhibition of mRNA for expression for TRPV1 and $Na_v1.8$ in DRG, which are important channels related to pain sensation and transmission [24]. Thus, demonstrating that DHA-derived molecules target the sensorial system. RvD5 administrated i.t. inhibited neuropathic pain induced by chemotherapy paclitaxel [25] suggesting its action in the sensorial system as well.

Inflammatory pain is induced by algesic molecules released by local and recruited immune cells [29]. Inflammatory cytokines and lipids act on their receptor on the innervating sensory neuron causing sensitization which lowers the neuronal threshold activation causing hyperalgesia (increased pain sensation) [24]. Thus, targeting the infiltration of inflammatory leukocytes accounts to induce analgesia. RvD5 inhibited the accumulation of $LysM^+$ and $CCR2^+$ leukocytes infiltration in synovial tissue after 30 days of chronic arthritis induced by TiO_2. Neutrophils recruitment contributes to pain induction with the release of PGE_2 [30], and $RvD5_{n\text{-}3\ DPA}$ through GRP101 inhibited joint edema and the release of PGE_2 in arthritis induced by arthritogenic serum in mice [26]. Herein, RvD5 inhibited mRNA expression of TNFα and pro-IL-1β in chronic arthritis induced by TiO_2. In aligning,

RvD5 inhibited nuclear translocation of p-NFκB and decreased the release of TNFα but no IL1-β in primed macrophages stimulated with TiO_2. Suggesting that modulatory activity in cytokines release by RvD5 is by inhibiting NFκB activation but not the inflammasome activation which is required for IL-1β maturation and release upon TiO_2 stimulus [31]. TNFα released in the joint induces pain in antigen-induced arthritis in rats and blocking it decreases nociception response [32]. Thus, RvD5 inhibited TNFα release in chronic arthritis induced by TiO_2 stimulus is aligned with its analgesic activity. In addition, anti-TNFα therapies have been suggested in cases of prosthesis loosening and bone degradation by decrease osteolysis [33, 34]. In a model of prothesis-induced osteolysis, etanercept inhibits calvaria osteolysis induced by titanium particles. Anti-TNFα therapies have side effects such as infections due to the role of TNFa during infectious diseases [19] and using SPM molecules would benefit patients since such molecules induce the resolution, increases the response to infections lowering the requirement of antibiotics rather than reducing the inflammatory responses and immune responses required to fight against infections [13]. It remains to be elucidated whether RvD5 inhibits the osteolysis in TiO_2-induced chronic arthritis. But is noteworthy that, resolvin E1 promotes bone regeneration in periodontitis [35] and decreases osteoclast differentiation and activity [36]. In addition, using a nano-pro-resolving mediator analog to Lipoxin A_4 (benzo-lipoxin A4, $bLXA_4$) counteracts bone loss with a 2-fold increase in bone regeneration compared to bLXA4 without the nanoformulation in periodontitis-induced bone loss in miniature pigs.

Oxidative stress in chronic arthritis-related to prosthesis occurs by nanoparticles increasing the production of free radicals and decreasing the antioxidant response in the knee joint [14, 37]. Macrophages uptake titanium nanoparticles inducing an oxidative response [38, 39]. Herein, RvD5 inhibited the oxidative by increasing the total antioxidant capacity and decreased the superoxide anion production accompanied by a decrease in the mRNA expression of the catalytic NADPH oxidase-2 sub-unit ($gp91^{phox}$) and iNOS, which produces nitric oxide that reacts with superoxide anion producing peroxynitrite [40]. Free radicals such as superoxide anion and peroxynitrite induce pain [41, 42]. Thus RvD5 inhibition of oxidative stress is aligned with its analgesic activity since improving antioxidant capacity reduces the availability of free radicals that induces pain. In agreement, MaR1 inhibited skin inflammation and damage induced by UVB radiation exposure in

mice by reducing the oxidative response, increasing the antioxidant capacity by restoring GSH levels, and decreasing the production of superoxide anion and mRNA expression for $gp91^{phox}$ [19]. Therefore, our data support that RvD5 is a conceivable approach in prosthesis and implants loosening nanoparticles and inducing chronic arthritis. Herein, RvD5 resolved the disease phenotype of TiO_2-induced chronic arthritis inhibiting nociceptive behavior and edema, inhibited the accumulation of polymorphonuclear and mononuclear $LysM^+$ and $CCR2^+$ cells in the knee joint. RvD5 reduced the deleterious actions of TiO_2 inhibiting TNFα production through inhibition of NFκB activation and oxidative stress.

Funding

Coordenação de Aperfeiçoamento de Pessoal de Nível Superior (CAPES; Finance Code 001), and Programa de Pesquisa para o SUS (PPSUS) grant supported by Ministério da Ciência, Tecnologia e Inovação (MCTI), Secretaria da Ciência, Tecnologia e Ensino Superior (SETI), Decit/SCTIE/MS through CNPq with the support of Fundação Araucária and Secretaria da Saúde do Estado do Paraná (SESA-PR), and Parana State Government (Brazil).

References

1. Khan, M., et al., *The epidemiology of failure in total knee arthroplasty: avoiding your next revision.* Bone Joint J, 2016. **98-B**(1 Suppl A): p. 105-12.

2. Sargeant, A. and T. Goswami, *Pathophysiological aspects of hip implants.* Journal of surgical orthopaedic advances, 2006. **15**(2): p. 111-2.

3. Cobelli, N., et al., *Mediators of the inflammatory response to joint replacement devices.* Nature Publishing Group, 2011. **7**(10): p. 600-608.

4. Wang, J., L. Wang, and Y. Fan, *Adverse Biological Effect of TiO(2) and Hydroxyapatite Nanoparticles Used in Bone Repair and Replacement.* Int J Mol Sci, 2016. **17**(6).

5. Dörner, T., et al., *Implant-related inflammatory arthritis.* Nature Clinical Practice Rheumatology, 2006. **2**(1): p. 53-56.

6. Goodman, S.B., *Wear particles, periprosthetic osteolysis and the immune system.* Biomaterials, 2007. **28**(34): p. 5044-8.

7. Danks, L., et al., *RANKL expressed on synovial fibroblasts is primarily responsible for bone erosions during joint inflammation.* Annals of the Rheumatic Diseases, 2016. **75**(6): p. 1187-1195.

8. O'Brien, W., et al., *RANK-Independent Osteoclast Formation and Bone Erosion in Inflammatory Arthritis.* Arthritis & Rheumatology, 2016. **68**(12): p. 2889-2900.

9. Serhan, C.N., N. Chiang, and J. Dalli, *The resolution code of acute inflammation: Novel pro-resolving lipid mediators in resolution.* Seminars in Immunology, 2015. **27**(3): p. 200-215.

10. Hsiao, H.-M., et al., *A novel anti-inflammatory and pro-resolving role for resolvin D1 in acute cigarette smoke-induced lung inflammation.* PloS one, 2013. **8**(3): p. e58258-e58258.

11. Croasdell, A., et al., *Resolvins attenuate inflammation and promote resolution in cigarette smoke-exposed human macrophages.* American journal of physiology. Lung cellular and molecular physiology, 2015. **309**(8): p. L888-901.

12. Arnardottir, H.H., et al., *Resolvin D3 Is Dysregulated in Arthritis and Reduces Arthritic Inflammation.* Journal of immunology (Baltimore, Md. : 1950), 2016(August).

13. Guerrero, A.T.G., et al., *Hypernociception elicited by tibio-tarsal joint flexion in mice: a novel experimental arthritis model for pharmacological screening.* Pharmacology, biochemistry, and behavior, 2006. **84**(2): p. 244-51.

14. Manchope, M.F., et al., *Naringenin mitigates titanium dioxide (TiO2)-induced chronic arthritis in mice: role of oxidative stress, cytokines, and NFkappaB.* Inflamm Res, 2018. **67**(11-12): p. 997-1012.

15. Sullivan, D.P., et al., *In vivo imaging reveals unique neutrophil transendothelial migration patterns in inflamed intestines.* Mucosal Immunol, 2018. **11**(6): p. 1571-1581.

16. Braga, T.T., et al., *CCR2 contributes to the recruitment of monocytes and leads to kidney inflammation and fibrosis development.* Inflammopharmacology, 2018. **26**(2): p. 403-411.

17. Marim, F.M., et al., *A method for generation of bone marrow-derived macrophages from cryopreserved mouse bone marrow cells.* PLoS One, 2010. **5**(12): p. e15263.

18. Katalinic, V., et al., *Gender differences in antioxidant capacity of rat tissues determined by 2,2'-azinobis (3-ethylbenzothiazoline 6-sulfonate; ABTS) and ferric reducing antioxidant power (FRAP) assays.* Comparative biochemistry and physiology. Toxicology & pharmacology : CBP, 2005. **140**(1): p. 47-52.

19. Cezar, T.L.C., et al., *Treatment with maresin 1, a docosahexaenoic acid-derived pro-resolution lipid, protects skin from inflammation and oxidative stress caused by UVB irradiation.* Sci Rep, 2019. **9**(1): p. 3062.

20. Babior, B.M., *NADPH oxidase.* Current Opinion in Immunology, 2004. **16**: p. 42-47.

21. Aktan, F., *iNOS-mediated nitric oxide production and its regulation.* Life Sci, 2004. **75**(6): p. 639-53.

22. Carr, A.J., et al., *Knee replacement.* The Lancet, 2012. **379**(9823): p. 1331-1340.

23. Basil, M.C. and B.D. Levy, *Specialized pro-resolving mediators: endogenous regulators of infection and inflammation.* Nat Rev Immunol, 2016. **16**(1): p. 51-67.

24. Pinho-Ribeiro, F.A., W.A. Verri, and I.M. Chiu, *Nociceptor Sensory Neuron–Immune Interactions in Pain and Inflammation.* Trends in Immunology, 2017. **38**(1): p. 5-19.

25. Luo, X., et al., *Resolvin D5 Inhibits Neuropathic and Inflammatory Pain in Male But Not Female Mice: Distinct Actions of D-Series Resolvins in Chemotherapy-Induced Peripheral Neuropathy.* Front Pharmacol, 2019. **10**: p. 745.

26. Flak, M.B., et al., *GPR101 mediates the pro-resolving actions of RvD5n-3 DPA in arthritis and infections.* J Clin Invest, 2020. **130**(1): p. 359-373.

27. Fattori, V., et al., *Specialized pro-resolving lipid mediators: A new class of non-immunosuppressive and non-opioid analgesic drugs.* Pharmacol Res, 2020. **151**: p. 104549.

28. Visel, A., C. Thaller, and G. Eichele, *GenePaint.org: an atlas of gene expression patterns in the mouse embryo.* Nucleic Acids Res, 2004. **32**(Database issue): p. D552-6.

29. Verri, W.A., et al., *Hypernociceptive role of cytokines and chemokines: Targets for analgesic drug development?* Pharmacology & Therapeutics, 2006. **112**(1): p. 116-138.

30. Cunha, T.M., et al., *Crucial role of neutrophils in the development of mechanical inflammatory hypernociception.* Journal of Leukocyte Biology, 2008. **83**(4): p. 824-832.

31. Kolling, J., et al., *Evaluation of the NLRP3 Inflammasome Activating Effects of a Large Panel of TiO2 Nanomaterials in Macrophages.* Nanomaterials (Basel), 2020. **10**(9).

32. Schaible, H.G., et al., *The role of proinflammatory cytokines in the generation and maintenance of joint pain.* Ann N Y Acad Sci, 2010. **1193**: p. 60-9.

33. Schwarz, E.M., R.J. Looney, and R.J. O'Keefe, *Anti-TNF-alpha therapy as a clinical intervention for periprosthetic osteolysis.* Arthritis Res, 2000. **2**(3): p. 165-8.

34. Childs, L.M., et al., *Efficacy of etanercept for wear debris-induced osteolysis.* J Bone Miner Res, 2001. **16**(2): p. 338-47.

35. Hasturk, H., et al., *Resolvin E1 regulates inflammation at the cellular and tissue level and restores tissue homeostasis in vivo.* J Immunol, 2007. **179**(10): p. 7021-9.

36. Herrera, B.S., et al., *An endogenous regulator of inflammation, resolvin E1, modulates osteoclast differentiation and bone resorption.* Br J Pharmacol, 2008. **155**(8): p. 1214-23.

37. Borghi, S.M., et al., *The flavonoid quercetin inhibits titanium dioxide (TiO2)-induced chronic arthritis in mice.* J Nutr Biochem, 2017. **53**: p. 81-95.

38. Olmedo, D.G., et al., *Effect of titanium dioxide on the oxidative metabolism of alveolar macrophages: an experimental study in rats.* J Biomed Mater Res A, 2005. **73**(2): p. 142-9.

39. Kang, J.L., et al., *Comparison of the biological activity between ultrafine and fine titanium dioxide particles in RAW 264.7 cells associated with oxidative stress.* J Toxicol Environ Health A, 2008. **71**(8): p. 478-85.

40. Szabo, C., H. Ischiropoulos, and R. Radi, *Peroxynitrite: biochemistry, pathophysiology and development of therapeutics.* Nat Rev Drug Discov, 2007. **6**(8): p. 662-80.

41. Ndengele, M.M., et al., *Cyclooxygenases 1 and 2 contribute to peroxynitrite-mediated inflammatory pain hypersensitivity.* The FASEB journal : official publication of the Federation of American Societies for Experimental Biology, 2008. **22**: p. 3154-3164.

42. Maioli, N.A., et al., *The superoxide anion donor, potassium superoxide, induces pain and inflammation in mice through production of reactive oxygen species and cyclooxygenase-2.* Brazilian journal of medical and biological research = Revista brasileira de pesquisas médicas e biológicas / Sociedade Brasileira de Biofísica ... [et al.], 2015. **48**(4): p. 321-31.

5. CONCLUSÃO

A dor articular envolve mecanismos inflamatórios periféricos, e sensoriais a nível periférico do DRG e central da medula espinal. Abordagens terapêuticas que resolvam o processo inflamatório periférico, modulem a atividade do nociceptor, inibam a ativação de células da glia e neuroinflamação na medula espinal são importantes no contexto da dor articular. Os SPMs são uma classe de moléculas com mecanismos de ação que induzem a resolução da inflamação, inibem a ativação do nociceptor, e neuroinflamação a nível da medula espinal. Neste trabalho demonstrou-se que a RvD5 induz a resolução do processo inflamatório reduzindo o infiltrado leucocitário e dano histopatológico, estresse oxidativo e expressão e de citocinas pró-inflamatórias. A nível do sistema sensorial, a RvD5 reduz a ativação de neurônios primários, e especial de neurônios peptidérgicos $CGRP^{+}$. A nível espinal a RvD5 inibe a neuroinflamação reduzindo a expressão de RNAm para marcadores da ativação de células da glia e expressão de citocinas pró-inflamatórias e do receptor ST2. Demonstrando que a RvD5 é uma abordagem interessante no contexto da dor articular que envolve mecanismos complexos. Portanto, a RvD5 se mostra eficaz modulando tanto o sistema imune induzindo a resolução da inflamação quanto no sistema somatossensorial resultando em uma redução da dor articular.

REFERÊNCIAS

ABBAS, A. K.; KUMAR, V.; FAUSTO, N. **Robbins & Cotran:Patologia -Bases Patológicas das Doenças**. Elsevier, 2016. 1440-1440 p.

AICH, A.; AFRIN, L. B.; GUPTA, K. Mast Cell-Mediated Mechanisms of Nociception. **Int J Mol Sci**, 16, n. 12, p. 29069-29092, Dec 4 2015.

ARNARDOTTIR, H. H.; DALLI, J.; NORLING, L. V.; COLAS, R. A. *et al.* Resolvin D3 Is Dysregulated in Arthritis and Reduces Arthritic Inflammation. **Journal of immunology (Baltimore, Md. : 1950)**, n. August, 2016.

BAISCH, B. L.; CORSON, N. M.; WADE-MERCER, P.; GELEIN, R. *et al.* Equivalent titanium dioxide nanoparticle deposition by intratracheal instillation and whole body inhalation: the effect of dose rate on acute respiratory tract inflammation. **Particle and fibre toxicology**, 11, p. 5-5, 2014.

BAS, D. B.; SU, J.; WIGERBLAD, G.; SVENSSON, C. I. Pain in rheumatoid arthritis: models and mechanisms. **Pain Manag**, 6, n. 3, p. 265-284, 2016.

BASBAUM, A. I.; BAUTISTA, D. M.; SCHERRER, G.; JULIUS, D. Cellular and molecular mechanisms of pain. **Cell**, 139, n. 2, p. 267-284, Oct 16 2009.

BORGHI, S. M.; MIZOKAMI, S. S.; PINHO-RIBEIRO, F. A.; FATTORI, V. *et al.* The flavonoid quercetin inhibits titanium dioxide (TiO2)-induced chronic arthritis in mice. **J Nutr Biochem**, 53, p. 81-95, Nov 5 2017.

BOTTARO, D.; SHEPRO, D.; PETERSON, S.; HECHTMAN, H. B. Serotonin, norepinephrine, and histamine mediation of endothelial cell barrier function in vitro. **Journal of Cellular Physiology**, 128, n. 2, p. 189-194, 1986.

BRAIN, S. D.; WILLIAMS, T. J. Interactions between the tachykinins and calcitonin gene-related peptide lead to the modulation of oedema formation and blood flow in rat skin. **Br J Pharmacol**, 97, n. 1, p. 77-82, May 1989.

BRAZ, J.; SOLORZANO, C.; WANG, X.; BASBAUM, Allan I. Transmitting Pain and Itch Messages: A Contemporary View of the Spinal Cord Circuits that Generate Gate Control. **Neuron**, 82, n. 3, p. 522-536, 2014.

BRENTANO, F.; SCHORR, O.; GAY, R. E.; GAY, S. *et al.* RNA released from necrotic synovial fluid cells activates rheumatoid arthritis synovial fibroblasts via Toll-like receptor 3. **Arthritis Rheum**, 52, n. 9, p. 2656-2665, Sep 2005.

BUSHNELL, M. C.; ČEKO, M.; LOW, L. A. Cognitive and emotional control of pain and its disruption in chronic pain. **Nature Reviews Neuroscience**, 14, n. 7, p. 502-511, 2013.

CHEN, J.; DONG, X.; ZHAO, J.; TANG, G. In vivo acute toxicity of titanium dioxide nanoparticles to mice after intraperitioneal injection. **Journal of applied toxicology : JAT**, 29, n. 4, p. 330-337, 2009.

CHIANG, N.; FREDMAN, G.; BACKHED, F.; OH, S. F. *et al.* Infection regulates pro-resolving mediators that lower antibiotic requirements. **Nature**, 484, n. 7395, p. 524-528, Apr 25 2012.

CHIU, I. M.; VON HEHN, C. A.; WOOLF, C. J. Neurogenic inflammation and the peripheral nervous system in host defense and immunopathology. **Nat Neurosci**, 15, n. 8, p. 1063-1067, Jul 26 2012.

CHU, C.; ARTIS, D.; CHIU, I. M. Neuro-immune Interactions in the Tissues. **Immunity**, 52, n. 3, p. 464-474, Mar 17 2020.

COBB, A. G.; SCHMALZREID, T. P. The clinical significance of metal ion release from cobalt-chromium metal-on-metal hip joint arthroplasty. **Proceedings of the Institution of Mechanical Engineers. Part H, Journal of engineering in medicine**, 220, n. 2, p. 385-398, 2006.

COBELLI, N.; SCHARF, B.; CRISI, G. M.; HARDIN, J. *et al.* Mediators of the inflammatory response to joint replacement devices. **Nature Publishing Group**, 7, n. 10, p. 600-608, 2011.

COELHO, F. M.; PINHO, V.; AMARAL, F. A.; SACHS, D. *et al.* The chemokine receptors CXCR1/CXCR2 modulate antigen-induced arthritis by regulating adhesion of neutrophils to the synovial microvasculature. **Arthritis Rheum**, 58, n. 8, p. 2329-2337, Aug 2008.

COX, J. J.; REIMANN, F.; NICHOLAS, A. K.; THORNTON, G. *et al.* An SCN9A channelopathy causes congenital inability to experience pain. **Nature**, 444, n. 7121, p. 894-898, Dec 14 2006.

CROASDELL, A.; THATCHER, T. H.; KOTTMANN, R. M.; COLAS, R. A. *et al.* Resolvins attenuate inflammation and promote resolution in cigarette smoke-exposed human macrophages. **American journal of physiology. Lung cellular and molecular physiology**, 309, n. 8, p. L888-901, 2015.

CUMPSTEY, A.; FEELISCH, M. Free Radicals in Inflammation. **Inflammation**, p. 695-726, 2017/12/11 2017. https://doi.org/10.1002/9783527692156.ch27.

CUNHA, F. Q.; CACINI, A. T.; FERREIRA, S. H. Inhibition of the release of a neutrophil chemotactic factor from macrophages partially explains the anti-inflammatory action of glucocorticoids. **Agents and actions**, 17, n. 3-4, p. 314-317, 1986.

CUNHA, F. Q.; POOLE, S.; LORENZETTI, B. B.; FERREIRA, S. H. The pivotal role of tumour necrosis factor alpha in the development of inflammatory hyperalgesia. **Br J Pharmacol**, 107, n. 3, p. 660-664, Nov 1992.

CUNHA, T. M.; VERRI, W. A.; SCHIVO, I. R.; NAPIMOGA, M. H. *et al.* Crucial role of neutrophils in the development of mechanical inflammatory hypernociception. **Journal of Leukocyte Biology**, 83, n. 4, p. 824-832, 2008.

CUNHA, T. M.; VERRI, W. A.; SILVA, J. S.; POOLE, S. *et al.* A cascade of cytokines mediates mechanical inflammatory hypernociception in mice. **Proceedings of the National Academy of Sciences of the United States of America**, 102, n. 5, p. 1755-1760, 2005.

DANKS, L.; KOMATSU, N.; GUERRINI, M. M.; SAWA, S. *et al.* RANKL expressed on synovial fibroblasts is primarily responsible for bone erosions during joint inflammation. **Annals of the Rheumatic Diseases**, 75, n. 6, p. 1187-1195, 2016.

DEAN, R. A.; COX, J. H.; BELLAC, C. L.; DOUCET, A. *et al.* Macrophage-specific metalloelastase (MMP-12) truncates and inactivates ELR+ CXC chemokines and generates CCL2, -7, -8, and -13 antagonists: potential role of the macrophage in terminating polymorphonuclear leukocyte influx. **Blood**, 112, n. 8, p. 3455-3464, Oct 15 2008.

DÖRNER, T.; HAAS, J.; LODDENKEMPER, C.; VON BAEHR, V. *et al.* Implant-related inflammatory arthritis. **Nature Clinical Practice Rheumatology**, 2, n. 1, p. 53-56, 2006.

DUNFORD, R.; SALINARO, A.; CAI, L.; SERPONE, N. *et al.* Chemical oxidation and DNA damage catalysed by inorganic sunscreen ingredients. **FEBS letters**, 418, n. 1-2, p. 87-90, 1997.

EBBINGHAUS, M.; UHLIG, B.; RICHTER, F.; VON BANCHET, G. S. *et al.* The role of interleukin-1beta in arthritic pain: main involvement in thermal, but not mechanical, hyperalgesia in rat antigen-induced arthritis. **Arthritis Rheum**, 64, n. 12, p. 3897-3907, Dec 2012.

ELLIOTT, M. R.; CHEKENI, F. B.; TRAMPONT, P. C.; LAZAROWSKI, E. R. *et al.* Nucleotides released by apoptotic cells act as a find-me signal to promote phagocytic clearance. **Nature**, 461, n. 7261, p. 282-286, Sep 10 2009.

FEIN, A. **Nociceptors and the perception of pain**. Farmington, CT: University of Connecticut Health Center, 2012 (Revised), 2012. 153-153 p.

FERREIRA, S. H.; FERRARI, L. F.; CUNHA, T. M.; NASCIMENTO, P. G. B. D. *et al.* Dor Inflamatória. *In*, 2009. p. 1438-1438.

FLAK, M. B.; KOENIS, D. S.; SOBRINO, A.; SMITH, J. *et al.* GPR101 mediates the pro-resolving actions of RvD5n-3 DPA in arthritis and infections. **J Clin Invest**, 130, n. 1, p. 359-373, Jan 2 2020.

FOXMAN, E. F.; CAMPBELL, J. J.; BUTCHER, E. C. Multistep navigation and the combinatorial control of leukocyte chemotaxis. **The Journal of cell biology**, 139, n. 5, p. 1349-1360, 1997.

GIERUT, A.; PERLMAN, H.; POPE, R. M. Innate immunity and rheumatoid arthritis. **Rheum Dis Clin North Am**, 36, n. 2, p. 271-296, May 2010.

GIRBL, T.; LENN, T.; PEREZ, L.; ROLAS, L. *et al.* Distinct Compartmentalization of

the Chemokines CXCL1 and CXCL2 and the Atypical Receptor ACKR1 Determine Discrete Stages of Neutrophil Diapedesis. **Immunity**, 49, n. 6, p. 1062-1076 e1066, Dec 18 2018.

GLOIRE, G.; PIETTE, J. Redox Regulation of Nuclear Post-Translational Modifications During NF-κB Activation. **Antioxidants & Redox Signaling**, 11, n. 9, p. 2209-2222, 2009.

GODINHO-SILVA, C.; CARDOSO, F.; VEIGA-FERNANDES, H. Neuro-Immune Cell Units: A New Paradigm in Physiology. **Annu Rev Immunol**, 37, p. 19-46, Apr 26 2019.

GOODMAN, S. B. Wear particles, periprosthetic osteolysis and the immune system. **Biomaterials**, 28, n. 34, p. 5044-5048, 2007.

GUDE, D. R.; ALVAREZ, S. E.; PAUGH, S. W.; MITRA, P. *et al.* Apoptosis induces expression of sphingosine kinase 1 to release sphingosine-1-phosphate as a "come-and-get-me" signal. **FASEB J**, 22, n. 8, p. 2629-2638, Aug 2008.

GUDES, S.; BARKAI, O.; CASPI, Y.; KATZ, B. *et al.* The role of slow and persistent TTX-resistant sodium currents in acute tumor necrosis factor-alpha-mediated increase in nociceptors excitability. **J Neurophysiol**, 113, n. 2, p. 601-619, Jan 15 2015.

GUERRERO, A. T. G.; VERRI, W. A.; CUNHA, T. M.; SILVA, T. A. *et al.* Involvement of LTB4 in zymosan-induced joint nociception in mice: participation of neutrophils and PGE2. **Journal of leukocyte biology**, 83, n. 1, p. 122-130, 2008.

GURR, J.-R.; WANG, A. S. S.; CHEN, C.-H.; JAN, K.-Y. Ultrafine titanium dioxide particles in the absence of photoactivation can induce oxidative damage to human bronchial epithelial cells. **Toxicology**, 213, n. 1-2, p. 66-73, 2005.

HARRIS, W. H. Wear and periprosthetic osteolysis the problem. **Clinical orthopaedics and related research**, n. 393, p. 66-70, 2001.

HARRIS, W. H.; SCHILLER, A. L.; SCHOLLER, J. M.; FREIBERG, R. A. *et al.* Extensive localized bone resorption in the femur following total hip replacement. **The Journal of bone and joint surgery. American volume**, 58, n. 5, p. 612-618, 1976.

HE, M.; KUBO, H.; MORIMOTO, K.; FUJINO, N. *et al.* Receptor for advanced glycation end products binds to phosphatidylserine and assists in the clearance of apoptotic cells. **EMBO Rep**, 12, n. 4, p. 358-364, Apr 2011.

HOLMSTRÖM, K. M.; FINKEL, T. Cellular mechanisms and physiological consequences of redox-dependent signalling. **Nature Reviews Molecular Cell Biology**, 15, n. 6, p. 411-421, 2014.

HSIAO, H. M.; THATCHER, T. H.; COLAS, R. A.; SERHAN, C. N. *et al.* Resolvin D1 reduces emphysema and chronic inflammation. **American Journal of Pathology**, 185, n. 12, p. 3189-3201, 2015.

JAMALUDDIN, M.; WANG, S.; BOLDOGH, I.; TIAN, B. *et al.* TNF-α-induced NF-κB/RelA Ser276 phosphorylation and enhanceosome formation is mediated by an ROS-dependent PKAc pathway. **Cellular Signalling**, 19, n. 7, p. 1419-1433, 2007.

JI, R.-R.; XU, Z.-Z.; GAO, Y.-J. Emerging targets in neuroinflammation-driven chronic pain. **Nature Reviews Drug Discovery**, 13, n. 7, p. 533-548, 2014.

JI, R. R.; NACKLEY, A.; HUH, Y.; TERRANDO, N. *et al.* Neuroinflammation and Central Sensitization in Chronic and Widespread Pain. **Anesthesiology**, 129, n. 2, p. 343-366, Aug 2018.

JIN, X.; GEREAU, R. W. Acute p38-Mediated Modulation of Tetrodotoxin-Resistant Sodium Channels in Mouse Sensory Neurons by Tumor Necrosis Factor. **Journal of Neuroscience**, 26, n. 1, p. 246-255, 2006.

JORDAN, P. M.; GERSTMEIER, J.; PACE, S.; BILANCIA, R. *et al.* Staphylococcus aureus-Derived alpha-Hemolysin Evokes Generation of Specialized Pro-resolving Mediators Promoting Inflammation Resolution. **Cell Rep**, 33, n. 2, p. 108247, Oct 13 2020.

JULIUS, D. TRP channels and pain. **Annu Rev Cell Dev Biol**, 29, p. 355-384, 2013.

JULIUS, D.; BASBAUM, A. I. Molecular mechanisms of nociception. **Nature**, 413, n. 6852, p. 203-210, 2001.

KASHEM, S. W.; RIEDL, M. S.; YAO, C.; HONDA, C. N. *et al.* Nociceptive Sensory Fibers Drive Interleukin-23 Production from CD301b+ Dermal Dendritic Cells and Drive Protective Cutaneous Immunity. **Immunity**, 43, n. 3, p. 515-526, Sep 15 2015.

KILPATRICK, L. E.; SUN, S.; LI, H.; VARY, T. C. *et al.* Regulation of TNF-induced oxygen radical production in human neutrophils: role of delta-PKC. **Journal of leukocyte biology**, 87, n. 1, p. 153-164, 2010.

LASTRUCCI, C.; BAILLIF, V.; BEHAR, A.; AL SAATI, T. *et al.* Molecular and cellular profiles of the resolution phase in a damage-associated molecular pattern (DAMP)-mediated peritonitis model and revelation of leukocyte persistence in peritoneal tissues. **FASEB J**, 29, n. 5, p. 1914-1929, May 2015.

LAUBER, K.; BOHN, E.; KROBER, S. M.; XIAO, Y. J. *et al.* Apoptotic cells induce migration of phagocytes via caspase-3-mediated release of a lipid attraction signal. **Cell**, 113, n. 6, p. 717-730, Jun 13 2003.

LAZAR, P.; REDDINGTON, M.; STREIT, W.; RAIVICH, G. *et al.* The action of calcitonin gene-related peptide on astrocyte morphology and cyclic AMP accumulation in astrocyte cultures from neonatal rat brain. **Neurosci Lett**, 130, n. 1, p. 99-102, Sep 2 1991.

LEE, Y. C.; CUI, J.; LU, B.; FRITS, M. L. *et al.* Pain persists in DAS28 rheumatoid arthritis remission but not in ACR/EULAR remission: a longitudinal observational

study. **Arthritis Res Ther**, 13, n. 3, p. R83, Jun 8 2011.

LEIPE, J.; GRUNKE, M.; DECHANT, C.; REINDL, C. *et al.* Role of Th17 cells in human autoimmune arthritis. **Arthritis Rheum**, 62, n. 10, p. 2876-2885, Oct 2010.

LEVY, B. D.; CLISH, C. B.; SCHMIDT, B.; GRONERT, K. *et al.* Lipid mediator class switching during acute inflammation: signals in resolution. **Nature immunology**, 2, n. 7, p. 612-619, 2001.

LOONEY, R. J.; SCHWARZ, E. M.; BOYD, A.; O'KEEFE, R. J. Periprosthetic osteolysis: an immunologist's update. **Current opinion in rheumatology**, 18, n. 1, p. 80-87, 2006.

LÓPEZ-SEPÚLVEDA, R.; GÓMEZ-GUZMÁN, M.; ZARZUELO, Maria J.; ROMERO, M. *et al.* Red wine polyphenols prevent endothelial dysfunction induced by endothelin-1 in rat aorta: role of NADPH oxidase. **Clinical Science**, 120, n. 8, p. 321-333, 2011.

LUO, X.; GU, Y.; TAO, X.; SERHAN, C. N. *et al.* Resolvin D5 Inhibits Neuropathic and Inflammatory Pain in Male But Not Female Mice: Distinct Actions of D-Series Resolvins in Chemotherapy-Induced Peripheral Neuropathy. **Front Pharmacol**, 10, p. 745, 2019.

MADERNA, P.; GODSON, C. Lipoxins: resolutionary road. **British journal of pharmacology**, 158, n. 4, p. 947-959, 2009.

MANCHOPE, M. F.; ARTERO, N. A.; FATTORI, V.; MIZOKAMI, S. S. *et al.* Naringenin mitigates titanium dioxide (TiO2)-induced chronic arthritis in mice: role of oxidative stress, cytokines, and NFkappaB. **Inflamm Res**, 67, n. 11-12, p. 997-1012, Dec 2018.

MANCHOPE, M. F.; CASAGRANDE, R.; VERRI, J. W. A.; MANCHOPE, M. F. *et al.* Naringenin: an analgesic and anti-inflammatory citrus flavanone. **Oncotarget**, 8, n. 3, p. 3766-3767, 2017.

MARADIT KREMERS, H.; LARSON, D. R.; CROWSON, C. S.; KREMERS, W. K. *et al.* Prevalence of total hip and knee replacement in the United States. **The Journal of Bone and Joint Surgery-American Volume**, 97, n. 17, p. 1386-1397, 2015.

MARTINEZ DE LA TORRE, Y.; LOCATI, M.; BURACCHI, C.; DUPOR, J. *et al.* Increased inflammation in mice deficient for the chemokine decoy receptor D6. **Eur J Immunol**, 35, n. 5, p. 1342-1346, May 2005.

MCCORMACK, D. G.; MAK, J. C.; COUPE, M. O.; BARNES, P. J. Calcitonin gene-related peptide vasodilation of human pulmonary vessels. **J Appl Physiol (1985)**, 67, n. 3, p. 1265-1270, Sep 1989.

MCDONALD, B.; PITTMAN, K.; MENEZES, G. B.; HIROTA, S. A. *et al.* Intravascular Danger Signals Guide Neutrophils to Sites of Sterile Inflammation. **Science**, 330, n. 6002, p. 362-366, 2010.

MCDOUGALL, J. J. Arthritis and pain. Neurogenic origin of joint pain. **Arthritis Res Ther**, 8, n. 6, p. 220, 2006.

MCNAMARA, C. R.; MANDEL-BREHM, J.; BAUTISTA, D. M.; SIEMENS, J. *et al.* TRPA1 mediates formalin-induced pain. **Proc Natl Acad Sci U S A**, 104, n. 33, p. 13525-13530, Aug 14 2007.

MCWILLIAMS, D. F.; WALSH, D. A. Pain mechanisms in rheumatoid arthritis. **Clin Exp Rheumatol**, 35 Suppl 107, n. 5, p. 94-101, Sep-Oct 2017.

MEDZHITOV, R. Origin and physiological roles of inflammation. **Nature**, 454, n. 7203, p. 428-435, 2008.

MILLAN, M. J. The induction of pain: an integrative review. **Progress in neurobiology**, 57, n. 1, p. 1-164, 1999.

MINNOCK, P.; FITZGERALD, O.; BRESNIHAN, B. Women with established rheumatoid arthritis perceive pain as the predominant impairment of health status. **Rheumatology (Oxford)**, 42, n. 8, p. 995-1000, Aug 2003.

MORAN, C. A.; MULLICK, F. G.; ISHAK, K. G.; JOHNSON, F. B. *et al.* Identification of titanium in human tissues: probable role in pathologic processes. **Human pathology**, 22, n. 5, p. 450-454, 1991.

MOTA, L.; KAKEHASI, A. M.; GOMIDES, A. P. M.; DUARTE, A. *et al.* 2017 recommendations of the Brazilian Society of Rheumatology for the pharmacological treatment of rheumatoid arthritis. **Adv Rheumatol**, 58, n. 1, p. 2, May 24 2018.

NDENGELE, M. M.; MUSCOLI, C.; WANG, Z. Q.; DOYLE, T. M. *et al.* Superoxide potentiates NF-kappaB activation and modulates endotoxin-induced cytokine production in alveolar macrophages. **Shock (Augusta, Ga.)**, 23, n. 2, p. 186-193, 2005.

NIETO, F. R.; CLARK, A. K.; GRIST, J.; CHAPMAN, V. *et al.* Calcitonin gene-related peptide-expressing sensory neurons and spinal microglial reactivity contribute to pain states in collagen-induced arthritis. **Arthritis Rheumatol**, 67, n. 6, p. 1668-1677, Jun 2015.

O'BRIEN, W.; FISSEL, B. M.; MAEDA, Y.; YAN, J. *et al.* RANK-Independent Osteoclast Formation and Bone Erosion in Inflammatory Arthritis. **Arthritis & Rheumatology**, 68, n. 12, p. 2889-2900, 2016.

OLD, E. A.; NADKARNI, S.; GRIST, J.; GENTRY, C. *et al.* Monocytes expressing CX3CR1 orchestrate the development of vincristine-induced pain. **J Clin Invest**, 124, n. 5, p. 2023-2036, May 2014.

ORTEGA-GOMEZ, A.; PERRETTI, M.; SOEHNLEIN, O. Resolution of inflammation: an integrated view. **EMBO Mol Med**, 5, n. 5, p. 661-674, May 2013.

PARADA, C. A.; TAMBELI, C. H.; CUNHA, F. Q.; FERREIRA, S. H. The major role of peripheral release of histamine and 5-hydroxytryptamine in formalin-induced nociception. **Neuroscience**, 102, n. 4, p. 937-944, 2001.

PERRETTI, M.; SOLITO, E. Annexin 1 and neutrophil apoptosis. **Biochem Soc Trans**, 32, n. Pt3, p. 507-510, Jun 2004.

PINHO-RIBEIRO, F. A.; BADDAL, B.; HAARSMA, R.; O'SEAGHDHA, M. *et al.* Blocking Neuronal Signaling to Immune Cells Treats Streptococcal Invasive Infection. **Cell**, 173, n. 5, p. 1083-1097 e1022, May 17 2018.

PINHO-RIBEIRO, F. A.; VERRI, W. A.; CHIU, I. M. Nociceptor Sensory Neuron–Immune Interactions in Pain and Inflammation. **Trends in Immunology**, 38, n. 1, p. 5-19, 2017.

PRILLER, J.; REDDINGTON, M.; HAAS, C. A.; KREUTZBERG, G. W. Stimulation of P2Y-purinoceptors on astrocytes results in immediate early gene expression and potentiation of neuropeptide action. **Neuroscience**, 85, n. 2, p. 521-525, Jul 1998.

QUADROS, A. U.; PINTO, L. G.; FONSECA, M. M.; KUSUDA, R. *et al.* Dynamic weight bearing is an efficient and predictable method for evaluation of arthritic nociception and its pathophysiological mechanisms in mice. **Sci Rep**, 5, p. 14648, Oct 29 2015.

RAJA, S. N.; CARR, D. B.; COHEN, M.; FINNERUP, N. B. *et al.* The revised International Association for the Study of Pain definition of pain: concepts, challenges, and compromises. **Pain**, 161, n. 9, p. 1976-1982, Sep 1 2020.

RAVICHANDRAN, K. S. Beginnings of a good apoptotic meal: the find-me and eat-me signaling pathways. **Immunity**, 35, n. 4, p. 445-455, Oct 28 2011.

REICHLING, D. B.; LEVINE, J. D. Critical role of nociceptor plasticity in chronic pain. **Trends in Neurosciences**, 32, n. 12, p. 611-618, 2009.

RIBEIRO, R. A.; SOUZA-FILHO, M. V.; SOUZA, M. H.; OLIVEIRA, S. H. *et al.* Role of resident mast cells and macrophages in the neutrophil migration induced by LTB4, fMLP and C5a des arg. **International archives of allergy and immunology**, 112, n. 1, p. 27-35, 1997.

ROCHA E SILVA, M. A brief survey of the history of inflammation. 1978. **Agents and actions**, 43, n. 3-4, p. 86-90, 1994.

SARGEANT, A.; GOSWAMI, T. Pathophysiological aspects of hip implants. **Journal of surgical orthopaedic advances**, 15, n. 2, p. 111-112, 2006.

SARIA, A. Substance P in sensory nerve fibres contributes to the development of oedema in the rat hind paw after thermal injury. **Br J Pharmacol**, 82, n. 1, p. 217-222, May 1984.

SCANNELL, M.; FLANAGAN, M. B.; DESTEFANI, A.; WYNNE, K. J. *et al.* Annexin-1

and peptide derivatives are released by apoptotic cells and stimulate phagocytosis of apoptotic neutrophils by macrophages. **J Immunol**, 178, n. 7, p. 4595-4605, Apr 1 2007.

SCHOLZ, J.; WOOLF, C. J. Can we conquer pain? **Nature Neuroscience**, 5, n. Supp, p. 1062-1067, 2002.

SCHUH, C. D.; PIERRE, S.; WEIGERT, A.; WEICHAND, B. *et al.* Prostacyclin mediates neuropathic pain through interleukin 1beta-expressing resident macrophages. **Pain**, 155, n. 3, p. 545-555, Mar 2014.

SERHAN, C. N. Pro-resolving lipid mediators are leads for resolution physiology. **Nature**, 510, n. 7503, p. 92-101, 2014.

SHARIF, K.; SHARIF, A.; JUMAH, F.; OSKOUIAN, R. *et al.* Rheumatoid arthritis in review: Clinical, anatomical, cellular and molecular points of view. **Clin Anat**, 31, n. 2, p. 216-223, Mar 2018.

SIDDIQUI, M. M. A.; YEO, S. J.; SIVAIAH, P.; CHIA, S.-L. *et al.* Function and quality of life in patients with recurvatum deformity after primary total knee arthroplasty: a review of our joint registry. **The Journal of arthroplasty**, 27, n. 6, p. 1106-1110, 2012.

SILVA, R. M.; TEESY, C.; FRANZI, L.; WEIR, A. *et al.* Biological response to nano-scale titanium dioxide (TiO2): role of particle dose, shape, and retention. **Journal of toxicology and environmental health. Part A**, 76, n. 16, p. 953-972, 2013.

SMOLEN, J. S.; ALETAHA, D.; MCINNES, I. B. Rheumatoid arthritis. **Lancet**, 388, n. 10055, p. 2023-2038, Oct 22 2016.

SOEVER, L. J.; MACKAY, C.; SARYEDDINE, T.; DAVIS, A. M. *et al.* Educational needs of patients undergoing total joint arthroplasty. **Physiotherapy Canada. Physiothérapie Canada**, 62, n. 3, p. 206-214, 2010.

SORKIN, L. S.; DOOM, C. M. Epineurial application of TNF elicits an acute mechanical hyperalgesia in the awake rat. **J Peripher Nerv Syst**, 5, n. 2, p. 96-100, Jun 2000.

SPECTOR, W. G.; WILLOUGHBY, D. A. VASOACTIVE AMINES IN ACUTE INFLAMMATION. **Annals of the New York Academy of Sciences**, 116, n. 3, p. 839-846, 1964.

ST PIERRE, C. A.; CHAN, M.; IWAKURA, Y.; AYERS, D. C. *et al.* Periprosthetic osteolysis: characterizing the innate immune response to titanium wear-particles. **Journal of orthopaedic research : official publication of the Orthopaedic Research Society**, 28, n. 11, p. 1418-1424, 2010.

SUNDFELDT, M.; CARLSSON, L. V.; JOHANSSON, C. B.; THOMSEN, P. *et al.* Aseptic loosening, not only a question of wear: a review of different theories. **Acta orthopaedica**, 77, n. 2, p. 177-197, 2006.

SVENSSON, C. I.; BRODIN, E. Spinal astrocytes in pain processing: non-neuronal cells as therapeutic targets. **Mol Interv**, 10, n. 1, p. 25-38, Feb 2010.

SZALLASI, A.; CORTRIGHT, D. N.; BLUM, C. A.; EID, S. R. The vanilloid receptor TRPV1: 10 years from channel cloning to antagonist proof-of-concept. **Nat Rev Drug Discov**, 6, n. 5, p. 357-372, May 2007.

TAKEUCHI, O.; AKIRA, S. Pattern Recognition Receptors and Inflammation. **Cell**, 140, n. 6, p. 805-820, 2010.

THEOHARIDES, T. C.; KEMPURAJ, D.; TAGEN, M.; CONTI, P. *et al.* Differential release of mast cell mediators and the pathogenesis of inflammation. **Immunological Reviews**, 217, n. 1, p. 65-78, 2007.

TORRES, M.; FORMAN, H. J. Redox signaling and the MAP kinase pathways. **BioFactors (Oxford, England)**, 17, n. 1-4, p. 287-296, 2003.

TRUMAN, L. A.; FORD, C. A.; PASIKOWSKA, M.; POUND, J. D. *et al.* CX3CL1/fractalkine is released from apoptotic lymphocytes to stimulate macrophage chemotaxis. **Blood**, 112, n. 13, p. 5026-5036, Dec 15 2008.

TRUONG, T. H.; CARROLL, K. S. Redox Regulation of Epidermal Growth Factor Receptor Signaling through Cysteine Oxidation. **Biochemistry**, 51, n. 50, p. 9954-9965, 2012.

TYLEK, K.; TROJAN, E.; REGULSKA, M.; LACIVITA, E. *et al.* Formyl peptide receptor 2, as an important target for ligands triggering the inflammatory response regulation: a link to brain pathology. **Pharmacol Rep**, Jun 8 2021.

VERRI, W. A.; CUNHA, T. M.; PARADA, C. A.; POOLE, S. *et al.* Hypernociceptive role of cytokines and chemokines: Targets for analgesic drug development? **Pharmacology & Therapeutics**, 112, n. 1, p. 116-138, 2006.

VERRI, W. A.; GUERRERO, A. T. G.; FUKADA, S. Y.; VALERIO, D. A. *et al.* IL-33 mediates antigen-induced cutaneous and articular hypernociception in mice. **Proceedings of the National Academy of Sciences of the United States of America**, 105, n. 7, p. 2723-2728, 2008.

VERRI, W. A.; SOUTO, F. O.; VIEIRA, S. M.; ALMEIDA, S. C. L. *et al.* IL-33 induces neutrophil migration in rheumatoid arthritis and is a target of anti-TNF therapy. **Annals of the Rheumatic Diseases**, 69, n. 9, p. 1697-1703, 2010.

WANG, J. X.; FAN, Y. B.; GAO, Y.; HU, Q. H. *et al.* TiO2 nanoparticles translocation and potential toxicological effect in rats after intraarticular injection. **Biomaterials**, 30, n. 27, p. 4590-4600, 2009.

WANG, Z.; MA, W.; CHABOT, J. G.; QUIRION, R. Cell-type specific activation of p38 and ERK mediates calcitonin gene-related peptide involvement in tolerance to morphine-induced analgesia. **FASEB J**, 23, n. 8, p. 2576-2586, Aug 2009.

WOODFIN, A.; VOISIN, M. B.; IMHOF, B. A.; DEJANA, E. *et al.* Endothelial cell activation leads to neutrophil transmigration as supported by the sequential roles of ICAM-2, JAM-A, and PECAM-1. **Blood**, 113, n. 24, p. 6246-6257, Jun 11 2009.

WOOLF, C. J. What is this thing called pain? **J Clin Invest**, 120, n. 11, p. 3742-3744, Nov 2010.

XANTHOS, D. N.; SANDKUHLER, J. Neurogenic neuroinflammation: inflammatory CNS reactions in response to neuronal activity. **Nat Rev Neurosci**, 15, n. 1, p. 43-53, Jan 2014.

YAMADA, H.; SAEGUSA, J.; SENDO, S.; UEDA, Y. *et al.* Effect of resolvin D5 on T cell differentiation and osteoclastogenesis analyzed by lipid mediator profiling in the experimental arthritis. **Sci Rep**, 11, n. 1, p. 17312, Aug 27 2021.

ZAKY, S.; ZAKY, C. S.; ABD-ELSAYED, A. Anatomy of the nervous system. *In*: ABD-ELSAYED, A. (Ed.). **Pain: A Review Guide**. Cham: Springer International Publishing, 2019. p. 3-8.

ZHANG, J.; WANG, X.; VIKASH, V.; YE, Q. *et al.* ROS and ROS-Mediated Cellular Signaling. **Oxidative Medicine and Cellular Longevity**, 2016, p. 1-18, 2016.

ANEXOS

ANEXO A – Aprovação Do Projeto Na Ceua De Artrite Induzida Por Antígeno E RvD5

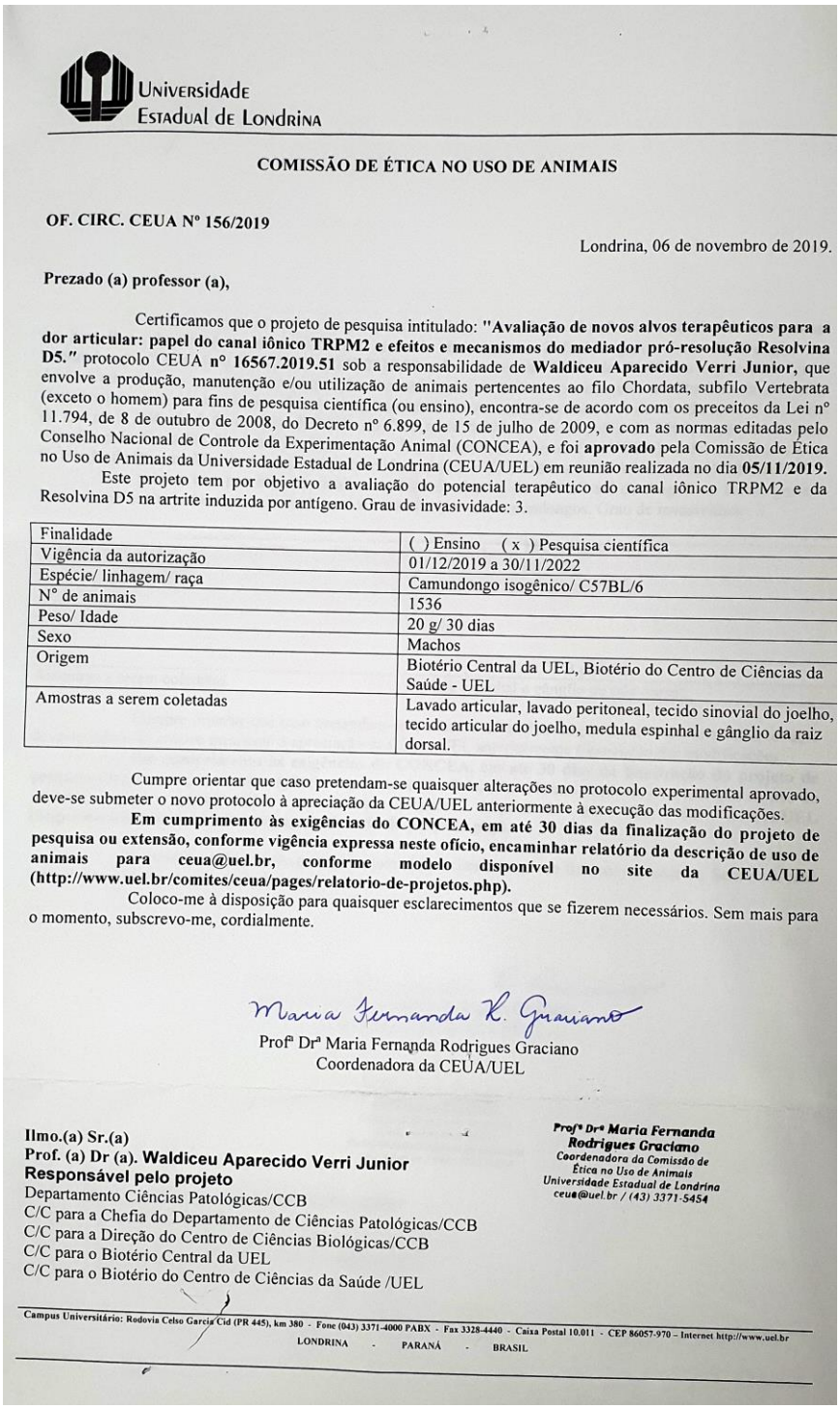

Universidade Estadual de Londrina

COMISSÃO DE ÉTICA NO USO DE ANIMAIS

OF. CIRC. CEUA Nº 156/2019

Londrina, 06 de novembro de 2019.

Prezado (a) professor (a),

Certificamos que o projeto de pesquisa intitulado: **"Avaliação de novos alvos terapêuticos para a dor articular: papel do canal iônico TRPM2 e efeitos e mecanismos do mediador pró-resolução Resolvina D5."** protocolo CEUA **nº 16567.2019.51** sob a responsabilidade de **Waldiceu Aparecido Verri Junior,** que envolve a produção, manutenção e/ou utilização de animais pertencentes ao filo Chordata, subfilo Vertebrata (exceto o homem) para fins de pesquisa científica (ou ensino), encontra-se de acordo com os preceitos da Lei nº 11.794, de 8 de outubro de 2008, do Decreto nº 6.899, de 15 de julho de 2009, e com as normas editadas pelo Conselho Nacional de Controle da Experimentação Animal (CONCEA), e foi **aprovado** pela Comissão de Ética no Uso de Animais da Universidade Estadual de Londrina (CEUA/UEL) em reunião realizada no dia **05/11/2019.**

Este projeto tem por objetivo a avaliação do potencial terapêutico do canal iônico TRPM2 e da Resolvina D5 na artrite induzida por antígeno. Grau de invasividade: 3.

Finalidade	( ) Ensino (x) Pesquisa científica
Vigência da autorização	01/12/2019 a 30/11/2022
Espécie/ linhagem/ raça	Camundongo isogênico/ C57BL/6
N° de animais	1536
Peso/ Idade	20 g/ 30 dias
Sexo	Machos
Origem	Biotério Central da UEL, Biotério do Centro de Ciências da Saúde - UEL
Amostras a serem coletadas	Lavado articular, lavado peritoneal, tecido sinovial do joelho, tecido articular do joelho, medula espinhal e gânglio da raiz dorsal.

Cumpre orientar que caso pretendam-se quaisquer alterações no protocolo experimental aprovado, deve-se submeter o novo protocolo à apreciação da CEUA/UEL anteriormente à execução das modificações.

Em cumprimento às exigências do CONCEA, em até 30 dias da finalização do projeto de pesquisa ou extensão, conforme vigência expressa neste ofício, encaminhar relatório da descrição de uso de animais para ceua@uel.br, conforme modelo disponível no site da CEUA/UEL (http://www.uel.br/comites/ceua/pages/relatorio-de-projetos.php).

Coloco-me à disposição para quaisquer esclarecimentos que se fizerem necessários. Sem mais para o momento, subscrevo-me, cordialmente.

Maria Fernanda R. Graciano

Profª Drª Maria Fernanda Rodrigues Graciano
Coordenadora da CEUA/UEL

Ilmo.(a) Sr.(a)
Prof. (a) Dr (a). Waldiceu Aparecido Verri Junior
Responsável pelo projeto
Departamento Ciências Patológicas/CCB
C/C para a Chefia do Departamento de Ciências Patológicas/CCB
C/C para a Direção do Centro de Ciências Biológicas/CCB
C/C para o Biotério Central da UEL
C/C para o Biotério do Centro de Ciências da Saúde /UEL

Profª Drª Maria Fernanda Rodrigues Graciano
Coordenadora da Comissão de Ética no Uso de Animais
Universidade Estadual de Londrina
ceua@uel.br / (43) 3371-5454

Campus Universitário: Rodovia Celso Garcia Cid (PR 445), km 380 - Fone (043) 3371-4000 PABX - Fax 3328-4440 - Caixa Postal 10.011 - CEP 86057-970 – Internet http://www.uel.br
LONDRINA - PARANÁ - BRASIL

ANEXO B – Aprovação Do Projeto Na Ceua De Rvd5 E Artrite Crônica Induzida Por TiO_2

Universidade Estadual de Londrina

COMISSÃO DE ÉTICA NO USO DE ANIMAIS

OF. CIRC. CEUA Nº 151/2016 **Londrina, 15 de Julho de 2016.**

Prezado Pesquisador,

Certificamos que o projeto intitulado **"Avaliação do efeito analgésico dos mediadores lipídicos pró-resolução resolvina D1 (RvD1) resolvina D2 (RvD2), resolvina D5 (RvD5), maresina 1 (Mar1), maresina 2 (Mar2), protectina (PD1), 15-epi-lipoxina A4 (ATLA4) e lipoxina A4 (LxA4) em modelo de artrite induzido por TiO_2"**, protocolo CEUA n° **11147.2016.40**, sob a responsabilidade de **Waldiceu Aparecido Verri Junior**, que envolve a produção, manutenção e/ou utilização de animais pertencentes ao filo Chordata, subfilo Vertebrata (exceto o homem), para fins de pesquisa científica (ou ensino), encontra-se de acordo com os preceitos da Lei nº 11.794, de 8 de outubro de 2008, do Decreto nº 6.899, de 15 de julho de 2009, e com as normas editadas pelo Conselho Nacional de Controle da Experimentação Animal (CONCEA), foi **aprovado** pela Comissão de Ética no Uso de Animais da Universidade Estadual de Londrina (CEUA/UEL), em reunião realizada em **05/07/2016**.

O objetivo do projeto investigar os mecanismos dos mediadores lipídicos pró-resolução RvD1, RvD2, RvD5, Mar1, Mar2, PD1, ATLA4 e LxA4 em modelo de hiperalgesia induzido por dióxido de titânio (TiO_2). Os animais serão divididos em gaiolas de polipropileno padrão medindo 41 X 34 X 16 CM (Insight®) no biotério de acordo com os grupos experimentais (máximo de 12 animais por gaiola), com livre acesso à água e ração e serão adaptados aos ambientes e condições experimentais com pelo menos 1 hora de antecedência em relação aos experimentos. Os procedimentos de cuidado e manuseio de animais estarão de acordo com as diretrizes da Associação Internacional de Estudo da Dor (IASP). A utilização de fármacos analgésicos não é realizada uma vez que estes podem interferir na resposta analisada, e desta forma prejudicar a interpretação dos resultados. A eutanásia será realizada por Isofluorano 1,5 a 3% em O_2 e serão posteriormente decapitados. GI 2.

Vigência do Projeto	01/01/2017 a 01/12/2022
Espécie/linhagem	Camundongo heterogênico / Swiss
Nº de animais	672
Peso/Idade	20-25 g / 2 meses
Sexo	Machos
Origem	Biotério Central / UEL
Amostras a serem coletadas	Articulação

Cumpre orientar que caso pretendam-se quaisquer alterações no protocolo experimental aprovado, deve-se submeter o novo protocolo à apreciação da CEUA/UEL anteriormente à execução das modificações.

Coloco-me à disposição para quaisquer esclarecimentos que se fizerem necessária. Sem mais para o momento, subscrevo, cordialmente,

Profa. Dra. Glaura Scantamburlo Alves Fernandes
Coordenadora da CEUA/UEL

Ilmo. Sr.
Prof. Dr. Waldiceu Aparecido Verri Junior
Coordenador do Projeto
Departamento de Ciências Patológicas / Centro de Ciências Biológicas
Com cópia para Coord. do Biotério Central/UEL; Chefe do Departamento de Ciências Patológicas e Diretor(a) do Centro de Ciências Biológicas

Campus Universitário: Rodovia Celso Garcia Cid (PR 445), km 380 - Fone (043) 3371-4000 PABX - Fax 3328-4440 - Caixa Postal 10.011 - CEP 86057-970 – Internet http://www.uel.br
LONDRINA - PARANÁ - BRASIL

ANEXO C – Artigo Publicado Durante O Doutoramento Na Revista Inflammation Research

Naringenin mitigates titanium dioxide (TiO_2)-induced chronic arthritis in mice: Role of oxidative stress, cytokines, and NFκB

Marília F. Manchope[a]; Nayara A. Artero[b]; Victor Fattori[a]; Sandra S. Mizokami[a]; Dimitrius L. Pitol[c]; João P. M. Issa[c]; Sandra Y. Fukada[d]; Thiago M. Cunha[e]; José C. Alves-Filho[e]; Fernando Q. Cunha[e]; Rubia Casagrande[b]; Waldiceu A. Verri Jr[a]*

[a]Departamento de Ciências Patológicas, Centro de Ciências Biológicas, Universidade Estadual de Londrina, Londrina, Brazil.

[b]Departamento de Ciências Farmacêuticas, Centro de Ciências de Saúde, Universidade Estadual de Londrina, Londrina, Brazil.

[c]Departamento de Morfologia, Fisiologia e Patologia Básica, Faculdade de Odontologia de Ribeirão Preto, Universidade de São Paulo , Ribeirão Preto, São Paulo, Brazil.

[d] Departamento de Física e Química, Faculdade de Ciências Farmacêuticas de Ribeirão Preto, Universidade de São Paulo , Ribeirão Preto, São Paulo, Brazil.

[e] Departamento de Farmacologia, Faculdade de Medicina de Ribeirão Preto, Universidade de São Paulo, Ribeirão Preto, São Paulo, Brazil.

***Author for correspondence: Prof. Waldiceu A. Verri Jr, Ph.D.** Present address: Departamento de Ciências Patológicas, Universidade Estadual de Londrina, Rod. Celso Garcia Cid Km480 PR445, CEP 86057-970, Cx Postal 10.011, Londrina, Paraná, Brasil. Tel: +55 43 3371 4979. Fax: +55 43 3371 4387. E-mails: waverri@uel.br or waldiceujr@yahoo.com.br

ABSTRACT

Objective To evaluate the effect and mechanisms of naringenin in TiO_2-induced chronic arthritis in mice, a model resembling prosthesis and implant inflammation.

Treatment Flavonoids are antioxidant and anti-inflammatory molecules with important anti-inflammatory effect. Mice were daily treated with the flavonoid naringenin (16.7-150 mg/kg, orally) for 30 days starting 24h after intra-articular knee injection of 3 mg of TiO_2.

Methods TiO_2-induced arthritis resembles cases of aseptic inflammation induced by prosthesis and/or implants. Mice were stimulated with 3 mg of TiO_2 and after 24h mice started to be treated with naringenin. The disease phenotype, treatment toxicity, histopathological damage, oxidative stress, cytokine expression and NFκB were evaluated after 30 days of treatment.

Results Naringenin inhibited TiO_2-induced mechanical hyperalgesia (96%), edema (77%), and leukocyte recruitment (74%) without inducing toxicity. Naringenin inhibited histopathological index (HE, 49%), cartilage damage (Toluidine blue tibial staining 49%, and proteoglycan 98%), and bone resorption (TRAP-stained 73%). These effects were accompanied by inhibition of oxidative stress ($gp91^{phox}$ 93%, NBT 83%, and TBARS 41%) cytokine mRNA expression (IL-33 82%, TNFα 76%, pro-IL-1β 100%, and IL-6 61%) and NFκB activation (100%).

Conclusion Naringenin ameliorates TiO_2-induced chronic arthritis inducing analgesic and anti-inflammatory responses with improvement in the histopathological index, cartilage damage, and bone resorption.

KEYWORDS: Flavonoids, Arthritis; Implant; Arthroplasty; Pain, Aseptic inflammation.

Introduction

Arthroplasty is a successful procedure in advanced cases of inflammatory arthritis including osteoarthritis and rheumatoid arthritis, and also in cases of fractures and

osteonecrosis that replaces the dysfunctional joint for a prosthesis [1, 2]. Exemplifying the importance of this procedure, nearly 7 millions of Americans had total knee or hip replacements in 2010 and until 2030 close to 11 millions of Americans will have total knee or hip replacements [3]. In this sense, arthroplasty is an efficient and successful procedure with a low relative-cost for terminal stage patients with dysfunctional joints [4]. Despite the success of the arthroplasty procedure, about 10-15% of the patients present osteolysis and failure in prosthesis-replaced dysfunctional joint due to immune-inflammatory [5] response to debris biomaterials of the prosthesis released by wearing [6].

The titanium dioxide (TiO_2) is a white and odorless powder used in designing prosthesis and implants in orthopedic and dentistry fields [7, 8]. There is evidence that TiO_2 is a contributing molecule to prosthesis or implants wear debris-induced inflammation. In agreement with the rationale that implants induce inflammation, a patient without a familiar history of rheumatic diseases developed implant-related arthritis due to titanium translocation from cervical cage implant to joints [9]. Furthermore, incubation of TiO_2 with patient's peripheral mononuclear blood cells induces TNFα release [9].TiO_2-induced chronic arthritis is a useful model in translational medicine to studying cellular and molecular mechanisms that involve TiO_2-triggered chronic joint inflammation and bone destruction. In fact, TiO_2 induces articular pain, knee edema, oxidative stress, IL-33, TNFα, IL-1β, and IL-6 inflammatory cytokines production, increased RANKL/RANK signaling pathway ultimately leading to joint destruction [10].

The flavonoid naringenin (4',5,7-trihydroxy-flavanone) is a polyphenol compound found in the human diet [11], mainly in citrus fruit including lemon, orange, tangerine, and grapefruit [12]. Mice oral intake of 200 mg of a Chinese extract containing naringenin is absorbed and plasma concentration is detected in 60 min. The elimination half-life of naringenin is 4.69 h and its elimination is almost complete in 24 h [13]. Regarding naringenin

pharmacological activities, this flavonoid is an analgesic molecule [14-16] acting through the activation of the analgesic signalling pathway NO−cGMP−PKG−K_{ATP} channel [14]. In addition to its analgesic action, naringenin reveals anti-inflammatory activity by inhibiting TNFα [14, 15], IL-1β [15, 16] and IL-6 [15] release in several models of inflammatory pain. Naringenin also inhibits RANKL-induced osteoclastogenesis and bone resorption through suppression of p38 MAPK phosphorylation inhibiting osteolysis in titanium particles-induced calvarial osteolysis [17].

In general, the inflammatory response includes the development of clinical signs such as increase in local or systemic temperature, erythema, edema and pain [18]. These clinical symptoms directly affect patients' quality of life [19]. The analgesic, anti-inflammatory and anti-osteolytic properties of naringenin [14-16, 20] would be important activities in the context of prosthesis-induced inflammation. Considering the physiopathology and clinical symptoms of prosthesis-induced arthritis as well as the pharmacological evidence on the activities of naringenin, we reason that naringenin has pharmacological potential on the treatment of prosthesis-induced arthritis. Thus, in the present study, we evaluated the therapeutic effect and mechanisms of action of naringenin in the pathogenesis of TiO_2-induced chronic arthritis.

Materials and Methods

General experimental procedures

In first series of experiments, mice (n = 6 per group per experiment) were stimulated in the right joint with an intra-articular (i.a.) injection of 3 mg of TiO_2 per knee joint as described previously [10]. Twenty four h after TiO_2 stimulus, mice were treated with titrated doses of naringenin (16.7, 50, or 150 mg/kg, per oral [p.o.]) [14]. Mechanical hyperalgesia and knee joint volume (e.g. edema) evaluation started 24h after TiO_2 stimuli and occurred before and after naringenin treatment (1, 3, 5, 7, and 24 h hours after naringenin treatment in the first day and 1 h after naringenin treatment once a day up to 30 days) [10, 21]. The

naringenin dose of 50 mg/kg was chosen based on the results of hyperalgesia and edema. Stomach and blood samples were harvested at the 30th day to evaluate possible side effects and toxic effects of chronic naringenin treatment. Parameters were stomach myeloperoxidase (MPO) activity, and plasmatic levels of aspartate transaminase (AST), alanine transaminase (ALT), urea, and creatinine. Knee joint and knee joint lavages were collected to histopathology (hematoxylin-eosin stain [HE]) and leukocytes recruitment analyses. Cartilage damage was determined with toluidine blue staining and patella proteoglycan levels. Bone resorption was evaluated by histochemical staining tartrate-resistant acid phosphatase (TRAP; a marker of osteoclasts) and RANKL/RANK/OPG signalling pathway by RT-qPCR. Oxidative stress was evaluated with gp91^{phox} mRNA expression [RT-qPCR], superoxide anion [nitroblue tetrazolium reduction levels], and lipid peroxidation (thiobarbituric acid reactive substances [TBARS]), pro-inflammatory cytokines mRNA expression (TNFα, proIL-1β, IL-6 and IL-33), and NFκB activation (ELISA) were analyzed with the mentioned methods. Free movements of animals were not altered by i.a. injection of TiO_2. The 30 days final time point was selected in preliminary experiments aiming to determine joint cartilage and bone damage [14], which were know not to occur before 7 days of TiO_2 inflammation [21]. All experiments were performed blinded.

Animals

Male Swiss mice weighing between 20-25 g from the Londrina State University, Londrina, Paraná, Brazil, were used in this study. Mice were housed in standard clear plastic cages with water and food *ad libitum*, light / dark cycle of 12 / 12h and controlled temperature (21°C). Mice were maintained in the vivarium of the Department of Pathology of Londrina State University for at least two days before experiments. Mice were used only once and were acclimatized to the testing room at least 1 hour before the experiments, which were conducted during the light cycle. Animal care and handling procedures were in accordance with the International Association for Study of Pain (IASP) guidelines and approved by the Londrina

State University Ethics Committee on Animal Research and Welfare (process number 11849.2015.19). All efforts were made to minimize the number of animals used and their suffering.

Test compounds

The compounds used in this study were saline solution (NaCl 0.9%; Frenesius Kabi Brasil Ltda, Aquiraz, CE, Brazil), Ethylenediaminetetraacetic acid disodium salt (EDTA; Synth, Diadema, SP, Brazil), and naringenin (Santa Cruz Biotechnology, Inc., 98%, Dalla, TX, USA). Titanium dioxide was purchased from Synth (Diadema, SP, Brazil) and particle size was < 1μm with an average of 862.2 nm as determined by size distribution analysis (Malvern Instruments Ltd, UK). Immediately before the injections, TiO_2 was suspended in sterile saline (10 μL) and naringenin was diluted in sterile saline solution. Naringenin (16.7, 50, or 150 mg/kg) and saline were administrated by p.o. in a volume of 100 μL.

Evaluation of articular mechanical hyperalgesia

The knee joint mechanical hyperalgesia was evaluated as previously described [22]. Briefly, in a quiet room, mice were placed individually in acrylic cages (12 x 10 x 17 cm) with a wire grid floor 15-30 minutes before the test for environmental adaption. An electronic pressure-meter test consisting of a hand-held force transducer fitted with a polypropylene tip (electronic von Frey Anesthesiometer; Insight, Ribeirão Preto, SP, Brazil) was used to evaluate mechanical articular nociception. For this model, a large tip (4.15 mm^2) was adapted to the probe. An increasing perpendicular force was applied to the central area of the plantar surface of the hind paw to induce a flexion movement of the tibiofemoral joint followed by paw withdrawal. The electronic pressure-meter apparatus automatically recorded the intensity of the force applied when the paw was withdrawn. The flexion-elicited mechanical threshold was expressed in grams (g) [22].

Articular edema measurements

Articular edema of the tibiofemoral joint was assessed through measurements of the transverse diameters using a caliper (Digmatic Caliper, Mitutoyo Corporation, Kanagawa,

Japan). Thickness values of the femorotibial joint were expressed as the percentage change by the ratio between the delta (the difference between the diameters measured before [basal value] and after TiO_2 i.a. injection) and basal value multiplied by 100.

Histopathology

Joints were fixed in 4% formaldehyde for two days before decalcification in NaOH/EDTA solution (pH 7.3-7.4) and processed for paraffin embedding. Tissue longitudinal sections (7 µm) were prepared and stained with HE. HE-stained tibiofemoral joint sections were examined blinded and scored by a pathologist using light microscopy, and the degree of synovial hyperplasia; inflammatory infiltrate and vascular proliferation were determined with modifications as described previously [23, 24]. The degrees of the following parameters were: a) synovial hyperplasia (from 0 = no pannus formation, to 3 = most severe pannus formation); b) inflammatory infiltrate (from 0 = no inflammation, to 3 = most severe inflammation; and c) vascularity (from 0 = no vascular proliferation, to 3 = most severe proliferation). Regarding vascular proliferation, it was considered the quantity of the capillary blood vessels. The final score was determined by summing all three parameters (a-c) resulting in a score for each sample expressed as the mean of 6 samples accordingly to the groups.

Myeloperoxidase activity

Myeloperoxidase (MPO) activity was used to evaluate possible naringenin-induced gastric damage, considering it´s activity increases with gastric damage induced by non-steroidal anti-inflammatory drugs [25]. Samples of the stomach were harvested in 50 mM K_2HPO_4 buffer (pH 6.0) containing 0.5% hexadecyl trimethylammonium bromide (HTAB) and kept at -86°C until use. Frozen samples were homogenized using a tissue turrax (Tissue-Tearor 985370, BioSpec Products, Bartlesville, OK, USA), centrifuged (2 min, 16,000 *g*, 4°C) and the resulting supernatant assayed using a spectrophotometer (Multiskan GO Microplate Spectrophotometer, ThermoScientific, Vantaa, Finland) for MPO activity determination at 450 nm. The MPO activity of samples was compared to a standard curve of neutrophils.

Briefly, 15 μL of sample was mixed with 200 μL of 50 mM phosphate buffer (pH 6.0), containing 0.167 mg/mL O-dianisidine dihydrochloride and 0.0005% hydrogen peroxide. Indomethacin (2.5 mg/kg, i.p., diluted in tris/HCl buffer, for 7 days) was used as positive drug control for stomach damage. The results were presented as MPO activity (number of neutrophils X 10^6 / mg of tissue).

Liver and kidney toxicity assays

Blood was harvested into microtubes containing 50 µL of the anticoagulant EDTA (5,000 IU/mL) and centrifuged (200 *g*, 10 min, 4 °C), and the plasma was separated. In order to determine naringenin-induced liver and kidney toxicity, plasma samples were used. Aspartate aminotransferase (AST) and alanine aminotransferase (ALT) were used as markers of hepatotoxicity, and acetaminophen was a positive drug control (650 mg/kg, intraperitoneal [i.p.], diluted in sterile saline, once). Urea and creatinine levels were used to evaluate nephrotoxicity, and diclofenac was a positive drug control (200 mg/kg, orally, diluted in sterile saline, once). Plasma samples were processed according to the manufacturer's instructions (Labtest Diagnóstico S. A., Brazil). Results were presented as U/mL (AST and ALT) or mg/dL (urea and creatinine) of plasma.

Evaluation of leukocyte migration

The total and differential counts of recruited leukocytes to the knee joint cavity were determined as previously described [26]. Briefly, knee joint cavities were washed with saline containing EDTA, which was recovered to evaluate total and differential cell counts. Total cell counts were performed in Neubauer chamber using Turk solution, and differential cell counts (100 cells per slide) were performed in slices stained with the panoptic kit (Laborclin, Pinhais, PR, Brazil) under a light microscope (Olympus CX31RTSF, Tokyo, Japan). Results were expressed as total leukocytes, polymorphonuclear, and mononuclear cells (cells x 10^3/ knee joint).

Proteoglycan assays

Proteoglycan degradation was evaluated using toluidine blue staining in samples processed for histopathology [21]. The percentage of stained areas (femoral and tibial cartilages) was measured using ImageJ 1.50i software. The load-bearing region was outlined in black and the same minimum (170) and maximum (255) threshold values for each sample analysis were used. Proteoglycan concentration was determined in patella using a colorimetric assay [27]. Briefly, the patella was carefully collected from mice and fixed with formaldehyde (4%) overnight using a shaker and decalcified in formic acid (5%) for 4 h using a shaker. Each patella sample was digested at 60°C for 16 h with 60 µL of papain digestion buffer (5 mg/ml) in calcium and magnesium-free PBS with 5 mM cysteine and 10 mM EDTA, pH 7.4. After reaching room temperature, samples were centrifuged for 10 min at 1000 *g* to collect the condensation droplets. Next, 50 µL of the supernatants and of serial chondroitin sulfate solutions (standard curve; 50–1000 mg/ml) was placed into 96-well plates. Then, 300 µL of a 1,9-dimethylmethylene blue (DMMB; 50 mg/L, Polysciences) solution was added to each well, and proteoglycan contents [21] were determined by spectrophotometer reading at 525 nm (Multiskan GO Microplate Spectrophotometer, ThermoScientific, Vantaa, Finland). The chondroitin 6-sulfate sodium salt from shark cartilage, a glucosaminoglycan (GAG) content was calculated from the standard curve. Results were presented as proteoglycan per milligram (mg) of tissue.

Histochemical stain for TRAP

TRAP was used as a histochemical marker of osteoclasts activation in 6 µm sections [10]. Sections were stained according to TRAP kit 387A (Sigma-Aldrich, St. Louis, MO, USA) and TRAP-positive cells appeared as dark purple. Digitally acquired images were analyzed in the ImageJ 1.44 software, using the threshold tool with color-based selection for positive staining analyzed in a total area of 3145728 pixels, which is a maximum area that can be acquired with our equipment (Olympus CX31RTSF, Tokyo, Japan coupled with lumenera Infinity 1 microscope camera, Ottawa, Canada). Three slices per sample of knee joint tissue

were analyzed and data were averaged. Results were expressed by total stained pixels of TRAP staining. Control and experimental knee joints were processed under the same conditions.

Nitroblue tetrazolium reduction

The superoxide anion production was determined by the reduction of the redox dye Nitroblue tetrazolium (NBT) [28]. Knee joint frozen tissue from mice were homogenized with 500 µL of saline using an ultra-turrax (Tissue-Tearor 985370, BioSpec Products, Bartlesville, OK, USA), centrifuged (10 min, 3,300 *g*, 4 °C) and 50 µL of the homogenate was placed in 96-well plate, followed by the addition of 100 µL of nitro blue tetrazolium solution (1 mg/mL) (NBT, Sigma) and maintained at 37°C in warm bath for 5 minutes. The supernatant was removed, and the formazan precipitated was then solubilized by adding 120 µL of 2 M KOH and 120 µL of dimeltisulfoxide (DMSO). The optical density was measured using a microplate spectrophotometer reader (Multiskan GO Microplate Spectrophotometer, Thermoscientific, Vantaa, Finland) at 600 nm. The NBT reduction levels were corrected per the total protein concentration and the results were presented as NBT reduction (OD/mg of protein).

Lipid peroxidation

Tissue lipid peroxidation was assessed by the levels of thiobarbituric acid reactive substances (TBARS) [29]. For this assay, TCA 10% was added to the homogenate and the mixture was centrifuged (3 min, 1000 *g*, 4 °C) to precipitate proteins. The protein-free supernatant was then separated and mixed with TBA (0.67%). The mixture was kept in a water bath (15 min, 100°C). Malondialdehyde (MDA), an intermediate product of lipid peroxidation, was determined by the difference between absorbance at 535 and 572 nm using a microplate spectrophotometer reader. The TBARS were corrected per the total protein concentration and results were presented as TBARS (ΔOD A_{535}-A_{572} /mg of protein) [29].

RT-qPCR

Knee joint were dissected 30 days after TiO2 and homogenized in TRIzol reagent®.

Total RNA was extracted by using the SV Total RNA Isolation System (Promega). The purity of total RNA was measured using a spectrophotometer (Multiskan GO Microplate Spectrophotometer, Thermoscientific, Vantaa, Finland) and the wavelength absorption ratio (260/280) was between 1.8 and 2.0 for all preparations. Reverse transcription of total RNA to cDNA and qPCR were carried out using GoTaq® 2-Step RT-qPCR System (Promega) and specific primers A no-reverse transcription control was applied for cDNA production (running the samples without adding reverse transcriptase enzyme) and a no-template control (NTC) was carried out for qPCR (running the qPCR reaction without cDNA). qPCR reaction was performed in StepOnePlus™ Real-Time PCR System (Applied Biosystems®). The relative gene expression was measured using the comparative $2^{-(\Delta\Delta Cq)}$ method. The primers used were: RANKL, sense: 5′-CAG AAG ATG GCA CTC ACT GCA-3′, antisense: 5′-CAC CAT CGC TTT CTC TGC TCT-3′; RANK, sense: 5′-CTA ATC CAG CAG GGA AGC AAAT-3′, antisense: 5′-GAC ACG GGC ATA GAG TCA GTTC-3′; osteoprotegerin (OPG), sense: 5′-GGA ACC CCA GAG CGA AAT ACA-3′, antisense: 5′-CCT GAA GAA TGC CTC CTC ACA-3′; $gp91^{phox}$, sense: 5′-AGC TAT GAG GTG GTG ATG TTA GTGG-3′, antisense: 5′-CAC AAT ATT TGT ACC AGA CAG ACT TGAG-3′; TNFα, sense: 5′-TCT CAT CAG TTC TAT GGC CC-3′, antisense: 5′-GGG AGT AGA CAA GGT ACAAC-3′; pro-IL-1β, sense: 5-′GAA ATG CCA CCT TTT GAC AGTG-3′, antisense: 5′-TGG ATG CTC TCA TCA GGA CAG-3′, IL-6 , sense: 5′-GAG GAT ACC ACT CCC AAC AGA CC,-3′, antisense: 5′-AAG TGC ATC ATC GTT GTT CAT ACA-3′, IL-33, sense: 5′-TCC TTG CTT GGC AGT ATCCA-3′, antisense: 5′-TGC TCA ATG TGT CAA CAG ACG-3′; glyceraldehyde 3-phosphate dehydrogenase (Gapdh), sense: 5′-CAT ACC AGG AAA TGA GCT TG-3′, antisense: 5′-ATG ACA TCA AGA AGG TGG TG-3′; β-actin: sense: 5′-AGC TGC GTT TTA CAC CCT TT-3’, antisense: 5′-AAG CCA TGC CAA TGT TGT CT-3′. The expression of Gapdh and β-actin mRNA were used as reference gene, and the results were

expressed as mRNA expression (normalized to Gapdh and β-actin).

NFκB activation

The knee joint samples were homogenized in 400 μL of the appropriate buffer containing protease inhibitors. The homogenates were centrifuged (10 min, 16,100 *g*, 4 ºC), and the supernatants were used to assess the levels of phosphorylated and total NFκB p65 subunit by ELISA using PathScan® kits (Cell Signaling) at 450 nm (Multiskan GO Thermo Scientific) according to the manufacturer's directions. The phosphorylated and total NFκB p65 subunit were corrected per the total protein concentration and results are expressed as NFκB activation (IoD phospho-p65/totalp65 ratio/mg of protein)

Statistical analysis

Results are presented as means ± SEM of measurements made on six mice in each group per experiment and are representative of two separate experiments. Two-way repeated measures analysis of variance (ANOVA) followed by Tukey's *post hoc* was used to compare all groups and doses at all times when responses were measured at different times after the stimulus injection. Differences between responses were evaluated by one-way ANOVA followed by Tukey's *post hoc* for data of single time point. Statistical differences were considered significant when $P < 0.05$.

Results

Naringenin inhibits TiO_2-induced mechanical hyperalgesia and edema without inducing toxicity

Mice were treated with naringenin (16.7, 50, or 150 mg/kg) by p.o. route starting 24 h after the i.a. injection of 3 mg/joint of TiO_2. Animals were treated daily for 30 days, 1 h before the articular mechanical hyperalgesia and edema measurements since naringenin peak-effect in mechanical hyperalgesia at day 1 occurred 1h after naringenin treatment (Fig 1a). The saline group did not present articular mechanical hyperalgesia (Fig. 1a) and edema (Fig. 1b). The i.a. injection of TiO_2 at day zero induced articular mechanical hyperalgesia (Fig. 1a) and edema (Fig. 1b) from 24-48 h after i.a. injection on the first day and subsequently from the 2^{nd} to 30^{th} day. All doses of naringenin inhibited TiO_2-induced articular mechanical

hyperalgesia at day 1. Naringenin effect lasted less than 24h, thus a daily treatment was required. Naringenin treatment inhibited TiO_2-induced articular mechanical hyperalgesia from the 2nd to 30th day. The dose of 16.7 mg/kg inhibited TiO_2-induced articular mechanical hyperalgesia from 1 to 5 h after the treatment (25-29 h after TiO_2 i.a. injection) on day one and up to 30 days. The dose of 50 mg/kg of naringenin inhibited TiO_2-induced articular mechanical hyperalgesia from 1 to 7 h after the treatment (25-31 h after TiO_2 i.a. injection) on day 1 and subsequently from day 2-30. In addition, the analgesic effect of the dose of 50 mg/kg of naringenin was statistically different compared to the other doses from days 2-30. The dose of 150 mg/kg of naringenin inhibited TiO_2-induced articular mechanical hyperalgesia only 5 h after naringenin treatment (29 h after TiO_2 i.a. injection) at day 1 and up to 30 days (Fig. 1a). Only the dose of 50 mg/kg of naringenin inhibited TiO_2-induced articular edema after 5 h after naringenin treatment (29 h after TiO_2 i.a. injection) at day 1 and from days 4-30. In addition, the inhibition of edema by the dose of 50 mg/kg of naringenin was statistically different compared to the other doses (Fig. 1b). Therefore, naringenin presented a bell-shaped dose-response curve with maximal effect with the dose of 50 mg/kg, which was chosen for the next experiments. At day 30, 1h after naringenin treatment, stomach, and blood samples were collected to evaluate if naringenin would induce gastric, hepatic, and renal damage. Naringenin did not induce MPO activity in stomach samples (Fig. 1c) or increase the levels of AST (Fig. 1d), ALT (Fig. 1e), urea (Fig. 1f), and creatinine (Fig. 1g) in the plasma. Therefore, chronic 30 days treatment with naringenin at a dose of 50 mg/kg did not induce detectable gastric, hepatic or renal lesion/damage. The treatment with positive control groups following previously established protocols demonstrates that the assays used can detect the selective tissue lesion markers [10, 28] (Fig. 1c-g).

Naringenin inhibits TiO_2-induced histopathological damage, recruitment of total leukocytes, polymorphonuclear, and mononuclear cells

Mice were treated daily for 30 days with naringenin (50 mg/kg, p.o.) starting 24 h after

the i.a. injection of 3 mg/joint of TiO_2. At day 30, 1h after naringenin treatment, knee joint was harvested to HE histopathology (Fig. 2a-g) evaluation and knee joint lavages were collected to count the number of total leukocytes (Fig. 2h), polymorphonuclear (Fig. 2i), and mononuclear cells (Fig. 2j). Naringenin inhibited TiO_2-induced synovial hyperplasia, inflammatory infiltrate, and vascular proliferation as observed in the histopathological index analyses (Fig. 2g). In agreement, naringenin inhibited TiO_2-induced recruitment of total leukocytes (Fig. 2h), polymorphonuclear (Fig. 2i) and mononuclear cells (Figure 2j) to the knee joint. Thus, naringenin reduced the recruitment of inflammatory cells induced by TiO_2 in the knee joint.

Naringenin inhibits TiO_2-induced cartilage erosion in the knee joint

Mice were treated as in Figure 2 and knee joint samples were collected for toluidine blue staining of cartilage and analyses (Fig. 3a-k). Patella samples were also collected for the determination of proteoglycan levels (Fig. 3i). TiO_2-decreased toluidine blue stained cartilage area (Fig 3b, e, h) in the tibia (Fig. 3b, h, k) but not in the femur (Fig. 3b, e, j) and patella proteoglycan content (Fig. 3i). Naringenin inhibited TiO_2-decreased toluidine blue staining cartilage in the tibia (Fig 3c, i, k) and patella proteoglycan content (Fig. 3l). These results demonstrate that naringenin inhibited TiO_2-induced cartilage destruction.

Naringenin inhibits TiO_2-induced bone resorption

Mice were treated as in Figure 2 and knee joint samples were collected to evaluate the TRAP staining (osteoclast marker) and the mRNA expression by RT-qPCR of the RANKL/RANK/OPG system. TiO_2 induced an increase of TRAP staining (Fig. 4b, e, g), and the RANKL mRNA expression (Fig. 4h), which were inhibited by naringenin treatment. TiO_2 did not alter the mRNA expression of RANK (Fig. 4i) and decreased OPG expression (Fig. 4j), but naringenin reduced the RANK mRNA expression and increased OPG mRNA expression. Therefore, naringenin inhibited TiO_2-induced dysregulation of markers of

increased bone resorption [10, 30, 31].

Naringenin inhibits TiO_2-induced oxidative stress

Animals were treated as in Figure 2 and knee joint samples were collected to evaluate the effect of naringenin on TiO_2-induced oxidative stress. TiO_2-induced an increase of $gp91^{phox}$ mRNA expression (Fig. 5a), and the production of superoxide anion (Fig. 5b) and lipid peroxidation (Fig. 5c), which were inhibited by naringenin treatment. Thus, demonstrating that naringenin not only inhibited TiO_2-induced oxidative stress, but also the upregulation of a NADPH oxidase (NOX)2 subunit involved in superoxide anion production [32].

Naringenin inhibits TiO_2-induced cytokines mRNA expression

Mice were treated as in Figure 2 and knee joint samples were collected to evaluate IL-33, TNFα, pro-IL-1β, and IL-6 mRNA expression. TiO_2-induced the expression of TNF-α (Fig. 6a), pro-IL-1β (Fig. 6b), IL-6 (Fig. 6c) and IL-33 (Fig 6d) mRNA expression, which were inhibited by naringenin treatment. Therefore, naringenin reduced the TiO_2-induced expression of pro-inflammatory cytokines involved in pain, edema, leukocyte recruitment and joint tissue degradation [30, 33-41, 26].

Naringenin inhibits TiO_2-induced NFκB activation

Considering that naringenin inhibited TiO_2-induced oxidative stress and the mRNA expression of enzymes and cytokines that are regulated by NFκB activation [42, 43], mice were treated as in Figure 2 and knee joint samples were collected to evaluate NFκB activation by ELISA (Fig. 7). TiO_2-induced an increase in phosphorylated p65 NFκB / total p65 NFκB ratio, indicating NFκB activation (phosphorylation), which was inhibited by naringenin treatment (Fig. 7). Therefore, naringenin inhibited the TiO_2-induced activation of a crucial pro-inflammatory transcription factor, NFκB. The present results were summarized in Fig. 8.

Discussion

Arthroplasty is an efficient and successful procedure to recover joint mobility and

functionality [4]. However, about 10-15% of the patients present intense inflammatory response triggered by wear debris released by biomaterials [6, 44]. TiO_2 is one of the main biomaterials used in the metallic prosthesis and implants and also a causative agent of articular inflammation and loosening of prosthesis and implants [9, 45]. In the present study, data show that naringenin reduced TiO_2-induced arthritic pain, edema and leukocyte recruitment to the knee joint. These beneficial effects were related to the reduction of oxidative stress and cytokine expression, which consequences of naringenin inhibition of TiO_2-induced NFκB activation. Naringenin effect occurred in a bell-shaped dose-response curve indicating that naringenin treatment reaches a maximum effect at a dose and increasing naringenin dose does not improve but rather reduces its efficacy. If naringenin goes through clinical testing, a dose-range for naringenin must be determined and increasing the dose indefinitely will not necessarily increase its efficacy. Considering that naringenin acts as an antioxidant, and other flavonoids such as myricetin inverse their antioxidant effects to pro-oxidant effect at high doses, it is reasonable to speculate that upon reaching the maximal antioxidant dose, higher doses of naringenin may start reducing the intended effect similarly to myricetin [46].

Evidence shows that the analgesic mechanisms of naringenin may encompass the targeting of nociceptive neurons function. For instance, naringenin modulates transient potential receptors (TRP) by blocking TRPV1 and TRPM3 and activating TRPM8 [47, 48]. Naringenin also activates the analgesic NO−cGMP−PKG−K_{ATP} channel signaling pathway [14, 16]. These data indicate that the analgesic effect of naringenin can also target the nociceptive neurons and not solely the peripheral inflammation as we demonstrated herein. In this sense, these results add to each other since present different perspectives. Naringenin presented a pronounced effect on TiO_2-induced knee edema, which lined up well with the inhibition of oxidative stress and cytokines since these molecules induce edema [49-51].

Depending on the underlying physiopathological mechanisms of the arthritis type and its degree of severity, therapeutic approaches may include the use of opioids, glucocorticoids, non-steroidal anti-inflammatory drugs, and disease modifying anti-rheumatic drugs [52]. Depending on the drug, doses, and chronicity of use, there are possible side effects including respiratory failure, addiction, gastrointestinal complications, hepatotoxicity, nephrotoxicity, cardiovascular effects and nausea [53]. The present evidence shows that naringenin is a safe drug given that long-term treatment (30 days) did not induce gastric, hepatic, or kidney damage. Corroborating the safety of naringenin, *in vitro* cell viability assay demonstrated that naringenin presents low toxicity when compared to other flavonoids, even at a high concentration such as 200 μM [54]. Short-term treatment (7 days) with naringenin also does not induce liver and stomach damage [16].

Herein, naringenin inhibited TiO_2-induced histopathological alterations including severe histopathological damage with vascular proliferation, increased leukocyte infiltration, and pannus formation (synovial hyperplasia) [10]. In agreement, naringenin reduces the histopathological alterations in monoiodoacetate (MIA)-induced osteoarthritis [55]. In addition, naringenin inhibited TiO_2-induced cartilage destruction and proteoglycan loss. We have previously observed that TiO_2-induced cartilage destruction with a decrease of proteoglycan content in the knee joint affects mainly the tibia [10]. In agreement with the present data, naringenin inhibits MIA- and IL-1β-induced metalloproteinases (MMP)-3 production in rats cartilage and primary cultured articular chondrocytes, respectively [55]. MMP play important role in cartilage destruction [56] and MMP-3 is well known for proteoglycan degradation and activation of procollagenases [57] This is a very important clinical benefit of naringenin since once the articular cartilage is destructed, there is no current treatment to heal it back to pre-disease condition [58].

The pronounced articular inflammation and cartilage destruction fuel the bone loss,

which predisposes to bone fractures and increases the severity of motor incapacity and pain. TiO_2 induced an increase of TRAP staining, which indicates the increase of osteoclastic activity in the bone. The TRAP staining aligned with the increase of RANKL and decrease of OPG mRNA expression since RANKL induces osteoclast formation and bone resorption and OPG inhibits the activity of RANKL [59, 60]. RANK expression was not altered indicating that the receptor for RANKL already has sufficient expression for the enhanced RANKL activity. Naringenin inhibited these alterations in bone metabolism induced by TiO_2, and also decreased RANK and increased OPG mRNA expression, which further supports the capacity of naringenin to reduce bone erosion. The cartilage loss facilitates the interaction of recruited neutrophils and osteoclasts. This neutrophil-osteoclast interaction induces osteoclast differentiation [61]. Thus, the cartilage loss and activated inflammatory cells account to increase bone loss.

Naringenin possesses *in vitro* and *in vivo* antioxidant activity [14, 16, 15, 54]. In fact, *in vitro* data show that naringenin presents scavenger ability at 40 μM and molecular docking demonstrated that naringenin reduces NADPH oxidase activation by inhibiting PKC-mediated $p47^{phox}$ phosphorylation by interacting with Gly-253 and Leu-251 amino acid residues [54]. In addition, *in vivo* data show that naringenin also increases Nrf2 activation, a transcription factor that is related to the expression of antioxidant molecules such as GSH [14, 16] suggesting that naringenin not only reduces ROS but also increases antioxidant defense. In agreement, naringenin inhibits oxidative stress in superoxide anion- [14] and carrageenan-induced [16] inflammatory pain, streptozotocin-induced diabetic neuropathy [62]. On the other hand, these effects of naringenin seem to impair neutrophils microbicidal activity. For instance, naringenin inhibits the killing of *Staphylococcus* aureus by neutrophils [63]. Therefore, given the relationship between oxidative stress and pain, the inhibition of the parameters herein evaluated is an important mechanism of naringenin to mitigate aseptic

inflammatory pain.

Phagocytes such as macrophages and neutrophils express the NOX2 that has gp91^{phox} as a subunit regulating superoxide anion production that in turn, will lead to the production of other ROS and in the end, lipid peroxidation [32]. TiO_2 enhances the phagocytic activity of neutrophils in a Syk (spleen tyrosine kinase)-dependent manner [64] and as consequence activates NADPH oxidase generating superoxide anion [65]. Naringenin inhibited TiO_2-enhanced gp91^{phox}mRNA expression, which corroborated the superoxide anion production and lipid peroxidation. In agreement, naringenin inhibits superoxide anion-induced oxidative stress inhibiting superoxide anion production, lipid peroxidation and gp91^{phox} mRNA expression [14]. ROS contribute to tissue lesion and accounts to cartilage and bone destruction [66-69]. Superoxide anion causes bone fragility due to lowering the turnover resulting in osteoporosis and impairing collagen cross-linking [70]. For instance, ROS, and in specific gp91^{phox} contributes to osteoclast differentiation [71], and naringenin inhibits RANKL-induced osteoclast differentiation and bone resorption [20]. Superoxide anion also induced hyperalgesia, edema, and leukocyte recruitment by further inducing the production of cytokines such as TNFα and IL-1β [14, 72], which were reduced by naringenin [14]. The superoxide anion-induced cytokine production depends on activating NFκB [72].

Herein, naringenin inhibited TiO_2-induced mRNA expression of IL-33, TNFα, IL-1β and IL-6. TiO_2 activates macrophages [9], which release pro-inflammatory cytokines, including TNFα [9], IL-1β [73] and IL-6 [74]. Naringenin inhibits TNFα, IL-1β, IL-6 and IL-33 in carrageenan-, LPS- and superoxide anion-induced inflammatory pain [15, 16, 14]. These cytokines participate in the chemoattraction of neutrophils [40, 26, 41]. TiO_2 also activates the recruited neutrophils[64] that participate in the destruction of cartilage and bone directly by releasing neutrophil extracellular traps (NETs). Releasing NETs results in histone citrullination, which is a mechanism involved in rheumatoid arthritis and also in TiO_2 and

implant-induced arthritis [75]. Cytokines produced by TiO_2 stimulus such as IL-33, IL-1β, and TNF-α that increase the release of MMP, activate chondrocytes and osteoclasts [26, 76]. Further, naringenin inhibits IL-1β-induced MMP-3 production in primary cultured articular chondrocytes [55]. TNFα and IL-6 induce osteoclastogenesis in osteoclast medium culture with synovial cells from RANK knockout mice, showing a RANK-independent manner to induces osteoclast formation[30]. Naringenin might also inhibit osteoclast formation in a RANK-independent manner since it reduces TNFα and IL-6 production in LPS-induced inflammation [15]. TiO_2 also enhances neutrophils phagocytosis in a Syk (spleen tyrosine kinase)-dependent manner[64] and activates NADPH oxidase generating superoxide anion [65]. And cytokines produced upon TiO_2 stimulus induce superoxide anion production. This result lined up with the inhibition of leukocyte recruitment, and also with the inhibition of oxidative stress, edema, cartilage destruction and bone degradation. In addition, evidence shows that naringenin reduces TNFα-induced ICAM-1 expression in human endothelial cells [77], a mechanism essential to leukocyte recruitment [78-80]. In chronic inflammation and neuropathic conditions IL-33 [33], TNFα [34], IL-1β [35] and IL-6 [36] activate sensory neurons, which is a nociceptive mechanism. In this sense, the inhibition of cytokine production is also an analgesic effect [81].

NFκB activation plays an essential role in the development and progression of arthritis once it is directly involved in the regulation of pro-inflammatory mediators production in the inflamed joint [82]. Herein, naringenin inhibited TiO_2-induced NFκB activation in the knee joint. NFκB signaling pathway also possesses an important role in RANKL-induced osteoclast formation given that NFκB selective inhibitors such as SC-514 (IKKβ inhibitor) and NBD (IKKγ inhibitor) block osteoclast differentiation [83]. Accumulated TiO_2 induces NFκB activation and TNFα release in the brain of rats [84], and in HepG2 cells [85]. Further, naringenin inhibits NFκB activation in MIA-induced osteoarthritis [55] and in LPS- and

carrageenan-induced inflammatory pain in mice [15, 16].Therefore, naringenin inhibition of NFκB activation is a consistent effect in varied models.

In conclusion, the present data suggest that naringenin ameliorates TiO_2-induced chronic arthritis. Naringenin mitigates TiO_2-induced inflammatory pain, knee edema, histopathological damage, leukocyte recruitment, cartilage erosion, and bone resorption by inhibiting oxidative stress, cytokine mRNA expression, and NFκB activation. Therefore, naringenin represents a promising therapeutic approach to mitigate the complications related to implant-induced aseptic inflammation.

Conflict of interest
The authors declare no conflict of interest.

Acknowledgments
We thank M.R.F.D.P., A.Z.Z. and M.M.B for the technical support and T.H.Z for the support in the Adobe Illustrator. This study was supported by grants from Conselho Nacional de Desenvolvimento Científico e Tecnológico (CNPq), São Paulo research Foundation (FAPESP) under grant agreements number 2011/19670-0 (Thematic project) and 2013/08216-2 (Center for Research in Inflammatory Disease-CRID), Coordenação de Aperfeiçoamento de Pessoal de Nível Superior (CAPES), and Programa de Pesquisa para o SUS (PPSUS) grant supported by Ministério da Ciência, Tecnologia e Inovação (MCTI), Secretaria da Ciência, Tecnologia e Ensino Superior (SETI), Decit/SCTIE/MS through CNPq with the support of Fundação Araucária and Secretaria da Saúde do Estado do Paraná (SESA-PR), and Parana State Government (Brazil).

References
1. Siddiqui MMA, Yeo SJ, Sivaiah P, Chia S-L, Chin PL, Lo NN. Function and quality of life in patients with recurvatum deformity after primary total knee arthroplasty: a review of our joint registry. The Journal of arthroplasty. 2012;27(6):1106-10. doi:10.1016/j.arth.2011.10.013.
2. Soever LJ, Mackay C, Saryeddine T, Davis AM, Flannery JF, Jaglal SB et al. Educational needs of patients undergoing total joint arthroplasty. Physiotherapy Canada Physiothérapie Canada. 2010;62(3):206-14. doi:10.3138/physio.62.3.206.
3. Maradit Kremers H, Larson DR, Crowson CS, Kremers WK, Washington RE, Steiner CA et al. Prevalence of total hip and knee replacement in the United States. The Journal of Bone

and Joint Surgery-American Volume. 2015;97(17):1386-97. doi:10.2106/JBJS.N.01141.
4. Carr AJ, Robertsson O, Graves S, Price AJ, Arden NK, Judge A et al. Knee replacement. The Lancet. 2012;379(9823):1331-40. doi:10.1016/S0140-6736(11)60752-6.
5. Cobelli N, Scharf B, Crisi GM, Hardin J, Santambrogio L. Mediators of the inflammatory response to joint replacement devices. Nature Publishing Group. 2011;7(10):600-8. doi:10.1038/nrrheum.2011.128.
6. Goodman SB. Wear particles, periprosthetic osteolysis and the immune system. Biomaterials. 2007;28(34):5044-8. doi:10.1016/j.biomaterials.2007.06.035.
7. Gurr J-R, Wang ASS, Chen C-H, Jan K-Y. Ultrafine titanium dioxide particles in the absence of photoactivation can induce oxidative damage to human bronchial epithelial cells. Toxicology. 2005;213(1-2):66-73. doi:10.1016/j.tox.2005.05.007.
8. Apostu D, Lucaciu O, Lucaciu GDO, Crisan B, Crisan L, Baciut M et al. Systemic Drugs That Influence Titanium Implant Osseointegration. Drug Metabolism Reviews. 2016:1-46. doi:10.1080/03602532.2016.1277737.
9. Dörner T, Haas J, Loddenkemper C, von Baehr V, Salama A. Implant-related inflammatory arthritis. Nature Clinical Practice Rheumatology. 2006;2(1):53-6. doi:10.1038/ncprheum0087.
10. Borghi SM, Mizokami SS, Pinho-Ribeiro FA, Fattori V, Crespigio J, Clemente-Napimoga JT et al. The flavonoid quercetin inhibits titanium dioxide (TiO2)-induced chronic arthritis in mice. J Nutr Biochem. 2017;53:81-95. doi:10.1016/j.jnutbio.2017.10.010.
11. Verri WA, Vicentini FTMC, Baracat MM, Georgetti SR, Cardoso RDR, Cunha TM et al. Flavonoids as anti-inflammatory and analgesic drugs: Mechanisms of action and perspectives in the development of pharmaceutical forms. In: Atta-ur-Rahman, editor. Studies in Natural Products Chemistry. 2012. p. 297-330.
12. Lee CH, Jeong TS, Choi YK, Hyun BH, Oh GT, Kim EH et al. Anti-atherogenic effect of citrus flavonoids, naringin and naringenin, associated with hepatic ACAT and aortic VCAM-1 and MCP-1 in high cholesterol-fed rabbits. Biochemical and biophysical research communications. 2001;284(3):681-8. doi:10.1006/bbrc.2001.5001.
13. Sun H, Dong T, Zhang A, Yang J, Yan G, Sakurai T et al. Pharmacokinetics of hesperetin and naringenin in the Zhi Zhu Wan, a traditional Chinese medicinal formulae, and its pharmacodynamics study. Phytother Res. 2013;27(9):1345-51. doi:10.1002/ptr.4867.
14. Manchope MF, Calixto-Campos C, Coelho-Silva L, Zarpelon AC, Pinho-Ribeiro FA, Georgetti SR et al. Naringenin Inhibits Superoxide Anion-Induced Inflammatory Pain: Role of Oxidative Stress, Cytokines, Nrf-2 and the NO-cGMP-PKG-KATPChannel Signaling Pathway. PloS one. 2016;11(4):e0153015-e. doi:10.1371/journal.pone.0153015.
15. Pinho-Ribeiro FA, Zarpelon AC, Mizokami SS, Borghi SM, Bordignon J, Silva RL et al. The citrus flavonone naringenin reduces lipopolysaccharide-induced inflammatory pain and leukocyte recruitment by inhibiting NF-κB activation. Journal of Nutritional Biochemistry. 2016;33:8-14. doi:10.1016/j.jnutbio.2016.03.013.
16. Pinho-Ribeiro FA, Zarpelon AC, Fattori V, Manchope MF, Mizokami SS, Casagrande R et al. Naringenin reduces inflammatory pain in mice. Neuropharmacology. 2016;105:508-19. doi:10.1016/j.neuropharm.2016.02.019.
17. Wang J, Fan Y. Lung injury induced by TiO2 nanoparticles depends on their structural features: Size, shape, crystal phases, and surface coating. International Journal of Molecular Sciences. 2014;15(12):22258-78. doi:10.3390/ijms151222258.
18. Ashley NT, Weil ZM, Nelson RJ. Inflammation: Mechanisms, Costs, and Natural Variation. The Annual Review of Ecology, Evolution, and Systematics 2012;43:385-406. doi:10.1146/annurev-ecolsys-040212-092530.
19. Smolen JS, Aletaha D, McInnes IB. Rheumatoid arthritis. Lancet. 2016;388(10055):2023-38. doi:10.1016/S0140-6736(16)30173-8.
20. Wang W, Wu C, Tian B, Liu X, Zhai Z, Qu X et al. The Inhibition of RANKL-Induced

Osteoclastogenesis through the Suppression of p38 Signaling Pathway by Naringenin and Attenuation of Titanium-Particle-Induced Osteolysis. International Journal of Molecular Sciences. 2014;15(12):21913-34. doi:10.3390/ijms151221913.
21. Wang JX, Fan YB, Gao Y, Hu QH, Wang TC. TiO2 nanoparticles translocation and potential toxicological effect in rats after intraarticular injection. Biomaterials. 2009;30(27):4590-600. doi:10.1016/j.biomaterials.2009.05.008.
22. Guerrero ATG, Verri WA, Cunha TM, Silva TA, Rocha FAC, Ferreira SH et al. Hypernociception elicited by tibio-tarsal joint flexion in mice: a novel experimental arthritis model for pharmacological screening. Pharmacology, biochemistry, and behavior. 2006;84(2):244-51. doi:10.1016/j.pbb.2006.05.008.
23. Yamanaka H, Goto K, Miyamoto K. Scoring evaluation for histopathological features of synovium in patients with rheumatoid arthritis during anti-tumor necrosis factor therapy. Rheumatol Int. 2010;30(3):409-13. doi:10.1007/s00296-009-1158-2.
24. Sun J, Hua B, Livingston EW, Taves S, Johansen PB, Hoffman M et al. Abnormal joint and bone wound healing in hemophilia mice is improved by extending factor IX activity after hemarthrosis. Blood. 2017;129(15):2161-71. doi:10.1182/blood-2016-08-734053.
25. Casagrande R, Georgetti SR, Verri WA, Dorta DJ, dos Santos AC, Fonseca MJV. Protective effect of topical formulations containing quercetin against UVB-induced oxidative stress in hairless mice. Journal of photochemistry and photobiology B, Biology. 2006;84(1):21-7. doi:10.1016/j.jphotobiol.2006.01.006.
26. Verri WA, Souto FO, Vieira SM, Almeida SCL, Fukada SY, Xu D et al. IL-33 induces neutrophil migration in rheumatoid arthritis and is a target of anti-TNF therapy. Annals of the Rheumatic Diseases. 2010;69(9):1697-703. doi:10.1136/ard.2009.122655.
27. Vieira SM, Cunha TM, Franca RF, Pinto LG, Talbot J, Turato WM et al. Joint NOD2/RIPK2 signaling regulates IL-17 axis and contributes to the development of experimental arthritis. J Immunol. 2012;188(10):5116-22. doi:10.4049/jimmunol.1004190.
28. Hohmann MSN, Cardoso RDR, Pinho-Ribeiro FA, Crespigio J, Cunha TM, Alves-Filho JC et al. 5-lipoxygenase deficiency reduces acetaminophen-induced hepatotoxicity and lethality. BioMed research international. 2013;2013:627046-. doi:10.1155/2013/627046.
29. Guedes RP, Bosco LD, Teixeira CM, Araújo ASR, Llesuy S, Belló-Klein A et al. Neuropathic pain modifies antioxidant activity in rat spinal cord. Neurochemical research. 2006;31(5):603-9. doi:10.1007/s11064-006-9058-2.
30. O'Brien W, Fissel BM, Maeda Y, Yan J, Ge X, Gravallese EM et al. RANK-Independent Osteoclast Formation and Bone Erosion in Inflammatory Arthritis. Arthritis & Rheumatology. 2016;68(12):2889-900. doi:10.1002/art.39837.
31. Danks L, Komatsu N, Guerrini MM, Sawa S, Armaka M, Kollias G et al. RANKL expressed on synovial fibroblasts is primarily responsible for bone erosions during joint inflammation. Annals of the Rheumatic Diseases. 2016;75(6):1187-95. doi:10.1136/annrheumdis-2014-207137.
32. Lambeth JD. NOX enzymes and the biology of reactive oxygen. Nature Reviews Immunology. 2004;4(3):181-9. doi:10.1038/nri1312.
33. Liu B, Tai Y, Achanta S, Kaelberer MM, Caceres AI, Shao X et al. IL-33/ST2 signaling excites sensory neurons and mediates itch response in a mouse model of poison ivy contact allergy. Proceedings of the National Academy of Sciences. 2016;113(47):E7572-E9. doi:10.1073/pnas.1606608113.
34. Jin X, Gereau RW. Acute p38-Mediated Modulation of Tetrodotoxin-Resistant Sodium Channels in Mouse Sensory Neurons by Tumor Necrosis Factor. Journal of Neuroscience. 2006;26(1):246-55. doi:10.1523/JNEUROSCI.3858-05.2006.
35. Binshtok AM, Wang H, Zimmermann K, Amaya F, Vardeh D, Shi L et al. Nociceptors Are Interleukin-1 Sensors. Journal of Neuroscience. 2008;28(52):14062-73.

doi:10.1523/JNEUROSCI.3795-08.2008.
36. Ebbinghaus M, Segond von Banchet G, Massier J, Gajda M, Brauer R, Kress M et al. Interleukin-6-dependent influence of nociceptive sensory neurons on antigen-induced arthritis. Arthritis Res Ther. 2015;17:334. doi:10.1186/s13075-015-0858-0.
37. Vieira SM, Lemos HP, Grespan R, Napimoga MH, Dal-Secco D, Freitas A et al. A crucial role for TNF-alpha in mediating neutrophil influx induced by endogenously generated or exogenous chemokines, KC/CXCL1 and LIX/CXCL5. Br J Pharmacol. 2009;158(3):779-89. doi:10.1111/j.1476-5381.2009.00367.x.
38. Mascarenhas DP, Pereira MS, Manin GZ, Hori JI, Zamboni DS. Interleukin 1 receptor-driven neutrophil recruitment accounts to MyD88-dependent pulmonary clearance of legionella pneumophila infection in vivo. J Infect Dis. 2015;211(2):322-30. doi:10.1093/infdis/jiu430.
39. Romano M, Sironi M, Toniatti C, Polentarutti N, Fruscella P, Ghezzi P et al. Role of IL-6 and its soluble receptor in induction of chemokines and leukocyte recruitment. Immunity. 1997;6(3):315-25.
40. Lan F, Yuan B, Liu T, Luo X, Huang P, Liu Y et al. Interleukin-33 facilitates neutrophil recruitment and bacterial clearance in S. aureus-caused peritonitis. Mol Immunol. 2016;72:74-80. doi:10.1016/j.molimm.2016.03.004.
41. Alves-Filho JC, Sonego F, Souto FO, Freitas A, Verri WA, Jr., Auxiliadora-Martins M et al. Interleukin-33 attenuates sepsis by enhancing neutrophil influx to the site of infection. Nat Med. 2010;16(6):708-12. doi:10.1038/nm.2156.
42. Poynter ME, Irvin CG, Janssen-Heininger YM. A prominent role for airway epithelial NF-kappa B activation in lipopolysaccharide-induced airway inflammation. J Immunol. 2003;170(12):6257-65.
43. Anrather J, Racchumi G, Iadecola C. NF-kappaB regulates phagocytic NADPH oxidase by inducing the expression of gp91phox. J Biol Chem. 2006;281(9):5657-67. doi:10.1074/jbc.M506172200.
44. Harris WH. Wear and periprosthetic osteolysis the problem. Clinical orthopaedics and related research. 2001(393):66-70.
45. Long M, Rack HJ. Titanium alloys in total joint replacement--a materials science perspective. Biomaterials. 1998;19(18):1621-39.
46. Chobot V, Hadacek F. Exploration of pro-oxidant and antioxidant activities of the flavonoid myricetin. Redox Rep. 2011;16(6):242-7. doi:10.1179/1351000211Y.0000000015.
47. Straub I, Mohr F, Stab J, Konrad M, Philipp SE, Oberwinkler J et al. Citrus fruit and fabacea secondary metabolites potently and selectively block TRPM3. British Journal of Pharmacology. 2013;168(8):1835-50. doi:10.1111/bph.12076.
48. Manchope MF, Casagrande R, Verri JWA, Manchope MF, Casagrande R, Verri JWA. Naringenin: an analgesic and anti-inflammatory citrus flavanone. Oncotarget. 2017;8(3):3766-7. doi:10.18632/oncotarget.14084.
49. Murakawa M, Yamaoka K, Tanaka Y, Fukuda Y. Involvement of tumor necrosis factor (TNF)-alpha in phorbol ester 12-O-tetradecanoylphorbol-13-acetate (TPA)-induced skin edema in mice. Biochem Pharmacol. 2006;71(9):1331-6. doi:10.1016/j.bcp.2006.01.005.
50. Seven A, Guzel S, Seymen O, Civelek S, Bolayirli M, Yigit G et al. Nitric oxide synthase inhibition by L-NAME in streptozotocin induced diabetic rats: impacts on oxidative stress. Tohoku J Exp Med. 2003;199(4):205-10.
51. Salvemini D, Wang ZQ, Wyatt PS, Bourdon DM, Marino MH, Manning PT et al. Nitric oxide: a key mediator in the early and late phase of carrageenan-induced rat paw inflammation. Br J Pharmacol. 1996;118(4):829-38.
52. Fattori V, Amaral FA, Verri WA. Neutrophils and arthritis: Role in disease and pharmacological perspectives. Pharmacological research. 2016.

doi:10.1016/j.phrs.2016.01.027.
53. Scott DL, Wolfe F, Huizinga TWJ. Rheumatoid arthritis. The Lancet. 2010;376(9746):1094-108. doi:10.1016/S0140-6736(10)60826-4.
54. Kongpichitchoke T, Hsu J-L, Huang T-C. Number of Hydroxyl Groups on the B-Ring of Flavonoids Affects Their Antioxidant Activity and Interaction with Phorbol Ester Binding Site of PKCδ C1B Domain: In Vitro and in Silico Studies. Journal of Agricultural and Food Chemistry. 2015;63(18):4580-6. doi:10.1021/acs.jafc.5b00312.
55. Wang CC, Guo L, Tian FD, An N, Luo L, Hao RH et al. Naringenin regulates production of matrix metalloproteinases in the knee-joint and primary cultured articular chondrocytes and alleviates pain in rat osteoarthritis model. Braz J Med Biol Res. 2017;50(4):e5714. doi:10.1590/1414-431X20165714.
56. Murphy G, Lee MH. What are the roles of metalloproteinases in cartilage and bone damage? Ann Rheum Dis. 2005;64 Suppl 4:iv44-7. doi:10.1136/ard.2005.042465.
57. Lin PM, Chen CT, Torzilli PA. Increased stromelysin-1 (MMP-3), proteoglycan degradation (3B3- and 7D4) and collagen damage in cyclically load-injured articular cartilage. Osteoarthritis Cartilage. 2004;12(6):485-96. doi:10.1016/j.joca.2004.02.012.
58. Steinert AF, Noth U, Tuan RS. Concepts in gene therapy for cartilage repair. Injury. 2008;39 Suppl 1:S97-113. doi:10.1016/j.injury.2008.01.034.
59. Hofbauer LC, Schoppet M. Clinical Implications of the Osteoprotegerin/RANKL/RANK System for Bone and Vascular Diseases. JAMA. 2004;292(4):490-. doi:10.1001/jama.292.4.490.
60. Boyle WJ, Simonet WS, Lacey DL. Osteoclast differentiation and activation. Nature. 2003;423(6937):337-42. doi:10.1038/nature01658.
61. Chakravarti A, Raquil M-A, Tessier P, Poubelle PE. Surface RANKL of Toll-like receptor 4–stimulated human neutrophils activates osteoclastic bone resorption. Blood. 2009;114(8).
62. Al-Rejaie SS, Aleisa AM, Abuohashish HM, Parmar MY, Ola MS, Al-Hosaini AA et al. Naringenin neutralises oxidative stress and nerve growth factor discrepancy in experimental diabetic neuropathy. Neurological Research. 2015;37(10):924-33. doi:10.1179/1743132815Y.0000000079.
63. Nishimura FdCY, de Almeida AC, Ratti BA, Ueda-Nakamura T, Nakamura CV, Ximenes VF et al. Antioxidant effects of quercetin and naringenin are associated with impaired neutrophil microbicidal activity. Evidence-based complementary and alternative medicine : eCAM. 2013;2013:795916-. doi:10.1155/2013/795916.
64. Gonçalves DM, Chiasson S, Girard D. Activation of human neutrophils by titanium dioxide (TiO2) nanoparticles. Toxicology in Vitro. 2010;24(3):1002-8. doi:10.1016/j.tiv.2009.12.007.
65. Masoud R, Bizouarn T, Trepout S, Wien F, Baciou L, Marco S et al. Titanium Dioxide Nanoparticles Increase Superoxide Anion Production by Acting on NADPH Oxidase. PLOS ONE. 2015;10(12):e0144829-e. doi:10.1371/journal.pone.0144829.
66. Callaway DA, Jiang JX. Reactive oxygen species and oxidative stress in osteoclastogenesis, skeletal aging and bone diseases. J Bone Miner Metab. 2015;33(4):359-70. doi:10.1007/s00774-015-0656-4.
67. Kim MS, Yang YM, Son A, Tian YS, Lee SI, Kang SW et al. RANKL-mediated reactive oxygen species pathway that induces long lasting Ca2+ oscillations essential for osteoclastogenesis. J Biol Chem. 2010;285(10):6913-21. doi:10.1074/jbc.M109.051557.
68. Rees MD, Hawkins CL, Davies MJ. Hypochlorite and superoxide radicals can act synergistically to induce fragmentation of hyaluronan and chondroitin sulphates. Biochem J. 2004;381(Pt 1):175-84. doi:10.1042/BJ20040148.
69. Henrotin YE, Bruckner P, Pujol JP. The role of reactive oxygen species in homeostasis and degradation of cartilage. Osteoarthritis Cartilage. 2003;11(10):747-55.

70. Nojiri H, Saita Y, Morikawa D, Kobayashi K, Tsuda C, Miyazaki T et al. Cytoplasmic superoxide causes bone fragility owing to low-turnover osteoporosis and impaired collagen cross-linking. J Bone Miner Res. 2011;26(11):2682-94. doi:10.1002/jbmr.489.
71. Kang IS, Kim C. NADPH oxidase gp91(phox) contributes to RANKL-induced osteoclast differentiation by upregulating NFATc1. Sci Rep. 2016;6:38014. doi:10.1038/srep38014.
72. Pinho-Ribeiro FA, Fattori V, Zarpelon AC, Borghi SM, Staurengo-Ferrari L, Carvalho TT et al. Pyrrolidine dithiocarbamate inhibits superoxide anion-induced pain and inflammation in the paw skin and spinal cord by targeting NF-κB and oxidative stress. Inflammopharmacology. 2016;24(2-3):97-107. doi:10.1007/s10787-016-0266-3.
73. St Pierre CA, Chan M, Iwakura Y, Ayers DC, Kurt-Jones EA, Finberg RW. Periprosthetic osteolysis: characterizing the innate immune response to titanium wear-particles. Journal of orthopaedic research : official publication of the Orthopaedic Research Society. 2010;28(11):1418-24. doi:10.1002/jor.21149.
74. Borgognoni CF, Mormann M, Qu Y, Schäfer M, Langer K, Öztürk C et al. Reaction of human macrophages on protein corona covered TiO_2 nanoparticles. Nanomedicine : nanotechnology, biology, and medicine. 2015;11(2):275-82. doi:10.1016/j.nano.2014.10.001.
75. Vitkov L, Krautgartner W-D, Obermayer A, Stoiber W, Hannig M, Klappacher M et al. The Initial Inflammatory Response to Bioactive Implants Is Characterized by NETosis. PLOS ONE. 2015;10(3):e0121359-e. doi:10.1371/journal.pone.0121359.
76. Wright HL, Moots RJ, Edwards SW. The multifactorial role of neutrophils in rheumatoid arthritis. Nature Reviews Rheumatology. 2014;10(10):593-601. doi:10.1038/nrrheum.2014.80.
77. Freischmidt A, Jürgenliemk G, Kraus B, Okpanyi SN, Müller J, Kelber O et al. Contribution of flavonoids and catechol to the reduction of ICAM-1 expression in endothelial cells by a standardised Willow bark extract. Phytomedicine. 2012;19(3-4):245-52. doi:10.1016/j.phymed.2011.08.065.
78. Martinelli R, Gegg M, Longbottom R, Adamson P, Turowski P, Greenwood J. ICAM-1-mediated endothelial nitric oxide synthase activation via calcium and AMP-activated protein kinase is required for transendothelial lymphocyte migration. Molecular biology of the cell. 2009;20(3):995-1005. doi:10.1091/mbc.E08-06-0636.
79. Dal Secco D, Moreira AP, Freitas A, Silva JS, Rossi MA, Ferreira SH et al. Nitric oxide inhibits neutrophil migration by a mechanism dependent on ICAM-1: Role of soluble guanylate cyclase. Nitric Oxide. 2006;15(1):77-86. doi:10.1016/j.niox.2006.02.004.
80. Kevil CG, Patel RP, Bullard DC. Essential role of ICAM-1 in mediating monocyte adhesion to aortic endothelial cells. American journal of physiology Cell physiology. 2001;281(5):C1442-7.
81. Verri WA, Cunha TM, Parada CA, Poole S, Cunha FQ, Ferreira SH. Hypernociceptive role of cytokines and chemokines: Targets for analgesic drug development? Pharmacology & Therapeutics. 2006;112(1):116-38. doi:10.1016/j.pharmthera.2006.04.001.
82. Simmonds RE, Foxwell BM. Signalling, inflammation and arthritis: NF- B and its relevance to arthritis and inflammation. Rheumatology. 2008;47(5):584-90. doi:10.1093/rheumatology/kem298.
83. Yu M, Qi X, Moreno JL, Farber DL, Keegan AD. NF-κB signaling participates in both RANKL- and IL-4-induced macrophage fusion: receptor cross-talk leads to alterations in NF-κB pathways. Journal of immunology (Baltimore, Md : 1950). 2011;187(4):1797-806. doi:10.4049/jimmunol.1002628.
84. Meena R, Kumar S, Paulraj R. Titanium oxide (TiO2) nanoparticles in induction of apoptosis and inflammatory response in brain. Journal of Nanoparticle Research. 2015;17(1):49-. doi:10.1007/s11051-015-2868-x.
85. Prasad RY, Simmons SO, Killius MG, Zucker RM, Kligerman AD, Blackman CF et al.

Cellular interactions and biological responses to titanium dioxide nanoparticles in HepG2 and BEAS-2B cells: Role of cell culture media. Environmental and Molecular Mutagenesis. 2014;55(4):336-42. doi:10.1002/em.21848.

Figures and Captions

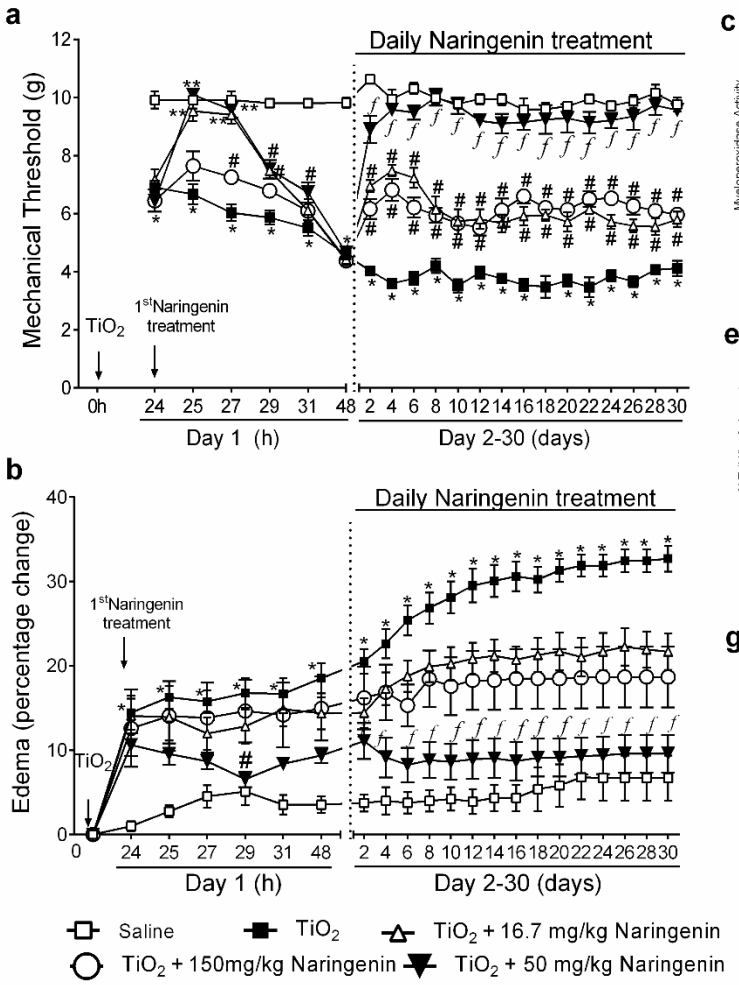

Fig. 1 Naringenin inhibits TiO_2-induced articular mechanical hyperalgesia and edema without inducing toxicity. Mice were treated daily for 30 days with naringenin (16.7, 50, or 150 mg/kg, p.o.) starting 24 h after intra-articular injection of TiO_2 (3 mg/joint). (a) Articular mechanical hyperalgesia and (b) edema were measured initially from 24-48 h (Day 1) after TiO_2 injection and subsequently every other day until day 30 after TiO_2 injection (Day 2 – 30). At the day 30, naringenin-induced (c) MPO activity in the stomach; (d) AST and (e) ALT plasmatic levels; (f) urea and (g) creatinine plasmatic levels were determined to evaluate treatment toxicity. As positive drug control for gastric, hepatic and

renal toxicity indomethacin (2.5 mg/kg, i.p., diluted in tris/HCl buffer, during 7 days); acetaminophen (650 mg/kg, i.p., diluted in saline); and diclofenac (200 mg/kg, p.o., diluted in saline, once) were used, respectively. Results are presented as mean ± SEM of six mice per group per experiment and are representative of two separate experiments. [*p < 0.05 compared to the saline group; #p < 0.05 compared to the TiO2 group; **p < 0.05 compared to the TiO2 and naringenin (150 mg/kg) groups; *f*p < 0.05 compared to the TiO2 and naringenin (16.7 and 150 mg/kg) groups (repeated measures two-way ANOVA (a,b) and one-way ANOVA (c-g) followed by Tukey's post hoc)].

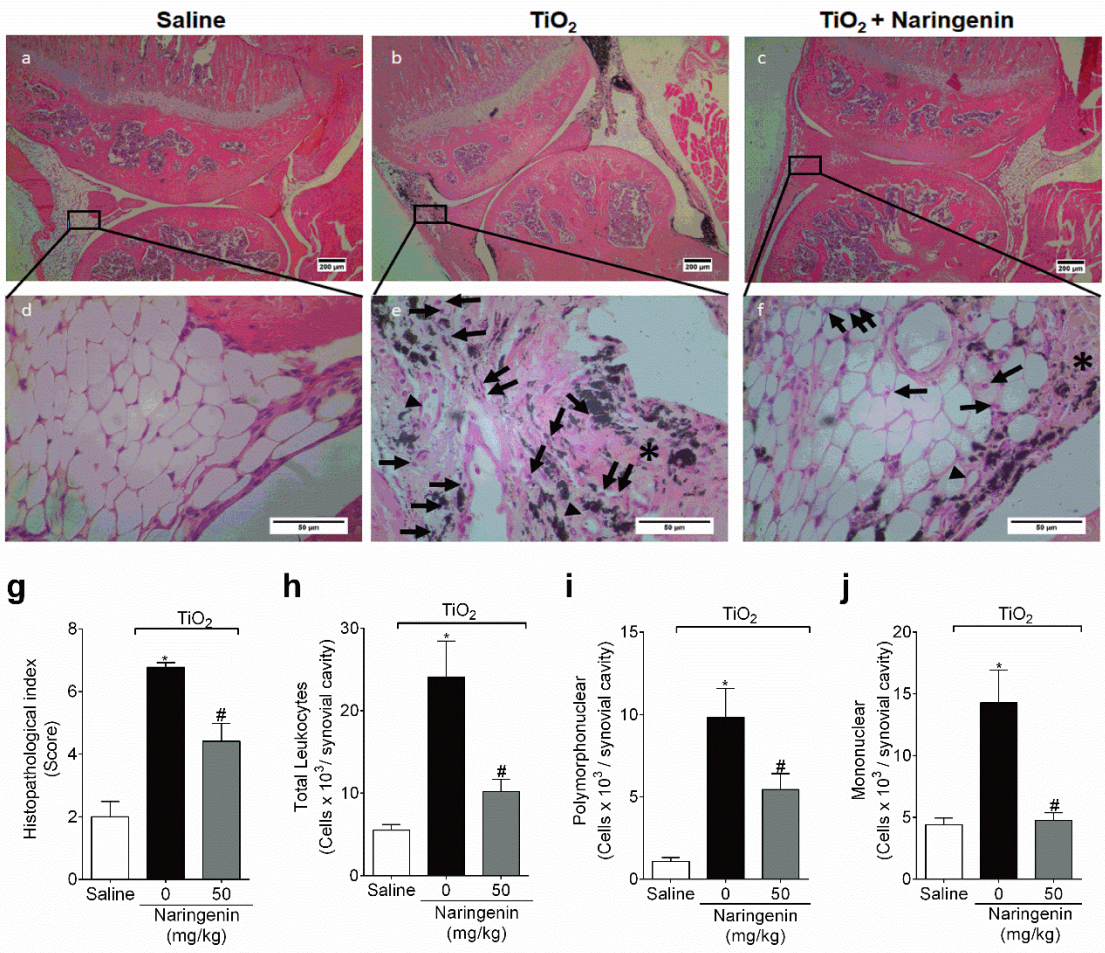

Fig. 2 Naringenin inhibits TiO_2-induced histopathological damage, recruitment of total leukocytes, polymorphonuclear and mononuclear cells. Mice were treated daily for 30 days

with naringenin (50 mg/kg, p.o.) starting 24 h after intra-articular injection of TiO_2 (3 mg/ joint). Histopathological analysis (a-f) and index (g), total leukocytes (h), polymorphonuclear (i), and mononuclear cells (j) count in knee joint lavages were evaluated 30 days after TiO_2 injection. The sites where the images of the Panels d–f were captured from Panels a–c. The parameters analyzed were (*) invasive pannus formation; leukocyte infiltration was represented by an arrow; and vascularity with an arrowhead. Saline (a and d); TiO_2 (b and e); and TiO_2 treated with naringenin (c and f). The samples were stained with HE. Original magnification 4× (scale bar 200 μm) and 40× (scale bar 50 μm), *n*=6. Results are presented as mean ± SEM of six mice per group per experiment and are representative of two separate experiments. [*$p < 0.05$ compared to the saline group; #$p < 0.05$ compared to the TiO_2 group (one-way ANOVA followed by Tukey's *post hoc*)].

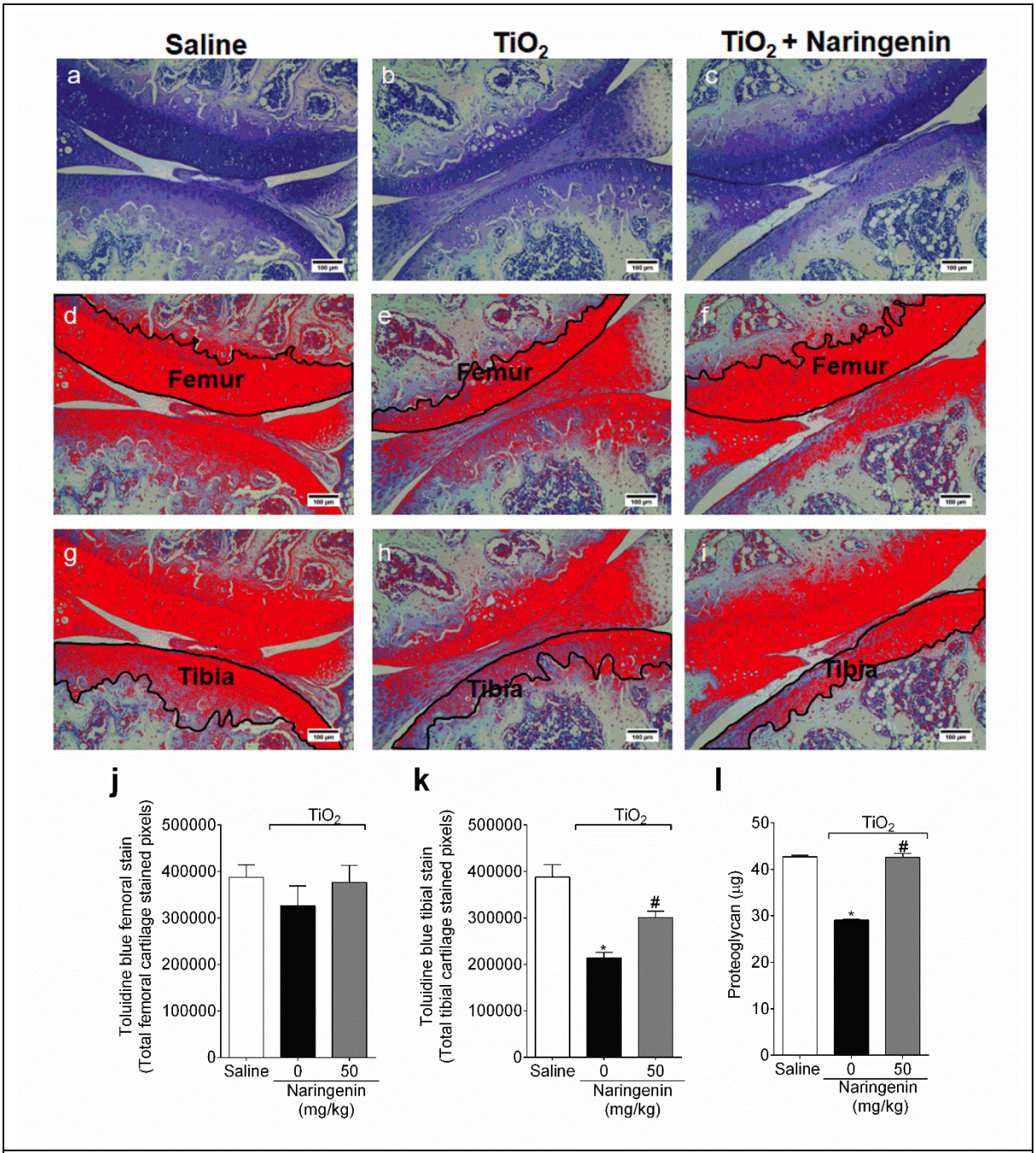

Fig. 3 Naringenin inhibits TiO_2-induced cartilage erosion in the knee joint. Mice were treated daily for 30 days with naringenin (50 mg/kg, p.o.) starting 24 h after intra-articular injection of TiO_2 (3 mg/ joint). (a-i) Toluidine blue staining quantification of (j) femoral and (k) tibial stained areas; and (l) quantitative quantification of proteoglycan levels in the knee joint samples were evaluated at 30th day. (a, d and g) Saline; (b, e, and h) TiO_2; and (c, f and i) TiO_2 treated with naringenin. The percentage of toluidine blue stained areas in the (j) femoral and (k) tibial cartilage in the load-bearing region were measured through the

area outlined in black. The panels d-f and panels g-i demonstrate the analysis performed in femur and tibia, respectively. Original magnification 10x (scale bar 100 µm), n = 6. Results are presented as mean ± SEM of six mice per group per experiment and are representative of two separate experiments. [*p < 0.05 compared to the saline group; #p < 0.05 compared to the TiO_2 (one-way ANOVA followed by Tukey's *post hoc*)].

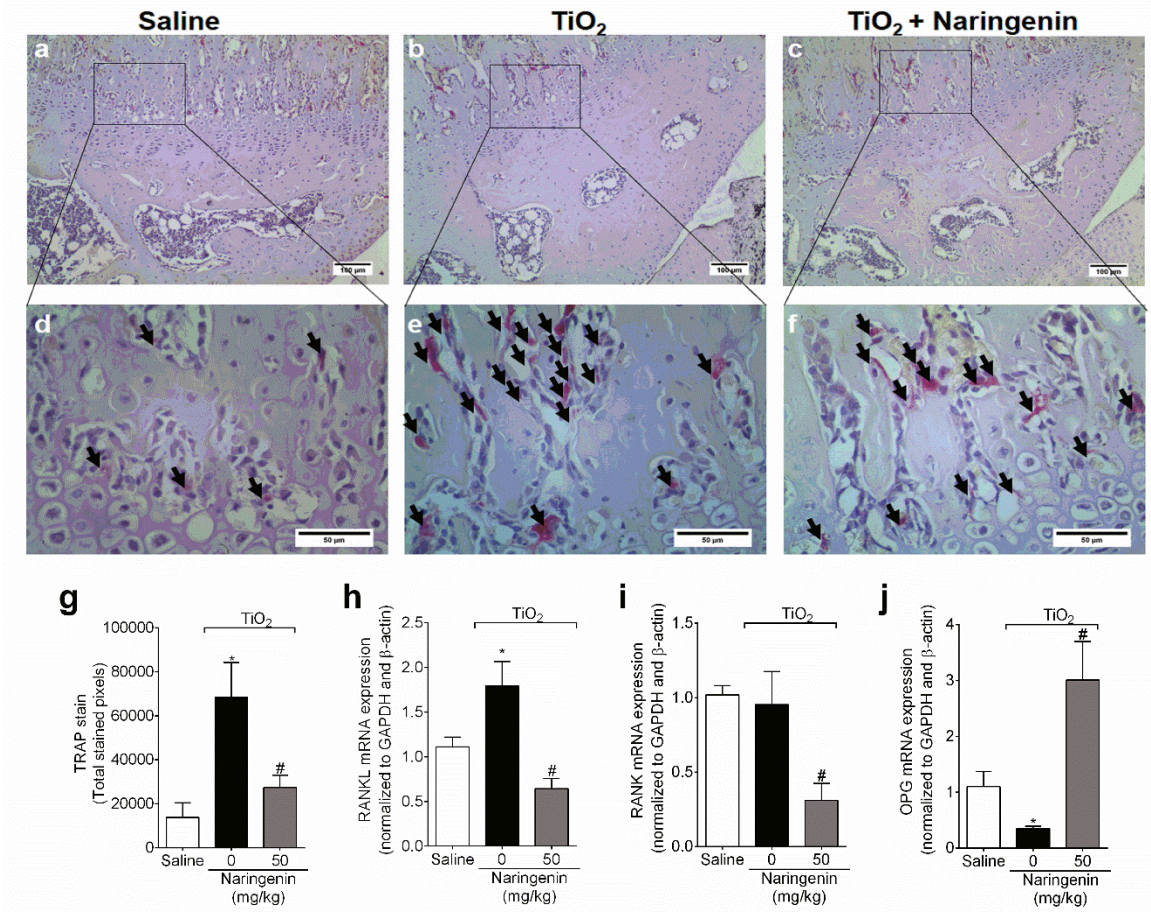

Fig. 4 Naringenin inhibits TiO_2-induced bone resorption. Mice were treated daily for 30 days with naringenin (50 mg/kg, p.o.) starting 24 h after TiO_2 i.a. injection (3 mg/joint). (a-f) TRAP histochemical staining; (g) quantitative analysis of TRAP-positive cells; (g) RANKL, (i) RANK; and (j) OPG mRNA expression were determined at 30th day. The areas delimited in rectangles in panels a-c represent the fields observed in panels d-f, that were used to determine (g) TRAP histochemical staining between the groups. Original

magnification 10x (scale bar 100 µm) and 40x (scale bar 50 µm), n = 6. Results are presented as mean ± SEM of six mice per group for histochemical stain and qPCR analysis per experiment and are representative of two separate experiments. [*p < 0.05 compared to the saline group; #p < 0.05 compared to the TiO_2 group (one-way ANOVA followed by Tukey's test)]

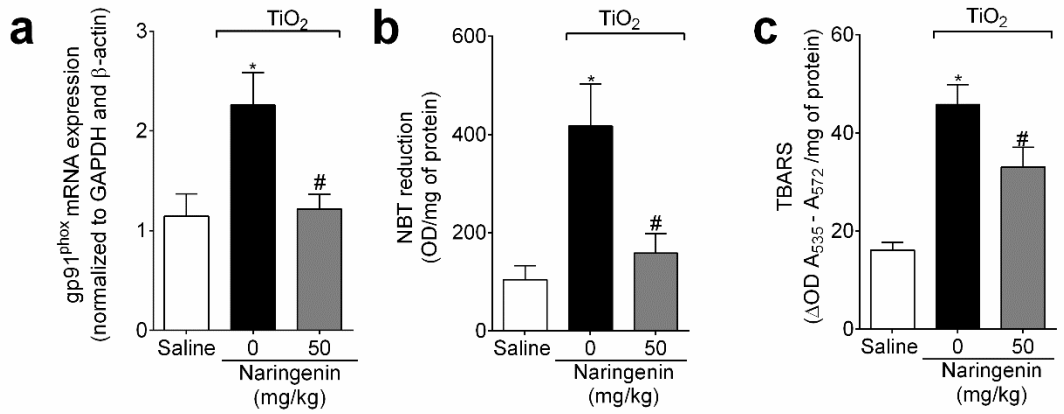

Fig. 5 Naringenin inhibits TiO_2-induced oxidative stress. Mice were treated daily for 30 days with naringenin (50 mg/kg, p.o.) starting 24 h after TiO_2 i.a. injection (3 mg/joint). (a) $gp91^{phox}$ mRNA expression, (b) superoxide anion production, and (c) TBARS levels were determined at 30th day after TiO_2 injection. Results are presented as mean ± SEM of six mice per group per experiment and are representative of two separate experiments. [*p < 0.05 compared to the saline group; #p < 0.05 compared to the TiO2 group (one-way ANOVA followed by Tukey's post hoc)].

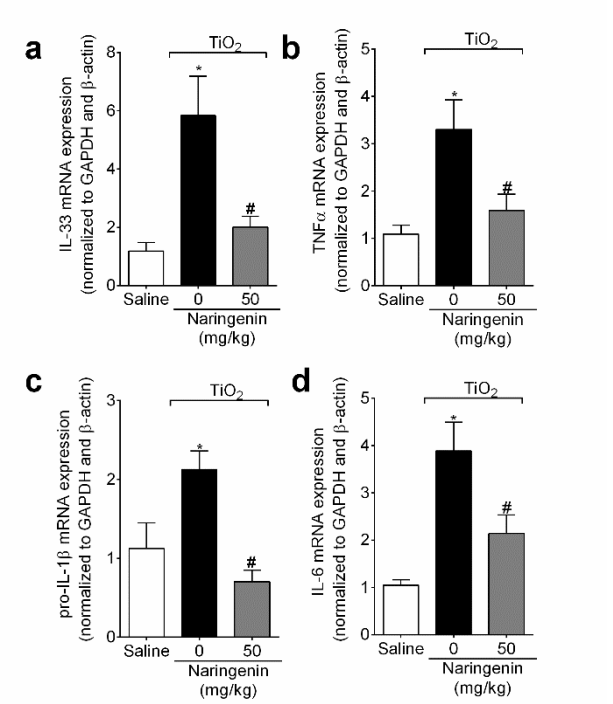

Fig. 6 Naringenin inhibits TiO_2-induced cytokines mRNA expression. Mice were treated daily for 30 days with naringenin (50 mg/kg, p.o.) starting 24 h after TiO_2 i.a. injection (3 mg/joint). (a) IL-33, (b) TNFα, (c) pro-IL-1β, and (d) IL-6, mRNA expression were determined by RT-qPCR 30 days after TiO_2 injection. Results are presented as mean ± SEM of six mice per group per experiment and are representative of two separate experiments. [*$p < 0.05$ compared to the saline group; #$p < 0.05$ compared to the TiO_2 group (one-way ANOVA followed by Tukey's *post hoc*)].

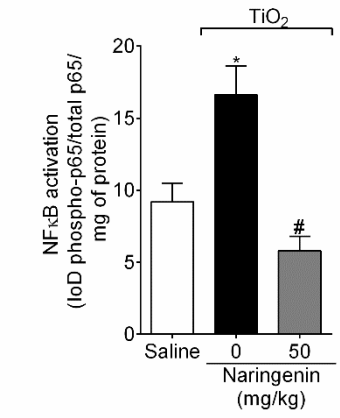

Fig. 7 Naringenin inhibits TiO_2-induced NFκB activation. Mice were treated daily for 30 days with naringenin (50 mg/kg, p.o.) starting 24 h after TiO_2 i.a. injection (3 mg/joint). NFκB activation determined 30 days after TiO_2 injection. Results are presented as mean ± SEM of six mice per group per experiment and are representative of two separate experiments. [*$p < 0.05$ compared to the saline group; #$p < 0.05$ compared to the TiO_2 group (one-way ANOVA followed by Tukey's *post hoc*)].

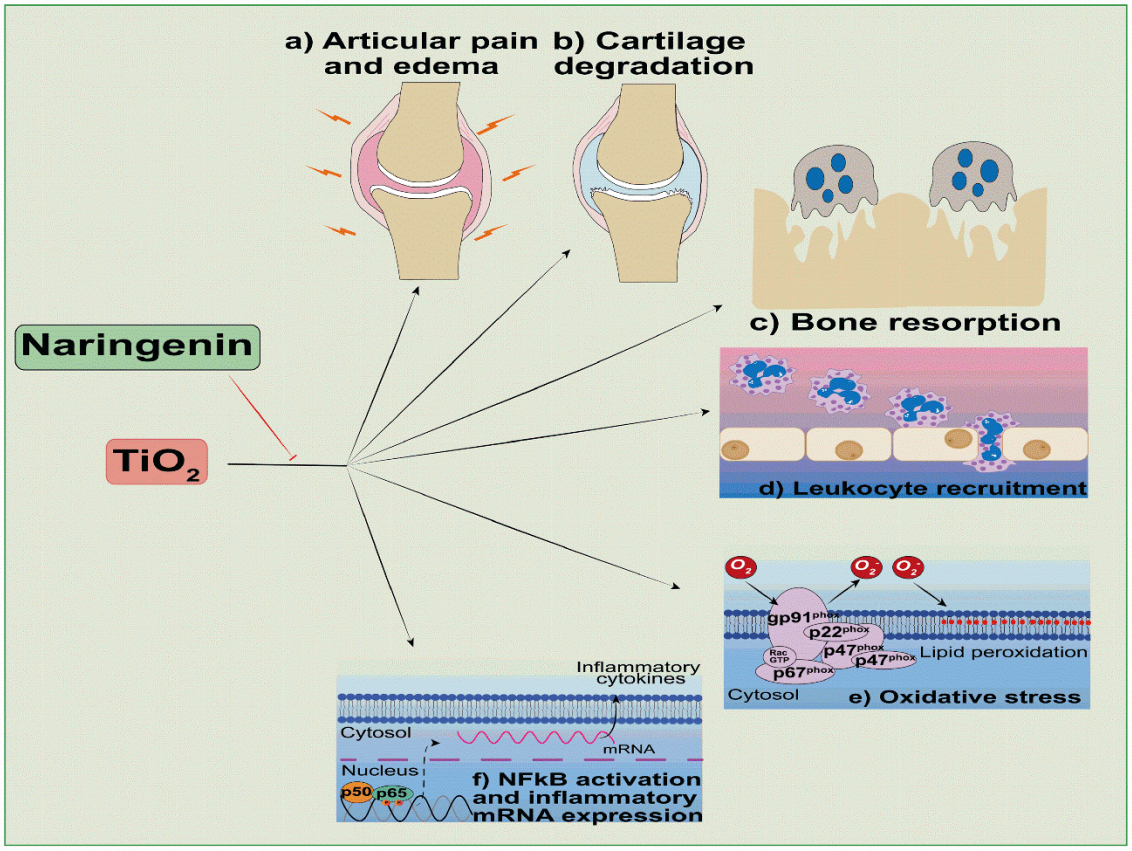

Fig. 8 Naringenin ameliorates TiO_2-induced chronic arthritis inhibiting a) articular pain and edema, b) cartilage degradation, c) bone resorption, d) leukocyte recruitment, e) oxidative stress, and f) NFκB activation and mRNA expression of inflammation biomarkers.

ANEXO D – Artigo Submetido Durante O Doutoramento Na Revista Natural Product Research

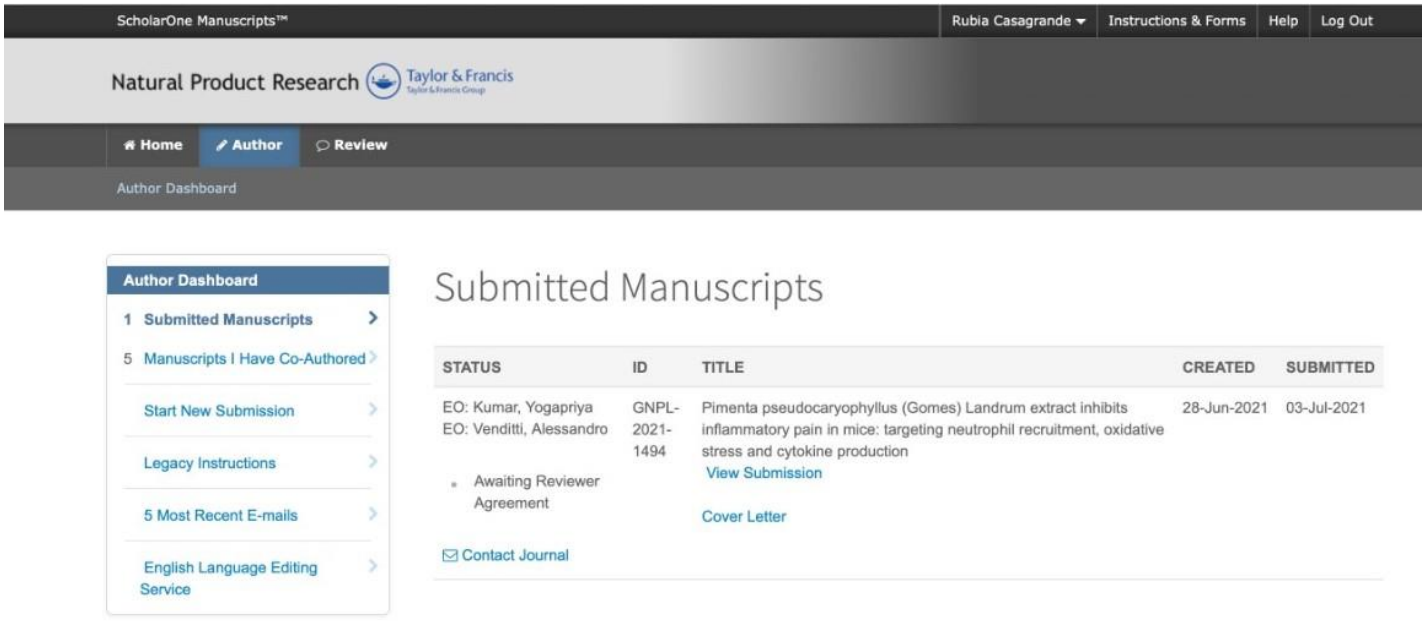

Natural Product Research

Pimenta pseudocaryophyllus (Gomes) Landrum extract inhibits inflammatory pain in mice: targeting neutrophil recruitment, oxidative stress and cytokine production

Journal:	*Natural Product Research*
Manuscript ID	GNPL-2021-1494
Manuscript Type:	Short Communication
Date Submitted by the Author:	03-Jul-2021
Complete List of Authors:	Manchope, Marília; Universidade Estadual de Londrina, Department of Pathology Mizokami, Sandra; Universidade Estadual de Londrina, Department of Pathology Ferraz, Camila; Universidade Estadual de Londrina Borghi, Sergio; Universidade Estadual de Londrina, Department of Pathology Vignoli, Josiane; Universidade Estadual de Londrina Camilios-Neto, Doumit; Universidade Estadual de Londrina Arakawa, Nilton; Universidade Estadual de Londrina, Department of Pharmaceutical Sciences Georgetti, Sandra; Universidade Estadual de Londrina, Ciências Farmacêuticas Verri, Waldiceu; Universidade Estadual de Londrina, Department of Pathology Casagrande, Rubia; Universidade Estadual de Londrina, Department of Pharmaceutical Sciences
Keywords:	Inflammation, Pain, Leukocytes, Oxidative stress, Cytokines

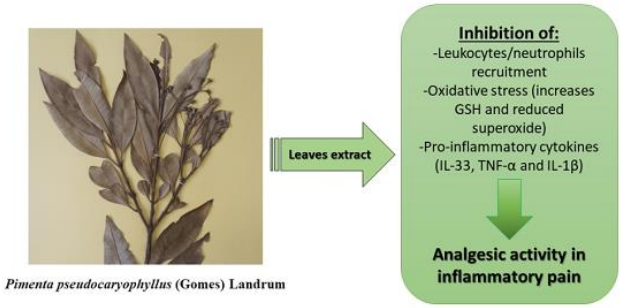

Pimenta pseudocaryophyllus (Gomes) Landrum

338x190mm (96 x 96 DPI)

Pimenta pseudocaryophyllus (Gomes) Landrum extract inhibits inflammatory pain in mice: targeting neutrophil recruitment, oxidative stress and cytokine production

Marília F. Manchope,[1,§] Sandra S. Mizokami,[1,§] Camila R. Ferraz,[1,2,§] Sergio M. Borghi,[1,3] Josiane A. Vignoli,[4] Doumit Camilios-Neto,[4] Nilton S. Arakawa,[2] Sandra R. Georgetti,[2] Waldiceu A. Verri Jr,[1] Rubia Casagrande[2*]

[1] Departamento de Ciências Patológicas, Centro de Ciências Biológicas, Universidade Estadual de Londrina, Rodovia Celso Garcia Cid, Pr 445, Km 380, Cx. Postal 10.011, Londrina, Paraná, 86057-970, Brazil.

[2] Departamento de Ciências Farmacêuticas, Centro de Ciências de Saúde, Universidade Estadual de Londrina, Avenida Robert Koch, 60, Londrina, Paraná, 86039-440 Londrina, Brazil.

[3] Centro de Pesquisa em Ciências da Saúde, Universidade Norte do Paraná, Rua Marselha, 591, Jardim Piza, Londrina, Paraná, 86041-140, Brazil.

[4] Departamento de Bioquímica e Biotecnologia, Centro de Ciências Extas, Universidade Estadual de Londrina, Rodovia Celso Garcia Cid, Pr 445, Km 380, Cx. Postal 10.011, Londrina, Paraná, 86057-970, Brazil.

[§]These authors contributed equally to this work.

***Author for correspondence**: Prof. Rubia Casagrande, PhD. Present address: Departamento de Ciências Farmacêuticas, Centro de Ciências de Saúde, Universidade Estadual de Londrina, Avenida Robert Koch, 60, Londrina, Paraná, 86039-440 Londrina, Brazil. Tel/Fax: +55 (43) 3371-2475. E-mail: rubiacasa@yahoo.com.br.

Pimenta pseudocaryophyllus (Gomes) Landrum extract inhibits inflammatory pain in mice: targeting neutrophil recruitment, oxidative stress and cytokine production

Abstract

Pimenta pseudocaryophyllus (Gomes) Landrum is a Brazilian native plant. Its antinociceptive property in the acetic acid-induced contortions was shown. However, the mechanisms by which it promotes analgesia are unknown. We demonstrated the analgesic effect of dried extract of *P. pseudocaryophyllus* in the following models of inflammatory pain; phenyl-p-benzoquinone, formalin, complete Freund's adjuvant and carrageenin, without motor impairment (rota-rod test). Its analgesic effect depends on inhibiting neutrophil recruitment, oxidative stress, and cytokine production. The present study advances in understanding the analgesic mechanisms of *P. pseudocaryophyllus*.

Keywords: Inflammation; pain; leukocytes; oxidative stress; cytokines.

1. Introduction

Pimenta pseudocaryophyllus (Gomes) Landrum is a plant found in Brazilian Atlantic forest (de Paula et al. 2012) popularly known as "pau-cravo", "louro-cravo", "craveiro-do-mato", "chá-de-bugre", and "cataia" (Landrum 1986). Its folk uses include the treatment of arthritis and fever (D'angelis and Negrelle 2014). Pain is a symptom of arthritis that diminishes quality of life of patients and is decisive to search medical treatment (Duenas et al. 2016). One study showed *P. pseudocaryophyllus* extract reduces acetic acid-induced abdominal contortions in mice (de Paula et al. 2012). However, other models of inflammatory pain were not evaluated and the mechanisms underpinning the analgesic property of *P. pseudocaryophyllus* extract were not explored, thus, these were the aims of the present study.

2. Results and discussion

2.1. Chemical characteristics of P. pseudocaryophyllus *extract*

The HPLC analysis of the ethanolic extract indicated the presence of rutin, eugenol and tannic acid as main compounds compared to reference standards (Figure S1). The UV data (λmax) of individual compounds were identified by reported value.

2.2. P. pseudocaryophyllus *extract inhibits inflammatory pain*

We performed dose-response curves using the PBQ (phenyl-p-benzoquinone)-induced abdominal writhing model and *P. pseudocaryophyllus* extract administration by s.c., p.o. gavage and i.p. (Figure 1(A)-(C)). The extract inhibited the two phases of formalin test (Figure 1(D)-(E)) and CFA overt pain-like behavior (Figure 1(F)). Only 3 mg/kg dose inhibited carrageenin-induced mechanical and thermal hyperalgesia (Figure 1 (G)-(H)). The extract did not cause motor capacity impairment or sedative-like effects (Figure (I)).

2.3. Inhibition of leukocyte recruitment, oxidative stress, and cytokine production

P. pseudocaryophyllus inhibited carrageenan-induced leukocyte recruitment (5h), especially neutrophils, observed by counting and identifying these cells (Figure 2 (A)-(B)), myeloperoxidase activity (Figure 2(C)) and using LysM-eGFP mice (Figure 2(D)-(E)). Carrageenin depleted GSH levels, and increased superoxide anion, IL-33, TNFα, and IL-1β production (3h), whilst *P. pseudocaryophyllus* inhibited all parameters (Figure 2 (F)-(J)). The control drug indomethacin presented the expected effects (Figure 1 and 2).

3. Experimental section

See Supplemental material.

4. Conclusions

P. pseudocaryophyllus is analgesic in varied models of inflammatory pain acting by inhibiting neutrophil recruitment, oxidative stress, and cytokine production.

Disclosure statement

The Authors declare no conflict of interest.

Acknowledgments

Funding was from CAPES, CNPq, FUNADESP, SETI/Araucaria Foundation, MCTI and Paraná State Government (PRONEX grant) (Brazil). We thank CMLP-UEL core facility, Prof. Terezinha Faria for preparing/donating the extract, and Elson F. S. Rossetto for the photograph of the *P. pseudocaryophyllus* voucher specimen 43025 from UEL Herbarium.

References

D'angelis A, Negrelle R. 2014. *Pimenta pseudocaryophyllus* (Gomes) Landrum: aspectos botânicos, ecológicos, etnobotânicos e farmacológicos. Rev Bras Pl Med. 16(3):607-617.

de Paula JA, Silva Mdo R, Costa MP, Diniz DG, Sa FA, Alves SF, Costa EA, Lino RC, de Paula JR. 2012. Phytochemical Analysis and Antimicrobial, Antinociceptive, and Anti-Inflammatory Activities of Two Chemotypes of Pimenta pseudocaryophyllus (Myrtaceae). Evid Based Complement Alternat Med. 2012:420715.

Duenas M, Ojeda B, Salazar A, Mico JA, Failde I. 2016. A review of chronic pain impact on patients, their social environment and the health care system. J Pain Res. 9:457-467.

Landrum LR. 1986. Campomanesia, Pimenta, Blepharocalyx, Legrandia, Acca, Myrrhinium and Luma (Myrtaceae). Flora Neotropica Monograph 45:1-179.

Figure captions

Figure 1. Analgesic effect of *P. pseudocaryophyllus* extract in PBQ- (A)-(C), formalin- (D)-(E), CFA- (F) and carrageenin hyperalgesia (G)-(H) without motor impairment in the rota-rod (I). Mice were pretreated (30 min) with the extract or vehicle by the indicated administration routes or i.p. if not stated. Indomethacin pretreatment (40 min). Results are mean ± SEM (6 mice/ group/ experiment, 2 separate experiments). *$p< 0.05$ vs. saline group, #$p< 0.05$ vs. vehicle group (One-way ANOVA followed by Tukey's *post hoc*).

Figure 2. *P. pseudocaryophyllus* extract inhibits carrageenin-induced leukocyte recruitment (A)-(B), myeloperoxidase activity (C), neutrophil migration (LysM-eGPF fluorescence) (D)-(E), oxidative stress (F)-(G) and cytokine production (H)-(J) in the paw skin. Mice were pretreated (30 min) with *P. pseudocaryophyllus* extract or vehicle. Indomethacin pretreatment (40 min). Results are mean ± SEM (6 mice/group/experiment, 2 separate experiments). *$p< 0.05$ vs. saline group, **$p<0.05$ vs. vehicle group (One-way ANOVA followed by Tukeys' *post hoc*).

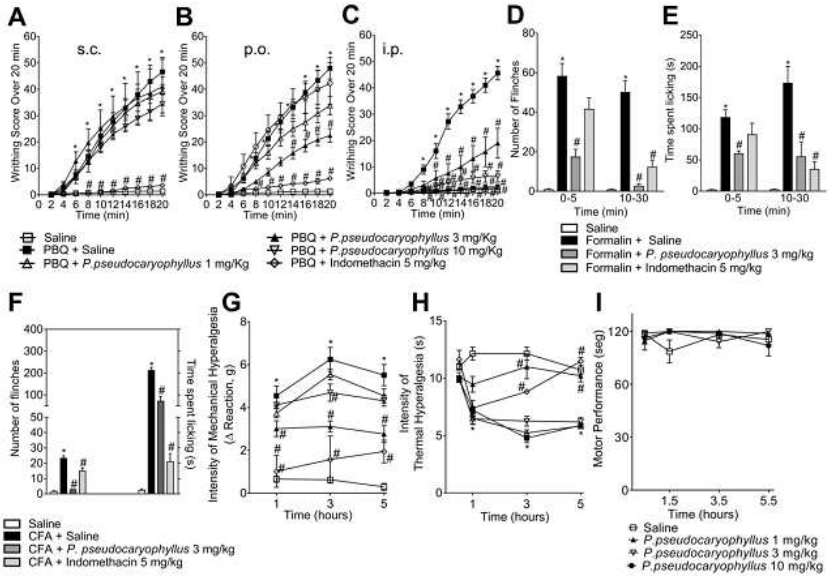

Figure 1. Analgesic effect of P. pseudocaryophyllus extract in PBQ- (A)-(C), formalin- (D)-(E), CFA- (F) and carrageenin hyperalgesia (G)-(H) without motor impairment in the rota-rod (I). Mice were pretreated (30 min) with the extract or vehicle by the indicated administration routes or i.p. if not stated. Indomethacin pretreatment (40 min). Results are mean ± SEM (6 mice/ group/ experiment, 2 separate experiments). *p< 0.05 vs. saline group, #p< 0.05 vs. vehicle group (One-way ANOVA followed by Tukey's post hoc).

298x211mm (300 x 300 DPI)

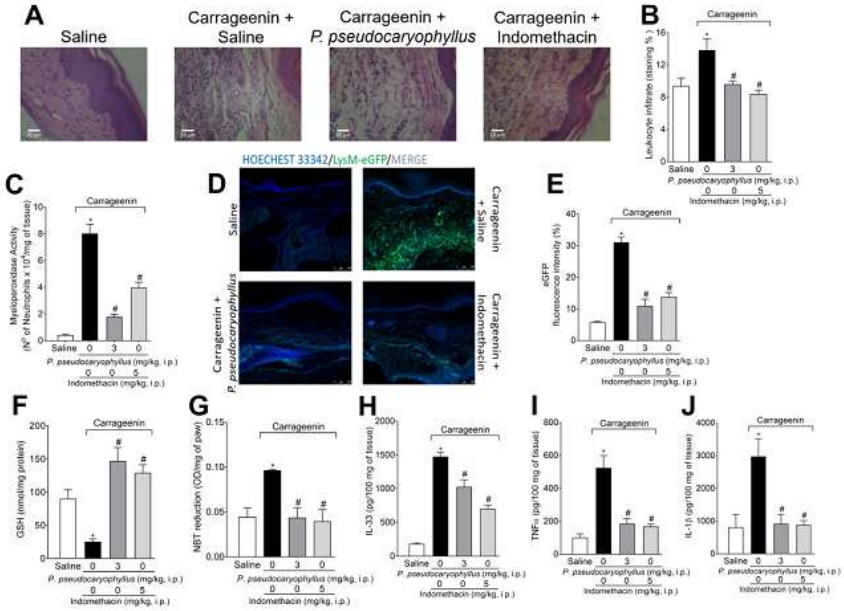

Figure 2. P. pseudocaryophyllus extract inhibits carrageenin-induced leukocyte recruitment (A)-(B), myeloperoxidase activity (C), neutrophil migration (LysM-eGPF fluorescence) (D)-(E), oxidative stress (F)-(G) and cytokine production (H)-(J) in the paw skin. Mice were pretreated (30 min) with P. pseudocaryophyllus extract or vehicle. Indomethacin pretreatment (40 min). Results are mean ± SEM (6 mice/group/experiment, 2 separate experiments). *p< 0.05 vs. saline group, **p<0.05 vs. vehicle group (One-way ANOVA followed by Tukeys' post hoc).

287x211mm (300 x 300 DPI)

SUPPLEMENTARY MATERIAL

Pimenta pseudocaryophyllus (Gomes) Landrum extract inhibits inflammatory pain in mice: targeting neutrophil recruitment, oxidative stress and cytokine production

Marília F. Manchope,[1,§] Sandra S. Mizokami,[1,§] Camila R. Ferraz,[1,2,§] Sergio M. Borghi,[1,3] Josiane A. Vignoli,[4] Doumit Camilios-Neto,[4] Nilton S. Arakawa,[2] Sandra R. Georgetti,[2] Waldiceu A. Verri Jr,[1] Rubia Casagrande[2*]

[1] Departamento de Ciências Patológicas, Centro de Ciências Biológicas, Universidade Estadual de Londrina, Rodovia Celso Garcia Cid, Pr 445, Km 380, Cx. Postal 10.011, Londrina, Paraná, 86057-970, Brazil.

[2] Departamento de Ciências Farmacêuticas, Centro de Ciências de Saúde, Universidade Estadual de Londrina, Avenida Robert Koch, 60, Londrina, Paraná, 86039-440 Londrina, Brazil.

[3] Centro de Pesquisa em Ciências da Saúde, Universidade Norte do Paraná, Rua Marselha, 591, Jardim Piza, Londrina, Paraná, 86041-140, Brazil.

[4] Departamento de Bioquímica e Biotecnologia, Centro de Ciências Extas, Universidade Estadual de Londrina, Rodovia Celso Garcia Cid, Pr 445, Km 380, Cx. Postal 10.011, Londrina, Paraná, 86057-970, Brazil.

[§]These authors contributed equally to this work.

***Author for correspondence**: Prof. Rubia Casagrande, PhD. Present address: Departamento de Ciências Farmacêuticas, Centro de Ciências de Saúde, Universidade Estadual de Londrina, Avenida Robert Koch, 60, Londrina, Paraná, 86039-440 Londrina, Brazil. Tel/Fax: +55 (43) 3371-2475. E-mail: rubiacasa@yahoo.com.br.

Abstract

Abstract

Pimenta pseudocaryophyllus (Gomes) Landrum is a Brazilian native plant. Its antinociceptive property in the acetic acid-induced contortions was shown. However, the mechanisms by which it promotes analgesia are unknown. We demonstrated the analgesic effect of dried extract of *P. pseudocaryophyllus* in the following models of inflammatory pain; phenyl-p-benzoquinone, formalin, complete Freund's adjuvant and carrageenin, without motor impairment (rota-rod test). Its analgesic effect depends on inhibiting neutrophil recruitment, oxidative stress, and cytokine production. The present study advances in understanding the analgesic mechanisms of *P. pseudocaryophyllus*.

Keywords: Inflammation; pain; leukocytes; oxidative stress; cytokines.

Experimental

Animals

Male Swiss mice (20-25 g) from the State University of Londrina (UEL), Brazil, were used in this study. Mice were housed in standard clear plastic cages with free access to food and water, a light/dark cycle of 12:12 h, and kept at 21°C. The heterogeneous Swiss strain was used for the most of experimental analysis in the present study, with exception of the immunofluorescent test evaluating the participation of migrating neutrophils to the mice paw tissue in the model. For the last analysis LysM-eGFP^{+} mice were used, which is a strain generated through its background C57BL/6 mouse, presenting enhanced green fluorescent protein (eGFP) expression controlled by the promoter of lysozyme M (LysM), an enzyme that is found predominantly in neutrophils granules and secreted upon cell activation (Wenzel et al. 2011). Animal care and handling procedures were approved by the "Animal Welfare and Ethics Committee of the UEL" (n° 28869.2014.87) and conducted following the guidelines and ethical standards of the International Association for the Study of Pain (IASP) in animals. For sample collection, mice were euthanized using a lethal dose of anaesthetic isoflurane 5% (Abbott Park, IL, USA), which was confirmed by dislocation of the cervical segment of the spinal cord followed by decapitation. All effort was carried out with the intension of reduce the total number of animals used in the study and their suffering.

Plant material, extract preparation and chemical characterization

P. pseudocaryophyllus (Gomes) Landrum is the only specie of Myrtaceae genus found in Brazil, mainly in mountainous and coastal regions of southern and southeastern Brazil, (e.g. Espírito Santo, São Paulo, Rio de Janeiro, Paraná, Santa Catarina, and Rio Grande do Sul States). The leaves of *P. pseudocaryophyllus* (Gomes) Landrum were

collected, with permission, in the month of December 2007, from São Jerônimo da Serra (Paraná, Brazil). After collection, the sample was identified and authenticated by Prof. Ana Odete Santos Vieira, Department of Chemistry, UEL, and a voucher specimen was deposited at the Herbarium of UEL (FUEL under the code 43025). The leaves of *P. pseudocaryophyllus* were dried at 40 ºC and 80 g of dried leaves coarsely powdered in industrial blender. The ethanolic extract (1:10) was obtained by exhaustive maceration at room temperature (25 ºC) for 12 days. The extract was filtered and concentrated under vacuum (yield 0.8 g). We reported the chemical characterization of the extract previously (Campanini et al. 2013; Campanini et al. 2014).

HPLC Analysis

The extract was analyzed by Shimadzu HPLC with a photodiode array detector (SPD-M10Avp), multisolvent delivery system (LC-10Avp), oven control system (CTO-10ASvp), and controlled software Class VP 6.14 software, Spherisob® column (C-18ODS) (250×4.6mm i.d.; particle size 5 µm; Waters), flow rate (1 mL/min), Panreac ® HPLC-grade solvents and Milli-Q-plus water filter systems (Millipore) was used with a gradient of acidified H_2O (2% formic acid; solvent A) and acetonitrile (2% formic acid; solvent B) - 0 min, 0% B; 5 min, 0% B; 20 min, 2.5% B; 30 min, 5% B; 50 min, 15%B; 60 min, 25% B; 65 min, 30%B; 70 min, 45%B; 75 min, 50%B; 80min, 70% B; 85 min, 90%B; 90min, 100%B; 95 min, 100% B; 110 min, 0% B), UV detection set to 280 and 340 nm and spectra were recorded for each main peak in the chromatograms, with 20 µL of volume injection. The following compounds were used as references (external standard): quercetin- 3-O-rutinoside (rutin, Sigma), eugenol (Sigma) and tannic acid (Synth).

Chemical compounds and stimuli

The following materials were obtained from the sources as indicated: Saline solution (NaCl 0.9%) from Frenesius Kabi Brasil Ltda (Aquiraz, CE, Brazil); carrageenin from Santa Cruz Biotechnology (Santa Cruz, CA, USA); DMSO, CFA, and PBQ from Sigma-Aldrich (St. Louis, MO, USA); formaldehyde from Mallinckrodt Baker S.A. (Mexico City, Mexico); and indomethacin from Prodome (Campinas, SP, Brazil).

General experimental procedures

Mice were pretreated with *P. pseudocaryophyllus* [1, 3 and 10 mg/kg; subcutaneous (s.c.), per oral (p.o.), and intraperitoneal (i.p.); diluted in 2% DMSO in saline) or vehicle (i.p., 2% DMSO in saline) 30 minutes before inflammatory stimuli. Indomethacin (i.p., 5 mg/kg, 40 min before the stimuli) was used as positive control drug. The writhing response was evaluated for 20 minutes after i.p. injection of (PBQ; 1890 μg/Kg; diluted in 2% DMSO in saline). Flinch and licking of the right paw were quantitated as a nociceptive behavior for 30 minutes after formalin 2% (25 μL/paw) or complete Freund's adjuvant (CFA; 10 μL/paw) intraplantar (i.pl.) injection in right paw. Mechanical hyperalgesia and thermal hyperalgesia were evaluated 1, 3 and 5 hours after carrageenin (300 μg; in 25 μL of saline/paw), and at 5 hours the animals were euthanized, and paw skin samples were collected for MPO activity determination and immunofluorescence assay. All inflammatory stimuli induced only ipsilateral hyperalgesia (in the paw in which the stimulus was injected). Cytokine production (TNF-α, IL-1β, and IL-33), GSH and NBT reduction (superoxide anion production) were measured in paw skin samples collected 3 hours after carrageenin injection. The doses of inflammatory stimuli applied, and assays were previously determined in our laboratory (Valerio et al. 2009; Campanini

et al. 2013; Maioli et al. 2015; Pinho-Ribeiro et al. 2016). Experimenters were always blinded to the experimental groups to avoid bias.

Overt pain-like behavioral assessment

Abdominal writhing was induced by i.p. injection of PBQ (1890 μg/Kg). Immediately after stimulus injection, each mouse was placed individually in a large glass cylinder, and nociceptive behaviors were evaluated by counting the total number of writhings occurring between 0 and 20 minutes after PBQ injection. The writhing is characterized by contraction of the abdominal muscles associated with a stretching of hind limbs. The intensity of the writhing response was expressed as the cumulative number of abdominal contortions over the period of 20 minutes. The number of paw flinches and the time spent licking the paw were determined between 0 and 30 min after i.pl. injection of formalin (2%; 25 μL/paw) or CFA (10 μL/paw) injection into the right paw. Each mouse was placed in a large glass cylinder immediately after formalin i.pl. injection, and the intensity of nociceptive behavior was quantified by counting the total number of paw flinches and the time (seconds) spent licking ipsilateral paw (Fattori et al. 2015).

Mechanical hyperalgesia assessment

The evaluations were conducted as previously described (Fattori et al. 2015). In a quiet room, animals were carefully positioned in individual spaces made of acrylic material (12×10×17 cm) with wire grid floors, 30 min before testing. Test applications consist of evoking a mice hind paw reflex with a hand-held force transducer (electronic aesthesiometer; Insight) adapted with a 0.5 mm^2 polypropylene tip. The investigator was initially trained to apply the tip perpendicularly to the plantar surface of the same hind paw for all evaluation periods, with a gradual increase in pressure. The end point

was characterized by removing the paw from the stimulus when the latter is sensitized, behavior that is followed by flinching movements. The intensity of pressure applied is then recorded automatically by the apparatus. Mice were tested basal condition and after treatment protocol and stimulus, and the value for each interval was an average of a minimum of three measurements. Data are presented by delta (Δ) withdrawal threshold (in g), calculated by subtracting the mean measurements obtained at 1, 3 or 5 h after i.pl. stimulus from the basal (zero h) mean measurements. Experimenter was always blinded to treatments of experimental groups to avoid biased measurements.

Thermal hyperalgesia assessment

Thermal hyperalgesia was assessed before and after i.pl. injection of carrageenan into the paw tissue. The test was performed as previously reported (Fattori et al. 2015). In sum, animals were individually positioned in a glass compartment with a width of 10 cm on a hot plate (Hot Plate HP-2002, Insight) kept at a maximum of 50°C. The end points used were animal jump, paw flinch or paw licking. The normal latency (reaction time) was 16.63± 0.10 s (mean ± S.E.M.; n = 72). A cut-off of 20 s was established to prevent thermal damage of paw skin tissue.

Motor performance assessment

To discard possible nonspecific muscle-relaxant or sedative effects of *P. pseudocaryophyllus* extract, mice motor performance was evaluated using the rota-rod test. The apparatus consisted of a bar with a diameter of 2.5 cm, subdivided into four compartments by disks 25 cm in diameter (Ugo Basile, model 7600). The bar rotated at a constant speed of 22 rotations per min. Mice were selected 24 h previously by eliminating those that did not remain on the bar for two consecutive periods of 180 s.

Mice were treated with saline or *P. pseudocaryophyllus* extract (1, 3 and 10 mg/kg), and the evaluations were performed 1.5, 3.5, and 5.5 h after treatment. The cutoff time used was 180 s (Borghi et al. 2013).

Histopathological analyses

Paw skin samples were collected 5 hours after carrageenan i.pl. injection, fixed in buffered formaldehyde, with subsequent embedding in paraffin. Longitudinal sections (5 µm) were prepared in cryostat (CM1520, Leica Biosystem) and stained with hematoxylin and eosin (H&E) for histopathological analysis. Images (4 sections per mice, and 6 mice per group) were analyzed using light microscopy (Olympus Life Science, model CX31RTSF, Tokyo, Japan) with magnification of 40x.

MPO activity measurement

The neutrophil mobilization to the paw tissue was assessed 5 hours after carrageenan i.pl. injection through the MPO kinetic activity assay (one paw per sample). Paw tissues were removed and added in 200 μL of 50 mM K_2PO_4 solution (pH 6.0), composed of hexadecyl trimethylammonium bromide (HTAB; 0,5%) and homogenized in ice-cold condition using a Tissue-Tearor (Biospec®). After this step, samples were centrifuged (16100 g for 2 min), and the resultant supernatants (15 μL) were blended with 200 μL 50 mM K_2PO_4 buffer, containing 0.167 mg/mL *o*-dianisidine dihydrochloride and 0.015% hydrogen peroxide. The MPO activity absorbance was determined by spectrophotometry at 450 nm (Multiskan GO Microplate Spectrophotometer, Thermo Fischer Scientific, Vantaa, Finland). The results present MPO activity in tested samples (neutrophils x 10^4/mg of paw skin) (Martinez et al. 2018).

Immunofluorescence analysis under confocal microscopy

To further confirm the inhibitory effect of *P. pseudocaryophyllus* upon neutrophils, paw samples of LysM-eGFP^{+} mice were collected 5 hours after carrageenan i.pl. injection, and were maintained in 4% paraformaldehyde (PFA) for 24 h. Subsequently, samples were transferred for 30% saccharose for additional 72 h. The skin samples were then embedded in optimum cutting temperature reagent (Tissue-Tek®, O.C.T. Compound, IA018, ProSciTech), and 15 micrometers (μm) sections were cut in a cryostat (CM1520, Leica Biosystem, Richmond, IL, USA). Sterile slides (4 sections per mice, and 6 mice per group) were mounted with a drop of mounting medium with DAPI (SlowFade™ Gold Antifade Moutant with DAPI; 1:1000 dilution; Thermo Fisher Scientific) to stain regular nucleus. The representative images (four slides per mice/four animal per group) and quantitative analysis were carried out using a confocal microscope (SP8, Leica Microsystems). The intensity of fluorescence was quantified in randomly selected fields of different groups by a blind evaluator to the experimental groups. Results are presented as the percentage of GFP fluorescent intensity (Martinez et al. 2018).

GSH assay

Samples of paw tissue were collected in 1.15% KCl 3 h after carrageenan i.pl. injection (four paws per sample) and maintained at -80 ºC for at least two days. Subsequently, samples were homogenized with 200 μL of 0.02 M ethylenediamine tetraacetic acid (EDTA). The homogenate was mixed with 25 μL of trichloroacetic acid (TCA) 50%, v/v and was homogenized three times over 15 min. The mixture was centrifuged under specific conditions (15 min x 1500 g x 4 ºC), and the resultant supernatant was added to 200 μL of TRIS buffer (0.2 M, pH 8.2), and 10 μL of 0.01M (5,5-dithio-bis-(2-nitrobenzoic acid) DTNB reagent. After 5 min, the absorbance was measured at 412 nm

against a blank reagent with no supernatant. A standard GSH curve was formed and use for calculations for GSH levels in samples. The results are expressed as GSH per mg of sample of protein.

NBT assessment

The quantification of superoxide anion concentrations in paw skin samples (10 mg/mL in 1.15% KCl) were performed through the NBT assay following previous protocol (Campanini et al. 2013). In brief, homogenates (in a volume of 50 μL) were added to a solution containing 100 μL of NBT (1 mg/mL) reagent using 96-well plates (37°C, 1 h). Next, samples were removed from all wells and the reduced formazan that remained fixed in the wells added to 120 μL of KOH 2 M and 140 μL of dimethyl sulfoxide (DMSO). Results were analysed spectrophotometrically. Data are presented as NBT reduction (OD/mg of tissue).

Determination of cytokine concentrations in samples

Cytokine levels (IL-33, TNF-α, and IL-1β) were quantified through enzyme-linked immunosorbent assay (ELISA) tests following the directions of the product package insert (eBioscience). For the presentation of results, standard curves for each cytokine were used for assimilating the data. Data were analyzed spectrophotometrically and are presented as picograms (pg) per 100 mg of paw tissue for each cytokine evaluated (Fattori et al. 2015).

Statistical analysis

Results are presented as means ± SEM of measurements made on six mice in each group per experiment and are representative of two separate experiments. Two-way analysis of

variance (ANOVA) was used to always compare the groups and doses when responses were measured at different times after the different stimulus injection. Analyzed factors were treatments, time, and time versus treatment interaction, and when interaction was significant one-way ANOVA followed by Tukey's *post hoc* was performed for each time point. Differences between responses were evaluated by one-way ANOVA followed by Tukey's *post hoc* for data of single time point. Statistical differences were considered significant when $P < 0.05$.

Supplementary figure

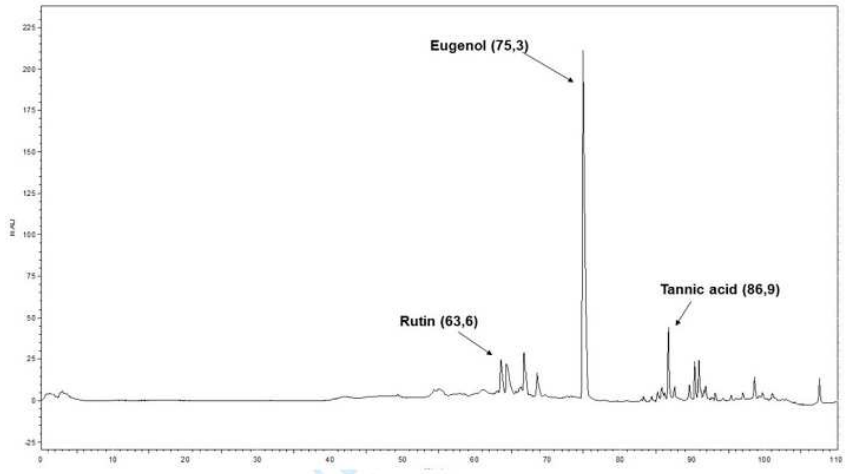

Figure S1. Identification of phenolic compounds of *P. pseudocaryophyllus* extract using HPLC.

References

Borghi SM, Carvalho TT, Staurengo-Ferrari L, Hohmann MS, Pinge-Filho P, Casagrande R, Verri WA, Jr. 2013. Vitexin inhibits inflammatory pain in mice by targeting TRPV1, oxidative stress, and cytokines. J Nat Prod. 76(6):1141-1149.

Campanini MZ, Custodio DL, Ivan AL, Martins SM, Paranzini MJ, Martinez RM, Verri WA, Jr., Vicentini FT, Arakawa NS, de JFT et al. 2014. Topical formulations containing Pimenta pseudocaryophyllus extract: In vitro antioxidant activity and in vivo efficacy against UV-B-induced oxidative stress. AAPS PharmSciTech. 15(1):86-95.

Campanini MZ, Pinho-Ribeiro FA, Ivan AL, Ferreira VS, Vilela FM, Vicentini FT, Martinez RM, Zarpelon AC, Fonseca MJ, Faria TJ et al. 2013. Efficacy of topical formulations containing Pimenta pseudocaryophyllus extract against UVB-induced oxidative stress and inflammation in hairless mice. J Photochem Photobiol B. 127:153-160.

Fattori V, Pinho-Ribeiro FA, Borghi SM, Alves-Filho JC, Cunha TM, Cunha FQ, Casagrande R, Verri WA, Jr. 2015. Curcumin inhibits superoxide anion-induced pain-like behavior and leukocyte recruitment by increasing Nrf2 expression and reducing NF-kappaB activation. Inflamm Res. 64(12):993-1003.

Maioli NA, Zarpelon AC, Mizokami SS, Calixto-Campos C, Guazelli CF, Hohmann MS, Pinho-Ribeiro FA, Carvalho TT, Manchope MF, Ferraz CR et al. 2015. The superoxide anion donor, potassium superoxide, induces pain and inflammation in mice through production of reactive oxygen species and cyclooxygenase-2. Braz J Med Biol Res. 48(4):321-331.

Martinez RM, Fattori V, Saito P, Melo CBP, Borghi SM, Pinto IC, Bussmann AJC, Baracat MM, Georgetti SR, Verri WA, Jr. et al. 2018. Lipoxin A4 inhibits UV radiation-induced skin inflammation and oxidative stress in mice. J Dermatol Sci.

Pinho-Ribeiro FA, Zarpelon AC, Fattori V, Manchope MF, Mizokami SS, Casagrande R, Verri WA, Jr. 2016. Naringenin reduces inflammatory pain in mice. Neuropharmacology. 105:508-519.

Valerio DA, Georgetti SR, Magro DA, Casagrande R, Cunha TM, Vicentini FT, Vieira SM, Fonseca MJ, Ferreira SH, Cunha FQ et al. 2009. Quercetin reduces inflammatory pain: inhibition of oxidative stress and cytokine production. J Nat Prod. 72(11):1975-1979.

Wenzel P, Knorr M, Kossmann S, Stratmann J, Hausding M, Schuhmacher S, Karbach SH, Schwenk M, Yogev N, Schulz E et al. 2011. Lysozyme M-positive monocytes mediate angiotensin II-induced arterial hypertension and vascular dysfunction. Circulation. 124(12):1370-1381.

ANEXO E – Dados Obtidos Durante O Doutorado Sanduíche No McNaughton Lab, King's College London (2018 – 2019)

1. PAPEL DO CANAL IÔNICO TRPM2 NA ARTRITE INDUZIDA POR ANTÍGENO (AIA)

Nesta primeira seção de resultados foram abordados os efeitos do bloqueio farmacológico [pré-tratamento com Ácido N (p-Amilcinamoil) antranílico (ACA)] do canal iônico TRPM2 no modelo de AIA bem como se fenótipo da resposta do ACA se assemelha ao fenótipo desenvolvido nos animais nocautes para o canal iônico TRPM2.

1.1. Efeito Do Bloqueador Farmacológico Do Canal Iônico TRPM2, ACA, Na Fase Aguda Da AIA

Nesta primeira etapa, experimentos foram realizados a fim de verificar a participação do TRPM2 na fase inicial da AIA. Os animais C57BL/6 foram previamente imunizados e pré-tratados com o bloqueador farmacológico ACA 2h antes do desafio i.a. com 100 µg de mBSA. Como pode-se observar na figura 1a, o bloqueio do canal TRPM2 inibiu a hipersensibilidade mecânica induzida pelo desafio com mBSA 1, 3, 5 e 7 h (Fig 1a). Além disso, o tratamento com ACA reduziu o edema induzido pelo mBSA, 7h após o desafio (Fig 1b) .

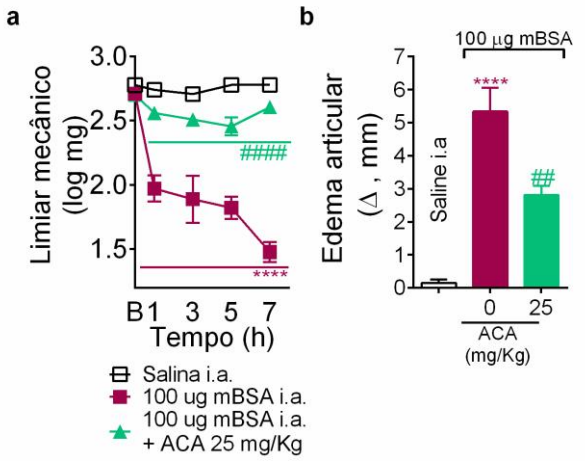

Fig 1 O tratamento farmacológico com o bloqueador do canal iônico TRPM2 inibe a hipersensibilidade mecânica e edema na AIA. Animais C57BL/6 previamente imunizados foram pré-tratados com 25 mg/Kg de ACA s.c. 2 horas antes de serem desafiados com 100 µg mBSA i.a. A hipersensibilidade mecânica (a) foi avaliada de 1-7h e o edema (b) 7 h após o desafio. Os valores foram expressos como a média ± E.P.M e analisados por ANOVA de duas ou uma via e pós teste de Tukey. Foram considerados significativos $^{****}p<0,0001$: grupo mBSA diferente do

grupo salina; ##p<0,01, ####p<0,0001: grupo mBSA diferente do grupo ACA. B: valores basais

Os leucócitos são essenciais na resposta da AIA, em especial os neutrófilos (Coelho et al., 2008). Além disso, o TRPM2 tem papel essencial no recrutamento de neutrófilos (Haraguchi et al., 2012). Desta forma, avaliou-se o efeito do bloqueio farmacológico do canal iônico TRPM2 no recrutamento de leucócitos induzido pelo desafio com mBSA. Animais C57BL/6 foram previamente imunizados e pré-tratados com ACA e desafiados após 2h com mBSA. Após 7h do desafio com o mBSA o lavado da cavidade articular foi coletado. O ACA inibiu o recrutamento de leucócitos totais (Fig 2a), polimorfonucleares (Fig 2b) e mononucleares (Fig 2c) 7h após o desafio com mBSA.

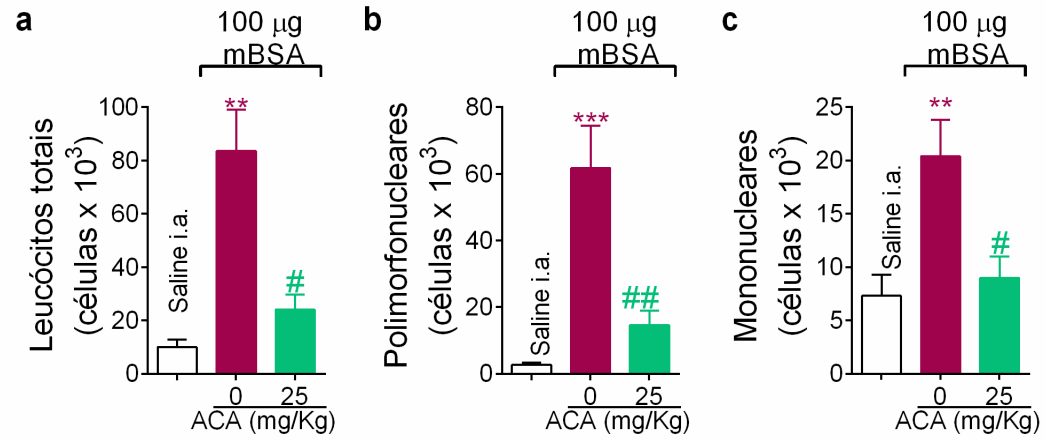

Fig 2 O tratamento farmacológico com o inibidor do canal iônico TRPM2 inibe o recrutamento leucocitário para a cavidade sinovial na artrite induzido por antígeno. Animais C57BL/6 previamente imunizados foram pré-tratados com 25 mg/Kg de ACA s.c. e desafiados com 100 µg mBSA i.a. após 2h do tratamento. Os leucócitos totais (a), polimorfonucleares (b) e mononucleares (c) foram avaliados após 7h do desafio com mBSA. Os valores foram expressos como a média ± E.P.M e analisados por ANOVA de uma via e pós teste de Tukey. Foram considerados significativos **p<0,01 e ***p<0,001: grupo mBSA diferente do grupo salina; #p<0,05 e ##p<0,01: grupo mBSA diferente do grupo ACA.

1.2. Camundongos TRPM2 Deficientes Apresentam Resposta Inflamatória Reduzida Na Fase Inicial Da AIA

Tendo em vista que o bloqueador farmacológico ACA não é seletivo para canal iônico TRPM2, podendo bloquear outros canais TRP (Harteneck et al., 2007), o modelo de AIA foi induzido também em animais deficientes para o canal iônico TRPM2 (TRPM2 KO) a fim de confirmar a participação do TRPM2 por meio de uma ferramenta genética além da farmacológica.

Os animais controle e nocautes foram imunizados previamente e desafiados i.a. com mBSA e a hipersensibilidade mecânica foi avaliada 1, 3, 5, 7 e 24 h após o desafio, e o edema foi avaliado 7 e 24 h após o desafio. Os animais TRPM2 nocautes apresentaram menor hipersensibilidade mecânica (Fig 3a) e edema articular (Fig 3b) quando comparados aos animais WT. A resposta dos animais TRPM2 KO foi semelhante aos animais tratados com o bloqueador ACA.

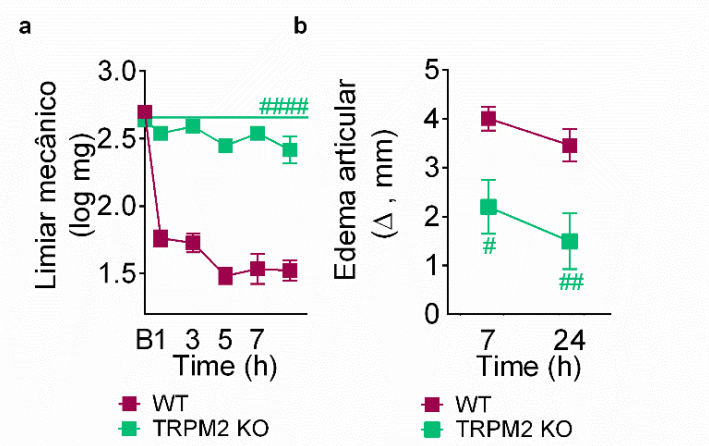

Fig 3 Hipersensibilidade mecânica e edema na AIA são reduzidos em animais TRPM2 nocautes. Animais C57BL/6 e C57BL/6 KO para o canal iônico TRPM2 foram imunizados e desafiados i.a com 100 µg mBSA. A hipersensibilidade mecânica foi avaliada 1-24h (a) e o edema (b) 7 e 24 h após o desafio intra-articular. Os valores foram expressos como a média ± E.P.M. e analisados por teste T. Foram considerados significativos $^{\#}p<0,05$, $^{\#\#}p<0,01$ e $^{\#\#\#\#}p<0,0001$:comparado aos animais C57BL/6 WT. B: valores basais

A fim de verificar o efeito do recrutamento de leucócitos nos animais deficientes para o canal iônico TRPM2, o modelo de AIA foi induzido em animais WT e TRPM2 KO. Os animais foram previamente imunizados e 21 dias após desafiados i.a. com 100 µg de mBSA. Após 24h do desafio com o mBSA o lavado da cavidade articular foi coletado. Como pode-se observar na figura 4, os animais TRPM2 KO apresentaram menor recrutamento de leucócitos totais (Fig 4a), polimorfonucleares (Fig 4b) e mononucleares (Fig 4c) comparados aos animais WT.

Desta forma demonstramos utilizando tanto ferramenta farmacológica como genética, a importância do canal TRPM2 na hipersensibilidade mecânica, edema e recrutamento leucocitário no protocolo agudo do modelo de AIA. Estes resultados corroboram com dados da literatura que demonstram a importância do TRPM2 no contexto da dor inflamatória em que animais nocautes pro TRPM2 apresentaram menor hipersensibilidade mecânica e recrutamento de neutrófilos após estímulo intraplantar com carragenina (Haraguchi et al., 2012).

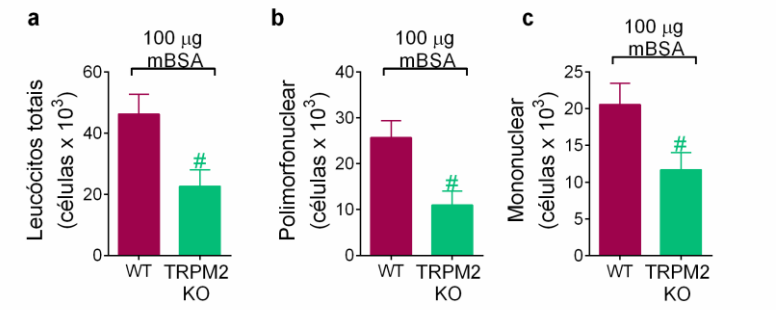

Fig 4. Os animais TRPM2 KO apresentam menor recrutamento leucocitário para a cavidade sinovial na AIA. Animais C57BL/6 e C57BL/6 KO para o canal iônico TRPM2 foram imunizados e desafiados i.a com 100 µg mBSA. A quantidade de leucócitos totais (a) polimorfonucleares (b) e mononucleares (c) foram avaliados 24h após o desafio. Os animais TRPM2 KO apresentaram menor recrutamento de leucócitos totais (a) polimorfonucleares (b) e mononucleares (c) 24h após o desafio com mBSA. Os valores foram expressos como a média ± E.P.M. e analisados por teste T. Foram considerados significativos $^{\#}p<0,05$,:comparado aos animais C57BL/6 WT.

1.3. Bloqueio Farmacológico Do Canal Iônico TRPM2 Na Fase Tardia Da AIA

Um protocolo prolongado de AIA foi utilizado a fim de mimetizar os períodos de re-agudização que ocorrem em pacientes com AR e verificar se existe diferença na participação do TRPM2 nas duas fases, aguda e crônica, da AIA. Para isso, animais C57BL/6 foram pré-tratados com ACA como no protocolo agudo da AIA e posteriormente o tratamento foi continuado a cada 24h por 10 dias. Os animais foram desafiados i.a. com mBSA 2h após o primeiro tratamento com ACA e posteriormente 120h após o primeiro desafio. A hipersensibilidade mecânica foi avaliada 1, 3, 5, 7 e 24, 29, 48, 53, 72, 77, 96, 101, 120, 125, 144, 149, 168, 173, 192, 197, 216, 221, 240, 245h, e o edema 7 e 29, 53, 77, 101, 125, 149, 173, 197, 221, 245h após o primeiro desafio. O bloqueador do canal iônico TRPM2 inibiu a hipersensibilidade mecânica (Fig 5a) após o 1º e 2º desafio, porém a intensidade do efeito foi diferente nas duas fases. Após o 1º desafio o efeito do ACA foi mais proeminente após o primeiro (1-7h) e segundo (29h) tratamentos, o qual foi diminuindo a partir do terceiro tratamento (53h). Interessantemente, quando os animais foram re-desafiados com mBSA, ou seja, um processo de re-agudizacao da doença, o efeito do ACA voltou a ser proeminente (125h), porém nos dias subsequentes esse efeito decaiu novamente. O edema (Fig 5b) foi inibido 7h após o primeiro desafio, e subsequentemente o edema articular do grupo ACA assemelhou-se ao grupo mBSA e foi diminuindo gradativamente. O edema foi inibido novamente

pelo tratamento com ACA após o 2º desafio (125h) e subsequentemente assemelhou-se ao grupo mBSA e foi diminuindo gradativamente e ao final da última medida no dia 10 o edema articular dos grupos mBSA e ACA estavam semelhantes ao grupo salina (Fig 5b).

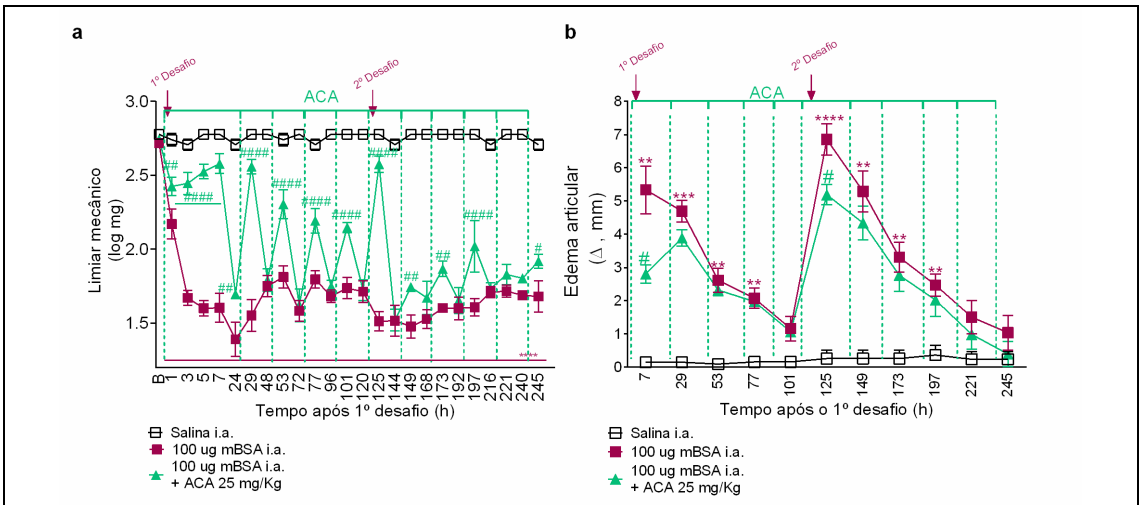

Fig 5 Efeito do bloqueador do canal iônico TRPM2 na hipersensibilidade mecânica e edema no protocolo prolongado de AIA. Animais C57BL/6 previamente imunizados foram tratados a cada 24 h com 25 mg/Kg de ACA s.c. Os animais receberam o primeiro desafio com 100 µg mBSA i.a. após 2h do primeiro tratamento com ACA. O segundo desafio com 100 µg mBSA i.a. foi administrado 120h depois do primeiro desafio. A hipersensibilidade mecânica (a) e edema (b) foram avaliados 1-245h após o primeiro desafio. Os valores foram expressos como a média ± E.P.M e analisados por ANOVA de duas via e pós teste de Tukey. Foram considerados significativos $^{**}p<0,01$, $^{***}p<0,001$, $^{****}p<0,0001$: grupo mBSA diferente do grupo salina; $^{\#}p<0,05$, $^{\#\#}p<0,01$, $^{\#\#\#\#}p<0,0001$: grupo mBSA diferente do grupo ACA. B: valores basais

1.4. Efeito Da Inibição Do Canal Iônico TRPM2 Na Produção De CXCL2 E TNFα Na AIA

Tendo em vista a importância do CXCL2 e TNFα na fisiopatologia da AIA (Coelho et al., 2008; Taylor and Feldmann, 2009), foi avaliado se o canal iônico TRPM2 poderia ser importante para a produção desses mediadores. Desta forma avaliou-se o efeito do tratamento com o bloqueador do TRPM2 ACA na produção CXCL2 e TNFα. Animais C57BL/6 foram previamente imunizados e pré-tratados com ACA e desafiados após 2h com mBSA. O tecido sinovial foi coletado 5 h após o desafio e a produção destes mediadores foi determinada por ELISA. Como podemos observar na figura 6, o desafio com mBSA induziu a produção de CXCL2 (Fig 6a) e TNFα (Fig 6b) e o pré-tratamento com o ACA reduziu a produção desses mediadores na membrana sinovial. O CXCL2 é a quimiocina responsável pelo recrutamento de neutrófilos para o foco inflamatório, o efeito do ACA em inibir a

produção do CXCL2 na AIA está de acordo com o efeito do ACA em inibir o recrutamento de neutrófilos na AIA (Fig 2b). Além disso, o TRPM2 é importante para a produção de CXCL2 em outros contexto que não o da AIA, animais nocautes para o TRPM2 estimulados com carragenina produzem menos CXCL2 4h após o estímulo (Haraguchi et al., 2012). Além disso monócitos nocautes para o TRPM2 quando estimulados com H_2O_2 produzem menos CXCL2 quando comparado a monócitos de animais WT (Yamamoto et al., 2008).

O TNFα é uma citocina de extrema importância na progressão da AR, possui efeitos catabólicos responsáveis pela degradação da cartilagem bem como que em ação conjunta com a IL-6 leva a osteoclastogenesis e reabsorção óssea (O'Brien et al., 2016). Além disso o TNFα tem papel importante na dor, reduz o limiar mecânico e térmico de ratos estimulados intraplantarmente com TNFα (Cunha et al., 1992) e ativa neurônios sensoriais nociceptivos do DRG (Schafers et al., 2003). A inibição da hipersensibilidade mecânica pelo bloqueio do TRPM2 pelo ACA na AIA pode ter relação com a inibição da produção TNFα pelo ACA na AIA.

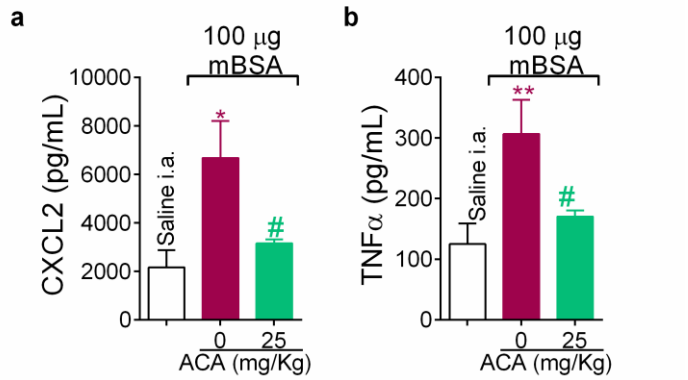

Fig 6. O tratamento farmacológico com o bloqueador do canal iônico TRPM2 inibe a produção de CXCL2 e TNFα no tecido sinovial na AIA. Animais C57BL/6 previamente imunizados foram pré-tratados com 25 mg/Kg de ACA s.c. e desafiados com 100 µg mBSA i.a. após 2h. Os níveis de CXCL2 (a) e TNFα (b) foram avaliados após 5h do desafio com mBSA. Os valores foram expressos como a média ± E.P.M e analisados por ANOVA de uma via e pós teste de Tukey. Foram considerados significativos $^{*}p<0,05$ e $^{**}p<0,01$: grupo mBSA diferente do grupo salina; $^{\#}p<0,05$: grupo mBSA diferente do grupo ACA.

1.5. Avaliação Da Expressão Do TRPM2 Na Medula Espinal, DRG, Linfonodos Poplíteo E Inguinal Na AIA

A fim de compreender qual o tecido em que o TRPM2 está desempenhando o seu papel no modelo de AIA, a expressão do RNAm para o TRPM2 foi avaliada na medula espinal, DRG, linfonodos poplíteo e inguinal por RT-

qPCR. Animais C57BL/6 foram previamente imunizados e desafiados no 21º e 26º dias i.a. com mBSA. A medula espinal, DRG, linfonodos poplíteo e inguinal foram coletados após 7h do primeiro desafio e 96h após o segundo desafio. Animais estimulados com salina i.a. ou *Naïves* (não imunizados) foram utilizados como controles. Foi observado aumento na expressão do RNAm para TRPM2 96h após o 2º desafio (Fig 7a) na medula espinal, e 7h após o primeiro desafio no linfonodo poplíteo (Fig 7c). Não foram observadas alterações significativas na expressão do TRPM2 no DRG (Fig 7b) e linfonodos inguinais (Fig 7d) nos tempos avaliados. Assim, estes dados. sugerem que o TRPM2 expresso na medula espinal e linfonodos poplíteos parecem desempenhar um papel importante na fisiopatologia da AIA.

A micróglia é um dos tipos celulares que apresentam o TRPM2 na medula espinal. No contexto da dor neuropática houve redução na ativação da micróglia em animais nocautes para o TRPM2 comparado aos WT após ligadura parcial do nervo ciático. Além disso a produção de CXCL2 foi reduzida em cultura primária de micróglia de animais TRPM2 nocautes estimulados com LPS comparado a cultura da micróglia de animais selvagens (Haraguchi et al., 2012). Na AIA existe a participação da micróglia no processo doloroso uma vez que o tratamento com o inibidor de micróglia minociclina inibe a mudança de descarga de peso nas patas do camundongo na AIA (Quadros et al., 2015).

As células T são de extrema importância no contexto da autoimunidade. O TPRM2 tem seu RNAm aumentando em células T $CD4^+$ após estimulação policlonal do receptor de célula T (Melzer et al., 2012). De maneira semelhante na AIA houve aumento na expressão do TRPM2 no linfonodo poplíteo 7h após o desafio com mBSA. O TRPM2 tem papel importante na proliferação de células T haja vista a redução da proliferação de células T nocautes para o TRPM2 comparado a células de animais WT estimulados com *beads* anti-CD3/CD28 (Melzer et al., 2012). Estudos posteriores precisam ser realizados para verificar se após o desafio com mBSA ocorre a proliferação de células T no linfonodo poplíteo de forma dependente de TRPM2.

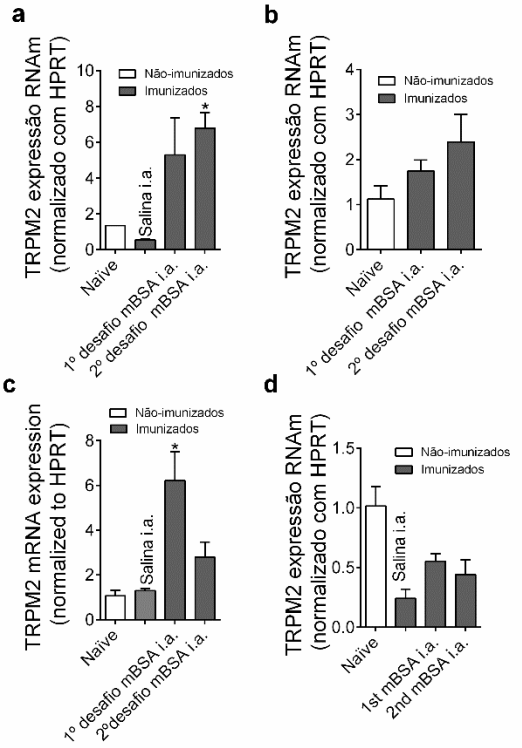

Fig 7 Expressão do RNAm do canal iônico TRPM2 na medula espinal, DRG, linfonodo poplíteo e inguinal. Animais C57BL/6 foram imunizados e desafiados no 21º dia e re-desafiados no 26º. A expressão do RNAm para o TRPM2 foi avaliada por RT-qPCR na medula espinal (a), DRG (b), linfonodo poplíteo (c) e inguinal (d). Os tecidos foram coletados após 7 h do primeiro desafio e 96h após o segundo desafio. Animais estimulados com salina i.a. ou *Naïves* foram usados como controles. Os resultados foram expressos como erro ± E.P.M e analisados por ANOVA de uma via e pós teste de Tukey. Foram considerados significativos $^{*}p<0,05$ comparado com o grupo *Naïve.*

Desta maneira foi demonstrando utilizando a ferramenta farmacológica de bloqueio do canal iônico TRPM2 ou genética com animais TRPM2 nocautes a importância do TRPM2 no controle da dor articular e inflamação com redução no recrutamento de células imunes na AIA. Além disso o bloqueio com ACA do TRPM2 inibiu a produção de CXCL2 e TNFα induzido pela AIA. Além disso, no contexto da AIA houve aumento da expressão do TRPM2 na medula espinal e linfonodo poplíteo. Portanto, a participação do TRPM2 no contexto da AIA é importante e os demais mecanismos celulares e moleculares da contribuição do TRPM2 na AIA ainda precisam ser elucidados.

2. PAPEL DO CANAL IÔNICO TRPM2 NA OSTEOARTRITE INDUZIDA POR MIA

Nesta próxima seção de resultados foram abordados os efeitos do bloqueio farmacológico do canal iônico TRPM2 no modelo de osteoartrite induzido por MIA.

2.1. Efeito Do Bloqueador Farmacológico Do Canal Iônico TRPM2 No Modelo De MIA

Animais C57BL/6 foram estimulados i.a. com 0,5 mg de MIA no dia 0 e a hipersensibilidade mecânica e edema foram avaliados nos dias 3, 7, 10, 14, 17, 21, 24 e 28 dias após o estímulo com MIA. O tratamento com o bloqueador do canal iônico TRPM2, ACA na dose de 25 mg/Kg s.c., foi realizado nos dias das medidas 2h antes da avaliação da hipersensibilidade mecânica e edema. Os animais desafiados com MIA desenvolveram hipersensibilidade mecânica, a qual foi reduzida parcialmente pelo tratamento com ACA (Fig 9a). O tratamento com o ACA inibiu a hipersensibilidade mecânica mais proeminentemente até 14 dias após o estímulo com MIA e posterior esse efeito analgésico foi diminuindo, possivelmente isso pode ter relação com o curso inflamatório que o MIA gera na articulação estimulada. De fato, foi demonstrado previamente que o modelo de osteoartrite com MIA induz processo inflamatório na articulação e sinovite, os quais são reduzidos ao longo do curso da doença (Takahashi et al., 2018). Este fato corrobora ainda com nossos resultados de edema articular (Fig 9b). O MIA induz edema articular nos primeiros 14 dias do curso da doença e o tratamento com ACA foi capaz de inibir este edema até o dia 10. Após 14 dias da injeção de MIA o edema regrediu ao nível basal, demonstrando assim que esse período inicial da doença no qual o efeito do ACA foi mais pronunciado deve-se, provavelmente, a uma ação anti-inflamatória. Demonstrando assim que o papel do TRPM2 na dor articular provavelmente é mais importante em contextos em que o processo inflamatório tem importante contribuição na fisiopatologia da doença. Por outro lado, como neurônios sensoriais expressam o TRPM2 e o efeito do ACA após a fase inflamatória local do modelo de osteoartrite induzido por MIA pode ser por reduzir a transmissão sináptica nociceptiva para o sistema nervoso central.

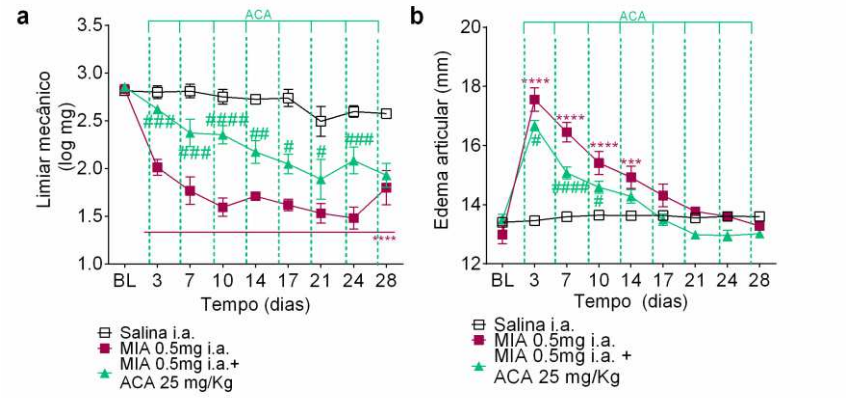

Fig 8 Efeito do bloqueador farmacológico do canal iônico TRPM2 na hipersensibilidade mecânica e edema no modelo de osteoartrite induzido por MIA. Animais C57BL/6 foram estimulados i.a. com 0,5 mg de MIA no dia 0. Animais foram tratados s.c. com 25 mg/kg nos dias 3, 7, 10, 14, 17, 21, 24 e 28 dias após o estímulo com MIA. A hipersensibilidade mecânica (a) e edema (b) foram avaliados 3, 7, 10, 14, 17, 21, 24 e 28 dias após o estímulo com MIA. Os valores foram expressos como a média ± E.P.M e analisados por ANOVA de duas via e pós teste de Tukey. Foram considerados significativos $^{****}p<0,0001$: grupo MIA diferente do grupo salina; $^{\#}p<0,05$, $^{\#\#}p<0,01$, $^{\#\#\#}p<0,001$ $^{\#\#\#\#}p<0,0001$: grupo MIA diferente do grupo ACA. B: valores basais

2.2. Expressão Do RNAm Para O Canal Iônico TRPM2 Na Medula Espinal E DRG Na Osteoartrite Induzida Por MIA

A expressão do RNAm para o canal iônico TRPM2 por RT-qPCR na medula espinal e DRG foi avaliada para determinar se o modelo de MIA induz um aumento na expressão deste canal iônico. Animais C57BL/6 foram estimulados i.a. com 0,5 mg de MIA e a medula espinal e DRG foram coletados 3, 7, 14, 21 e 30 dias após o estímulo. Observou-se uma tendência no aumento da expressão do TRPM2 na medula espinal (a), porém devido a variabilidade dentro do grupo não foi observada diferença significativa entre os animais estimulados com MIA e os animais *Naïves* (não estimulados). No DRG não se observou alterações significativas na expressão do TRPM2 (b).

No contexto da dor articular induzido pelo MIA a ativação da micróglia tem papel importante. Ratos estimulados com MIA apresentaram ativação da micróglia 7, 14, 21 e 28 dias após o estímulo i.a. com MIA. Além disso a inibição da micróglia pelo tratamento de minociclina inibiu a ativação da micróglia e a hipersensibilidade mecânica no 28º dia após o estímulo com MIA (Sagar et al., 2011). Tendo em vista a importância do TRPM2 na ativação da micróglia, observou-se a redução na ativação da micróglia em animais nocautes para o TRPM2 comparado aos WT após ligadura parcial do nervo ciático (Haraguchi et al., 2012).

Estudos posteriores precisam ser realizados para verificar se o efeito do ACA na hipersensibilidade mecânica podem ter relação com a inibição da ativação da micróglia pelo bloqueio do TRPM2.

Este projeto verificou que o TRPM2 no contexto da dor articular induzido pelo MIA, e aumento deste canal na medula espinal pode ter contribuição importante para a manutenção dolorosa no contexto do modelo de MIA. Os mecanismos celulares e moleculares ainda precisam ser investigados para determinar as células e vias que o TRPM2 pode vir estar participando para a manutenção da dor articular.

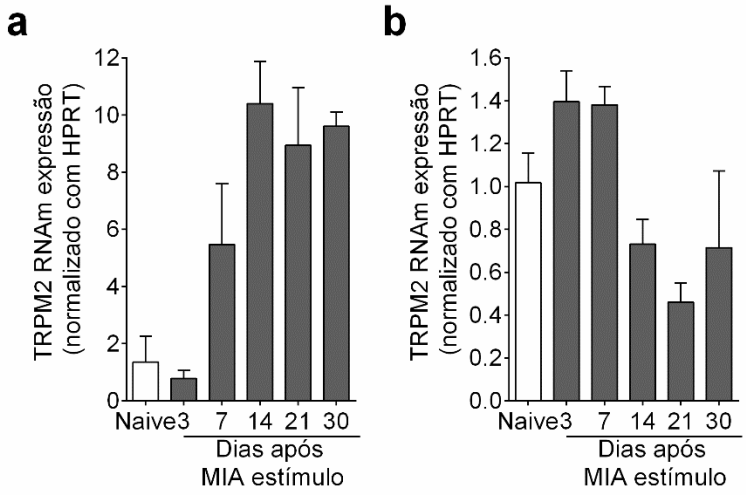

Fig 9 Expressão do RNAm do canal iônico TRPM2 na medula espinal e DRG. Animais C57BL/6 foram estimulados i.a. com 0,5 mg de MIA. A expressão do RNAm para o TRPM2 foi avaliada por RT-qPCR na medula espinal (a) e DRG (b). Os tecidos foram coletados 3, 7, 14, 21 e 30 dias após a injeção i.a. com MIA. Animais *Naïves* foram usados como controles. Os resultados foram expressos como erro ± E.P.M e analisados por ANOVA de uma via e pós teste de Tukey. Foram considerados significativos $p<0,05$.

3. AVALIAÇÃO DE ANTICORPOS COMERCIAIS PARA MARCAÇÃO DO CANAL IÔNICO TRPM2

Com o intuito de determinar em qual tipo celular oTRPM2 estava presente, foi avaliado a especificidade de 3 anticorpos comerciais distintos contra o canal iônico TRPM2. Para isso, animais C57BL/6 WT e TRPM2 KO foram estimulados i.p. com 500 µg de carragenina – estimulo inflamatório que induz recrutamento de células para o local (Mizokami et al., 2016) – e o lavado peritoneal foi coletado após 24h. A suspensão celular foi citocentrifugadas e o ensaio de imunofluorescência realizado. Os 3 anticorpos testados Ab11169 (Abcam – Fig

10a,b) SAB2108271 (Sigma-Aldrich – Fig 10c,d) e ACC-043 (Alomone – Fig 10e,f) apresentaram ligação inespecífica uma vez que podemos observar marcação positiva nas células recrutadas pelo estímulo com carragenina em animais deficientes para o canal iônico TRPM2.

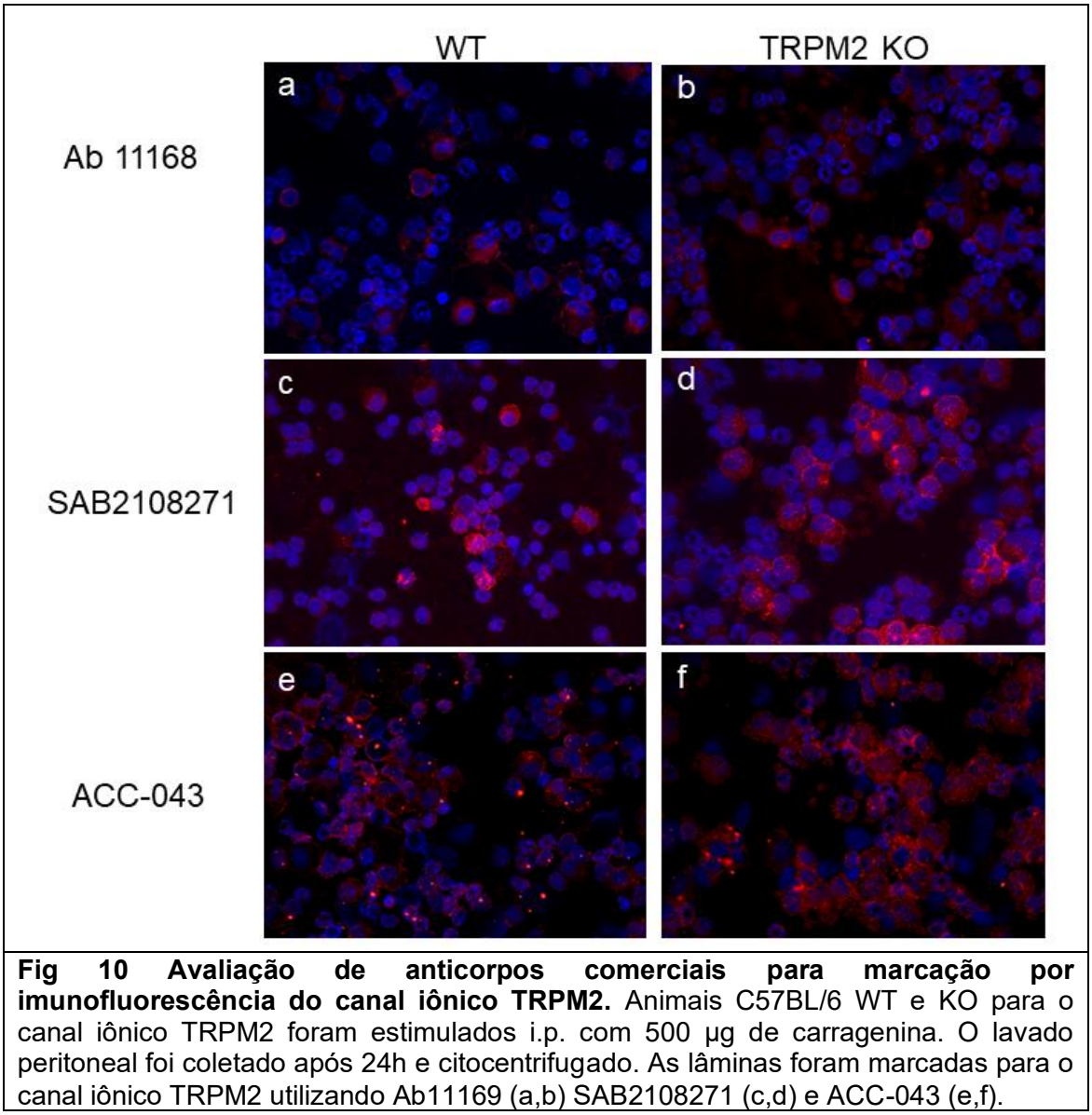

Fig 10 Avaliação de anticorpos comerciais para marcação por imunofluorescência do canal iônico TRPM2. Animais C57BL/6 WT e KO para o canal iônico TRPM2 foram estimulados i.p. com 500 µg de carragenina. O lavado peritoneal foi coletado após 24h e citocentrifugado. As lâminas foram marcadas para o canal iônico TRPM2 utilizando Ab11169 (a,b) SAB2108271 (c,d) e ACC-043 (e,f).

Referências

Coelho, F. M., Pinho, V., Amaral, F. A., Sachs, D., Costa, V. V., Rodrigues, D. H., Vieira, A. T., Silva, T. A., Souza, D. G., Bertini, R., Teixeira, A. L., Teixeira, M. M., 2008. The chemokine receptors CXCR1/CXCR2 modulate antigen-induced arthritis by regulating adhesion of neutrophils to the synovial microvasculature. Arthritis Rheum 58, 2329-2337.

Cunha, F. Q., Poole, S., Lorenzetti, B. B., Ferreira, S. H., 1992. The pivotal role of tumour necrosis factor alpha in the development of inflammatory hyperalgesia. Br J Pharmacol 107, 660-664.

Haraguchi, K., Kawamoto, A., Isami, K., Maeda, S., Kusano, A., Asakura, K., Shirakawa, H., Mori, Y., Nakagawa, T., Kaneko, S., 2012. TRPM2 contributes to inflammatory and neuropathic pain through the aggravation of pronociceptive inflammatory responses in mice. J Neurosci 32, 3931-3941.

Harteneck, C., Frenzel, H., Kraft, R., 2007. N-(p-amylcinnamoyl)anthranilic acid (ACA): a phospholipase A(2) inhibitor and TRP channel blocker. Cardiovasc Drug Rev 25, 61-75.

Melzer, N., Hicking, G., Gobel, K., Wiendl, H., 2012. TRPM2 cation channels modulate T cell effector functions and contribute to autoimmune CNS inflammation. PLoS One 7, e47617.

Mizokami, S. S., Hohmann, M. S., Staurengo-Ferrari, L., Carvalho, T. T., Zarpelon, A. C., Possebon, M. I., de Souza, A. R., Veneziani, R. C., Arakawa, N. S., Casagrande, R., Verri, W. A., Jr., 2016. Pimaradienoic Acid Inhibits Carrageenan-Induced Inflammatory Leukocyte Recruitment and Edema in Mice: Inhibition of Oxidative Stress, Nitric Oxide and Cytokine Production. PLoS One 11, e0149656.

O'Brien, W., Fissel, B. M., Maeda, Y., Yan, J., Ge, X., Gravallese, E. M., Aliprantis, A. O., Charles, J. F., 2016. RANK-Independent Osteoclast Formation and Bone Erosion in Inflammatory Arthritis. Arthritis & Rheumatology 68, 2889-2900.

Quadros, A. U., Pinto, L. G., Fonseca, M. M., Kusuda, R., Cunha, F. Q., Cunha, T. M., 2015. Dynamic weight bearing is an efficient and predictable method for evaluation of arthritic nociception and its pathophysiological mechanisms in mice. Sci Rep 5, 14648.

Sagar, D. R., Burston, J. J., Hathway, G. J., Woodhams, S. G., Pearson, R. G., Bennett, A. J., Kendall, D. A., Scammell, B. E., Chapman, V., 2011. The contribution of spinal glial cells to chronic pain behaviour in the monosodium iodoacetate model of osteoarthritic pain. Mol Pain 7, 88.

Schafers, M., Lee, D. H., Brors, D., Yaksh, T. L., Sorkin, L. S., 2003. Increased sensitivity of injured and adjacent uninjured rat primary sensory neurons to exogenous tumor necrosis factor-alpha after spinal nerve ligation. J Neurosci 23, 3028-3038.

Takahashi, I., Matsuzaki, T., Kuroki, H., Hoso, M., 2018. Induction of osteoarthritis by injecting monosodium iodoacetate into the patellofemoral joint of an experimental rat model. PLoS One 13, e0196625.

Taylor, P. C., Feldmann, M., 2009. Anti-TNF biologic agents: still the therapy of choice for rheumatoid arthritis. Nat Rev Rheumatol 5, 578-582.

Yamamoto, S., Shimizu, S., Kiyonaka, S., Takahashi, N., Wajima, T., Hara, Y., Negoro, T., Hiroi, T., Kiuchi, Y., Okada, T., Kaneko, S., Lange, I., Fleig, A., Penner, R., Nishi, M., Takeshima, H., Mori, Y., 2008. TRPM2-mediated Ca2+influx induces chemokine production in monocytes that aggravates inflammatory neutrophil infiltration. Nat Med 14, 738-747.